NORTH ATLANTIC TREATY ORGANISATION

RESEARCH AND TECHNOLOGY ORGANISATION

AC/323(AVT-007)TP/25

www.rta.nato.int

RTO TECHNICAL REPORT **TR-AVT-007-V2**

Technologies for Propelled Hypersonic Flight

(Technologies des vols hypersoniques propulsés)

Volume 2 – Subgroup 2: Scram Propulsion

This report documents the results of the Applied Vehicle Technology Panel Working Group 10, Subgroup 2.

Published January 2006

NORTH ATLANTIC TREATY ORGANISATION

RESEARCH AND TECHNOLOGY ORGANISATION

AC/323(AVT-007)TP/25

www.rta.nato.int

RTO TECHNICAL REPORT **TR-AVT-007-V2**

Technologies for Propelled Hypersonic Flight

(Technologies des vols hypersoniques propulsés)

Volume 2 – Subgroup 2: Scram Propulsion

This report documents the results of the Applied Vehicle Technology Panel Working Group 10, Subgroup 2.

The Research and Technology Organisation (RTO) of NATO

RTO is the single focus in NATO for Defence Research and Technology activities. Its mission is to conduct and promote co-operative research and information exchange. The objective is to support the development and effective use of national defence research and technology and to meet the military needs of the Alliance, to maintain a technological lead, and to provide advice to NATO and national decision makers. The RTO performs its mission with the support of an extensive network of national experts. It also ensures effective co-ordination with other NATO bodies involved in R&T activities.

RTO reports both to the Military Committee of NATO and to the Conference of National Armament Directors. It comprises a Research and Technology Board (RTB) as the highest level of national representation and the Research and Technology Agency (RTA), a dedicated staff with its headquarters in Neuilly, near Paris, France. In order to facilitate contacts with the military users and other NATO activities, a small part of the RTA staff is located in NATO Headquarters in Brussels. The Brussels staff also co-ordinates RTO's co-operation with nations in Middle and Eastern Europe, to which RTO attaches particular importance especially as working together in the field of research is one of the more promising areas of co-operation.

The total spectrum of R&T activities is covered by the following 7 bodies:

- AVT Applied Vehicle Technology Panel
- HFM Human Factors and Medicine Panel
- IST Information Systems Technology Panel
- NMSG NATO Modelling and Simulation Group
- SAS Studies, Analysis and Simulation Panel
- SCI Systems Concepts and Integration Panel
- SET Sensors and Electronics Technology Panel

These bodies are made up of national representatives as well as generally recognised 'world class' scientists. They also provide a communication link to military users and other NATO bodies. RTO's scientific and technological work is carried out by Technical Teams, created for specific activities and with a specific duration. Such Technical Teams can organise workshops, symposia, field trials, lecture series and training courses. An important function of these Technical Teams is to ensure the continuity of the expert networks.

RTO builds upon earlier co-operation in defence research and technology as set-up under the Advisory Group for Aerospace Research and Development (AGARD) and the Defence Research Group (DRG). AGARD and the DRG share common roots in that they were both established at the initiative of Dr Theodore von Kármán, a leading aerospace scientist, who early on recognised the importance of scientific support for the Allied Armed Forces. RTO is capitalising on these common roots in order to provide the Alliance and the NATO nations with a strong scientific and technological basis that will guarantee a solid base for the future.

Published January 2006

ISBNs 92-837-0041-4 / 978-92-837-0041-8

Technologies for Propelled Hypersonic Flight

(RTO-TR-AVT-007-V2)

Executive Summary

In 1998, in the wake of the successful WG 18, the new RTO AVT Panel endorsed the creation of a new Working Group on "Technologies for Propelled Hypersonic Flight", RTO AVT WG 10.

The aim of this new Working Group was:

- To address selected critical issues related to propelled hypersonic flight;
- To review the associated state of the art for analysis and design; and
- To recommend activities for further developments.

Three (3) Subgroups were created to structure the activities of the Working Group (WG):

- **Subgroup 1** dealt with reviewing fundamental aspects on plug nozzles, analysing altitude adaptation aspects and wake closure phenomena, studying influence of external flow on thrust, and addressing design methods including thrust vector control and flight extrapolation.
- **Subgroup 2** addressed the physical modelling aspects associated with scram combustion; a review was given on fuels, turbulence mixing, ignition and flame holding prediction capabilities as well as vitiation.
- **Subgroup 3** screened a large number of test cases for CFD validation; selected well-defined sets of experiments, repeated in some cases older experiments with updated instrumentation and this for six areas where CFD validation was deemed essential: boundary layer instability and transition; real gas flows; laminar viscous inviscid interaction; shock-shock interactions; shock wave turbulent boundary layer interaction; and base flows with and without plumes.

A very fruitful exchange of information and stimulating discussions among all members of the Working Group resulted in an **unprecedented effort** to improve the technologies for hypersonic flight. High standards for the selection and evaluation of test cases for CFD validation were applied.

The present WG allowed and promoted "harmonization" of otherwise dispersed activities. The Working Group expressed their vision that in the future, joint "in flight research" programmes could be set up under the auspices of NATO and in collaboration with Russia, as advances in hypersonic flight require strong collaboration on improvements of aerothermodynamic capabilities, i.e. numerical, experimental and flight test techniques.

Technologies des vols hypersoniques propulsés
(RTO-TR-AVT-007-V2)

Synthèse

En 1998, suite aux activités très positives du GT18, le nouveau Comité AVT de la RTO a avalisé la création d'un nouveau Groupe de travail sur les « Technologies du vol hypersonique propulsé », le GT10 AVT de la RTO.

L'objectif de ce nouveau Groupe de travail était le suivant :

- Aborder des aspects critiques sélectionnés en rapport avec le vol hypersonique propulsé ;
- Passer en revue l'état de l'art correspondant pour l'analyse et la conception ;
- Recommander des activités en vue de développements futurs.

Trois sous-groupes ont été constitués afin de structurer les activités du Groupe de travail (GT) :

- Le **sous-groupe 1,** dont la mission consistait à étudier les aspects fondamentaux des tuyères à noyau central, à analyser les aspects d'adaptation à l'altitude et les phénomènes de fermeture du sillage, à étudier l'influence de l'écoulement externe sur la poussée, et à aborder les méthodes de conception incluant le contrôle du vecteur-poussée et l'extrapolation du vol.
- Le **sous-groupe 2,** dont le travail consistait à étudier les aspects de la modélisation physique associés à la combustion supersonique ; une étude ayant notamment porté sur les carburants, le mélange de turbulence, les capacités de prévision d'allumage et de tenue de flamme ainsi que la viciation.
- Les travaux du **sous-groupe 3** ont couvert un grand nombre d'essais types aux fins de validation par CFD; le sous-groupe a sélectionné des batteries d'essais bien définies, réitéré, dans certains cas, des expériences déjà faites dans le passé à l'aide d'instruments modernes, ce dans six domaines où la validation par CFD était jugée essentielle : instabilité et transition de la couche limite ; dynamique des gaz réels ; interaction laminaire visqueuse/non-visqueuse ; interactions choc-choc ; interaction onde de choc/couche limite turbulente ; et écoulement de culot avec ou sans panache.

L'échange d'informations très fructueux et les débats passionnés qui ont eu lieu entre tous les membres du Groupe de travail se sont traduits par le déploiement **d'efforts sans précédent** en vue d'améliorer les technologies du vol hypersonique. Des normes rigoureuses de sélection et d'évaluation des essais types effectués dans le cadre de la validation CFD ont été appliquées.

Le présent GT a par ailleurs permis et favorisé « l'harmonisation » d'autres activités dispersées. Le Groupe de travail a indiqué qu'à l'avenir, les programmes de « recherche en vol » conjoints pourraient être organisés sous l'égide de l'OTAN et en collaboration avec la Russie, les progrès dans le domaine du vol hypersonique requérant une étroite collaboration pour optimiser les capacités aérothermodynamiques, telles que les techniques numériques, expérimentales et d'essais en vol.

Table of Contents

Foreword

This Final Report includes final contributions by participants in the NATO RTO AVT WG 10, Subgroup 2 – SCRJ. Participation came from European industries, and European and US research organizations, including the military. The purpose stated since the beginning of this NATO RTO activity (June 1998) was to single out, and then focus on, the key areas of SCRJ design and operation in need of investigating; this in order to help in moving SCRJ engines from conceptual objects in need of laboratory tests a step closer to actual propulsion systems.

Although not all the work envisaged and encompassed by this goal has been accomplished, I think that substantial progress was made toward a better understanding of some, if not most, of the truly key issues in SCRJ engines, and therefore of the potential ways of solving the peculiar problems of SCRJ design and operation.

It is regrettable that proprietary and security issues have prevented full sharing of information among participants, by which faster and perhaps better progress would have accomplished. Nevertheless, even with all constraints, this Report includes, I hope, useful information, some of which was previously unavailable. New information was produced by the willingness and time made freely available by most participants while also performing their institutional duties.

In fact, without the time, help, patience and persistence of the people who volunteered to write the Chapters describing key SCRJ technologies, this Report could not have been possible. I wish to seize this opportunity to thank all participants in this Subgroup for their priceless collaboration.

I also want to acknowledge Dr. F. Cuoco (now at FiatAvio), Dr. F. Tomassi and Dr. A. Ingenito who have taken the burden of handling, editing, collating and re-organizing many times the countless messages and files exchanged during the course of this work, taking in stride my haste, and sometimes my temper.

Rome, March 2003

AVT Working Group 10

CHAIRMAN

Mr. Jean Muylaert
ESTEC, Aerothermodynamic Section
Postbus 299
2200 AG Noorwijk
THE NETHERLANDS
Jean.Marie.Muylaert@esa.int

CO-CHAIRMAN

Dr. Ajay Kumar
NASA Langley Research Center
Mail Stop 285
Hampton, VA 23681
USA
a.kumar@larc.nasa.gov

SUBGROUP CHAIRMEN

Prof. Marcello Onofri
Universita degli Studi di Roma
La Sapienza
Dipartimento Meccanica Aeronautica
Via Eudossiana, 18
00184 ROMA
ITALY
onofri@onofri.ing.unioma1.it

Prof. Claudio Bruno
Universita degli Studi di Roma
La Sapienza
Dipartimento Meccanica Aeronautica
Via Eudossiana, 18
00184 ROMA
ITALY
cbruno@dma.ing.uniroma1.it

Prof. Doyle Knight
Dept of Mechanical & Aerospace
Engineering
Rutgers University
98, Brett Road
Piscataway, NJ 08854-8058
USA
knight@jove.rutgers.edu

MEMBERS

BELGIUM
D. Fletcher, VKI
P. Hendrick, ERM
J. Muylaert, ESTEC
J. Wendt, VKI

FRANCE
D. Arnal, ONERA
B. Aupoix, ONERA
M. Bouchez, MATRA
M. Calabro, EADS
F. Chalot, Dassault Aviation
B. Chanez, ONERA
J. Delery, ONERA
D. Devezeaux, ONERA
P. Donguy, SNECMA
C. Dujarric, ESAHQ
M. Dussauge, Univ. Marseille
F. Falempin, MBDA
P. Novelli, ONERA
P. Reijasse, ONERA
P. Rostand, Dassault Aviation

GREECE
A. Panaras, Univ. Athens

GERMANY
W. Beck, DLR
G. Hagemann, EADS
H. Immich, EADS

GERMANY (cont'd)

W. Koschel, DLR
P. Sacher, EADS
R. Schwane, ESTEC

ITALY

S. Borrelli, CIRA
C. Bruno, Univ. Roma
D. D'Ambrosio, Univ. Torino
L. Guerra, ALENIA
M. Onofri, Univ. Roma
M. Pandolfi, Univ. Torino

THE NETHERLANDS

P. Bakker, TUD
W. Bannink, TUD
R. Veraar, TNO

SWEDEN

A. Boman, Volvo
J. Olsson, FOI

UNITED KINGDOM

T. Cain, DERA
J. Harvey, Imperial College

UNITED STATES

I. Blankson, NASA Lewis
G. Candler, Univ. Minnesota
D. Davis, USAF
P. Drummond, NASA Langley
J. Hicks, NASA Dryden
M. Holden, CALSPAN
T. Jackson, USAF
R. Kimmel, USAF
D. Knight, Rutgers Univ.
A. Kumar, NASA Langley
L. Maurice, USAF
J. Moss, NASA Langley
S. Murthy, Purdue Univ.
T. Nguyen, Aerojet
K. Numbers, USAF
E. Reshotko, Case Western Reserve Univ.
W. Saric, Arizona State Univ.
J. Schetz, Princeton
J. Schmisseur, USAF
G. Seibert, USAF
D. Van Wie, APL
S. Walker, USAF

RUSSIA

M. Ivanov, ITAM
A. Maslov, ITAM
A. Zeldovodov, ITAM

Acknowledgements

I would like to express my sincere thanks to all the members of this Working Group; thanks to their sustained, free of charge and high quality work we were able to improve understanding and capabilities for hypersonic sustained flight phenomena.

I would also like to acknowledge in particular my co-chair Dr. Ajay Kumar, who has supported me throughout the lifetime of this Working Group, as well as my Subgroup Chairmen Prof. Marcello Onofri, Prof. Claudio Bruno and Prof. Doyle Knight. Without their driving enthusiasm, the Working Group would never have been so successful. Thanks to the Subgroup Chairmen, these present documents will undoubtedly be used in the coming years, as a reference for hypersonic design tools evaluation.

Jean Muylaert
Chair RTO AVT WG 10

OVERVIEW

1.1 HISTORICAL BACKGROUND

The history of this Working Group dates back to 1987 when the former Fluid Dynamics Panel (FDP) from AGARD organized a symposium on hypersonics in Bristol. (AGARD CP-428). In those days, NASP in the US and HERMES in the EU required significant advances in hypersonics and there was a need to improve existing hypersonic facilities including instrumentation, as well as to develop new ones in particular the high enthalpy facilities. As a result, Dr. R. Graves and Prof. E. Reshotko founded the ad hoc Study Group on hypersonic research and technology, covering 4 technology groups:

- Rarefied flows;
- Viscous interactions and transition;
- High enthalpy facilities; and
- Hypersonic wind tunnel instrumentation.

The original contributors of this ad hoc Group on hypersonics were: S. Bogdonoff, J. Delery, C. Dujarric, J. Ginoux, R. Graves, M. Holden, K. Kienappel, J. Leynaert, E. Reshotko, M. Thery and J. Wendt. The ad hoc Study Group organized their meetings and in the course of their work identified research needs.

In 1992, the ad hoc Study Group recommendations were followed up by the creation of the AGARD Working Group 18 “Hypersonic Experimental and Computational Capability, Improvements and Validation”, chaired by K. Kienappel and W. Saric.

In addition to the usual practice of gathering and collecting the existing knowledge base, this Working Group (WG) also coordinated specific transatlantic cooperation:

- The planetary probe campaigns in high enthalpy facilities; and
- The Halis / Orbiter testing including flight extrapolation activities.

The WG 18 attracted all the disciplines in hypersonics; its life time was extended, covering a period from 1992 to 1997 and resulted finally in AGARD AR-319.

1.2 CREATION OF RTO AVT WG 10

In 1998, in the wake of the successful WG 18, the new RTO AVT Panel endorsed the creation of a new Working Group on “Technologies for Propelled Hypersonic Flight”, RTO AVT WG 10. The Working Group was set up initially for a period of 3 years.

The aim of this new Working Group was:

- To address selected critical issues related to propelled hypersonic flight;
- To review the associated state of the art for analysis and design; and
- To recommend activities for further developments.

Following the successful modus operandi of WG 18, this new Working Group updated further the knowledge base in hypersonics and coordinated specific transatlantic experiments associated with hypersonic CFD validation. In particular, a series of experiments on generic configurations were performed in different hypersonic facilities either because of the complementarity’s in nature or because

of the required redundancy allowing experimental uncertainty analysis. This aspect of its activities attracted again a large group active in hypersonics, not only under NATO countries but also from Russia.

An extension till 2003 was granted by the RTO. This extension allowed the completion of large-scale experiments in US, in EU, as well as in Russia, and the associated numerical rebuilding activities to take place, followed by an in-depth discussion on physical model validation.

Three (3) Subgroups were created to structure the activities of the Working Group:

- **Subgroup 1** on 'Plug Nozzles', headed by Prof. M. Onofri;
- **Subgroup 2** on 'Scram Propulsion', headed by Prof C. Bruno; and
- **Subgroup 3** on 'CFD Validation for Hypersonic Flight', headed by Prof. D. Knight.

Subgroup 1 dealt with reviewing fundamental aspects on plug nozzles, analysing altitude adaptation aspects and wake closure phenomena, studying influence of external flow on thrust, and addressing design methods including thrust vector control and flight extrapolation.

Three (3) test cases for CFD validation were identified:

- Axisymmetric full length annular plug;
- A truncated plug nozzle; and
- 3-D linear clustered plug nozzle.

Computational contributors from Europe and US participated in detailed validation activities, addressed shortcomings, and conclusions were drawn on the applicability of CFD tools for design and verification.

Subgroup 2 addressed the physical modelling aspects associated with scram combustion; a review was given on fuels, turbulence mixing, ignition and flame holding prediction capabilities as well as vitiation. In particular, the Subgroup discussed the approach to be used in the design process: how to combine tests and numerical simulations to design scram engines with required margins; components modeling and testing; performance prediction; tip to tail computations etc.

Subgroup 3 screened a large number of test cases for CFD validation; selected well-defined sets of experiments, repeated in some cases older experiments with updated instrumentation, and this for six areas where CFD validation was deemed essential:

- Boundary layer instability and transition;
- Real gas flows;
- Laminar viscous inviscid interaction;
- Shock-shock interactions;
- Shock wave turbulent boundary layer interaction; and
- Base flows with and without plumes.

A very fruitful exchange of information and stimulating discussions among all members of the Working Group resulted in an **unprecedented effort** to improve the technologies for hypersonic flight. The WG felt that they employed high standard for the selection and evaluation of test cases for CFD validation.

The present WG allowed and promoted "harmonization" of otherwise dispersed activities.

Because of this important added value, the WG recommended to proceed with their activities by focussing on advances associated with "further improvements of the **aerothermodynamic capabilities for flight prediction**".

The Working Group expressed their vision, and hoped that in the future, joint "in flight research" programmes could be set up under the auspices of NATO and in collaboration with Russia.

Indeed, advances in hypersonic flight require strong collaboration on improvements of aerothermodynamic capabilities, i.e. numerical, experimental and flight test techniques.

INTRODUCTION

While problem areas still exist in Supersonic Combustion Ramjets (SCRJ), its technology is nevertheless progressing towards military application. This Final Report contains discussions and calculations relevant to the SCRJ problem areas identified at the beginning of the activities by this Subgroup. ITAR, sensitivity and proprietary issues have prevented a full analysis of certain topics: some were explored only at the qualitative level, while others should be carried out later. The military implications of SCRJ technology is such that this is to be considered unavoidable if not acceptable.

Participants in this Subgroup agreed that SCRJ technology, filled as it is with challenges, is ready to be tested for certain applications. With the understanding that Chapters 1-9 of this report are representative of only what is already available and understood in the open literature, the Conclusions and Recommendations sections at the end of each chapter indicate that (with the usual caveat from scientists) critical areas such as mixing, supersonic combustion, scaling and ground testing are approaching the maturity level enabling stepping up to flight testing of SCRJ-powered vehicles. It is important also to realize that problem areas outlined in these chapters are amenable to technological solutions either being tested now or that can be tested in the short term. This conclusion is supported by recent information from US supersonic combustion tests and by the successful Australian flight test of a scramjet engine.

The general consensus was that SCRJ engines are likely to be viable for tactical missiles, e.g., for future Air Guided Missiles and also, possibly, for reconnaissance vehicles and cruise missiles. In this context, ground testing may be very effective to reduce the uncertainties (and therefore the cost) of flight tests; this is made possible by appropriately accounting for the differences in chemistry (and thus for the effect of air vitiation) as detailed in Chapter 4.

This report identifies many key areas in need of further work. However, recent supersonic combustor experiments in the US are very encouraging in that they indicate that kerosene-based fuels pose fewer problems than anticipated in the past, thus paving the way to tactical applications. Hydrogen may remain the fuel for long range (strategic) SCRJ-powered vehicles, and (likely) that for part of trajectory of accelerators.

Experiments mentioned, and others planned or in progress in France, indicate regenerative cooling and flame anchoring is not only possible, but also feasible within the range of materials and flight conditions to be expected either now or in the near future.

Simulating SCRJ flowfields is an area of growing importance to predict the effect of new geometry or combustion strategies. While work presented in this report indicates that supersonic turbulent combustion is still poorly understood, (e.g., see Chapter 6) current Large Eddy Simulation (LES) in conjunction with appropriate Sub-Grid Scale (SGS) models is becoming increasingly useful. SGS modelling is in fact key to develop practical SCRJ combustors software. In this context, any SGS model must be capable of simulating ignition and flame anchoring, and thus must embody adequate chemical kinetics. This is especially true in the case of regeneratively-cooled SCRJ chambers, where endothermic fuels decompose into simpler hydrocarbons via complex chemistry. Perhaps even more critical is the need of software that can integrate all SCRJ functional blocks and their flowfield (“tip to tail”) to predict overall performance (thrust, fuel consumption, drag). This task was recognized as very important by this Subgroup, but could not be performed within the available time scale and resources.

This Subgroup is aware that non-NATO countries exploring SCRJ technology include China (that has explicitly classified SCRJ as a key area for government support since 1997), India (with Russian technical support in the subsonic RJ portion of the flight trajectory), Japan, and others. While detailed information is sketchy, it still hints to the possibility that work in this field may be progressing more rapidly in non-NATO countries than within NATO, with the exception of the US.

Based on this, and other, information it is therefore recommended that, to speed progress in scramjet-powered applications, work should be carried out at least in the following areas:

- Kerosene fuels reforming technology and its integration with SCRJ combustors;
- Ignition and flame anchoring at flight Mach numbers 5-6 and above;
- Fuel-air mixing and combustion (using cavities, pilot flames and wall fuel injection);
- Effects of air vitiation and scaling on ground testing, enabling extrapolation to flight; and
- Robust simulation of scramjet flowfields using Computational Fluid Dynamics.

In France, and also Italy there is strong interest in continuing or initiating ground testing of SCRJ. This Subgroup thinks that SCRJs are of more than technical importance to NATO, that they should be supported as a critical technology, and that this technology needs investing in human and financial resources to produce the results of which it is potentially capable.

CHAPTER 1: OVERVIEW OF NATO BACKGROUND ON SCRAMJET TECHNOLOGY

Phil Drummond, Marc Bouchez and Charles R. McClinton
J. Philip Drummond, D.Sc., P.E.
NASA Langley Research Center
j.p.drummond@larc.nasa.gov
Marc Bouchez
Propulsion Department
EADS - AEROSPATIALE – MATRA MISSILES
8, rue Le Brix , 18020 BOURGES CEDEX , France
marc.bouchez@missiles.aeromatra.com
Charles R. McClinton
Hyper-X Project Office at NASA Langley
c.r.mcclinton@larc.nasa.gov

1.1 INTRODUCTION

The purpose of the present overview is to summarise the current knowledge of the NATO contributors. All the topics will be addressed in this chapter, with references and some examples. This background enhances the level of knowledge of the NATO scramjet community, which will be used for writing the specific chapters of the Report. Some previous overviews have been published on scramjet technology worldwide. One of the most documented within the available overviews on scramjet technology worldwide is [D1] from Dr. Tom Curran.

NASA, DOD, the U.S. industry and global community have studied scramjet-powered hypersonic vehicles for over 40 years. Within the U.S. alone, NASA, DOD (DARPA, U.S. Navy and USAF), and industry have participated in hypersonic technology development. Over this time NASA Langley Research Center continuously studied hypersonic system design, aerothermodynamics, scramjet propulsion, propulsion-airframe integration, high temperature materials and structural architectures, and associated facilities, instrumentation and test methods. These modestly funded programs were substantially augmented during the National Aero-Space Plane (X-30) Program, which spent more than $3B between 1984 and 1995, and brought the DOD and other NASA Centers, universities and industry back into hypersonic. In addition, significant progress was achieved in all technologies required for hypersonic flight, and much of that technology was transferred into other programs, such as X-33, DC-X, X-37, X-43, etc. In addition, technology transfer impacted numerous other industries, including automotive, medical, sports and aerospace.

The future development of scramjet and hypersonic technology within the USA falls under the NASA Advanced Space Transportation Program and yet to be defined DOD interests. A complete plan will be completed in 2002. This current ASTP program is a comprehensive program designed to complete technology development and demonstration by 2018, leading to a Space Shuttle replacement vehicle IOC by 2025. This program is focused on the NASA third generation goal, which is to reduce cost and increase reliability and safety. Assuming 1000-2000 flights per year, the 3rd generation goals are $100/lb. of payload to LEO, and a 10^{-6} failure rate. These stretch goals can not be achieved using rocket propulsion. This program includes system analysis, focused and generic research and technology development, and ground and flight technology demonstrators. Systems studies are being used to evaluate numerous vehicle architectures: single stage to orbit (SSTO) and two stage to orbit (TSTO), vertical and horizontal takeoff, hydrogen, hydrocarbon and dual-fuel, as well as alternate propulsion systems. Propulsion systems generally fall into two categories: Rocket-based and turbine-based. Both approaches use dual-mode scramjets over much of the flight envelope, from Mach 3 or 4 to Mach 12 to 15. Rocket based combined cycle (RBCC) systems use rockets in the scramjet duct for low speed acceleration and/or orbital insertion. Turbine based combined cycle (TBCC) systems use turbine based engines for low speed acceleration, and some form of rocket for orbital insertion. In TSTO systems, the propulsion options double. The program is also developing the critical technologies identified by the system studies. These range from structures and materials, to tires to operational and integrated vehicle health monitoring (IVHM).

* Hypersonic Airbreathing Propulsion Branch, NASA Langley Research Center, Hampton, Virginia
† MBDA – France, Flight Dynamics and Propulsion Department, Bourges, France
‡ Hyper-X Program Office, NASA Langley Research Center, Hampton, Virginia

The French national Research and Technology Program for Advanced Hypersonic Propulsion (PREPHA) ended in 1999. It aimed at acquiring a first know-how for the hydrogen-fueled scramjet, which could be combined with other airbreathing modes (particularly ramjet) and rocket mode for powering future reusable space launchers. It gave the opportunity to acquire a first know-how in scramjet and dual-mode ramjet components design (inlet, combustor, injection struts and nozzle) and hypersonic airbreathing vehicle system studies (design and performance evaluation for space launchers, missiles and experimental flight vehicles) [A1]. The French Aeronautics and Space Research Center (ONERA) and EADS Aerospatiale Matra Missiles (now in the new MBD.A Missiles Systems European group and its "MBDA-F" French subsidiary) have been major contributors to the PREPHA Program.

In France, after the end of the National PREPHA program, MBDA-F and ONERA have taken the initiative in starting further works to preserve the intellectual and material investment and to improve mastery of hypersonic airbreathing propulsion. Since 1997, ONERA and DLR are leading the in house research program JAPHAR (Joint Airbreathing Propulsion for Hypersonic Application Research) [A5]. This program aims at studying a hydrogen fueled dual mode ramjet working in the Mach number range from 4 to 8. It also aims at defining a methodology for ground and flight performance demonstration. That includes the definition of a possible experimental vehicle able to autonomously fly in the given Mach number range [A6]. MBDA-F leads a cooperation with Moscow Aviation Institute (MAI) to develop a dual-mode dual fuel ramjet, operating from Mach 3 to Mach 12 with a variable geometry. MBDA-F and EADS-Launch Vehicles (EADS-LV) are also developing an innovative technology for fuel-cooled composite material structures. Under the aegis of the French MoD, MBDA-F and ONERA are leading the PROMETHEE R&D program to improve knowledge on hydrocarbon fueled dual mode ramjet for missile application. Its aims at developing a propulsion system able to power a missile from Mach 2 to Mach 8. First phase is expected to end in 2002 [A16].

Previously, in Germany, some cooperative work has been performed with Russia on hypersonic flight testing issues and on scramjet flowpath technology at TsAGI (Jukowsky, Russia).

Contribution to the education of students is also one of the important elements of this scramjet technology effort. Students, young scientists or technicians are often enthusiastic to be associated, even for only several months on scramjet technology development efforts [B10], [B18].

1.2 SYSTEM STUDIES

1.2.1 REUSABLE SPACE LAUNCHERS

The USA focused on SSTO technology during the NASP era. The program failed because of naively optimistic projected costs and schedules. After NASP (1984-1994) NASA initiated several hypersonic technology programs: the LaRC/DFRC Hypersonic X-Plane Program, Hyper-X, in 1996; the GRC Trailblazer in 1997; and the MSFC Advanced Reusable Transportation ART technology program in 1997, Bantam in 1997, Spaceliner-D and finally, just "Spaceliner" in 1999. Of these programs only Hyper-X and ART build on the technology gains of the X-30 program. The Hyper-X Program focused on extending scramjet powered vehicle technology to flight, elevating as much technology as possible, and validating, in flight, the design systems, computational fluid dynamics (CFD), analytical and experimental methods required for this complex multi-disciplinary problem. The smaller ART program focused on rocket based combined cycle (RBCC—i.e. single duct air augmented ramjet/dual mode scramjet)) wind tunnel testing of alternate airframe integrated scramjet flowpath concepts.

Currently, all US space access focused hypersonics propulsion is incorporated under the NASA Marshall Space Flight Center (MSFC) led "third-generation" (Venture-star replacement), "Spaceliner" Program. The third generation goal is to reduce cost and increase reliability and safety. Assuming 1000-2000 flights per year, the 3rd generation goals are $100/lb. of payload to LEO, and 10-6 failure rate. These stretch goals can not be achieved using rocket propulsion. This program includes systems analysis, focused and generic research and technology development, and ground and flight technology demonstrators. Systems study being used to evaluate numerous vehicle architectures including permutations of single stage to orbit (SSTO) or two stage to orbit (TSTO), vertical or horizontal takeoff, hydrogen, hydrocarbon or dual-fuel, as well as various propulsion systems. Propulsion systems studied generally fall into two categories: Rocket-based or turbine-based. Both approaches use dual-mode scramjets over much of the flight envelope, from Mach 3 or 4 to Mach 12 to 15. Rocket based combined cycle (RBCC) systems use rockets in the scramjet duct for low speed acceleration and/or orbital insertion. Turbine based combined cycle (TBCC) systems use turbine based engines for low speed acceleration, and some form of rocket for orbital insertion. In TSTO systems, the propulsion options double. Current high fidelity analysis is limited to NASP derived air breathing launch vehicles. These single stage vehicles close at near one million pounds take off gross weight for 50,000 pounds to low earth orbit. Low speed engine selection and uncertainty in combined/combination engine performance and weight can change vehicle weight by 40

percent, as shown in figure 1. Two stage systems tend to fall within this same band, but have an uncertainty in closed weight.

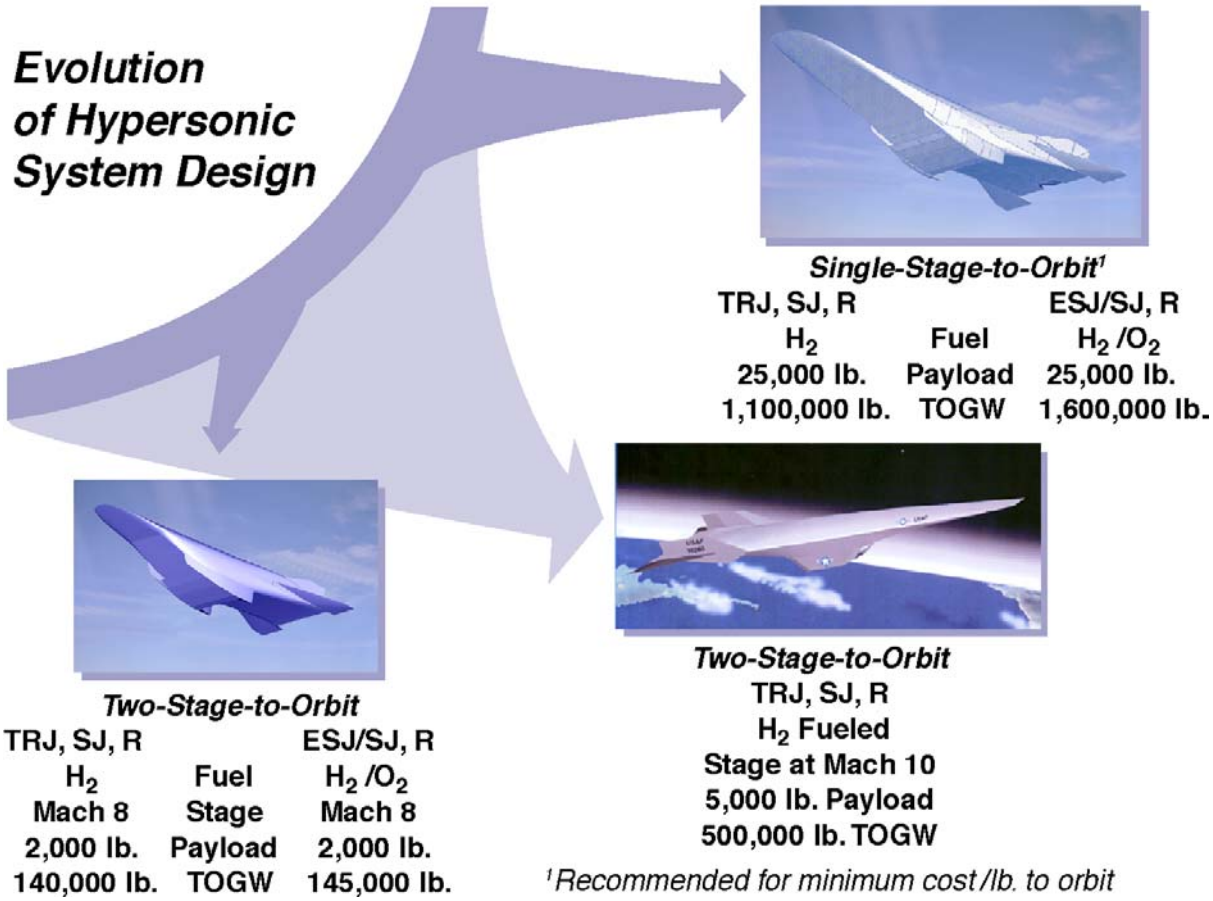

Figure 1: Vision Vehicle (Space Access).

During the 1980s, several national programs were undertaken around the world to study combined propulsion for space launchers and to acquire needed technologies. Some system studies were performed in France to evaluate combined propulsion interest for space launchers. These studies, considering TSTO and SSTO vehicles, concluded that combined propulsion didn't present any advantage if the airbreathing phase is limited to subsonic combustion (maximum flight Mach number 6/6.5). Then it was decided to continue studies by exploring the possibility to use supersonic combustion. In this way, the French national Research and Technology Program for Advanced Hypersonic Propulsion (PREPHA) started in 1992 under the aegis of Ministry of Defense, Ministry of Research and Technology, National Space Agency ([C7]).

Four concepts of combined propulsion systems, using slush hydrogen as fuel, have been considered at the beginning of the PREPHA: two twin-duct concepts which are turborocket-scramjet-rocket and turbojet-dual mode ramjet-rocket; two one-duct concepts which are rocket-dual mode ramjet-rocket and ejector dual mode ramjet-rocket ([C17] and [C18]). After integration of these propulsion systems on the generic vehicle, trajectories simulation allowed selection of the rocket—dual mode ramjet—rocket concept (in separate ducts) and to improve, step by step, airframe and propulsion system design [C19]. Finally, these studies concluded that there was the feasibility of a vehicle able to fulfill the mission with a total take-off mass of 487.3 metric tons without payload or 540 t with a payload of 5 metric tons [C20].

Figure 2: PREPHA vehicle (550 metric tons Take-off weight)

In addition, some ESA (European Space Agencies) programs have been conducted in the 90's utilizing SSTO with scramjet and other cycles [B12]. In two of these programs (FESTIP 1 and 2), Belgium has realized studies on pre-design and trajectory calculations for SSTO and TSTO using scramjets, high speed ramjets, RBCC and other cycles [E1].

In the scope of the WRR co-operation between MBDA-F and MAI, several topics have been addressed, including system studies (for the air-breathing engine point of view) and technological work [B3, B9, B24, B25, B26]. The results obtained during the WRR Prototype development phase in term of propulsive performance and cooling system technology have been used to determine how the fully variable geometry of the two-mode ramjet could really impact on the global performance of a SSTO vehicle [A12]. A WRR-type engine has been defined and integrated to the generic SSTO vehicle designed during the PREPHA Program. The accessible performance of this vehicle have been compared with those obtained with the same vehicle powered by the final version of the fixed geometry two-mode ramjet designed during the PREPHA Program. This study indicated a real interest of variable geometry for the combustor: the increase of performance seems much higher than the increase of weight (actuators…). In parallel with the propulsion-oriented WRR space launcher system studies by MBDA-F and MAI , ONERA is still continuing some system studies to assess the interest of a possible use of a high-speed airbreathing system for space launcher application [A20].

1.2.2 MISSILES

It is generally assumed that the first application of high-speed airbreathing propulsion will be missiles or the strategic UAV ([A13] and [A14]). In France, after several in-house studies [D3], a generic missile is studied within the PROMETHEE program, in order to more deeply study the military application and to develop some needed specific technologies ([A15] and [A16]). The technical program is oriented by the conceptual design of a generic air-to-ground missile. A variable geometry engine concept has been selected. Its preliminary design study is under enhancement. This design study allows performances to be determined and to mass budget characteristics to numerical flight simulation codes in order to estimate the achievable global performance of the missile. The generic mission which has been considered is the air-launch air to ground concept, but other may be derived.

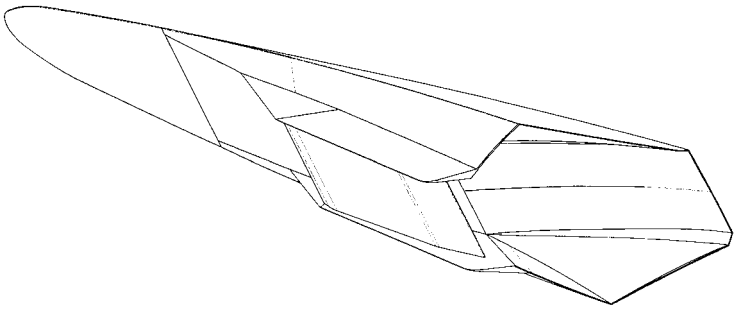

Figure 3: Artist view of PROMETHEE missile.

In the US, a lifting body scramjet missile concept was developed under the DARPA ARRMD. Demonstration of the hydrocarbon-fueled engine is currently underway in ground facilities and it will be flown on the X-43C. Within the DOD several military hypersonic programs emerged in the USA after NASP. These programs include the USAF AFRL Hypersonic Technology (HyTech) program [D7], the Defense Advanced Research Projects Agency (DARPA) Affordable Rapid Response Missile Demonstrator (ARRMD) Program, the USN Rapid Response Missile Program and the Army Scramjet Technology Development Program.

Figure 4: ARRMD Missile

1.2.3 AIRCRAFT

In France, only very preliminary studies have been performed with scramjet-powered aircraft (i.e., the Mach 5 civil transport or higher Mach number commercial or military aircraft, mainly from the propulsion point of view.) No application of hypersonic civilian transports is currently being considered in the US. In addition to the missiles programs, the USAF Aeronautical Systems Center, in collaboration with the Air Combat Command, has conducted a Future Strike study, which included hypersonic aircraft. With this renewed interest in hypersonic vehicles, requirements are being discussed which can only be met with hypersonic systems. These include the USAF CONUS-based Expeditionary Aerospace Force concepts, and “control of the complete aerospace continuum” [U15].

Some potential hypersonic aircraft concepts and capabilities are presented in figure 5.

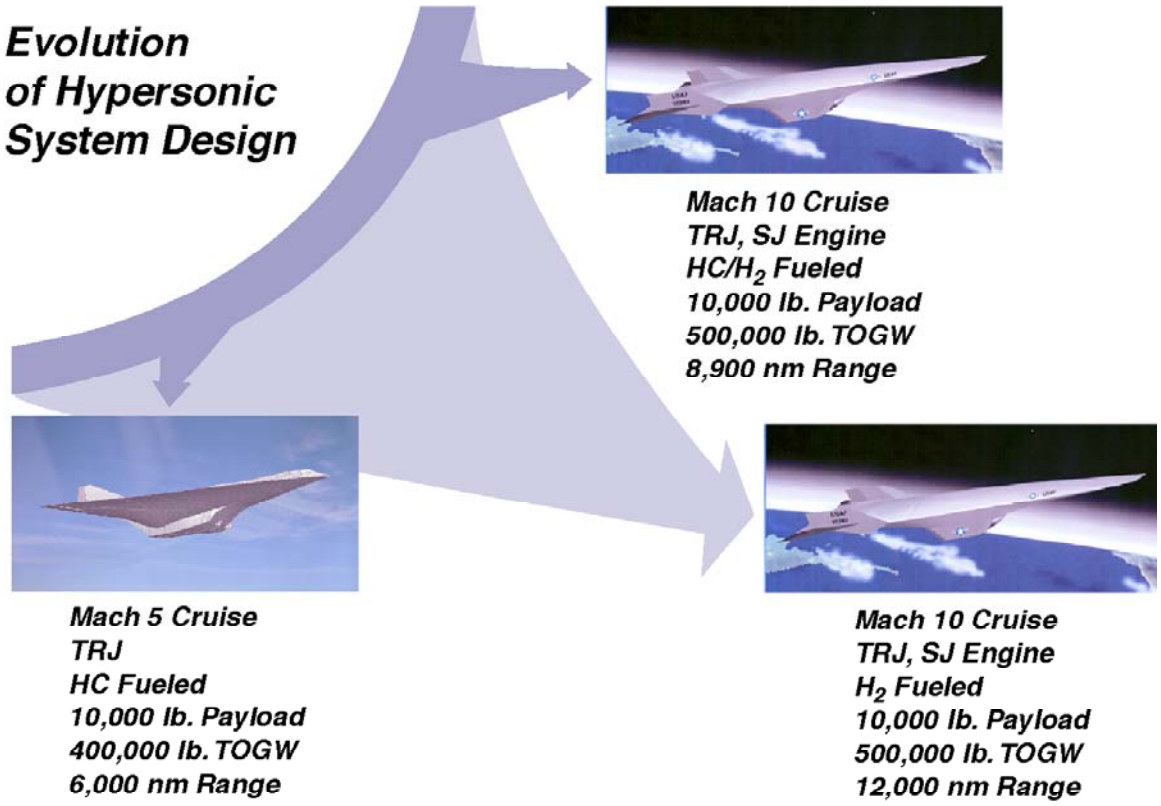

Figure 5: Hypersonic aircraft concepts

1.3 DESIGN TOOLS

1.3.1 TEST FACILITIES

It is currently necessary to simulate the flight operation of a scramjet engine in ground based facilities. The NASA Langley Research Center Scramjet Test Complex is made up of five facilities, the Direct Connect Supersonic Combustion Test Facility, the Combustion Heated Scramjet Test Facility, the Arc-Heated Scramjet Test Facility, the 8-ft. High Temperature Tunnel, and the Hypersonic Pulse Facility. The Langley Direct-Connect Supersonic Combustion Test Facility (DCSCTF) is used to test ramjet and scramjet combustor models in flows with stagnation enthalpies duplicating that of flight at Mach numbers between 4 and 7.5. Results of the tests are typically used to assess the mixing, ignition, flameholding, and combustion characteristics of the combustor models. The facility operates "directly connected" to the combustor model with the entire facility test gas mass flow passing through the model. The combustor model may exhaust freely (into the test cell), or directly (connected) to an air-ejector or to a 70-ft diameter vacuum sphere. Nozzle geometric simulations can also be added at the exit of the combustor models.

The Langley Combustion Heated Scramjet Facility (CHSTF) has historically been used to test complete (inlet, combustor, and partial nozzle) subscale scramjet component integration models in flows with stagnation enthalpies duplicating that of flight at Mach numbers from 3.5 to 6. The CHSTF uses a hydrogen, air, and oxygen heater to obtain the flight stagnation enthalpy required for engine testing. Oxygen is replenished in the heater to obtain a test gas with the oxygen mole fraction of air (0.2095). The facility may be operated with either a Mach 3.5 or 4.7 nozzle. Either gaseous hydrogen or gaseous hydrocarbon (both at ambient temperature) may be used as the primary fuel in the scramjet engines tested in the CHSTF. A 20-percent silane, 80-percent hydrogen mixture (by volume) is available for use in the scramjet model as an igniter/pilot gas to aid in the combustion of the primary fuel.

The Langley Arc-Heated Scramjet Test Facility (AHSTF) is used for tests of component integration models of airframe integrated scramjet engines at conditions experienced at flight Mach numbers of 4.7 to 8. Results are used to assess the performance of the scramjet, to optimize the design of the components, and to optimize fueling schemes. Typical models include the inlet, isolator, combustor, and a significant portion of the nozzle and are hydrogen and silane fueled. The flow at the exit of the facility nozzle simulates the flow entering

a scramjet engine module in flight, which has been processed by the forebody shock of the vehicle. The total enthalpy of the flight condition is achieved by electrically heating the air with a Linde arc heater. Run times normally range from 30 sec at flight Mach number of 8 simulated conditions to 60 sec at flight Mach number of 4.7 simulated conditions.

The Langley 8-Foot High Temperature Tunnel (8-Ft HTT) is a combustion-heated hypersonic blowdown-to-vacuum wind tunnel that provides duplication of total flight enthalpy for Mach numbers of 4, 5, and 7 through a range of altitude from 50,000 to 120,000 ft. The open-jet test section is 8 ft in diameter and 12-ft long. The test section will accommodate very large models, air-breathing hypersonic propulsion systems, and structural and thermal protection system (TPS) components. Stable wind tunnel test conditions can be provided up to about 60 seconds. Additional simulation capabilities are provided by a radiant heater system that can be used to simulate ascent or entry heating profiles. The high-energy test medium is the combustion products of air and methane that are burned in a pressurized combustion chamber. Oxygen is added for air-breathing propulsion tests. Hypersonic air-breathing propulsion system tests are performed with the propulsion test article (e.g. NASP concept demonstration engine, Hyper-X flight vehicle) attached to a model support pedestal mounted on an external force measurement balance. Propellant fuel (e.g. gaseous hydrogen, liquid hydrocarbon) and purge gases are supplied to the test article by the facility.

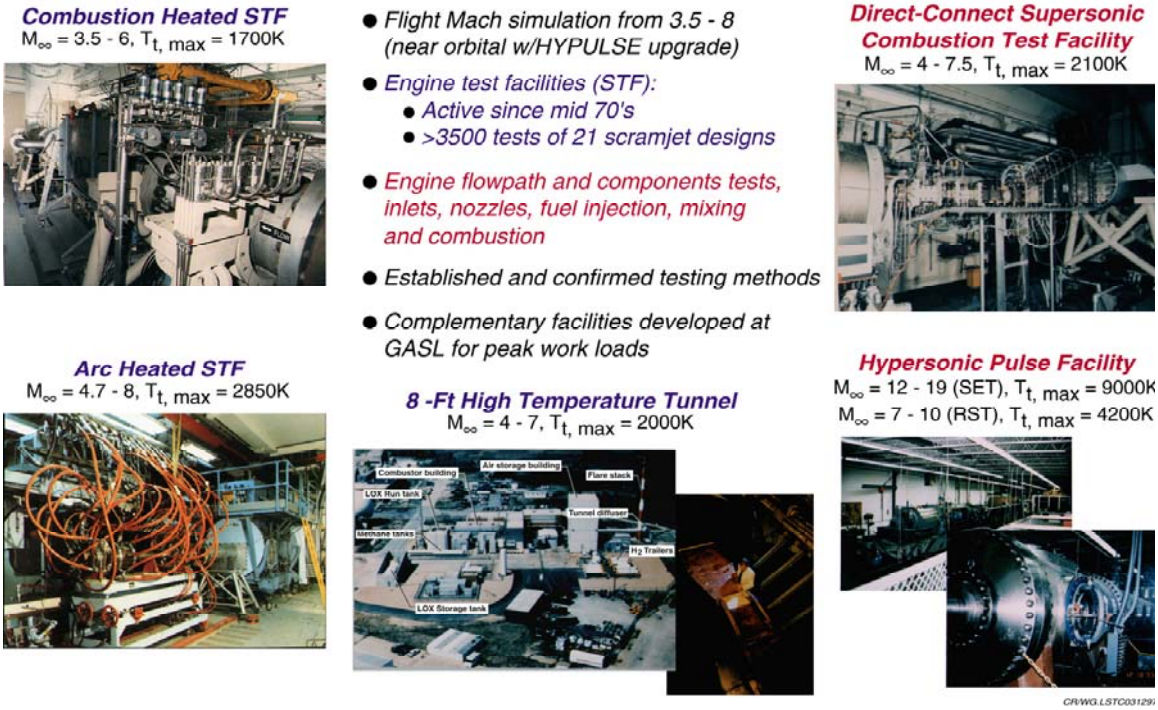

Figure 6: NASA Langley Scramjet Test Complex

The Hypersonic Pulse Facility (HYPULSE) is a dual-mode shock tunnel facility. It can operate in both a reflected shock tunnel mode and a shock-expansion mode. A 7 ft diameter test section is available for aerothermodynamic and propulsion testing for models up to 15 feet long. HYPULSE is operated as a Ludweig tube to reproduce flight conditions up to Mach 2, as a reflected shock tunnel for flight conditions from Mach 4 to Mach 12, and as a shock expansion tube for flight conditions from Mach 12 to Mach 25. When operated in the tunnel mode, HYPULSE expands the test gas to Mach 6.5 using a 26" diameter axisymmetric nozzle. Optical access is provided for schlieren images and for laser diagnostics, and instrumentation is available for collecting measurements from pressure, heat transfer, and temperature transducers.

The Arnold Engineering and Development Center (AEDC) facilities in Tennessee are used for endurance tests of high-speed engines or currently, engines at moderate Mach number [D5]. The NASA Hypersonic Test Facility at Glenn Research Center is used to do free jet tests up to Mach 7 conditions with no

water or CO2 in the incoming air [D6]. A GASL test facility is used to simulate trajectory variations, thanks to a high area-ratio axis-movable nozzle.

Thanks to the PREPHA program, ONERA and MBDA-F extended the simulation capabilities of the French ramjet test facilities up to Mach 7.5 flight conditions and 100 kg/s of air ([A2] and [A3]). Two facilities have been used extensively: the ATD 5 test cell of ONERA Palaiseau and the MBDA-F hypersonic test rig of Bourges-Subdray ramjet test facility. The first facility is limited in size (4 kg/s and 4 MPa with 2400 K of stagnation conditions, 10 seconds of test) but able to reproduce Mach 7.5 conditions. The second facility (Subdray) is currently limited to Mach 6.5 conditions, but with higher mass flow (up to 100 kg/s at 8 MPa, two minutes test duration). These are water-vitiated facilities.

New optical diagnostic methods are under development, which will allow exploration of the flow into the combustion chamber in an industrial facility [A22], [D4]. Up to now the laser-induced optical methods are mostly used in laboratories or more academic supersonic combustion configurations [A16] [A21]. Using available pulsed high enthalpy tunnels to reach higher stagnation test conditions is also under consideration in Europe [D11], [D15].

1.3.2 SYSTEM ANALYSIS, CFD AND MODELING

The key to any hypersonic vehicle development or technology program is a credible preliminary system analysis to identify the technical requirements and guide technology development. The complexity of the hypersonic airbreathing system and the small thrust margin dictate that a thorough system analysis be performed before any focused technology development is started. System analysis is executed on four levels. The lowest level, designated “0,” does not require a physical geometry. The level zero analysis utilizes ideal engine cycle performance, historical L/D and Cd values for aerodynamic performance, design tables (or weight fractions) for structure and components weight, “rocket equation” for flight trajectory, and estimates for packaging. This analysis does not require a specified vehicle, engine flowpath or systems definition. All higher levels of analysis require a vehicle, engine flowpath shape and operating modes, system definition, etc.

The next level of system analysis, referred to herein as Level 1, utilizes uncertified cycle performance and/or CFD, impact theory, unit or uncertified finite element model (FEM) weights, single equation packaging relations, and energy state vehicle performance. This level of analysis does not capture operability limits, and thus has large uncertainties.

Level 2 analysis utilizes “certified,” methods; i.e., the user has sufficient relevant experience. This level uses the same methods for propulsion, aerodynamics, structure and weights (but certified), trimmed 3-DOF (degree of freedom) vehicle performance analysis and multiple equation, linear or non-linear packaging relations. Certification is only achieved by demonstration that the methods used work on the class of problems simulated (this relates to the method, as well as the operator applying that method). For example, at level 2 analytical models utilize corrections for known errors, such as inlet mass spillage, relevant empirical fuel mixing models [U1], shear and heat flux models [U2], etc. This empirical approach is based on experimental (wind tunnel tests, structural component tests, etc) data. Higher level methods (CFD, FEM) are used to refine the vehicle and propulsion system closure.

The highest design level (level 3) is achieved only by having a significantly large fraction of the actual vehicle manufactured and tested. Wind tunnel and other ground testing provide less verification than flight tests. Although numerous components have been built and ground tested, flight data is required for the highest level of design. This has not yet been done for a hypersonic airbreathing vehicle (see §1.6 below). Whatever the level of system analysis, closure is achieved by sizing the vehicle so that the propellant fraction required (for the mission) is equal to the propellant fraction available (packaged within the sized vehicle). However, the reported closure weight is only as good as the lowest level of analysis used in the “closure.”

Computational fluid dynamics (CFD) has multiple roles in the design of a hypersonic propulsion system. It primarily serves as an engineering tool for detailed design and analysis [U3]. In addition, results from CFD analyses provide input data for cycle decks and performance codes. Finally, CFD has several applications in engine test programs to develop an engine concept. CFD is first used to guide the test setup and to determine the proper location for placement of instrumentation in the engine. It has also proven to be an effective tool for determining the effects of a facility on testing; for example, the effects of contaminants in a combustion heated facility on an engine combustor test. During and following a test, CFD is useful to predict flowfield measurements as a complement to measured data. Various computational strategies are utilized in inlet, combustor, and nozzle of a scramjet engine.

Computational analyses of inlets typically employ codes that solve the Euler equations, or Euler codes iterated with the boundary layer equations for viscous effects, for initial analyses. More detailed calculations

utilize either the parabolized Navier-Stokes equations, or the full Navier-Stokes equations if significant flow separation must be considered. All of the calculations typically solve the steady-state equations so that simulations can be completed in reasonable times. Turbulence is modeled using either algebraic or two-equation turbulence models with empirical compressibility corrections and wall functions. Transition models are not currently being employed. Thermodynamic properties are generally determined by assuming that the inlet flow behaves as a perfect gas or equilibrium air. Calculations are conducted on fixed grids of 100,000 to 3,000,000 points in multizone domains. A limited degree of dynamic grid adaptation is employed when necessary. There is a serious need for the development of advanced transition and turbulence models. This is likely the most limiting area for accurate modeling of inlet flowfields. Promising work is now underway to develop new algebraic Reynolds stress turbulence models with governing equations that can be efficiently solved [U4], [U5]. For non-equilibrium flows, the differential Reynolds stress equations must be solved, however, and further work is necessary for this to be done more efficiently. Advances in large eddy simulation, with the development of subgrid scale models appropriate to high-speed compressible flow, may also allow this technique to be applied to inlet flows in the future [U6]. Finally, work is needed to develop improved transition models for inlet flows, particularly with flows exhibiting adverse pressure gradients. Some models are quite operational to predict the transition beginning zone, but generally not its end.

Computations of combustor flowfields typically employ codes that solve either the parabolized or full Navier-Stokes equations, depending upon the region of the combustor being modeled and the degree of flow separation and adverse pressure gradient being encountered. Steady-state methods are normally used with limited unsteady analyses for mixing studies or the analysis of combustion instabilities. Turbulence is again modeled using algebraic or two-equation models with empirical compressibility corrections and wall functions. There is a limited use of models to account for turbulence-chemistry interactions based on probability density functions. Thermodynamic properties are determined utilizing perfect gas or, in some cases, real gas models. Chemical reaction is modeled with reduced reaction set, finite rate models. For the hydrogen-air reactions occurring in a hydrogen-fueled scramjet, a typical reaction mechanism includes nine chemical species and eighteen chemical reactions, although other mechanisms are employed as the case dictates [U7]. Hydrocarbon-fueled scramjet concepts are modeled with much more complex mechanisms that must be further reduced to allow practical computations. Calculations in each case are typically conducted on fixed structured grids of 200,000 to 8,500,000 points in multizone domains. Typical run times on a Cray C-90 computer range from 10 to over 300 hours. Many of the future technology needs for combustor simulations follow from the needs for inlets described earlier, but several of the additional requirements will be more difficult to achieve. For combustor modeling, a factor of ten improvement in the efficiency of steady-state and temporal Navier-Stokes codes will be needed to carry out the required calculations with the necessary accuracy and design turn-around time. Multigrid methods again offer promise for significantly enhancing convergence rates, but the application of multigrid methods to reacting flows also results in additional challenges for success with the method [U8]. Current research to apply multigrid methods to high-speed reacting flows has resulted in a significant improvement in convergence rates over single grid methods. Dynamic grid adaptation will become even more important for capturing the complex flow structure in combustors, in particular the shock-expansion and vortical structure in the flow. Proper resolution of vortical flow requires very high resolution to conserve angular momentum. Again, there is a serious need for improved turbulence modeling in high speed reacting flows, both to model the turbulence field and to properly couple the effects of turbulence on chemical reaction and reaction on turbulence. Promising work is again taking place in this area using several approaches [D8]. Techniques using velocity-composition probability density functions have been successfully applied to incompressible reacting flows, and this work is now being extended [U9] to model compressible reacting flows. Work is also underway to apply Large Eddy Simulation (LES) techniques to compressible reacting flows. Subgrid scale models for the LES of these flows are currently being developed. Recent work utilizing a filtered mass density function for the LES of turbulent reacting flows appears particularly promising for the future [U6]. Finally, further work is needed to simplify the modeling of chemical reaction in combustor flowfields. Methods for systematically reducing the number of reactions in a full reaction mechanism are required to reduce the computational work [U10].

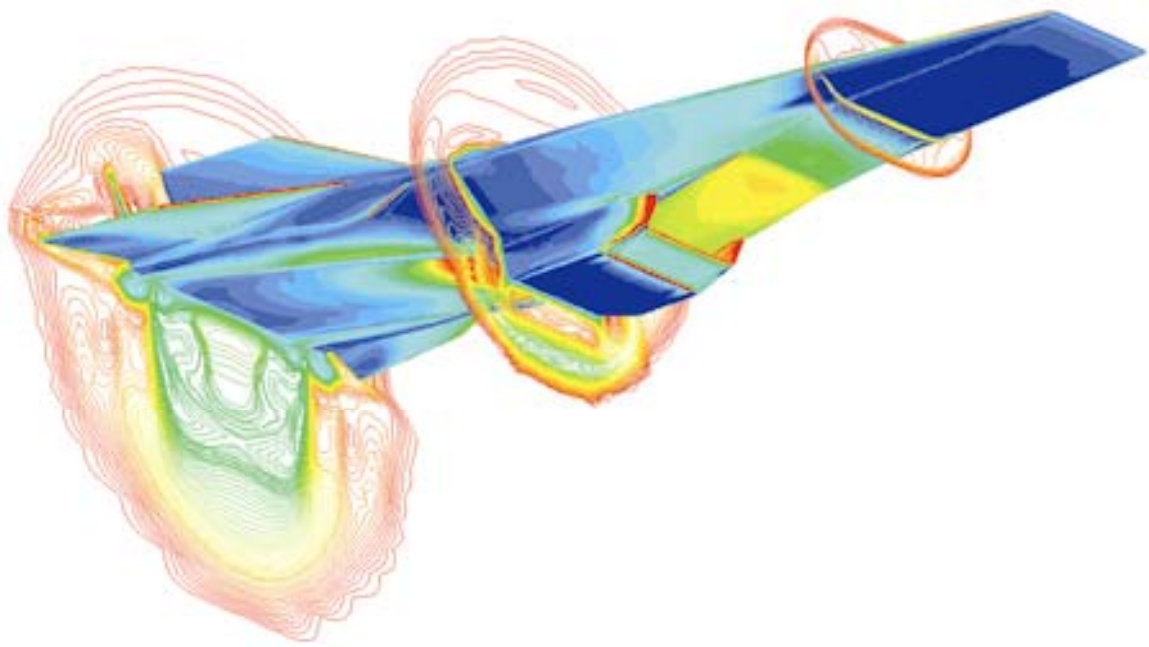

Figure 7: Hyper-X nose-to-tail and generic combustor computational solution

Computations of nozzle flowfields are usually conducted with Euler codes, or Euler codes iterated with boundary layer calculations for initial engineering design studies; and with either parabolized or full Navier-Stokes codes for more detailed studies. Steady-state methods are normally employed. Turbulence is modeled by algebraic or two-equation models with empirical compressibility corrections and wall functions. Perfect gas or, when necessary, real gas models are used to determine thermodynamic properties. Chemical reaction is modeled with reduced kinetics models as utilized in the upstream combustor flow. Finite rate analyses are required throughout the nozzle to assess the continuing degree of reaction, and to determine the extent of recombination reactions that add to the available thrust. Calculations for complete nozzles are typically carried out on structured grids of 100,000 to 500,000 nodes grouped in multizone domains. Future technology needs for nozzle simulations, even though less demanding, follow very similar lines to the requirements for combustor simulations. Dynamic grid adaptation will be useful for capturing shock structure and resolving possible wall separation due to shock-boundary layer interactions. There is a further need for improved turbulence models, particularly for capturing the nozzle wall boundary layer relaminarization created by the favorable pressure gradient. Algebraic Reynolds stress turbulence models offer significant promise for describing these flowfields [U4], [U5]. The reduced kinetics models currently being applied to nozzle flows appear to be reasonably accurate, although some further work to improve the description of recombination may be warranted. In addition, methods of accurately predicting the combustion process and the recombination process with a small reaction set will expedite solution times.

In Europe CFD is also a big concern for high-speed propulsion development. In this view, a research program is in progress at ONERA and with MBDA-F and several research laboratories to improve the accuracy of physical models thanks to a very detailed basic test. Integration of the improved models into the code and the global validation are led together by ONERA and AMM. This effort is focused on the MSD code, initially developed by ONERA to simulate internal aerodynamic flows, which has been upgraded in cooperation between ONERA and MBDA-F to perform subsonic and supersonic reactive flow simulations. It solves the unsteady, 3D, averaged Navier-Stokes equations by a finite volume algorithm on multi-domain structured curvilinear grids [C2]. It includes multi-species capability and takes into account the variations of gases' thermodynamic properties with the temperature. The MSD code has been used in France by industrial or research labs, for basic configurations up to actual combustors such as CHAMOIS scramjet. It is able to compute the heat release, to predict the ignition process (with hydrogen as fuel), and to roughly represent the liquid injection and associated droplets in turbulent 3D flow [D8], [D2], [C11], [C13].

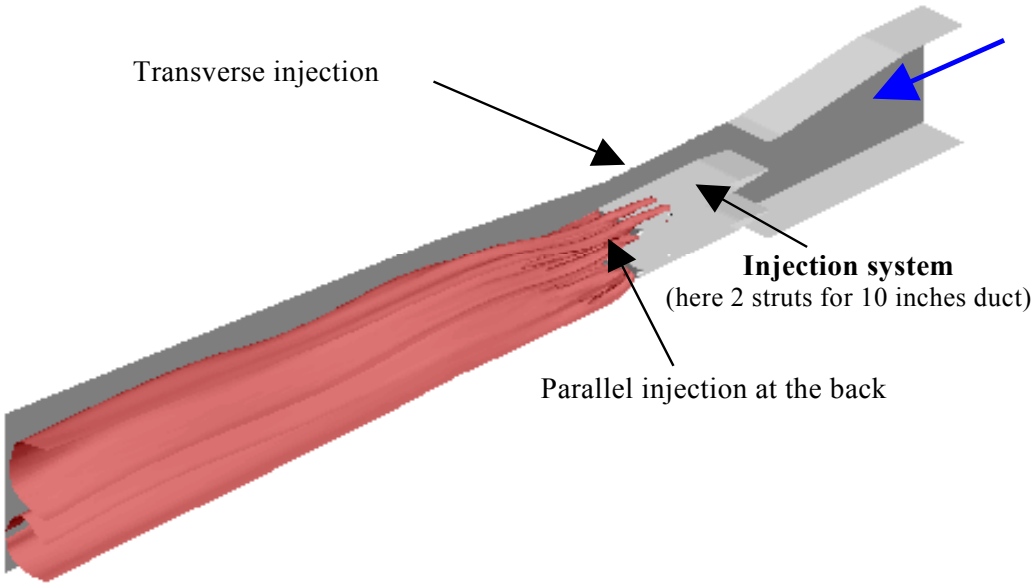

Figure 8: CFD analysis of CHAMOIS scramjet combustor

In France, since 1993, CFD analysis has been systematically associated with test results. The MSD code and associated models have been demonstrating since 1994 the capacity of reproducing qualitatively the thermal blockage phenomenon due to excessive heat release resulting from insufficiently distributed heat release. But they still have difficulties:

- To predict on a sufficiently extended range the hydrocarbon/air kinetic effect (ignition, …)
- To predict the facility effect in case of water or CO2 vitiation
- To quantitatively predict the thermal blockage ER of a given scramjet combustor
- To quickly perform accurate 3D nose-to-tail flow computations.
- To give quantitative information on hot spots and local heat transfer locations
- To compute a real size, actual, regeneratively cooled scramjet combustor, in case of hydrocarbon fuel (catalytic or thermal decomposition, …) and/or composite materials (non-isotropic and porous).

Two test facilities are used in the JAPHAR program for checking the diffusion/mixing/combustion process with all available optical diagnostic systems: the M11 test bench of DLR at Lampoldshausen (test section: 40x50mm², Mach 2 nozzle) and the LAERTE test bench, developed during the PREPHA Program (test section 45x45mm², Mach 2 nozzle). The database obtained is used to validate the physical models, issued from PREPHA program and which have been implemented in the MSD code and used for scramjet design and test analysis.
Several LES or DNS codes and basic computations have been performed in France (supersonic mixing or reactive layer, interaction with an incoming shock, turbulence enhancement, …). But, up to now, the results have not been directly used or applied to the validation of CFD modeling.

Because of the time needed to improve the CFD tools and because of the speed of computer capabilities enhancement, it seems that the main effort has to be in modeling (turbulence, combustion, boundary layer transition and separation, coupling, …).

1.4 SCRAMJET FLOWPATH

1.4.1 FOREBODY AND INLET

During the PREPHA program, a generic forebody was tested in the ONERA S4MA wind tunnel with wall pressure and thermal flux measurements, utilization of total and static pressure rakes in the plane of the inlet entrance and infrared thermography. Some specific CFD parametric studies have been performed in addition during JAPHAR studies [A8].

Significant inlet issues for hypersonic airbreathing propulsion lie primarily in the areas of configuration and inlet unstart. The design of 2-D, axisymetric, and 3-D inlets for a multitude of applications from auxiliary systems to primary propulsion systems (turbojet, ramjet, scramjet) can be accomplished. Usually these designs accept some pre-idea of the capture shape and overall requirements (mass flow, contraction ratio, pressure rise, total pressure recovery, etc). Computer codes are sometimes used to generate the grids for complex three-dimensional shapes, although 2-D and sidewall compression configurations do not require this step. Shock diagrams are laid out, followed by boundary layer thickness corrections and then applications of variable geometry to meet the Mach number range.

After completing the preliminary design, the inlet is evaluated experimentally. Full Navier-Stokes computer codes are then used, first to be validated by comparison with the experimental data and then to evaluate inlet performance and other parameters that are not easily obtained by the experimental program. Often models are not tested (or cannot be) over the Mach number range, and data are extrapolated with the aid of analytical tools. Scale is also extrapolated as small models are expanded to flight vehicles.

Knowledge of inlet starting is important for all inlets, but is especially valuable for fixed geometry designs. Usually the surest way of obtaining inlet-starting information is through an experimental program. Because inlet contraction ratios are usually increased to the limit to obtain maximum performance, the “startability” of an inlet is typically very hard to predict with accuracy. This is understandable considering the possibility of having two or more real experimental flow solutions. Small variations in the tunnel flow, incoming boundary layer characteristics, and even model wall temperature can affect starting. Inlets can also pulse-start in the wind tunnel, and this must be compensated by providing a method of unstarting and then restarting the inlet during test. Small, relatively inexpensive models are usually used to get this information, but extrapolating the data to larger models and to flight scale is not assuredly accurate. Larger inlet models may be found to start easier in a large test facility, but an even larger flight article may not start again if it has to swallow a thick vehicle boundary layer that was not be simulated in the wind tunnel test.

PREPHA considered a fixed combustor geometry to limit the technological difficulties. Then, a propulsive stream tube geometry was adapted thanks to a variable capture area inlet which gave as much as possible an adapted geometrical contraction ratio variation as a function of the Mach number. This kind of inlet has been studied in France for several years [C8]. The basic concept [C9] has been adapted to the needs and constraints of the SSTO generic vehicle. A modular model was tested at Mach 5 and 7 in the ONERA R2Ch wind tunnel with a particular device helping the inlet start. This allowed a geometrical contraction ratio superior to 4 in spite of high deviation angles limiting the length, and then the mass, of an operational inlet. A new model definition has been realised for a second experiment at Mach 2 to 5.5 (ONERA S3MA wind-tunnel) aiming at defining maximum contraction ratio, effects of forebody boundary layer thickness, and maximum deviation angle on the compression ramps.

During the JAPHAR program, two types of 2D inlets were studied: a mixed, external/internal, compression inlet studied at DLR with testing in the H2K and TMK wind-tunnels, and an internal compression inlet, designed from the PREPHA program, tested by ONERA in the S3MA wind-tunnel from Mach 3.5 to Mach 5.5 [A8].

1.4.2 FUELS

Candidate scramjet fuels include hydrogen, hydrocarbons, pyrophorics, and exotic high-energy-density fuels. Hydrogen ignition and combustion will occur in moderately-heated air under very lean conditions, and is rapid enough that scramjet combustion is possible over a reasonable length. Furthermore, because H2 ignition and combustion can be sustained at strain rates 10 to 30 times higher than in flames using gaseous light-hydrocarbons (HCs) at typical temperatures, hydrogen is the necessary/preferred fuel for airbreathing scramjets based on reactivity alone. Also, liquid H2 is very effective for active cooling of vehicle structures, which is required at high speed. Unfortunately, liquid (or slush) H2 is difficult to store and handle on a routine basis, and it has three to four times a lower energy density than typical storable hydrocarbons.

Although HCs heated during active cooling will become more reactive, such increases are limited without significant decomposition. So-called storable endothermic fuels may be catalytically hydroformed, dehydrogenated and/or cracked in-situ, so that additional heat is absorbed and resultant fuel fragments (including H2 and CO) become more reactive. However, such heterogeneous catalytic processes are difficult to accomplish, reproduce, and control without forming significant carbon deposits on catalysts and within fuel passages and injectors. Pyrophorics (e.g. 20 mole percent silane in H2) ignite spontaneously and burn when injected into air, and thus make good ignition and piloting aids. However they are not endothermic, and they usually carry molecular weight penalties, are toxic, and produce troublesome condensed phase products (e.g. silica).

Finally, fuel chemists working over the last 40 years have devised a number of so-called exotic high-energy-density fuels (e.g. cubane, various strained-ring compounds, polymeric BxNyHz, and liquid H2 gelled with light HCs), and/or organic additives (e.g. nitrates, nitrites, nitro compounds, ethers and peroxides) with improved reactivity and energy release. Typical problems with these materials are stability, safe storage and handling under field conditions, toxicity, and increased cost; however, these problems are not necessarily insurmountable.

The use of gaseous or liquid hydrogen is currently planned in France, Germany, Italy, and the USA. In the US, the HyTech program has cracked the endothermic barrier by catalytic regenerative cooling. This allows operation to 1300F using JP7 fuel with little if any cooling. In France, for supersonic missiles without active cooling, new very high density fuels have been formulated and flight-tested. Production, ageing, storage, regulation, injection and combustion are demonstrated thanks to a specific advanced development [C4]. Some preliminary work has been done on the use of liquid hydrocarbon for regeneratively-cooled higher speed engines, within the scope of the PROMETHEE program [D10], [D11] or during PTAH-SOCAR cooled structures experimental evaluation [D12]. This work is currently under development in France.

1.4.3 COMBUSTOR

In the past, the design of a combustor flowpath utilized an experimental procedure consisting mostly of trials and errors. With direct-connect tests, a supersonic nozzle is attached to a facility heater with the nozzle exit flow conditions simulating the combustor entrance conditions for a ramjet or scramjet. A combustor duct, containing fuel injectors, is attached to the supersonic nozzle and the area variation of the combustor flow path is altered (experimentally) to achieve desired pressure and reacted fuel distributions. With freejet engine tests (or, semi-direct-connect tests), a ramjet or scramjet engine, typically with a truncated forebody and a truncated aftbody/nozzle, is placed within a facility test cabin, and tests are then conducted during which the engine geometry is varied such that the desired performance is achieved. More recently, engines (or test articles) have been constructed with high contraction ratio inlets which compress the freestream flow to higher levels than have been attempted in the past. Pre-test calculations are typically conducted where a CFD solution of the inlet yields the flow properties at the throat. A simple chemical equilibrium quasi-one-dimensional calculation is then conducted to indicate how much fuel injection and combustion could be achieved within the combustor before the flow becomes choked. These relatively simple calculations alert the researcher of any possible performance problems to be expected before construction or testing of the engine occurs.

The design of the combustor flowpath must also include choosing the location and type of fuel injectors. Various fuel injection mixing “recipes” are available to help the engineer with this task [U11, U16]. The “Langley Mixing Recipe” was developed during the early 70’s as a way to correlate fuel injection mixing efficiency with downstream distance for scramjets operating in the mid-speed range of Mach 4 to 8. More recently, computational methods have been used to study and optimize fuel injector components and to assess and optimize fuel injectors installed in the engine flowpath [U12]. Combining computational methods with earlier engineering design techniques has been found to offer the best strategy for scramjet combustor design.

Within the scope of PREPHA, an experimental combustor, named CHAMOIS, has been developed by AMM. In spite of its limited dimensions (entrance area of 212 x 212 mm2), this combustor presents as much as possible the same difficulties as a large operational combustor such as fuel injection by struts, wall/injection strut interaction, strut/strut interaction, upstream flow non uniformity (boundary layer and shock waves). One-, two- and three-dimensional numerical studies have allowed the definition of its combustor geometry. Then, several CHAMOIS test series (1994, 1995, 1996, and 1997) have been successfully performed. The tests have been done in connected pipe mode, with uniform or heterogeneous incoming airflow, in the MBDA-F Bourges-Subdray test facility under Mach 6 conditions ([C12] and [C13]). A liquid-kerosene-fueled CHAMOIS combustor has been tested in the same facility in 1997 and the flow has been computed [D2].

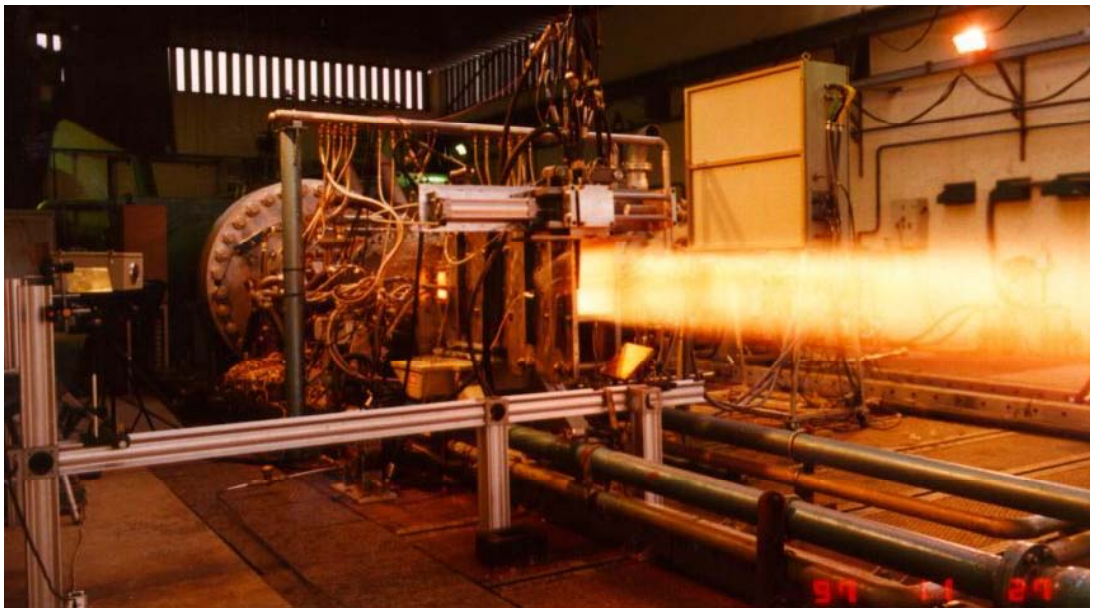

Figure 9: CHAMOIS scramjet testing in Bourges-Subdray

During PREPHA, in order to obtain some data at Mach 7.5 flight conditions and to observe the water vitiation effects, a new small combustor (100 x 100 mm² at the entrance) has been developed for a complementary test in ATD 5 facility at Mach 7.5 conditions with vitiated air and at Mach 6 conditions with more or less vitiated air thanks to the heat exchanger supplying the test facility (1000 K pure air). Moreover, this small combustor, called MONOMAT, has been used to analyse the transonic combustion mode in order to confirm the feasibility of the thermally choked dual mode ramjet [D13].

The JAPHAR dual mode ramjet powering the vehicle exceeds the envelope of the ATD5 test facility at ONERA Palaiseau Test Center, which provides Mach 7.5 flight conditions but for a limited air mass flow of 4 kg/s (water vitiated air). Considering that it is not possible to design a subscale model of the engine by following a scientific methodology, it has been decided to develop a smaller model, based on the same concept, but not homothetic, and to validate the whole design methodology on this concept. The vehicle engine and its integration to the airframe are being studied only by numerical simulation. Then, a stainless steel heat-sink model (entrance cross section of 100x100mm²) has been designed and manufactured by ONERA. It is equipped with only one strut at the upstream injection level and two struts at the downstream injection level. Today, ONERA is performing a direct-connected pipe test. The combustion chamber has been tested at Mach 4.9, 6.3 and 7.4 conditions. It has been possible to obtain subsonic combustion with a stable thermal throat at the end of the chamber. At higher Mach number, supersonic combustion was sustained.

With partial support of DGA, MBDA-F and the Moscow Aviation Institute (MAI) are developing a large scale prototype of a dual mode dual fuel ramjet with a fully variable geometry combustion chamber (Ref [A9]). This engine, called Wide Range Ramjet (WRR), has the challenging specifications, such as operation from at least Mach 3 up to Mach 12, use of movable panels during operation along the trajectory, modification of the internal geometry by a control-command computer connected with sensors on the engine in order to maximize the performance in real time, use of subsonic and then supersonic combustion, use of kerosene and then hydrogen as fuels, and a large scale engine (entrance area of 0.05m2, several meters length). This engine is under final manufacturing and is to be tested at Bourges-Subdray when the corresponding funding will be available. The cold structural framework of the WRR Prototype has been manufactured and major components have been developed and tested including kerosene with mixed bubbles of hydrogen, an ignition device, and a 3D-shape injection strut [A10]. More than half of the necessary cooled panels called Heat Protective Elements, have been realized. The control code has been written, tested and validated with simulation of prototype operation (waiting for the test), taking into account the transient actual behaviour of each actuator. The PROMETHEE combustor mock-up (212 mm width, scale 1 in height, stainless steel heat sink) has been designed at MBDA-F and will be tested in ONERA ATD test cells in 2002.

1.4.4 NOZZLE

Design of the scramjet internal nozzle and the external nozzle is performed in concert with the combustor design activity using a similar design strategy as described earlier. The nozzle flowfield is characterized by much of the flow physics of the combustor, but there are additional requirements including high velocities and high

initial temperatures, significant divergence and skin friction losses, potential relaminarization of the flow, energy-bound chemical radicals that will not relax in a finite nozzle length, and excited vibrational states. The favorable pressure gradient in the nozzle eliminates concerns with shock-boundary layer interaction and separation. Nozzle design still utilizes facility testing, but significant success had been achieved with computational modeling and design using programs ranging from Euler through full Navier-Stokes codes.

PREPHA gave France several results for nozzle and aft-body design of scramjet-powered vehicles. Basic research has led to a better knowledge of the evolution of the boundary layer along the expansion ramp and the interaction between the jet and the external boundary layer at the exit of a Single Expansion Ramp Nozzle (SERN). In the field of concepts definition, a numerical approach has been used to determine the influence of different parameters including length of the cowl, movable or fixed flap, and the expansion ramp profile [C10]. In order to allow a general evaluation of the FLU3M code in the case of the nozzle and afterbody, a generic model with an internal hydrogen burner has been tested in S4MA wind tunnel in Modane [C4].

1.4.5 INTEGRATION WITH OTHER MODES

1.4.5.1 DUAL-MODE SCRAMJET (SUBSONIC THEN SUPERSONIC COMBUSTION IN THE SAME ENGINE)

Dual-mode ramjet design operational limits are generally set by vehicle architecture (SSTO/TSTO, etc.) and engine cycle selection. For SSTO RBCC vehicles, the dual mode scramjet generally is designed to operate from Mach 3 to 12 - 15. It must include variable geometry for control of contraction ratio and combustor area-length. For an over/under TBCC, the scramjet will be expected to operate from Mach 3.5 – 4.2 to Mach 15. The higher scramjet “takeover” speed is based on high-speed turbine-based engines, which remain more efficient than scramjets to a higher Mach number, as US studies concluded. The USA’s dual-mode scramjet design is essentially that discussed in the next paragraph.

During the PREPHA program, different airbreathing propulsion systems, with a fixed geometry duct, were considered and their comparison led to selection of a dual mode ramjet concept (subsonic combustion up to Mach ~6 flight conditions then supersonic combustion) with a first quasi-constant cross section combustion chamber, used for supersonic combustion (first injection level), placed upstream of a diverging one, which is used for subsonic combustion with thermal throttling (second injection level). The fixed-geometry dual-mode scramjet of JAPHAR is based on the same concept as the double combustion chamber dual mode ramjet, selected during the PREPHA Program and also studied during the Radiance project. The WRR Prototype used a movable geometry (during the test) and a geometrical throat. Its test (planned in 2002) will give extensive time-dependant information on ram to scram transition by controlled contour modification.

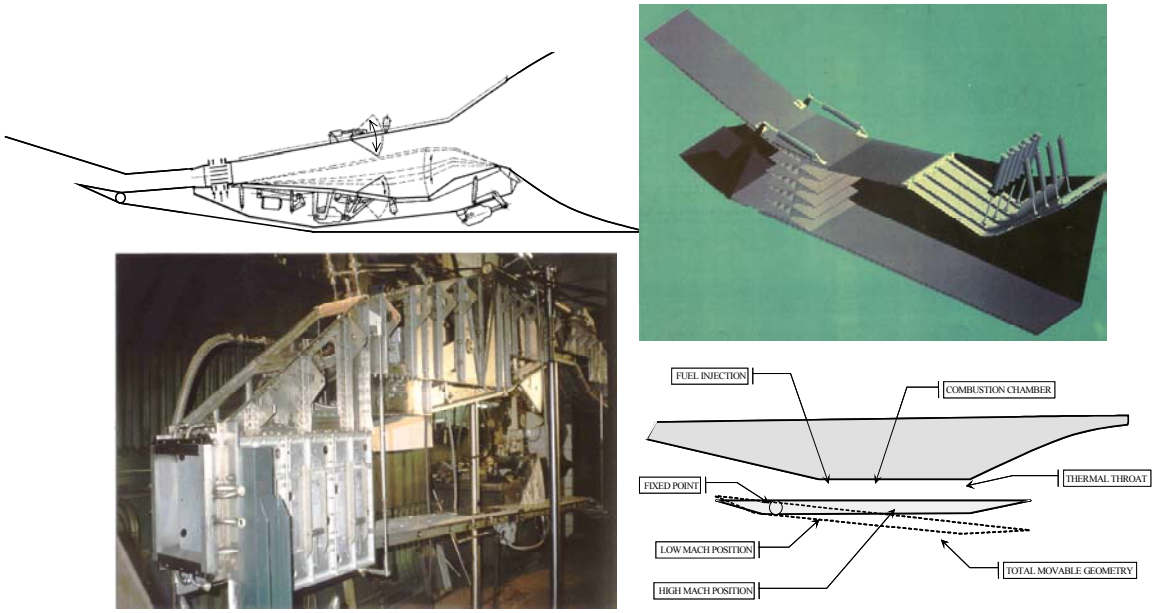

Figure 10: Examples of variable geometry dual-mode ramjets

For the PROMETHEE missile, the selected engine is a variable geometry dual-mode ramjet operating from Mach 1.8 to Mach 8. The geometry variation is achieved by the cowl wall rotation around an axis placed upstream the minimum cross-section. At low flight Mach number, the combustion is subsonic thanks to thermal choking.

1.4.5.2 ROCKET INTEGRATED IN THE AIRBREATHING DUCT

For missile applications, due to the 2D cross section of the scramjet combustor, solid propellant boosters (required to accelerate the vehicle from its launch up to airbreathing engine start) are not integrated but are external and jetissonable. For single stage to orbit (SSTO) access to space (ATS) missions, a rocket is required for the final stage of boost, orbital insertion, orbital maneuvering and de-orbit. A candidate for a SSTO vehicle is the rocket based combined cycle (RBCC) engine. RBCC engines utilize an air-augmented rocket for low speed, a ramjet/scramjet for mid-speed, and a rocket for high-speed operation. The NASA Marshall Space Flight Center is leading a program to develop an RBCC propulsion system to demonstrate the technology for future launch systems. A RBCC propulsion system may be tested in a program (X-43B) that is follow-on to the Hyper-X program later in this decade.

Only paper studies were carried on in Western Europe on this topic. In the scope of the French PREPHA program, the study of a generic SSTO vehicle led to conclude that the best type of air-breathing engine could be the dual-mode-ramjet (subsonic then supersonic combustion) [B1] [B2] with separate rockets for take-off and final acceleration. An extensive technology work has been investigated [B4] [B5] [B6] [B7] [B8] [B13].

1.4.5.3 DETONATION-BASED CYCLES (ODWE AND PDE)

Work was begun in the early 1990's at NASA Langley to study the feasibility of both Oblique Detonation Wave Engines (ODWE) and shock induced combustion engines. The premixed shock induced combustion (PMSIC) concept utilizes a strong shock to initiate combustion of a fuel-air premixture at the entrance to the engine combustor with the idea of significantly shortening the combustor of a scramjet. Computational studies were completed, and model design was begun, but the program did not continue to the stage of testing [D16]. There was also work during this period to computationally study oblique wave detonation engines [U13] and pulse detonation engines.

The WRR concept is –theoretically- designed to be used in ODWE mode instead of conventional scramjet after Mach 10. Several 1D and 2D computations have only been performed. ODWE basic studies have been experimentally demonstrated at ENSMA/CNRS laboratory at Poitiers, under Mach 10 conditions, with hydrogen as fuel.

There is currently an effort underway in USA and in France to explore pulsed detonation engine (PDE) concepts. Some preliminary integrations of PDE or PDR (rocket) concepts into a scramjet have been investigated [U17]. One of the common scientific challenges of the PDE and ODWE is the theory and the mastering of detonation of imperfectly mixed gases. Recent studies have shown that realistic, attainable performance limits the useful lower and upper Mach number limit of the PDE. Therefore, a careful realistic review of this engine will continue as it is being developed, to determine whether it is useful for hypersonic systems.

1.4.5.4 ASSOCIATION WITH TURBO-DUCTS

NASA Langley and Air Force studies show that scramjets integrated with a high speed turbojet, in an "over-under" configuration, may provide optimum vehicles in terms of take-off gross weight, reliability, operating cost and safety. Turbojets have high reliability, vis-a-vis rockets. Integration of the two engine flowpaths is currently in the conceptual stage. Previous design, dating to the late 60's, has included wind tunnel tests of propulsion-airframe integration issues for these over-under engine systems.

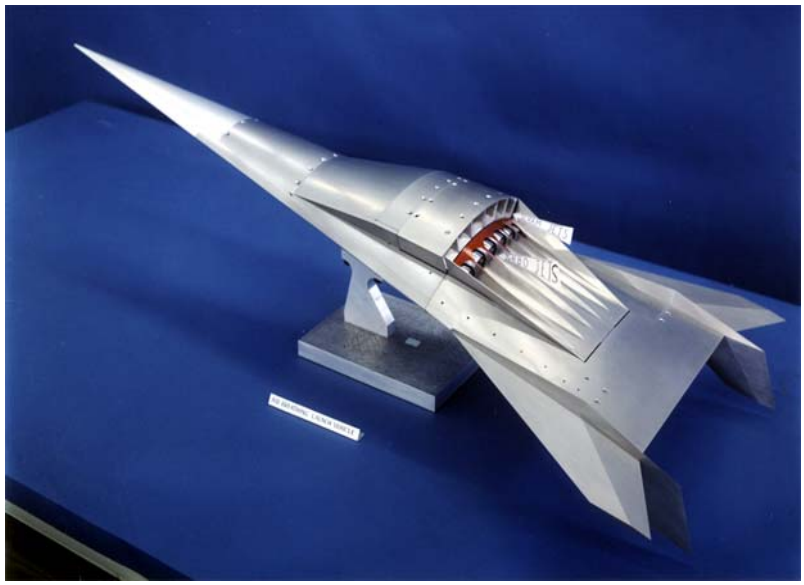

Figure 11: "Over-under" turbo-ramjet.

1.4.5.5 COOLED-AIR SECONDARY DUCT

Liquid-air systems have been studied in the USA, Europe and Japan. US studies have shown that liquid air rocket based combined cycle engines are competitive with turbojet-scramjet systems for space access [U16]. Several paper studies have been performed in Europe on this topic, in particular during ESA/CEPS studies (non-liquefied air, see [B12]) and PREPHA (air collection during cruise, see [A4]).

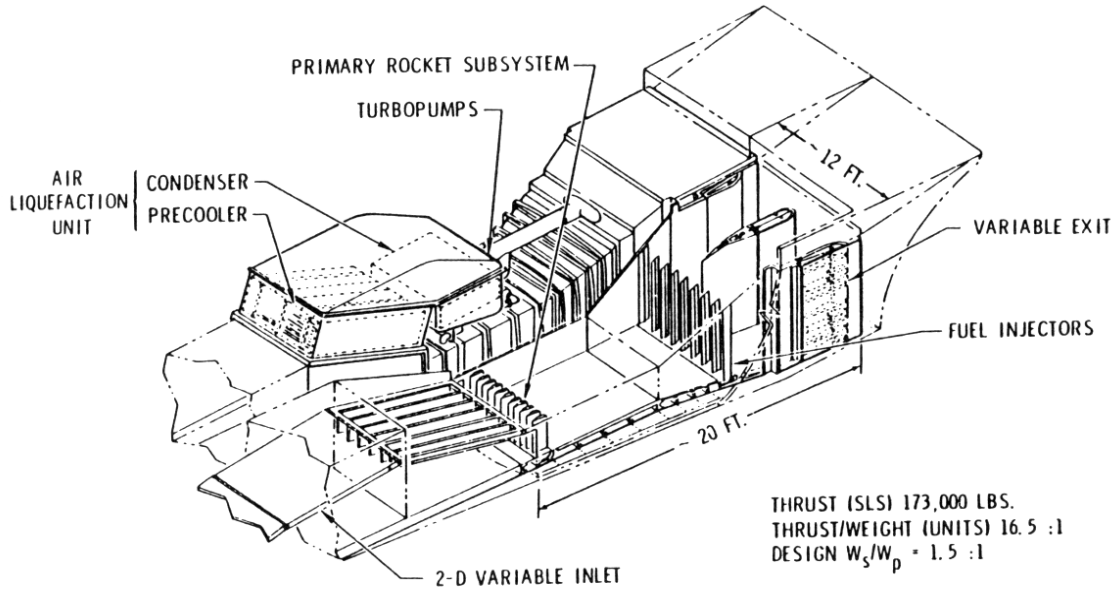

Figure 12: ScramLACE system

1.4.6 AIRFRAME INTEGRATION

Hypersonic airbreathing configurations are characterized by a highly integrated propulsion flowpath and airframe systems [U13]. Propulsion/Airframe Integration (PAI) research for this class of vehicle is focused on understanding various component interactions and their effects on integrated vehicle aero-propulsive performance. Advanced airframe-integrated concepts seek to exploit these interactions to maximize performance

and improve stability and control characteristics. Investigations of these phenomena require a range of analytical, computational and experimental methods [U15].

Airframe-propulsion integration has been studied extensively in France and Germany, but only using computations of different levels [A1] [B2] [D11] [B12] [B19] [B25]. Testing demonstration and associated methodology has been prepared, but no specific experimental work has yet been conducted in Western Europe.

Much of the US present capabilities and experience in this area is derived from support of various NASA hypersonic programs, such as the National Aerospace Plane (NASP) and the Hyper-X (X-43A) Program. A survey of work from these programs represents the state of the art in this research area. The development of the X-43A configurations provides an opportunity to evaluate testing and analytical capabilities and highlight some areas of opportunity for improvements in methodology leading to the development of a full-scale scramjet-powered flight vehicle. Among the advancements in PAI, experimental wind tunnel testing of a complete scramjet powered vehicle configuration was accomplished for the first time, and powered aerodynamics was validated at Mach 7.

1.5 MATERIALS AND STRUCTURES

Structural concepts for hypersonic vehicles and propulsion systems evolve with the design of the overall system. Many of the current concepts use either cold integral or non-integral graphite/epoxy LH2 tanks (developed and successfully tested under the X-30 and used in the DC-X and X-33). A mechanically attached insulated multi-wall insulation (IMI) thermal protection system (TPS) is used on the windward side, and the now obsolete tailored advanced blanket insulation (TABI) is base lined for the lee side. This combination provides a lightweight TPS with durable external skin. Wing and tail structure is titanium metal matrix composite, developed for the X-30. The engine primary structure is graphite-polyimide (being demonstrated on the X-37). Regeneratively cooled copper, aluminum, and high temperature superalloy panels are utilized in the engine and a convectively cooled process developed and verified for the X-30 cooled engine and vehicle sharp leading edges.

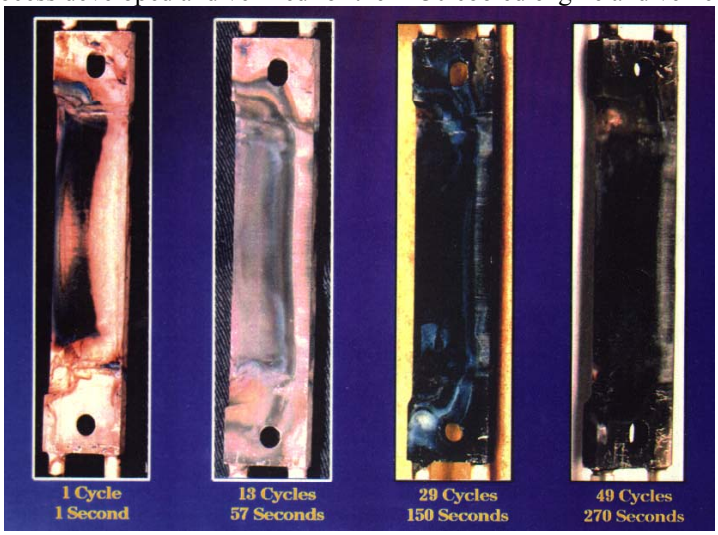

Figure 13: Test of engine heat exchangers and leading edges (Ref. U17)

The WRR project gave and will give the opportunity to acquire a substantial know-how for the design and the experimental validation of the active cooling systems usable in a dual mode ramjet for the different components, including injection struts, combustor walls, movable panels and hinges [A11]. In the framework of the WRR program more than 30 concepts of cooled panels have been developed for protecting the fixed and movable combustion chamber walls. Most of these studied cooled panels, called HPEs (Heat Protective Elements), and are based on metallic structures. Then, in order to maintain the temperature of the hot wall under the relatively limited capacity of the steel alloys, it is necessary to use both 3D configurations, in particular multi-layer architectures, such as the “two stages” HPE (material FeCrAl), and heat exchange enhancement systems in the cooling channels. Each of these HPE concepts has been tested in the MAI facility, in which a hydrogen fueled scramjet combustion chamber is used as a high temperature gas generator. The HPE tested (100x200 mm²) is placed at the scramjet chamber exit. A wedge is facing the HPE tested in order to create a shock wave whose interaction with the HPE increases the heat flux. For both metallic and composite materials versions, the future developments of cooled panels, or cooled integral structure, will take advantage of the large database collected during the WRR cooperation. Reference [D14] is a synthesis of this know-how.

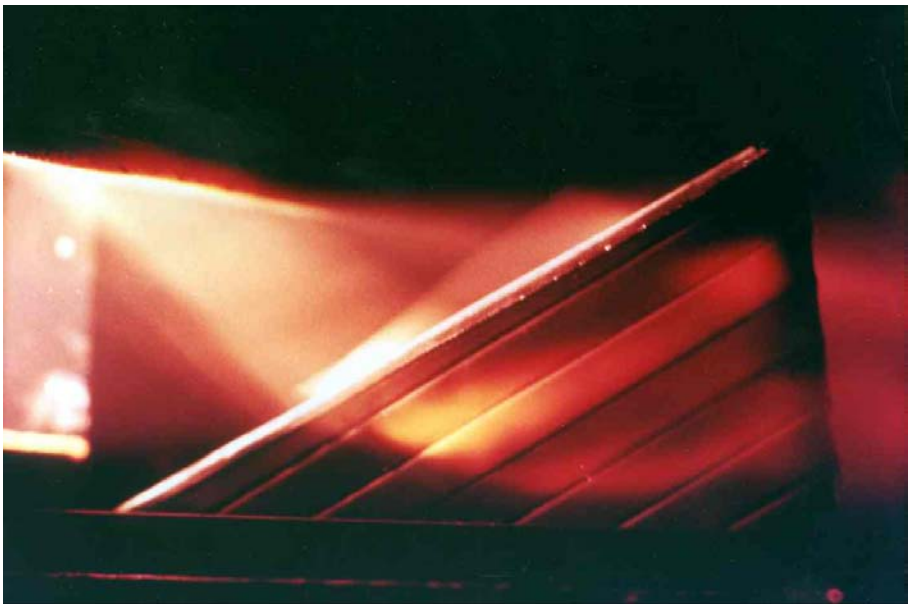

Figure 14: Hot test of WRR component (scramjet leading edge)

Recent French studies lead to considering combustion chamber technologies based on the use of thermo-structural composite materials cooled by the fuel. In this field, very limited works have been performed by EADS and SNECMA during the PREPHA program with basic tests performed at ONERA [A1]. Under the aegis of DGA and the USAF, ONERA and SNECMA are working with Pratt & Whitney in the A3CP program for endothermic fuel cooled composite materials structures ([A17]). The technology developed consists of manufacturing channels in a composite material sheet (C/SiC) and brazing a second composite material sheet to form a cooled panel. The program is dealing with the different difficulties related to this kind of cooled panel, including composite materials brazing technology able to sustain high temperature (> 1000 K), compatibility between material, endothermic fuel and possible catalyst, and fuel leakage through composite material porosity. A first hot test of A3C panel is planned in 2002.

Between 1993 and 1996, MBDA-F and EADS-Launch Vehicles (EADS-LV) led the project St ELME (French acronym for Advanced Injection System Through High Mach Number Flow). This project consisted in designing, manufacturing and testing in the CHAMOIS scramjet a high performance scramjet injection strut [A18].

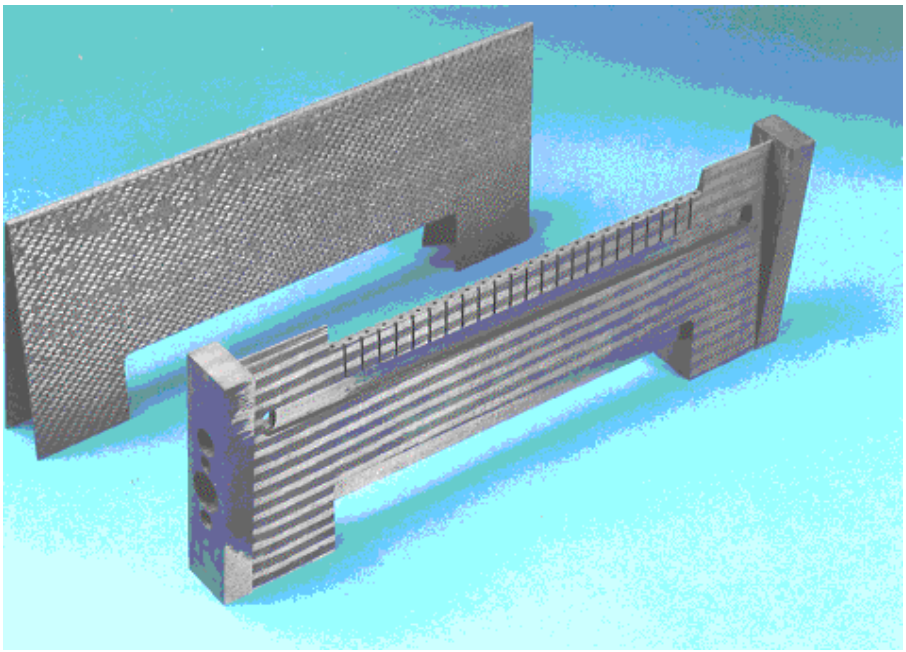

Figure 15: SAINT-ELME injection strut in thermostructural composite

Today, MBDA-F and EADS-LV are focusing their in-house effort on the development of a low cost, highly reliable and effective technology for the fuel-cooled composite material structure, particularly usable for the walls of a ramjet/scramjet combustion chamber. This technology, called PTAH-SOCAR (French acronym for Weaved Wall Applied to Hypersonic – Simple Operational Composite for Advanced Ramjet), takes advantage of the EADS-LV know-how in the field of pre-form manufacturing and particularly of its mastery for weaving the fibrous structure [A19]. Three different composite panels have been successfully tested since July 2001 with gaseous nitrogen and liquid kerosene as coolant and with a maximum wall temperature of 1850K. In connection with flowpath design and engine integration, prolonged testing of flight worthy scramjet engines has been investigated in the US (see §6.3, [A17], [B16]).

1.6 FLIGHT TESTING

1.6.1 HYPER-X

The primary goals of the Hyper-X Program are to validate the airframe-integrated, dual-mode, scramjet-powered vehicle in flight and provide databases for validation of design methods and tools [U14]. This will be accomplished using data from the X-43-A vehicle under powered conditions at Mach 7 and 10, and unpowered conditions down to subsonic flight. In preparation for these X-43 flights, refinement of the vehicle design using optimization methods was required to assure that the small, compact X-43 vehicle accelerates. In addition, every detail of the hypersonic system was evaluated, including the high Mach number, high dynamic pressure stage separation. The most extensive hypersonic aerodynamic, propulsion and thermal database ever generated for this class of vehicle is being used to develop autonomous flight controls, size TPS and reduce risk for this first ever scramjet-powered hypersonic flight. [B14]

The X-43A mission of June 2001, the first in a series of three, was lost moments after the X-43A and its launch vehicle were released from the wing of the NASA B-52 carrier aircraft. Following launch vehicle ignition, the combined launch vehicle and X-43A experienced structural failure, deviated from its flight path and was deliberately terminated. The board studying the June 2 loss of the first X-43A mission expects to find more than one factor responsible for the loss. After complete analysis of the failure, a new flight test will be planned.

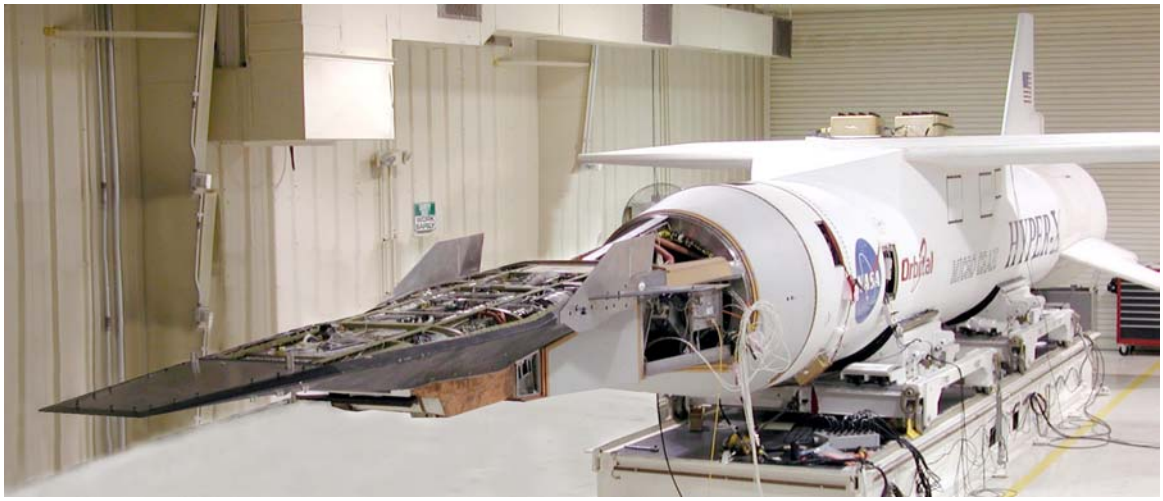

Figure 16: The Hyper-X vehicle integration

1.6.2 CIAM – "KHOLOD" SCRAMJET FLIGHT TESTS

This axisymmetric, dual-mode scramjet had been flight tested by Russia, first with internal funding (1991), then in 1993 and 1995, in cooperation with France [C14], with participation of three specialists also members of the present RTO subgroup. The last tests were performed within the scope of a CIAM-NASA cooperation. This test series provided ground and flight data at similar free stream conditions, showing similar results. This test also provided insight into autonomous flight controls.

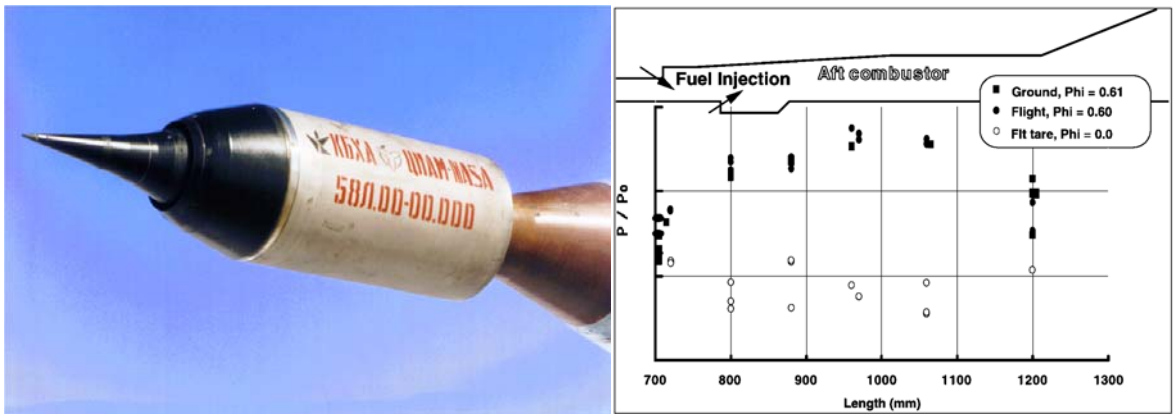

Figure 17: Kholod Russian experimental system.

1.6.3 ASTP – HYPERSONIC DEVELOPMENT FOR SPACE ACCESS

The future development of scramjet and hypersonic technology within the USA falls under the NASA Advanced Space Transportation Program and yet to be defined DOD interests. A complete plan will be completed in 2002.

The ASTP program is a comprehensive program designed to complete technology development and demonstration by 2018, leading to a Space Shuttle replacement vehicle by 2025. Propulsion systems generally fall into two categories: rocket-based and turbine-based combined cycles. Both approaches use dual-mode scramjets over much of the flight envelope, from Mach 3 or 4 to Mach 12 to 15. The program is also developing the critical technologies identified by the system studies. These range from structures and materials, to tires to operational and Integrated Vehicle Health Monitoring (IVHM).

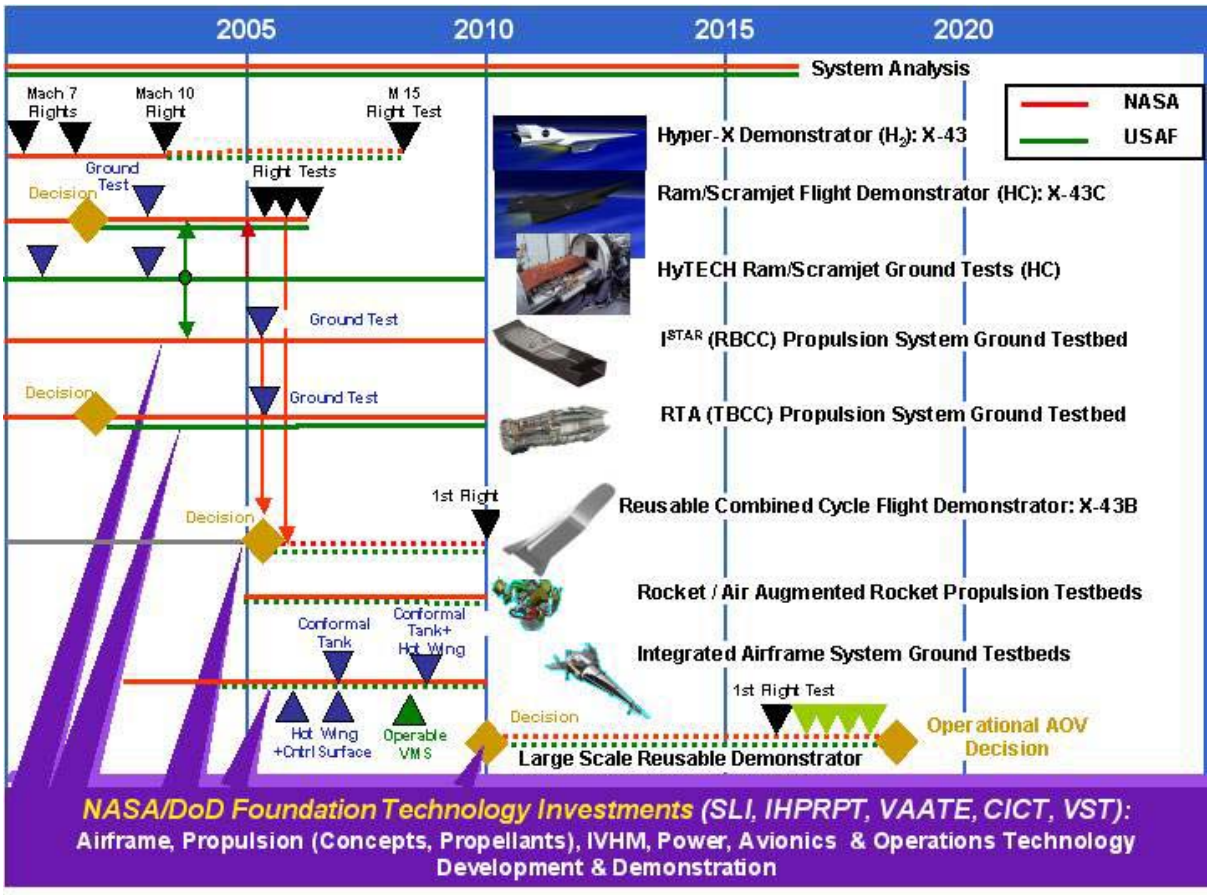

Figure 18: The Advanced Space Transportation Roadmap.

In addition, the program features both ground and flight demonstrations of key technologies, such as scramjet, RBCC and TBCC propulsion systems and major airframe structures. In the current plan, and in the conceptual designs, plans are being developed for scramjet flight demonstrators, ground testing RBCC and TBCC demonstrators, and a flight demonstration of either the RBCC or TBCC configuration. The current program is also calling for a large-scale flight vehicle, which would demonstrate all propulsion and other system technology. This phased, incremental program is designed to focus technology development, take to flight only systems which have heritage in ground/wind tunnel development, delay vehicle architecture selection until flight data is obtained, and meet the NASA and USAF 2025 IOC.

The first flight demonstrator is currently called the X-43C. It is a slightly scaled up version of the X-43 with 3 HyTech hydrocarbon engines, which were developed for the AARMD program. These flightweight, hydrocarbon-fueled and -cooled engines were developed and will be supplied by the USAF. NASA will provide the vehicle, integrated to fit the existing engines, and fly three vehicles using the same approach used by the Hyper-X Program, i.e. rocket-boosted, and not recovered. These vehicles will be boosted to Mach 5, demonstrate acceleration from Mach 5-7, duel-mode ramjet mode transition from ramjet to scramjet mode, and engine performance, operability and durability. Test times will be on the order of 4-6 min. This small step will produce the first regenerative cooled, flightweight scramjet powered vehicle, and represents an affordable, incremental step up from Hyper-X. (The Hyper-X team, with help from the USAF and other NASA centers will execute this program, with first flight scheduled for 2005). This will also be the first flight weight scramjet engine system built in the USA since the NASA Hypersonic Research Engine, which completed wind tunnel testing in 1972.

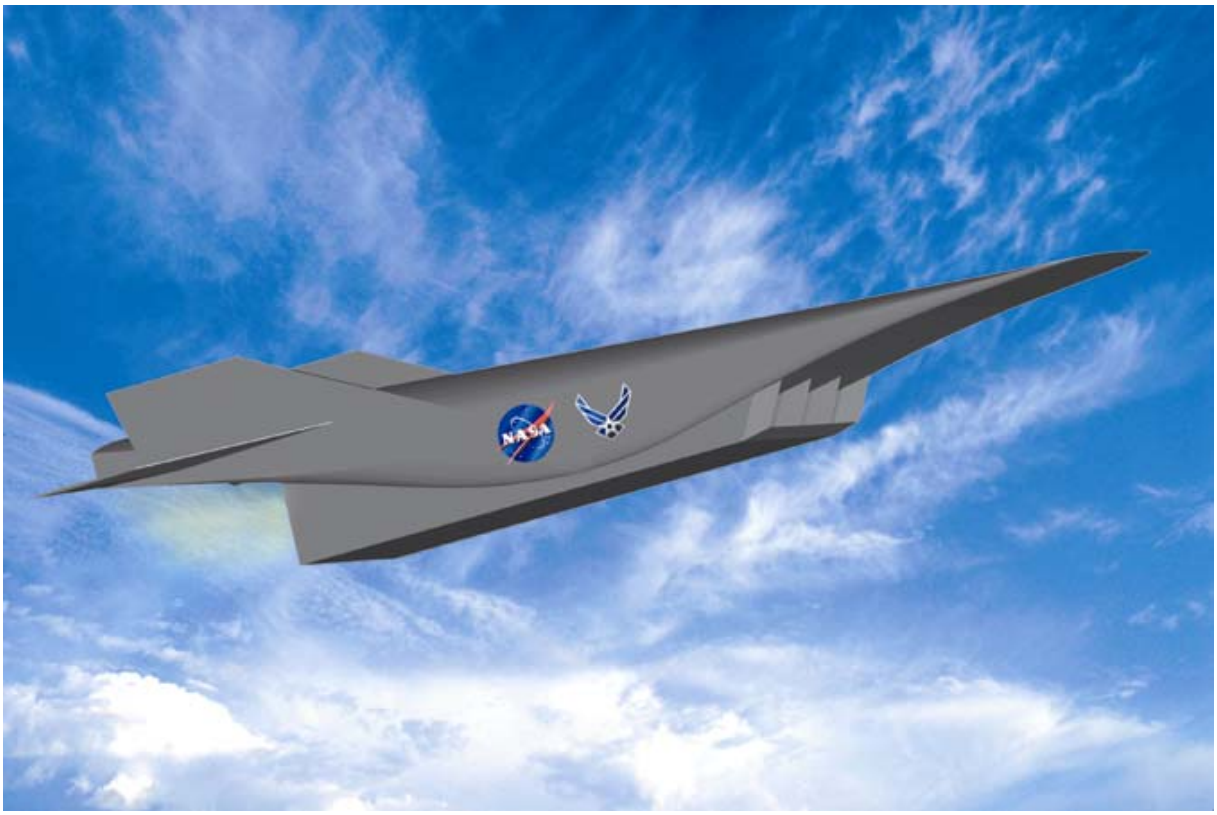

Figure 19: The X-43C Vehicle.

Following ground development and testing of both a flightweight RBCC and TBCC, and completion of a conceptual design for flight testing, one engine system will be selected for flight-testing. As currently envisioned, this engine system will be tested using an air launched version of the X-43 lifting body configuration called the X-43B. The vehicle will be dropped from the NASA B-52, will then accelerate to Mach 7, and glide to a dead stick landing, much like the X-15. Current studies indicate that by using hydrocarbon fuel to reduce vehicle size, this vehicle should be between 13 - 15 meters long, and weigh about 25,000 pounds at drop. Two vehicles are currently envisioned. Each will be required to fly 25 missions without major engine replacements/repairs. This reusable flight vehicle will provide the first real data on operation/costs for this class of vehicles. Depending on budgets, these vehicles can be flying by 2008-12. This vehicle is likely to be a jointly funded DOD-NASA program with the first flight in 2008.

Other ground demonstrators are being considered in the US for large airframe structural elements.

Following completion of the X-43C, the ASTP will evaluate system studies and requirements for "Hypervelocity" scramjet operations. A hypervelocity scramjet demonstrator is being investigated. This would utilize LH2, be rocket boosted, and validate LH2 fueled/cooled scramjet engine operation in the Mach 12-15 speed range. Because of budget considerations, this vehicle is envisioned as Hyper-X scale.

The final demonstrator leading to an operational vehicle will fold together all of the available technology, will be based on the selected vision vehicle, and demonstrate all propulsion modes and other key technologies. Engine cycle(s), vehicle architecture, number of stages, and fuel will be based on a down select from the system studies. Clearly this vehicle demonstrator will be a large undertaking. But, it will have significantly lower risk than the X-30 or X-33 because of the incremental approach that will be utilized. This demonstrator is scheduled for ASTP in 2010 - 2012, and first flight 2015-2017.

1.6.4 EUROPE FLIGHT TESTING ISSUES (PROBABLY WITH RUSSIA)

Considering difficulties and cost of test facilities on one hand, the extreme sensitivity of the aero-propulsive balance on the other hand, it is clear that scramjet technology development needs substantial flight testing. A demonstrator of an operational vehicle being very expensive and the associated technical risk being very high, such a flight experiments should begin with the development of small experimental vehicles.

The limited French participation to the tests by CIAM (Moscow), of boosted "Kholod" axisymmetric hydrogen-fueled engines was a first step [C14]. However, the design of the Kholod engines tested is very close to the HRE or ESOPE combustors design (ground tested in USA and in France in 1970s) and the limited height of the combustion chamber is not representative of a large operational scramjet. Beyond this first step, an analysis of needs evaluated the ability of a large set of typical experimental vehicles to comply with these requirements [C15].

From the results obtained, ONERA and MBDA-F sketched some self-powered experimental vehicles [C16].

For JAPHAR experimental vehicles, a height of 100mm has been chosen for the combustion chamber entrance to be representative of a space launcher application. A combustion chamber of this height requires the use of injection struts. Due to the height of the combustion chamber chosen, the generic experimental vehicle is relatively large (~10m long). Two 400mm wide propulsion system modules power it. On the basis of a preliminary design, some design studies have been performed to optimize the general configuration of the experimental vehicle [A7] and particularly the forebody shape [A8].

All these efforts, planned in discussions with the scientific community (ONERA, AMM, CNRS, DLR, Russian institutes), would lead to a small scale experimental vehicle, able to demonstrate in flight, whatever the final applications, the ability to develop a dual mode ramjet to accelerate a vehicle from Mach 2 to Mach 8.

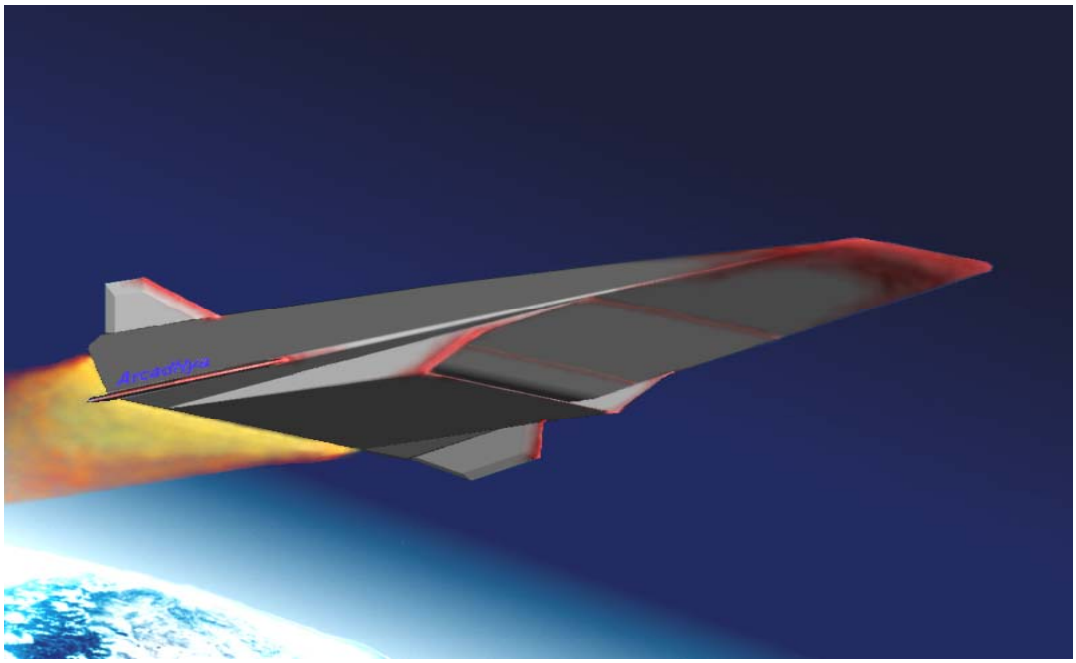

Figure 20: Artist view of airbreathing hypersonic experimental vehicle

1.7 CONCLUSIONS AND RECOMMENDATIONS

Significant advancements have been made in high-speed airbreathing propulsion. Many of these advancements have been discussed in this working group report. These advancements are finally being exploited in the first years of this new century.

Access-to-space requirements that must be addressed include reusable vehicles able to provide rapid (on demand) access to low earth orbit at significantly reduced cost and with increased reliability. There is also a need for development of hypersonic, airbreathing missiles to provide rapid response against time sensitive/critical targets and to counter threats from hostile hypersonic weapons. Possibly, hypersonic aircraft concepts could be considered to reach rapidly any critical area and provide a platform for reconnaissance and defense. For all these possible applications, it is necessary to master the technology of dual-mode ramjet able to efficiently operating from Mach 1.5/2 to Mach 8/12, depending of application.

Progress in high-speed airbreathing propulsion is therefore critical for the NATO Alliance and several topics should be addressed, as shown on Figure 21.

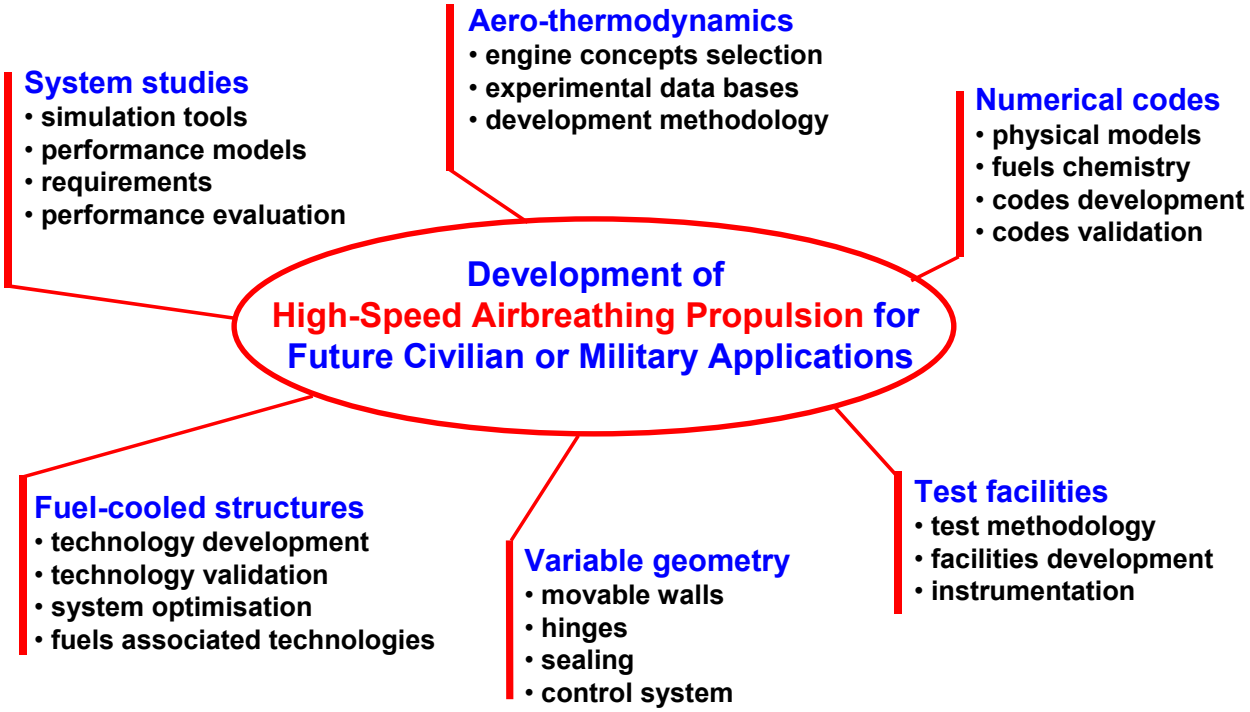

Figure 21: Key research areas for dual-mode ramjets mastering

These key-points will benefit from:

- System studies and mission analysis
- CFD enhancement
- Ground testing.

Figure 22 shows the two major key issues for hypersonic airbreathing propulsion:

1. To define and validate a design methodology predicting the aero-propulsive balance of the high speed vehicle, whatever its type, its size and the application, with the accuracy required to guarantee the design margins mandatory for an operational development. Due to the extreme sensitivity of the aeropropulsive balance and to the limitations of ground test facilities (in particular air vitiation, size , test duration and/or maximum flight Mach number), this methodology must closely combine partial tests and CFD tools. Validation of such methodology can only be by flight testing.
2. To demonstrate capability of building SCRJ combustion chambers, with fuel-cooled structures, variable geometry, minimum weight, endurance and operability. With system studies as guidelines, technology "bricks" can be developed at component level. But, when a sufficient technology readiness level will be reached for each component, an engine demonstrator will have to be designed, built and tested at least

on-ground (for a first demonstration prior to an operational development, a flight technology demonstration does not appear mandatory).

Following these two steps further research and technology development efforts should be focused on :

1. Flight testing of an autonomous vehicle, based on demonstrated understanding of the aero-propulsive balance (planned in 2002 in the US and 2010-2012 in France). This vehicle can be a simple experimental vehicle without any technology demonstration purpose. But it must be fitted out with a very extensive measurement system allowing to determine accurately the flight conditions and the contribution of each propulsion system component.
2. Ground testing of a flight-worthy regeneratively-cooled dual-mode ramjet engine (planned in 2003 in the US, in 2010 in France)

After these two key milestones will be reached, it will be possible to undertake the development of an operational vehicle, with possible flight testing of a technology demonstrator, if necessary.

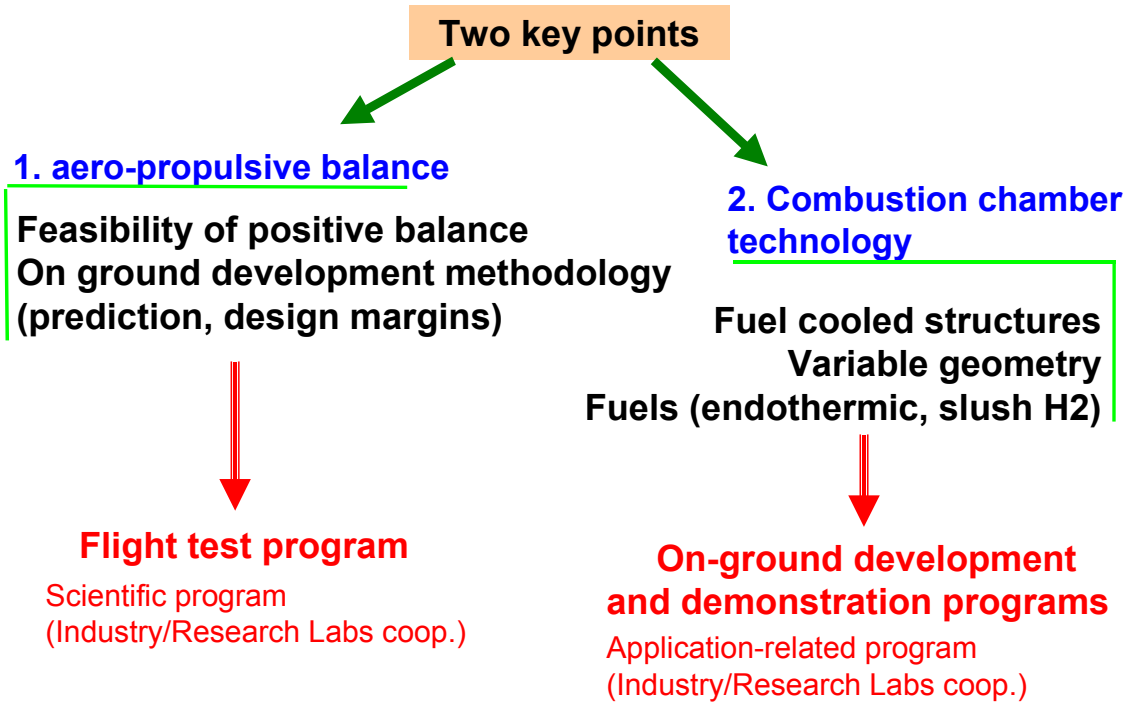

Figure 22: Main directions for dual-mode ramjet development

1.8 REFERENCES

[A1] F. FALEMPIN, D. SCHERRER, G. LARUELLE, Ph. ROSTAND, G. FRATACCI
French Hypersonic Propulsion programme PREPHA - Results, Lessons and Perspectives
AIAA - 98 – 1565 - Norfolk

[A2] A. CHEVALIER, F. FALEMPIN
Review of new French facilities for PREPHA Program
AIAA - 95 - 6128 - Chattanooga - 1995

[A3] F. FALEMPIN
Ramjet/Scramjet technology – French capabilities
AIAA - 99 – 2377 – Los Angeles

[A4] F. FALEMPIN
French hypersonic program PREPHA - System studies synthesis
XIII ISABE - Chattanooga - 1997

[A5] F.FALEMPIN, W. KOSCHEL

Combined rocket and air-breathing propulsion - European perspectives
3d International Symposium on Space Propulsion - Beijing - 1997

[A6] Ph. NOVELLI, W. KOSCHEL
JAPHAR: a joint ONERA-DLR research project for high-speed airbreathing propulsion
XIV ISABE - Florence - IS 7091 - 1999

[A7] Th. EGGERS, Ph. NOVELLI
Design studies for a Mach 8 dual mode ramjet flight test vehicle
AIAA – 99 - 4877 - Norfolk

[A8] Ph. DUVEAU, R. HALLARD, Ph. NOVELLI, Th. EGGERS
Aerodynamic perf. analysis of the hypers. airbreathing vehicle JAPHAR
XIV ISABE - Florence - IS 7286 - 1999

[A9] M.BOUCHEZ, V.LEVINE,F.FALEMPIN
D.DAVIDENKO, V. AVRASHKOV,
Airbreathing space launcher – interest of a fully variable geometry propulsion system – status in 1999
AIAA - 99 – 2376 – Los Angeles

[A10] M. BOUCHEZ, V. LEVINE, V. AVRASHKOV, D. DAVIDENKO, F. FALEMPIN
France-Russia partnership on hypersonic Wide Range Ramjet: status in 1999
AIAA – 99 – 4845 - Norfolk

[A11] F. FALEMPIN, V. LEVINE, V. AVRASHKOV, D. DAVIDENKO, M. BOUCHEZ
MAI/AEROSPATIALE Cooperation on a hypersonic Wide Range Ramjet:
evaluation of thermal protection systems
XIV ISABE - Florence - IS 7140 - 1999

[A12] M.BOUCHEZ, V.LEVINE, V. AVRASHKOV, D. DAVIDENKO,
P. GENEVIEVE
Airbreathing space launcher interest of a fully variable propulsion system
AIAA – 2000 – 3340 - Huntsville

[A13] L. SERRE
Hypersonic UAV for reconnaissance in the depth
AGARD 594 - Athens – 1997

[A14] L. SERRE, F. FALEMPIN
High altitude high-speed UAV for reconnaissance operations
Projection of forces international symposium
AAAF – Paris – Dec. 99

[A15] F. FALEMPIN, L. SERRE
The French PROMETHEE Program – Main goals and status in 1999
AIAA – 99 – 4814 – Norfolk

[A16] F. FALEMPIN, L. SERRE
The French PROMETHEE Program – status in 2000
AIAA – 2000 – 3341 – Huntsville

[A17] D.G. MEDWICK, J.H. CASTRO, D.R. SOBEL, G. BOYET, J.P. VIDAL
Direct fuel cooled composite structure
XIV ISABE - Florence - IS 7284 – 1999

[A18] M. BOUCHEZ, E. SAUNIER, P. PERES, J. LANSALOT
Advanced carbon/carbon injection strut for actual scramjet
AIAA – 96 – 4567

[A20] L. SERRE
Towards a low risk airbreathing SSTO program: a continuous robust PREPHA based TSTO
AIAA - 99 - 4946 - Norfolk

[A21] U. BRUMMUND, B. MESNIER
Flow field visualization of non-reacting and reacting supersonic flows in a scramjet model combustor using non-intrusive optical diagnostic
8th Int. Symposium of Flow Visualization, Sorrento, Italy, 1998

[A22] M. BOUCHEZ
Status of measurement techniques for supersonic and hypersonic ramjets in industrial facilities
XIV ISABE - Florence - IS 7168 - 1999

[B1] F. Falempin, D. Scherrer, G. Laruelle, Ph. Rostand, G. Fratacci, J.L.Schultz, *French hypersonic propulsion program PREPHA -results, lessons & perspectives* , AIAA - 98 - 1565 - Norfolk

[B2] F. Falempin, *PREPHA Program - System studies synthesis*, XIII ISABE - Chattanooga - 1997

[B3] A. Chevalier, V. Levine, M. Bouchez, D. Davidenko, *French-Russian Partnership on Hypersonic Wide Range Ramjets*, AIAA - 96 - 4554

[B4] W.B. Scott, *Space Access' LaunchSsystem Based on Airbreathing Ejector Ramjet*, Aviation Week and Space Technology, March 30, 1998

[B5] W.J.D. Escher, R.E. Schnnurstein, A Retrospective on Early Cryogenic Primary Rocket Subsystem Designs as Integrated Into RBCC Engines, AIAA-93-1944

[B6] W.J.D. Escher, *Synerjet for Earth/orbit Propulsion: revisiting the 1966 NASA/Marquardt Composite (airbreathing/rocket) propulsion study*, AIAA 96-3040

[B7] M.J. Bullman, A. Siebenhaar, RBCC propulsion for Space Launch, IAF-95-S.5.02

[B8] R. Engers, D. Cresci, C. Tsai, A combined Cycle Engine Test Facility, AIAA-95-6152

[B9] M. Bouchez et al. *French-Russian Partnership on Hypersonic Wide Range Ramjet: status in 1999* AIAA-99-4845, Norfolk, Hypersonics Conference, November 1999

[B10] J. Olds et al., *Hyperion: An SSTO Vision Vehicle Concept Utilizing Rocket-Based Combined Cycle Propulsion,* AIAA 99-4944

[B12] A. Wagner et al., *Integration of a Combined Engine Propulsion System into a SSTO launcher*, 1995, AIAA-95-6044

[B13] DE Pryor, EH Hyde, WJD Escher, *Development of a 12-thrust chamber kerosene/oxygen primary rocket subsystem for an early (1964) air-augmented rocket ground test system*, AIAA 99-4896

[B14] V. Rausch, C. McClinton, J. Sitz, *Hyper-X program overview,* ISABE-99-7213

[B16] NASA RFP (NASA Lewis) NASA RESEARCH ANNOUNCEMENT Air-Breathing Launch Vehicle (ABLV) Rocket-Based Combined Cycle (RBCC) Propulsion System Materials, Structures, And Integrated Thermal Management , 1998, NRA-98-LERC-2 (FINAL)

[B17] F. Falempin, L Serre, *The Promethee Program – Status in 2000,* AIAA–2000-3341, Huntsville, Joint Propulsion Conference, June 2000

[B18] M. Bouchez, *High speed propulsion: a ten years Aerospatiale-Matra education contribution*, AIAA-99-4894, Norfolk, November 1999

[B19] T. Bonnefond, F. Falempin, P. Viala: *Study of a Generic SSTO Vehicle Using Airbreathing Propulsion*, AIAA-96-4490-CP

[B23] Ph. Novelli, W. Koschel*, JAPHAR: a joint ONERA-DLR research project for high-speed airbreathing propulsion*, XIV ISABE - Florence - IS 7091 - 1999

[B24] Marc Bouchez, Vadim Levine, François Falempin, Dmitri Davidenko, Valery Avrashkov, *Airbreathing space launcher interest of a fully variable geometry propulsion system*, AIAA-98-3728, Cleveland, Joint Propulsion Conference, June 1998

[B25] Marc Bouchez, Vadim Levine, François Falempin, Dmitri Davidenko, Valery Avrashkov, , *Airbreathing space launcher interest of a fully variable geometry propulsion system*, AIAA-99-2376, Los Angeles, Joint Propulsion Conference, June 1999

[B26] Marc Bouchez, Vadim Levine, Dmitri Davidenko, Valery Avrashkov, Pascal Genevieve, *Airbreathing space launcher interest of a fully variable geometry propulsion system and corresponding French Russian Partnership*, AIAA-2000-3340, Hunstville, Joint Propulsion Conference, July 2000

[C2] Ph. Novelli, D. Scherrer, D. Gaffié

Scramjet flowfields investigation by numerical simulation
XIIth ISABE - Melbourne - 1995

[C4] F. Falempin
Overview of French Research Center ONERA activities on hypersonic airbreathing propulsion
XII ISABE - Melbourne - 1995
published in Australian Mechanical Engineering Transactions - vol.ME20 N°4 - 1995

[C7] M. Sancho, Y. Colin, C. Johnson
The French hypersonic research program PREPHA
AIAA - 96 - Norfolk

[C8] P. Garnero, I. Auneau, Ph. Duveau
Design and optimization methods for scramjet inlets
AIAA - 95 - 6017 - Chattanooga - 1995

[C9] F. Falempin, Ph. Duveau
variable capture area inlets - application to space launchers
AGARD CP 498 - Fort Worth - 1991

[C10] P.Perrier, M. Rapuc, P. Rostand, R. Hallard,
D. Regard, A. Dufour, O. Penanhoat
Nozzle and afterbody design for hypersonic airbreathing vehicles
AIAA - 96 - 4548 - Norfolk

[C11] D. Scherrer, O. Dessornes, N. Montmayeur,
O.Ferrandon
Injection studies in the French hypersonic technology program
AIAA - 95 - 6096 - Chattanooga

[C12] M. Bouchez, J-V. Hachemin, C. Leboucher
D. Scherrer, D. Saucereau
Scramjet combustor design in French PREPHA program - status in 96
AIAA - 96 - 4582 - Norfolk

[C13] M. Bouchez, Y. Kergaravat,D. Scherrer,
M. Souchet,D.Saucereau
Scramjet combustor design in French PREPHA Program - final status in 1998
AIAA - Norfolk - April 1998

[C14] A. Roudakov, Y. Schickmann, V. Semenov,
Ph. Novelli, O. Fourt
Flight testing an axisymmetric scramjet - Russian recent advances
IAF - 93 - S.4.485 - Gratz

[C15] F. Falempin, Ph. Vancamberg, R. Thevenot,
Ph. Girard, H. Joubert
Hypersonic airbreathing propulsion: flight tests needs
AIAA - 95 - 6013 - Chattanooga

[C16] F. Falempin, M. Forrat, J. Baldeck,
E. Hermant
Flight test vehicles: A mandatory step in scramjet development
AIAA - 92 - 5052 - Orlando

[C17] R. Zendron, P. Bellande, B. Forrat, D. Scherrer
Comparison of different propulsive systems for air-breathing launcher
AIAA - 95 - 6077 - Chattanooga

[C18] C. Rothmund, D. Scherrer, F. Levy, M.Bouchez
Propulsion system for airbreathing launcher in the French PREPHA program
AIAA - 96 - 4498 - Norfolk

[C19] T. Bonnefond, F. Falempin, P. Viala
Study of a generic SSTO vehicle using airbreathing propulsion
AIAA - 96 - 4490 - Norfolk

[C20] F. Falempin
PREPHA program - System studies synthesis
XIII ISABE - Chattanooga - 1997

[C22] M. Bouchez, E. Saunier, P. Peres, J. Lansalot
"Advanced carbon/carbon injection strut for actual scramjet"
AIAA - 96 - 4567 - Norfolk - 1996
[C23] F. Falempin, W. Koschel
Combined rocket and airbreathing propulsion - European perspectives
3d International on Space propulsion
Beijing - August 1997

[D1] E.T. Curran, "Scramjet Engines: The First Forty Years," AIAA Journal of Propulsion and Power, Vol. 17, No. 6, November-December 2001

[D2] E. Dufour, M. Bouchez: "Post-Experimental Computations of a Kerosene-Fueled Scramjet," AIAA-2001-1817, Kyoto, Japan, April 2001

[D3] M. Bouchez, X. Montazel, E. Dufour: "Hydrocarbon fueled airbreathing propulsion for high speed missiles," AIAA 98-3729, Joint Propulsion Conference, Cleveland, 1998

[D4] M. Bouchez, O. Legras, V. Avrashkov, et al.: "RAPIERE: An innovative industrial optical measurement system for scramjet flows," AIAA-2001-1861, Kyoto, Japan, April 2001

[D5] Garrard, Doug and Rigney, Sharon: "Building for the Future—AEDC's Investment in Hypersonic Aeropropulsion T&E," AIAA 2000-2644, 21st AIAA Aerodynamic Measurement Technology and Ground Testing Conference, June 19-22, 2000, Denver, Colorado.

[D6] Thomas, S. R.; Trefny, C. J.; and Pack, W. D.: "Operating Capability and Current Status of the Reactivated NASA Lewis Research Center Hypersonic Tunnel Facility." AIAA 95-6146 and NASA TM-106808, April 1995.

[D7] O.A. Powell, J.T. Edwards, R.B. Norris, K.E. Numbers, J.A. Pearce: "Development of Hydrocarbon-fueled Scramjet
Engines: the Hypersonic Technology (HyTech) Program," AIAA Journal of Propulsion and Power, Vol. 17, No. 6, November-December 2001.

[D8] D. Gaffie, U. Wepler, P. Magre, W. Koschel, Ph. Novelli: Numerical Investigation of Supersonic Reacting Hydrogen Jets in a Hot Air Coflow at AIAA-2001-1864, Kyoto, Japan, April 2001.

[D9] Walther, R., Sabelnikov V. , Koschel, W., Koronsvit, Y., Ivanov, V. "Investigations into the aerodynamic characteristics of Scramjet components," ISABE 97-7085.

[D10] B. Heinrich, Agnes Luc-Bouhali, F. Ser, C. Vigot: "Endothermic Liquid Fuels: Some Chemical Considerations on the Cooling Processes," AIAA-2001, Kyoto, Japan, April 2001.

[D11] L. Serre, F. Falempin, "PROMETHEE: the French Military Hypersonic Propulsion program," AIAA-2001-1871, Kyoto, Japan, April 2001.

[D12] F. Falempin, M. Bouchez, T. Salmon, P. Lespade, V. Avrashkov: "An Innovative Technology For Fuel-Cooled Composite Materials Structure", AIAA-2001-1880, Kyoto, Japan, April 2001.

[D13] Jourdren, Christine and Dessornes O.: "One Strut Scramjet Chambers Studies In The Frame Of The PREPHA Program.", AIAA 98-1560, Norfolk, USA, April 1998.

[D14] M. Bouchez, Dual-Mode Ramjet Thermo-Mechanical Design And Associated Performance, AIAA-2001-1918, Kyoto, Japan, April 2001.

[D15] Walter H. Beck "Modifications to the DLR High Enthalpy Shock Tunnel HEG for Measurements on Supersonic Combustion", AIAA-2001, Kyoto, Japan, April 2001.

[D16] G.P. Menees, H.G. Adelman, J.L. Cambier, J.V. Bowles, "Wave Combustors for Trans-Atmospheric Vehicles," Journal of Propulsion and Power, Vol. 8, N3, 1992, pp. 709-713.

[E1] Hendrick, P., VPSC: a Vehicle Parametric Sizing Code, AIAA-2001-1846, Kyoto, April 2001.

[U1] Anderson, G.Y. and Rogers, R.C.: A Comparison of Experimental Supersonic Combustor Performance with an Empirical Correlation of Non Reactive Mixing Results. NASA TM X-2429, Oct. 1971.

[U2] Pinckney, S.Z.: Turbulent Heat-Transfer Prediction Methods for Application to Scramjet Engines. NASA TN D-7810, 1974. Conference. Norfolk, Va. AIAA, Nov. 1999.

[U3] Drummond, J. P.: Supersonic Reacting Internal Flow Fields. Numerical Approaches to Combustion Modeling, Chapter 12, ed. E. Oran and J. Boris, American Institute of Aeronautics and Astronautics, Washington D. C., 1991. Also NASA-TM-103480, 1992.

[U4] Adumitroaie, V., Colucci, P. J., Taulbee, D. B., and Givi, P., LES, DNS and RANS for the Analysis of High-Speed Turbulent Reacting Flows, Annual Report, NASA Grant NAG 1-1122, 1994.

[U5] Girimaji, S. S, A Galilean Invariant Explicit Algebraic Reynolds Stress Model for Curved Flows, NASA CR-198340, pp. 1-28 June 1996.

[U6] Jaberi, F. A., Colucci, P. J., James, S., Givi, P., and Pope, S. B., Filtered Mass Density Function for Large Eddy Simulation of Turbulent Reacting Flows, J. Fluid Mechanics, Vol. 401, 85-121, 1999.

[U7] Jachimowsik, C. J., An Analytical Study of the Hydrogen-Air Reaction Mechanism with Application to Scramjet Combustion, NASA TP-2791, Feb. 1988.

[U8] Edwards, J. R., Development of an Upwind Relaxation Multigrid Method for Computing Three-Dimensional Viscous Internal Flows, AIAA Paper 95-0208, Jan. 1995.

[U9] Delarue, B. J., and Pope, S. B., Calculation of Subsonic and Supersonic Turbulent Reacting Mixing Layers Using Probability Density Function Methods, Physics of Fluids, Vol. 10, 487-498, 1998.

[U10] Mass, U., and Pope, S. B., Simplifying Chemical Kinetics: Intrinsic Low-Dimensional Manifolds in Composition Space, Combustion and Flame, Vol. 88, pp. 239-264, 1992.

[U11] Anderson, G.Y.: Supersonic Combustion Ramjet Performance. NASA TM X-968, Feb. 1964.

[U12] McClinton, C.R.: CFD Support of NASP Design. AIAA 90-3252, Sept. 1990.

[U13] Heiser, William H. and Pratt, Davis T.: Hypersonic Airbreathing Propulsion. AIAA Education Series. AIAA, Inc., Washington, D.C., USA. 1994.

[U14] Rausch, et. al. Hyper-X Program Overview, Presented 7th International Spaceplanes and Hypersonic Systems and Technology Conference. Norfolk, Va. AIAA, Nov. 1999.

[U15] Hunt, J. L., Eiswirth, E. A., NASA's Dual-Fuel Airbreathing Hypersonic Vehicle Study. AIAA CP-96-4591, 7th International Space Planes and Hypersonics Systems & Technology Conference, Nov. 1996.

[U16] McClinton,C.R; Andrews, E.H.; and Hunt,J.L: Engine Development for Space Access: Past, Present and Future. Paper no. 2001-1074, XV ISOABE Conference, Bangalore, India, Sept. 2001.

[U17] Escher, W. J. D. and Flornes, B. J., A Study of Composite Propulsion Systems. Marquardt Company Report 25.194. Final Report, Sep. 1966.

CHAPTER 2: FUELS

L. Q. Maurice, T. Edwards, F. Cuoco, C. Bruno, P. Hendrick

Lourdes Q. Maurice, Ph.D., P.E.
Office of Environment and Energy (AEE-3)/Federal Aviation Administration
800 Independence Avenue, S.W.
Washington, D.C. 20591
Lourdes.Maurice@faa.gov
T. Edwards
AFRL/PRTG, Bldg. 490, 1790 Loop Rd. N
WPAFB OH 45433-7103
james.edwards@wpafb.af.mil
F. Cuoco, DLR-Lampoldshäusen
francesco.cuoco@dlr.de
C. Bruno
University of Rome "La Sapienza"
Via Eudossiana 18, 00185 ROMA – ITALY
c.bruno@dma.ing.uniroma1.it
P. Hendrick
Royal Military Academy, Applied Mechanics Dept.
Av. De la Renaissance 30, 1000 Brussels - Belgium
Patrick.Hendrick@rma.ac.be

MISSION: The primary aim of AVT-10 is to assess the status of hypersonic technologies and make recommendations to NATO regarding the feasibility and usefulness of hypersonic systems to meet NATO future military challenges.

Hence, it is first necessary to understand the basic differences in requirements between military and civilian high-speed aircraft. These differences are outlined in Figure 1.

Figure 1. Differences between military and civilian high-speed systems requirements

2.1 INTRODUCTION

On-board reforming and cracking are appealing processes in order to enhance the quality and operability of fuels for hypersonic propulsion[1].

These processes seem suitable for several reasons. They both are endothermic, thus very suitable for thrust chamber cooling. No other reactant (but fuel) is needed in the case of cracking. Using appropriate catalysts, fuel conversion into light compounds (like H2, C2H2 or CH4) could also minimize soot formation associate with pure thermal cracking. Steam reforming needs appreciable quantities of steam[2].

The end product of reforming/cracking is HC much lighter than the original fuels (e.g. JP-8).

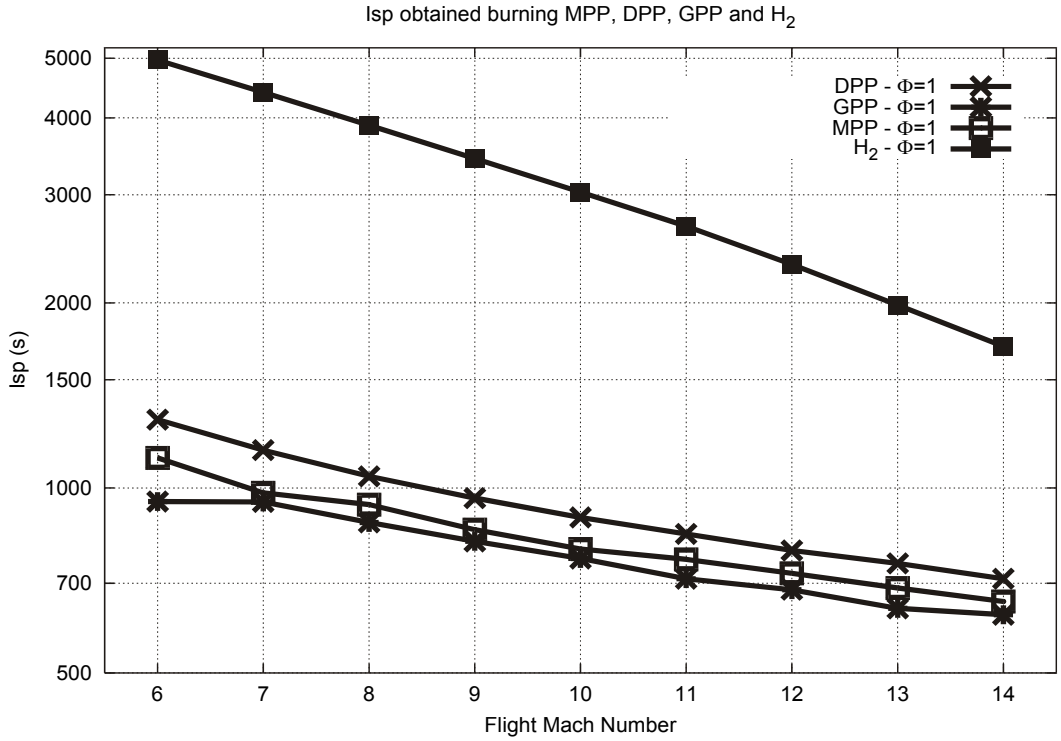

Figure 2: Isp vs Flight Mach number (MPP= methanol pyrolysis products, GPP= ethylene glycol p.p., DPP= dimethyl glycol ether p.p.) [3]

Light hydrocarbons combustion has several positive effects, like higher combustion rates, faster vaporization and mixing, faster chemical ignition, and lower soot production. Moreover light hydrocarbons yield higher performance (Isp) than typical jet fuels (see fig.1). Using H2 could pose problems due its high tankage volumes required; on the contrary storing, CH4 or heavier hydrocarbons is much more feasible and is conducive to smaller hypersonic vehicles [2]. Therefore, predicting the products of cracking/reforming performed at temperatures and pressures representative of hypersonic flight becomes a critical step toward implementing this technology in future hypersonic propulsion.

In this paper we present results of modeling steam reforming and cracking using the DSMOKE (Double precision Simulation Model Of Kinetic Equations) software, developed at the Chemical Engineer Department of the Polytechnic of Milan [4] and several detailed kinetics mechanisms. The DSMOKE predictions are compared with experimental data supplied by TDA in order to validate the code and, especially, the kinetics databases utilized. Our aim is to show that it is possible to simulate the complex phenomena occurring during steam reforming and cracking by means of a relative simple tool and to obtain acceptable results with different reactants and conditions.

2.2 THE USE OF HYDROGEN VERSUS HYDROCARBONS FOR NATO HYPERSONIC VEHICLES

2.2.1 SINGLE FUEL ON THE BATTLEFIELD

The concept of using a single fuel on the battle originated after the Second World War, with the objective of simplifying the logistic supply chain for petroleum products. The move toward a single battlefield fuel truly began in the 1970's when NATO Air Forces agreed to change their operational fuel from the wide cut F-40 (US JP-4) to the less flammable kerosene fuel F-34 (US JP-8). A primary reason for this change was improved flight and ground safety based largely on US experiences during the Vietnam conflict. Hence, AVT-10 must carefully consider the implications of suggesting a weapon system fueled by liquid hydrogen.

Another major consideration of using a single F-34 (US JP-8) fuel is that the fuel is based on the fuel used for civil aviation. F-34 and JP-8 are the civil equivalents Jet-A-1 and Jet-A with a military additive package. Hence, the single battlefield fuel concept would have significant logistics advantages in terms of availability throughout the world. In 1988, NATO nations agreed through the AC/112 NATO Pipeline Committee on the acceptance of the Single Fuel Concept [2]. The concept is defined as:

"To achieve equipment interoperability through single fuel for use on the battlefield and for land based air operations, ensuring that the specification of the fuel is standardized with its commercial equivalent in common use in NATO Europe, and that the physical and chemical characteristics of the fuel are such that it can be introduced, stored, transported and distributed by the NATO Pipeline System."

In the United States, the Single Fuel Concept was adopted in March 1988 with issuance of Department of Defense (DoD) Directive 4140.43 titled Fuel Standardization. Since the issuance of the DoD Directive, the US has successfully used the Single Fuel Concept in a) Operation Just Cause (Panama), b) Operation Desert Shield/Storm, c) Operation Comfort (Turkey), d) Somalia, e) Haiti, f) Bosnia and g) Kosovo. The U.S. Army is committed to full implementation by 2010, and to train in peace as they fight in war.

Hence, a feasible hypersonic weapon system must consider not only hydrocarbon fuels, but specifically F-34 (JP-8), other than for pre-fueled vehicles (accelerators).

A cryogenic fuel, such as hydrogen, is an attractive propellant for hypersonic systems both from energetic and vehicle coolant perspectives. The constant pressure specific heat (Cp) of typical jet fuels at 344 K (160 oF) lies in the range from 2.15 to 2.30 kJ/kg K (0.51 to 0.55 BTU/lb oF). By contrast the constant pressure specific heat of hydrogen at 343 K (158 oF) is 14.38 kJ/kg K (3.44 BTU/lb oF). However, hydrogen's low energy density may result in aerodynamically unattractive vehicles. Cryogenic propellants also pose logistic and safety concerns, as evidenced by ground personnel requirements for cryogenic versus solid propellant rockets. Moreover, availability and cost considerations (Table 1) presently limit the use of hydrogen to specialty applications [3]. Hydrocarbon fuels have been shown to be competitive with cryogenic hydrogen for hypersonic cruise and two-stage-to-orbit (TSTO) airbreathing applications due to their much higher density and logistical benefits [e.g., 4, 5]. Furthermore, all-hydrocarbon orbital launch vehicle concepts might potentially provide payload fractions in the 3-4% range, a marked improvement over present shuttle class vehicles [6], albeit with an associated increase in complexity.

An alternative to hydrocarbon fuels, the Russian "AJAX" concept of steam reforming of liquid hydrocarbon fuels for hypersonic vehicles, has been discussed by Gurijanov and Harsha [7]. The concept is essentially a two-stage steam reforming process, with individual optimization of catalysts and temperatures for each stage. The first stage is steam cracking of the kerosene fuel to form primarily methane; the second stage is the highly endothermic steam reforming of methane to form CO and H2. Steam reforming offers a very large heat sink potential, at the expense of combustor heat release. Some data obtained recently in the USA with steam reformer Pt catalysts are given in Figures 3 through 5. These data have been modeled and is discussed further below.

Fuel	Formula	Freeze Point °C	Flash Point °C	Net Heating value kJ/m^3	Viscosity @ -40 °C mm^2/s	Cost** $/liter	Heat Sink
Hydrogen	H_2	-259.2	Gaseous	8133	0.0084 (0 C)	16.33	high
JP-7	$C_{12}H_{24}$	-44	63	34423	17	0.8	
JP-8	$C_{12}H_{22}$	-50	38	34674	10	0.24	
JP-10	$C_{10}H_{16}$	-79	54	39441	19	2.94	low
		↑ operability	↑ safety	↑ range	↑ operability	↑ economics	↑ cooling

Table 1. Properties of typical aviation fuels [3]*

*Hydrogen included for comparison
**Price paid by U.S. Air Force in 1998

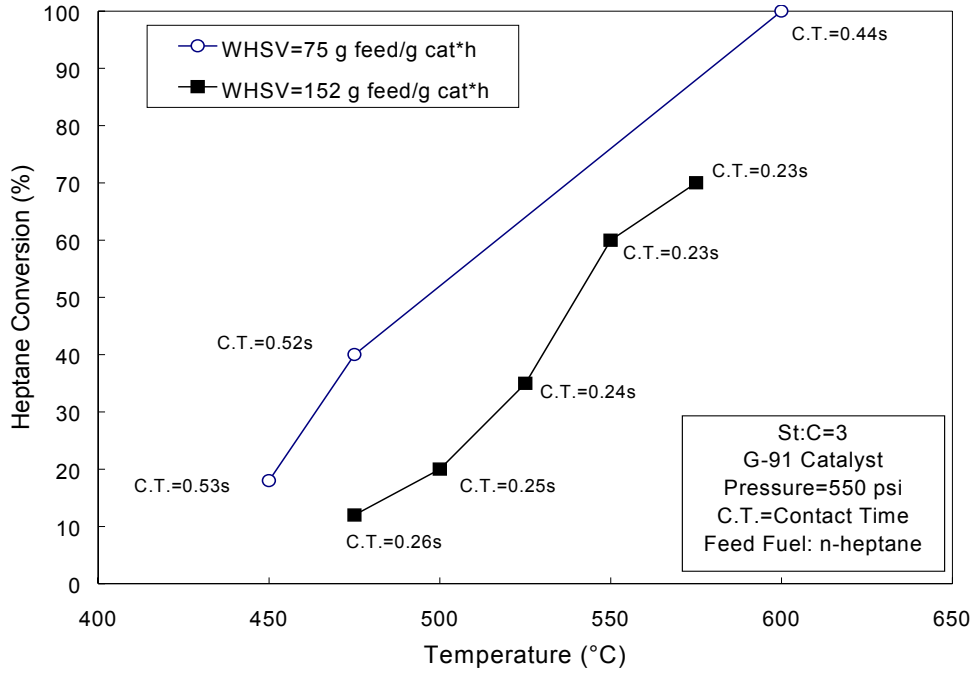

Figure 3: 1st stage n-heptane steam reforming results (courtesy of Dr. Dave Wickham, TDA, Inc.)

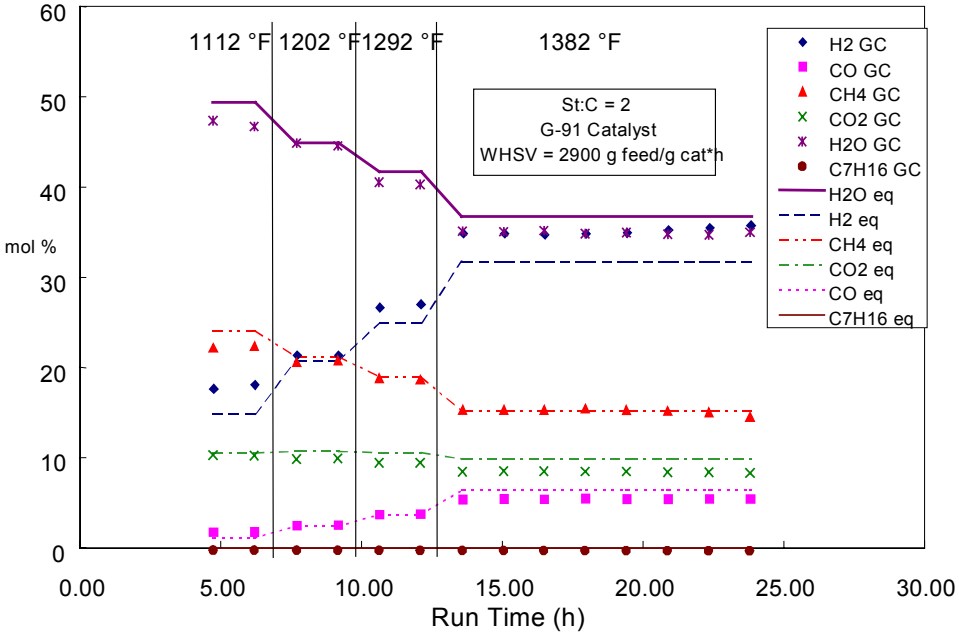

Figure 4: 2nd stage n-heptane steam reforming results (courtesy of Dr. Dave Wickham, TDA, Inc.)

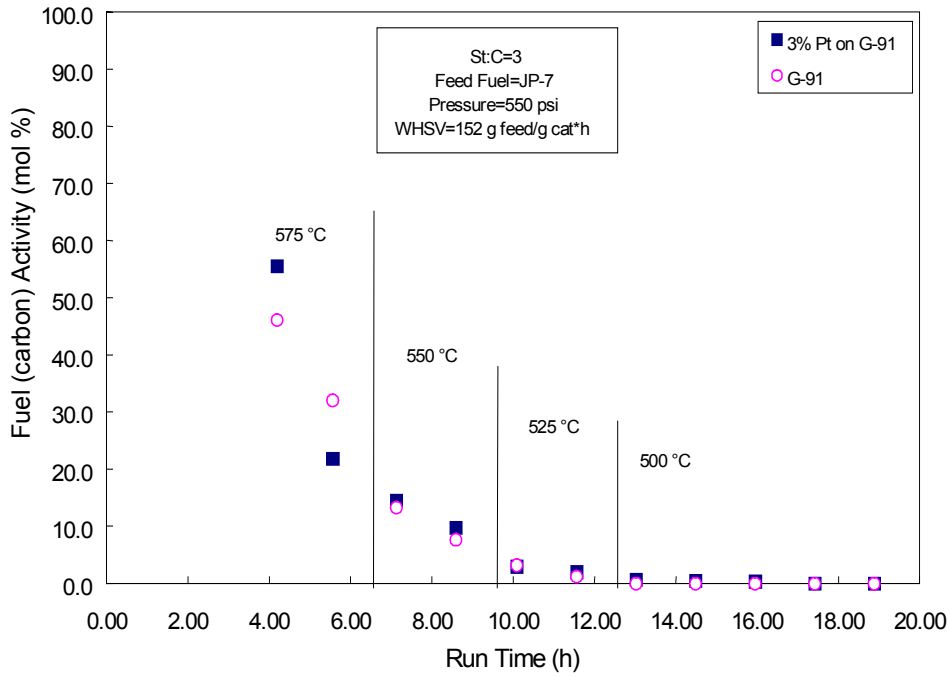

Figure 5: JP-7 steam reforming catalyst activity (courtesy of Dr. Dave Wickham, TDA, Inc.)

2.3 COOLING REQUIREMENTS FOR VARIOUS MANNED AND UNMANNED MILITARY SYSTEMS

The history of hydrocarbon fuel development has recently been reviewed by Maurice et al. [8]. The development of JP-7 for the U.S. SR-71 initiated a path to "high temperature fuels" development. The U.S. Air Force funded the Monsanto Research Corporation in the late 1950s characterized the effect of supercritical temperature exposure on liquid hydrocarbons and defined the new concept of an "endothermic fuel." Endothermic fuels feature an additional heat sink over that of conventional fuels by undergoing heat absorbing chemical reactions that are supported by energy extracted from heated air [9], (i.e. aerodynamically heated inlet air or compressor bleed). Laboratory data were generated which showed that, potentially, a large number of fuel components could reliably cool well into the supercritical regime. The results were succinctly presented at the 5th AGARD Colloquium in April, 1962 [10]. The use of endothermic fuels to power hypersonic vehicles will likely be realized in the 21st century.

Access into space either will require the use of airbreathing and rocket propulsion, in stages or integrated in a combined cycle. Hypersonic hydrocarbon fueled propulsion (Mach 4 - 10), with ramjets or scramjets, requires fuels that are stable at high temperatures and under extremely high heat fluxes. First generation endothermic fuels that chemically decompose into energetic gases via zeolite catalyst driven cracking reactions and provide 8 - 12 times the heat sink of JP-8 have been developed and are being tested in hypersonic propulsion system concepts. These fuels provide the cooling for structural integrity and durability of the propulsion system and convert the fuel into components that can be burned in a high Mach number (supersonic) combustor.

The heat sink requirements of a fuel have long been recognized [3], and there is generally quantitative agreement between various system trade studies. A plot of typical fuel heat sink requirements as a function of Mach number for both manned and unmanned systems is shown in Figure 6 [11]. A similar estimate is presented in Heiser and Pratt [12] for only engine cooling demand, and consequently their required heat sink at a given Mach number is somewhat lower than shown in Figure 5. The fuel heat sink required is dependent upon the engine design and size, cooling scheme design, structural materials selected, and cooling required by the airframe and other sub systems (such as avionics and flight controls). The heat capacity (Cp), and thus the sensible heat sink potential ($C_p\Delta T$, where ΔT is the available rise in bulk fuel temperature) of liquid hydrocarbon fuels computed is significantly lower than that offered by hydrogen as previously discussed. However, it was recognized in the late 1960s and early 1970s that heat sink in a fuel could be derived from two sources: the traditional sensible heat sink derived from heating of the fuel, as well as a chemical heat sink induced via fuel endothermic reactions [11].

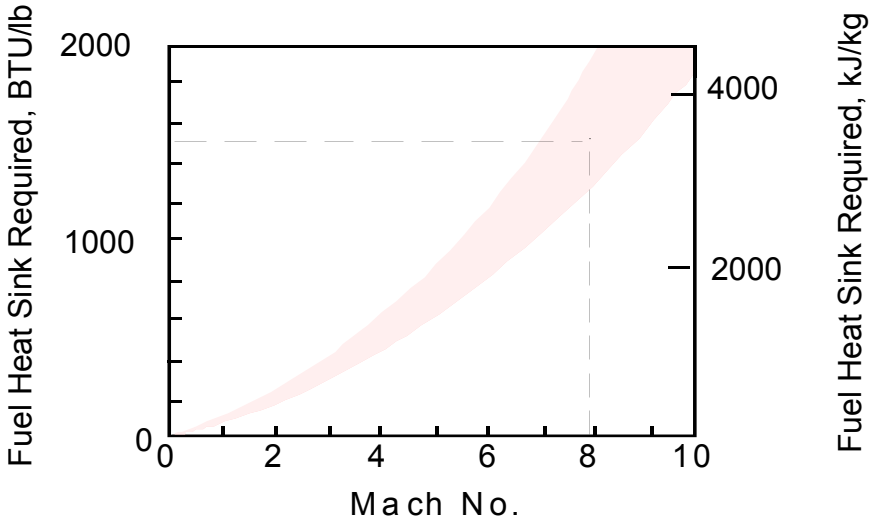

Figure 6: Heat sink required as a function of Mach number [11]. Lower bound - missiles, upper bound - aircraft.

At first glance there appears to be a contradiction between the terms endothermic and fuels. The outcome of a chemical reaction is either absorption or release of energy, and the latter is clearly essential to generate propulsive thrust. However, in the context of jet fuels, endothermic pertains to a class of reactions that take place in the fuel system prior to ignition. Endothermic fuels feature an additional heat sink over that of conventional fuels by undergoing heat absorbing chemical reactions that are supported by energy extracted from heated air, (i.e. aerodynamically heated inlet air or compressor bleed). The extent of the necessary endothermic reaction can vary from 0 % to nearly 100 % over the flight envelope as a function of cooling load requirements.

Endothermic fuel reactions can enable the use of airbreathing propulsion at hypersonic flight speeds without resorting to cryogenic propellants [3, 11, 13]. The relationship between fuel temperature and heat sink for thermally cracking of a kerosene-class hydrocarbon is shown schematically in Figure 7 [11, 14]. Typical kerosene-class fuels yield a total sensible heat sink of approximately 2300 kJ/kg (1000 BTU/lb) for fuels heated from ambient to 1000 K (1340 oF) [11]. By contrast, the heat sink for hydrogen under comparable conditions is 10,000 kJ/kg (4300 BTU/lb).

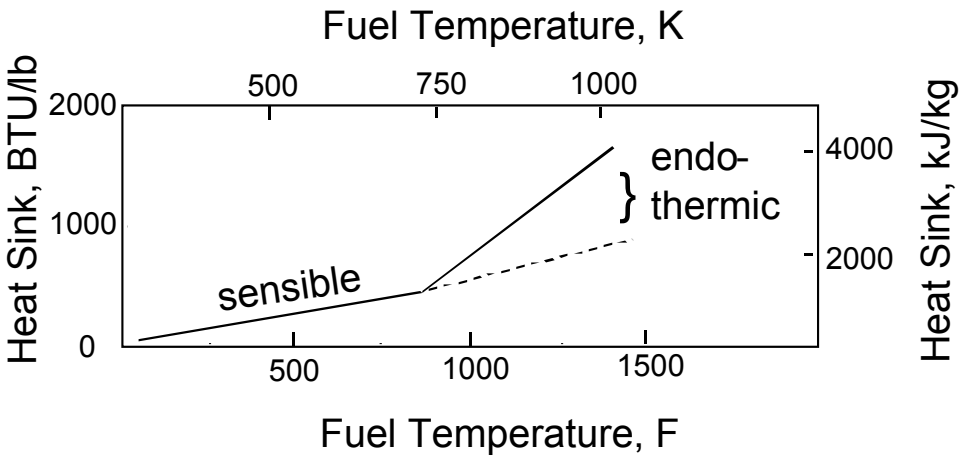

Figure 7: Notional diagram of fuel heat sink as a function of temperature.

2.3.1. CHARACTERISTICS OF ENDOTHERMIC FUELS

The chemical compositions of endothermic fuels have not been precisely defined to date. Nevertheless, it is apparent that these specialty fuels will comprise saturated linear and cyclic hydrocarbon molecules featuring at least seven carbon atoms. There are several options in selecting an endothermic fuel, as summarized in Table 2. Moreover, when the heat sinks of candidate fuels are compared in terms of propulsive energy (heat of combustion), hydrocarbons clearly became competitive with hydrogen (Table 3). The thermal decomposition reactions of hydrocarbon fuels feature a substantial activation energy barrier, and hence offer a potential heat sink. Moreover, the resulting heat of combustion of decomposition products remain essentially unchanged or slightly increased. Many types of fuel decomposition reactions have been considered for endothermic applications, including dehydrogenation, dehydrocyclization, dedimerization, cracking and steam reforming. Reaction classes and potential endotherms are defined in Table 2.

These endothermic reactions may be effected via either catalytic or thermal means. Whilst thermally driven endothermic reactions reduce fuel system complexity, catalytically-driven reactions afford enhanced reaction product selectivity and lower operational temperatures [11,14]. Dehydrogenation and cracking have received the most attention by far both in the U.S. and Russia [11, 13]. Consequently, these reactions are discussed next in some detail.

endothermic reaction	Reaction types	theoretical chemical heat sink, kJ/kg unreacted fuel	calc. heat of combustion of endothermic products, kJ/kg unreacted fuel
C_7H_{14} (methylcyclohexane) --> C_7H_8 (toluene) + 3 H_2	dehydrogenation	2190	45800
C_7H_{16} (*n*-heptane) --> C_7H_8 (toluene) + 4 H_2	dehydrocyclization	2350	47300
$C_{10}H_{10}$ (dicyclopentadiene) --> 2 c-C_5H_5	dedimerization	621	43630
$C_{12}H_{24}$ (kerosene) --> C_2H_4 (ideal)	cracking	3560	47200
$C_{12}H_{24}$ --> CH_4, C_2H_4, C_2H_6, etc. (actual)	cracking	<<3500	
$C_{12}H_{24}$ + 6 H_2O --> 9 CH_4 + 3 CO_2 (AJAX stage 1) CH_4 + H_2O --> CO + 3 H_2 (AJAX stage 2) Net: $C_{12}H_{24}$ + 15 H_2O --> 9 CO + 3 CO_2 + 27 H_2	steam reforming steam reforming steam reforming	net: (stage 1+2) 5490*	net: (stage 1+2) 21240
$2NH_3$ --> N_2 + 3 H_2	dehydrogenation	2720	19280
CH_3OH --> CO + 2 H_2	dehydrogenation	4000	20,420
2 CH_4 --> C_2H_2 + 3 H_2	addition/ dehydrogenation	11765	62,860
Benzene (C_6H_6) --> 3 C_2H_2	ring fracture of aromatics	7650	48280
Decalin ($C_{10}H_{18}$) --> naphthalene ($C_{10}H_8$) + 5 H_2	dehydrogenation	2210	40700

Table 2. Chemical heat sink values for various endothermic fuels [3]. Heat sink for kerosene calculated using dodecane heat of formation as an approximation. *Heat sink for steam reforming on total propellants (fuel + water).

Naphthenic (cycloparaffin) fuels can be dehydrogenated to aromatics and hydrogen. The classic example of this type of reaction is the catalytic dehydrogenation of methylcyclohexane (MCH, c-C7H14) to toluene (C7H8) and hydrogen [11].

$$c\text{-}C_7H_{14} \quad = \quad C_7H_8 \quad + \quad 3H_2$$

This reaction provides a theoretical endothermic heat sink of 2190 kJ/kg (940 BTU/lb).
Supported platinum catalysts in packed beds have been used to demonstrate chemical heat sinks for dehydrogenation of methylcyclohexane near the theoretical value of 2190 kJ/kg (940 BTU/lb). Heat fluxes up to 170 W/cm2 (150 BTU/ft2-s) have been achieved. The reaction yield could approach near 100%, dependent upon the amount of heating supplied. The U.S. Air Force sponsored large efforts at the Shell Development Corporation in the 1960s and early 1970s and Allied-Signal Aerospace in the 1980s and early 1990s to study catalytic dehydrogenation of fuels for advanced systems [3]. The Allied-Signal work culminated in the testing of a coupled endothermic fuel/air heat exchanger reactor and combustor [3].

Fuel	Heat of combustion kJ/kg	Total heat sink (chemical + physical) at 1000 K (1340 °F) kJ/kg	Ratio of heat sink/heat of combustion
H_2	128823	13931	0.108
Norpar 12	43654	3950	0.090
C_7H_{14} (methylcyclohexane)	45800	5074	0.110
CH_3OH	20420	5897	0.289

Table 3. Cooling capacities of candidate endothermic fuels as a function of propulsive efficiency (heat of combustion) [3].

Another plausible reaction, which affords a high endothermic heat sink, is cracking of liquid hydrocarbon fuels [11,13,14]. The cracking reaction will naturally occur at higher temperatures than dehydrogenation, or it may be enhanced through the use of catalysts or chemical initiators. The endothermicity of this reaction depends strongly on the products produced. For example, the cracking reaction of n-decane may proceed via a number of paths producing hydrogen and a variety of smaller hydrocarbons. The realizable theoretical endothermicity for n-decane cracking is dependent on the products of reaction. The production of acetylene affords the maximum theoretical endothermic heat sink of 9800 kJ/kg (4200 BTU/lb).

$$n\text{-}C_{10}H_{22} \quad = \quad 5C_2H_2 \quad + \quad 6H_2$$

Unfortunately, acetylene production requires reaction temperatures above 1000 K (1340 °F), which exceed reactor and catalyst materials limits, and demands unrealizable catalyst product selectivity (the ability of the catalyst to enhance the formation of desired products) [14].

The production of ethylene, a more saturated compound, reduces the theoretical endothermic heat sink to 3600 kJ/kg (1545 BTU/lb).

$$n\text{-}C_{10}H_{22} \quad = \quad 5C_2H_4 \quad + \quad H_2$$

The temperature necessary for equivalent conversions is lower, ensuring the survival of the heat exchangers and catalysts, but catalyst product selectivity remains problematic. Finally, production of saturated compounds, which feature negative heats of formation, further decreases the endothermic heat sink.

In reality, cracking produces a mix of products, from both endothermic and exothermic reactions. The products are dependent both on catalyst product selectivity and reactor operating conditions such as temperature, pressure and residence time. The endothermic cracking of a normal paraffin blend with average carbon number 12 (Norpar 12) in the presence of inexpensive, commercially available zeolite catalysts at 1000 K (1340 oF) has been investigated experimentally by Sobel and Spadaccini [14]. The product efflux consisted primarily of low molecular weight alkenes and alkanes (ethylene, propene, propane, ethane and methane) and hydrogen. An actual total heat sink of approximately 3950 kJ/kg (1700 BTU/lb) at 1000 K (1340 oF) was measured; the chemical heat sink was 1740 kJ/kg (750 BTU/lb). At higher temperatures, both increased sensible and chemical heat sinks can be obtained. Ianovski [13] showed a total heat sink of 5000 kJ/kg (2150 BTU/lb) at 1170 K (1650 oF) for cracking of endothermic fuel T-15. T-15 is referred to as a fuel which has properties that "are not distinguished from the standard jet fuels such as Russian T-6 or American JP-7". The resulting products from all experiments featured attractive combustion characteristics.

Other alternatives have been presented to the "standard" cracking and dehydrogenation endothermic reactions such as the "AJAX" concept discussed above [7]. Other non-hydrocarbon fuels, such as methanol and ammonia, could conceivably be used for applications where heat sink requirements are more pressing than heat release. Another example of a highly endothermic fuel is the reaction of methane to form acetylene and hydrogen [15]. However, it must be recognized that these reactions will not proceed to 100% completion as written in Table 2, but instead yield other intermediate products with associated lower heat sinks. The endothermic reaction selection for the first fielded liquid hydrocarbon-fueled hypersonic vehicle will most likely be either cracking or dehydrogenation.

For catalytically-driven fuel reactions, the Arrhenius rate expressions differ from those governing thermal cracking. The reactions are modeled to occur at the surface of catalyst particles or catalyst-coated

surfaces, with the surface temperature replacing the fuel temperature in the Arrhenius expression for the rate constant [11, 14, 16]. Naturally, at high fuel temperatures both thermal and catalytic reactions occur, with surface (catalytic) reactions promoted by high surface temperatures. Consequently, catalyst-coated heat transfer surfaces are preferred to packed beds, because wall-coated catalysts expose the fuel to the highest temperature at the catalyst surface. By contrast, in packed beds the fuel transfers heat to the catalyst, so the fuel catalyst interface is the coolest surface in the system. It may also be noted that chemical initiators can be used to enhance the fuel reaction rate [13, 17, 18].

2.4 REQUIREMENTS AND STATUS OF SOFTWARE TO GENERATE PHYSICAL AND CHEMICAL PROPERTIES AT SUPERCRITICAL CONDITIONS FOR CANDIDATE HYDROCARBON FUELS FOR HYPERSONIC SYSTEMS.

There are several sources of data for fuel properties over a wide range of temperature and pressure. The source in most widespread use is the Coordinating Research Council Report 530 –"Handbook of Aviation Fuel Properties" [19]. This handbook contains a wide variety of physical property data for aircraft and missile fuels. The Defense Energy Supply Center also provides a database for specification properties measured for the various purchases of JP-8 [20]. This database allows the assessment of the variation of specification physical properties with time and/or location. Also available are commercial physical property codes used in the petroleum industry, where a petroleum fraction (gasoline, kerosene, etc.) is characterized by general available measures, such as boiling range and specific gravity (density). An example of such a code is PPDS2 by NEL [21]. Typical JP-8 data used as input is shown in Table 3. Data from several of these types of calculations are available, which include density, viscosity, thermal conductivity, and heat capacity [22-25]. These types of calculations have been in widespread use for more than 50 years to characterize petroleum fractions. Another option is to approximate the multi-component fuels with surrogates consisting of a much smaller number of components [26]. Then, the fuel properties can be calculated by a code such as PPDS2 or NIST's Supertrapp [27]. A published JP-8 surrogate is shown in Table 4 [28]. A comparison of several calculations of density is shown in Figure 8. The results of the various calculations are usually consistent. However, at high temperatures (Figure 9) there are significant discrepancies in density predictions. New data and refined predictions are needed at high temperatures.

Table 3 – Typical JP-8 properties used for PPDS2 calculations

Boiling range, K	
10%	446
30%	473
50%	483
70%	495
90%	527
Specific gravity	0.809

Table 4 -JP-8 surrogate [28].

Compound	wt %
iso-octane	5.0
methyl cyclohexane	5.0
m-xylene	5.0
cyclooctane	5.0
decane	15.0
butyl benzene	5.0
1,2,4,5 tetramethyl benzene	5.0
tetralin	5.0
dodecane	20.0
1-methyl naphthalene	5.0
tetradecane	15.0
Hexadecane	10.0

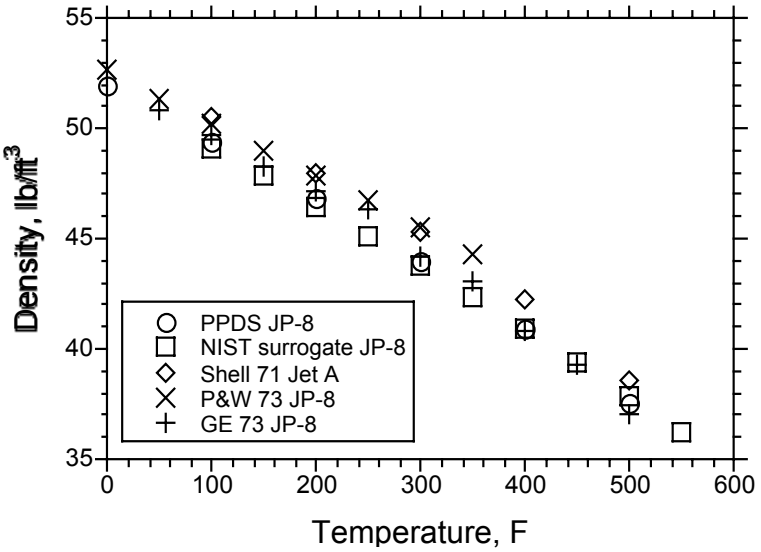

Figure 8: Comparison of various calculations for fuel density: PPDS [20] NIST Supertrapp [27] using Table 4 surrogate, and three other data sets [22, 25, 26].

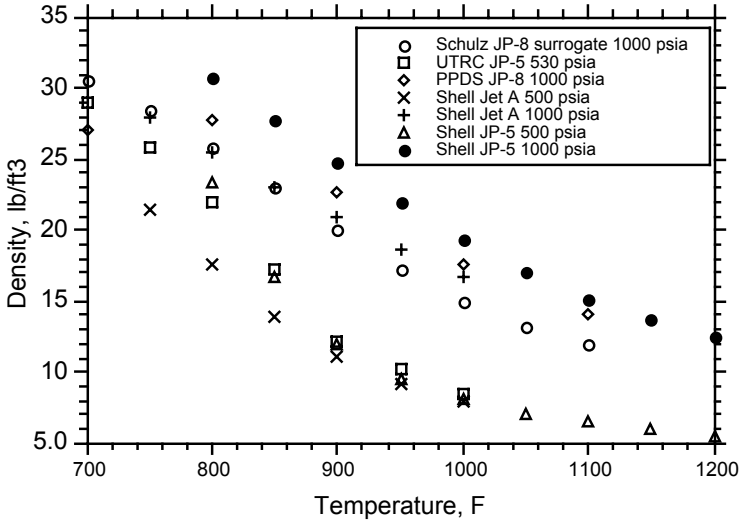

Figure 9: Comparison of various calculations for fuel density at higher temperatures.

2.5 ENDOTHERMIC FUEL MODELING

2.5.1 PREDICTIVE TOOLS – STEAM REFORMING FUEL REACTIONS COMPUTATIONS

In order to reproduce the set of experimental data from TDA research inc., (shown above) a number of simulations have been performed by the university of Rome group. The strategy consisted of (1) reproduce the data by means of a general purpose kinetics model ("SOXKERO"); (2) analyze the results obtained in the first step and, (3) develop new kinetics model ("newstref") based on those reactions which have the strongest influence on the steam reforming mechanism. Several simulations were done, changing the inlet conditions for

the reacting flow. Different conditions were considered, i.e. different pressures, steam-methane ratios (Sc), outlet temperatures, and flow rates.

A plug flow reactor, was assumed dimensioned as in the tda experiments, and simulated three different thermal behaviors: adiabatic, isothermal, and a linear temperature profile. In this last case the outlet temperature (Tout) was fixed to that measured in the experiments, and the inlet temperature (Tin) increased. this means the reactor had a decreasing temperature profile if Tin>Tout, or if Tout>Tin.

These calculations were done using the dsmoke software tool, simulating a sequence of reactors and equipment like splitters and mixers. In the simulations, the scheme used is simple: two different streams with flow rate values set to obtain, after mixing, the nominal steam-methane ratio, were mixed and sent to the plug flow unit (see figure 10).

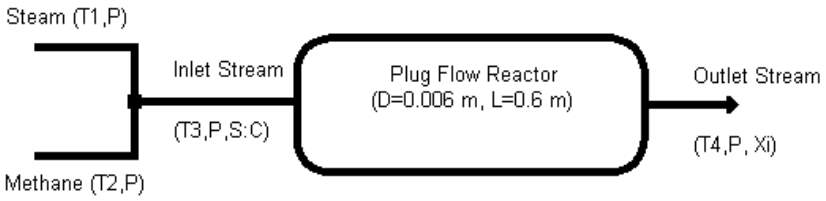

Figure 10: Scheme of the simulated system

During reaction emphasis was placed on methane conversion, inside temperature, and molar fractions of the most important compounds involved in steam reforming, namely CH4, H2O, H2, CO, and CO2. However, the trends of other species were also assessed.

2.5.2 THE GENERAL KINETICS MODEL

The first step of this work was to simulate the experimental data by using a general kinetics model (called SOXKERO) supplied as default in the DSMOKE code.

2.5.3 ADIABATIC CASE

In Figure 11 some results are presented for the adiabatic plug flow reactor (PFR) (P=37.4 atm, SC=1). In the figure some of the mole fractions of the principal species versus the inlet temperatures (T3) are shown. The simulated data do not fit very well the experimental ones (see Figure 12) We notice, for the same amount of unconverted methane, a greater production of hydrogen than measured and a higher concentration of residual steam. This may mean that under the conditions assumed, the general kinetic model is emphasizing principally the thermal cracking reactions while the mechanism involving steam reforming reactions is underestimated. Furthering this tentative conclusion is also small amount of carbon monoxide in the outlet stream; in general this molecule is an index of the importance of steam reforming reactions by the model used (a small percentage of CO indicates the influence of cracking larger than steam reforming). Moreover, a broad range of heavier species was predicted in the outlet stream and shown in Figure 13: among them, significant quantities of C2H6 and C2H4; but also of other heavy molecules like, pyrene, C10H8, C12H8 and others typical of cracking.

Following the species trends during the reaction time one can see that the reactions occur mainly during the first 2-3 minutes, and in the reactor sections in which the inside T is higher. Since the general process is endothermic, the T decreases moving further along the reactor, and the kinetics slow down and tend to an asymptotic limit. In these adiabatic simulations the outlet temperatures predicted are very much lower than the experimental ones. To make the simulated Tout equal to the real case, it was found necessary to send an input stream with a Tin >1600°C (too high even for a stainless steel!). From these considerations, it was concluded the adiabatic PFR was not a realistic assumption when trying to reproduce the real data, and hence it was not used in subsequent simulations.

2.5.4 ISOTHERMAL CASE

The isothermal case is at the other end of the spectrum compared to the adiabatic assumption above and expected to give better solution. Attention was focused on the data at high pressure (550 psi – 37.4 atm:) testing several carbon/steam ratios, steam flow rate (F1) and the inlet temperature (T3). Only some the results are presented in Figures14-18: in the same figures we report, for sake of simplicity, the experimental data and the results obtained by the other kinetic model used later in going further in simulations (see above).

One can immediately see that at low temperature the agreement is still not satisfactory. We observe again a larger than measured production of H2 and little unconverted CH4, as if the general kinetics was faster in the simulation than during experiments. This behavior is observed at almost every temperature. Only at the highest temperatures, the kinetic rate of the simulations seems to be equal to what measured. To explain these facts, and keeping in mind the high surface/volume ratio of the reactor, it can be conjectured wall quenching may occur in the experiments that the DSMOKE code could not reproduce. At high temperature, the alloying elements of the stainless steel (Ni and Cr) may have, instead, a catalytic effect in the dehydrogenation reactions.

At this same p=550 psi, changing the s:c ratios to 1.5 does not change the behavior of simulations. Again, an over-prediction of H2 in the simulated test is noted, arguably caused by the leading role played by cracking reactions.

2.5.5 LINEAR TEMPERATURE PROFILE CASE

In this case, the temperature inside the reactor was assumed to have a linear profile from the inlet to the outlet (set like in the experimental data). In Figures 18-20 select results are presented. Figure 18 shows results for the highest pressure used. Again, for the same H2 production predicted (Ti=1300 K) a smaller conversion of steam, under-predicted CO in the outlet stream and, approximately, the same CH4 conversion. As can be seen in Figure 18, the other simulated linear T profiles (Ti=1250 K, Ti=1200 K, Ti=1150 K) yield increasingly poorer results. These results can be summarized concluding that arguably the principal path followed by this model is cracking reactions.

Figures 19 and 20 show the results for p=30.6atm and S:C=1 and S:C=2.77 respectively; for these conditions the residual methane is greater for the low SC ratio (%CH4 $\cong$ 13%) than for the high SC ratio (%CH4 $\cong$ 20%). Simulations provide different answers: the methane conversion is smaller for the low S:C ratio than the high one. For the conditions of Figure 18, since the general kinetics is slower in the simulation, under-predicted H2 and a smaller conversion of steam is observed. By contrast, for S:C=2.77, a greater production of hydrogen than measured and, as a consequence, a greater conversion of steam is observed.

2.5.6 CONCLUSIONS

The results of this batch of simulations can be summarized as following point:

- the "*SOXKERO"* (default) model used was developed mainly to simulate petrochemical processes and, in particular, cracking processes. The results tend to show this feature: cracking has a decisive influence in the global system reactivity;
- the disagreement between experimental data and simulated tests may be explained also by the catalytic effects some alloying elements present in the stainless steel might have. If this is case, the "*SOXKERO*" and DSMOKE were unable to provide realistic answers (DSMOKE cannot simulate surface chemistry). Moreover, geometry and dimensions of the reactor should be accounted for: the experimental equipment has a large surface/volume ratio and this will enhance catalytic experimental effects even if per se not so obvious.

2.5.7 MODIFIED KINETICS MODEL

Following the results above, a second kinetics model was developed. The basic philosophy was to include a larger number of reactions involved in steam reforming. More reactions were added to the model in order to strengthen the production on hydrogen following the interaction of methane and its radicals with the OH radicals. Then we slightly modified the activation energy of the most important reactions in the methane dehydrogenation chain ($CH_{x+1} \rightarrow CH_x+H$), and those that can give water ($CH_{x+1}+OH \rightarrow CH_x+H_2O$). Some of the results of this new model (called "*newstref*") are presented in figures 14-17[1]. In a general overview of these graphs, one can see that this new model gave us not so good results. The considerations done for the former model (*SOXKERO)* are still good for this latter (see how, at p=37.4atm and at low temperature (1108 K) the real

[1] In these figures some results obtained using a third kinetics model ("*2000"*) are shown. This model was developed from a more complete kinetics scheme than *SOXKERO*'s source, but without modifying the kinetic parameters, as in *NEWSTREF*.

kinetics is slower than the simulated, with the opposite behavior at high temperature (1211 K). As stated above, the behavior at p=30.6 atm (450 psi) is very interesting: at low s:c ratio (1.34) we observe a faster real kinetics. Increasing the SC ratio (and the steam flow rate) the simulated kinetics become faster and faster while the real one slows. The lack of experimental data doesn't allow to say whether this behavior occurs at other pressure or the data, in these conditions, are not perfectly reliable. For every condition (see Figures 14-17), the answers of the different models are approximately the same, so we argued that modifying only kinetic parameters of few important reactions was not enough to balance cracking and reforming phenomena. For this reason, we created another kinetics model. The intent was to approximate, as much as possible, the catalytic effects of Ni and Cr present in stainless steel. Both these metals, commonly used in refining process, are very effective for dehydrogenation. By weakening C-H bonds (whose strengths, depending on their position in the molecule, is 90-110 kcal/mol), H* and other light radicals are quickly generated. The latter are generally oxidized *in situ,* preventing formation of heavy cracking products. To roughly simulate catalytic behaviour, we doubled the efficiency of the generalized reaction $R+H_2 > RH + H^*$ and switched off several radicals producing reactions. This means that radicals are almost completely depleted as soon as they are created, so cracking is no longer the most important reaction pathway. In other words, light species kinetics was artificially enhanced to the detriment of heavy species production.

This new model (called "*KINEX*") gave us the best results, as one can see from figures 21-25 (simulations done with a linear t profile reactor): at every pressure, the difference between the simulations and the experimental tests are very little. Only in those conditions discussed previously (p=30.2 atm, S:C=2.77), the agreement was not satisfactory (see figure 24). Our model seems not to be general and that was expected: a perfect fitting between experimental data and results obtained by a mono-dimensional kinetics code without a catalysis model looks unfeasible.

2.5.8 CONCLUSIONS

It is possible to use a simple kinetic model to predict the real behavior of a methane-steam reforming systems. In order to have a more precise and reliable model, a realistic reactor model must be assumed. Hence, a kinetic model in which the catalytic effects of stainless steel of the reactor are involved should be developed.

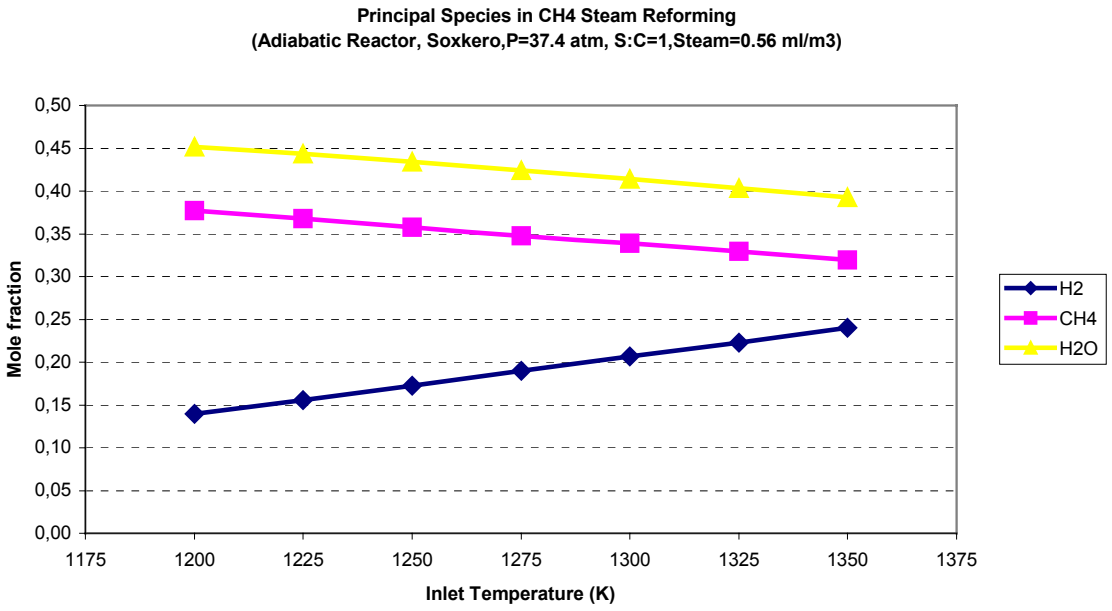

Figure 11: Results for adiabatic reactor using the general kinetic model (Soxkero, P=37.4 atm, S:C=1)

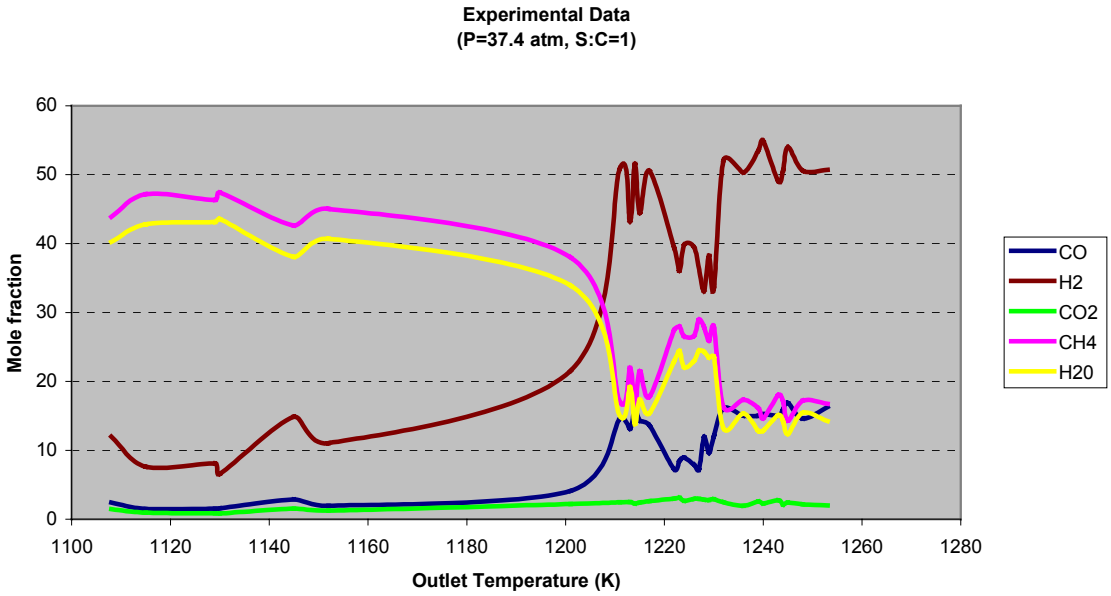

Figure 12: Experimental data (P=37.4 atm, S:C=1)

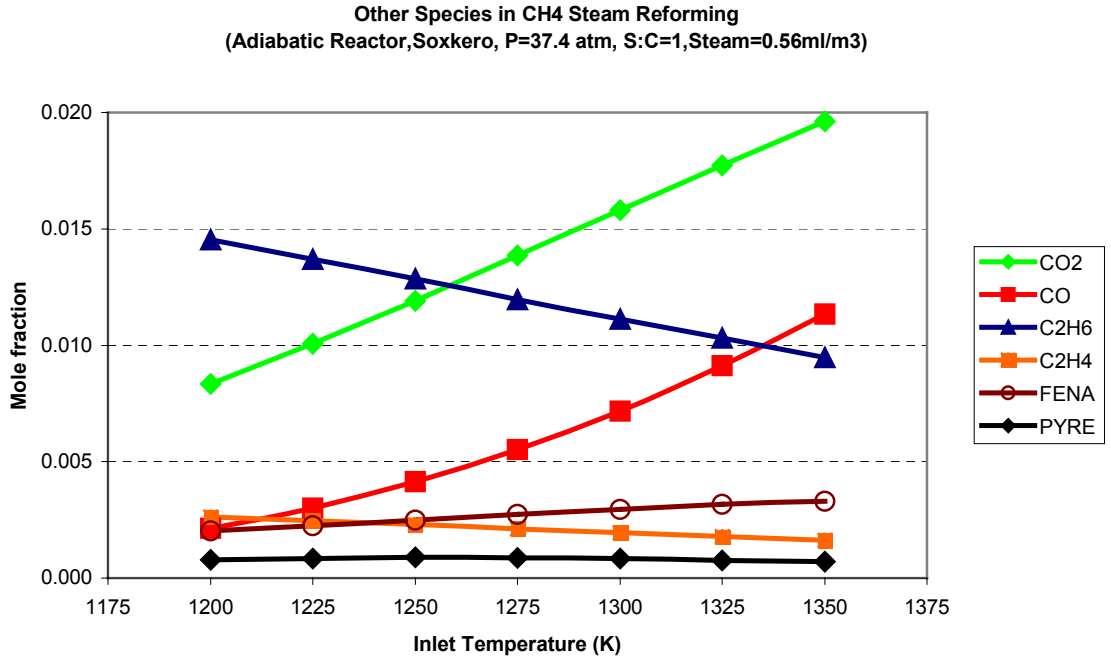

Figure 13: Other species in adiabatic reactor simulations (Soxkero, P=37.4 atm, S:C=1)

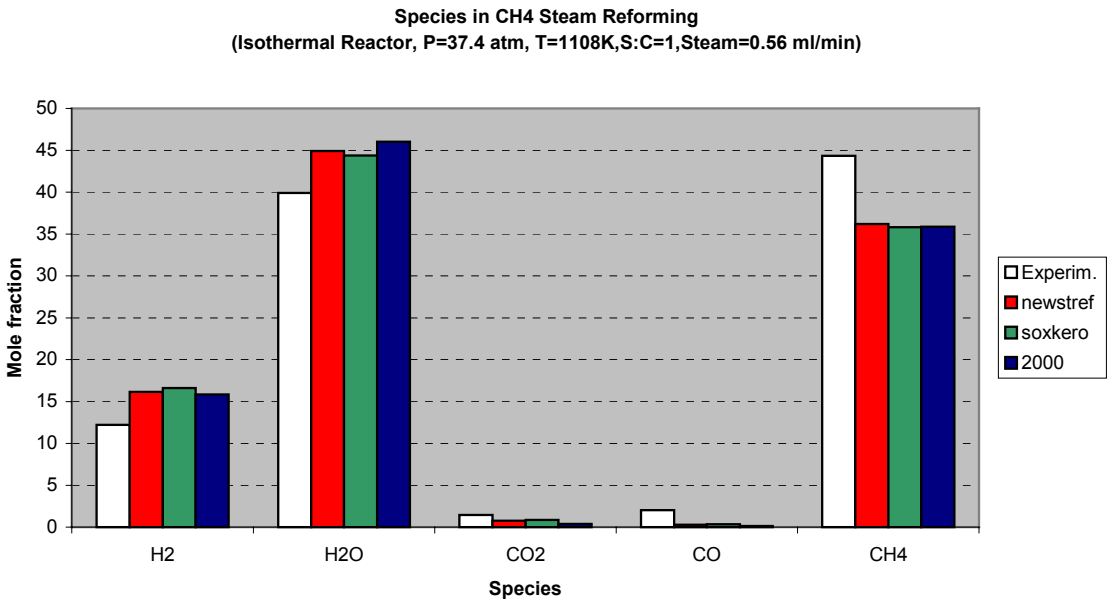

Figure 14: Results for isothermal reactor using three different kinetic model (P=37.4 atm)

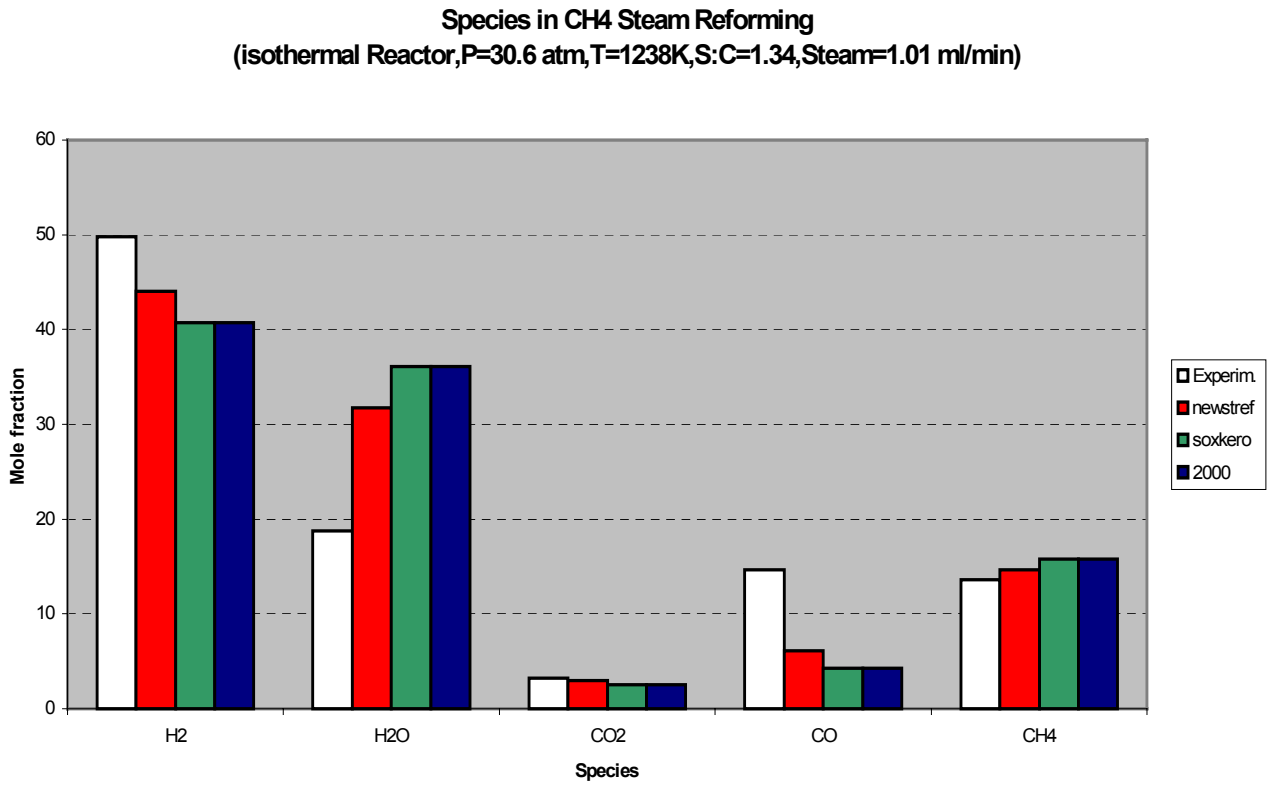

Figure 15: Results for isothermal reactor using three different kinetic model (P=30.6 atm)

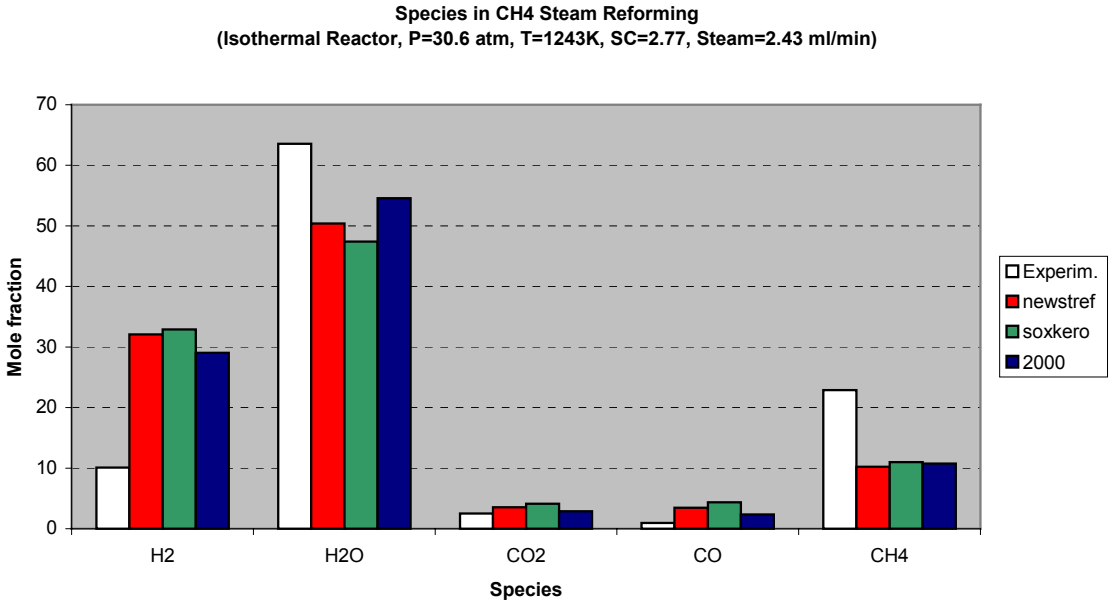

Figure 16: Results for isothermal reactor using three different kinetic model (P=30.6 atm)

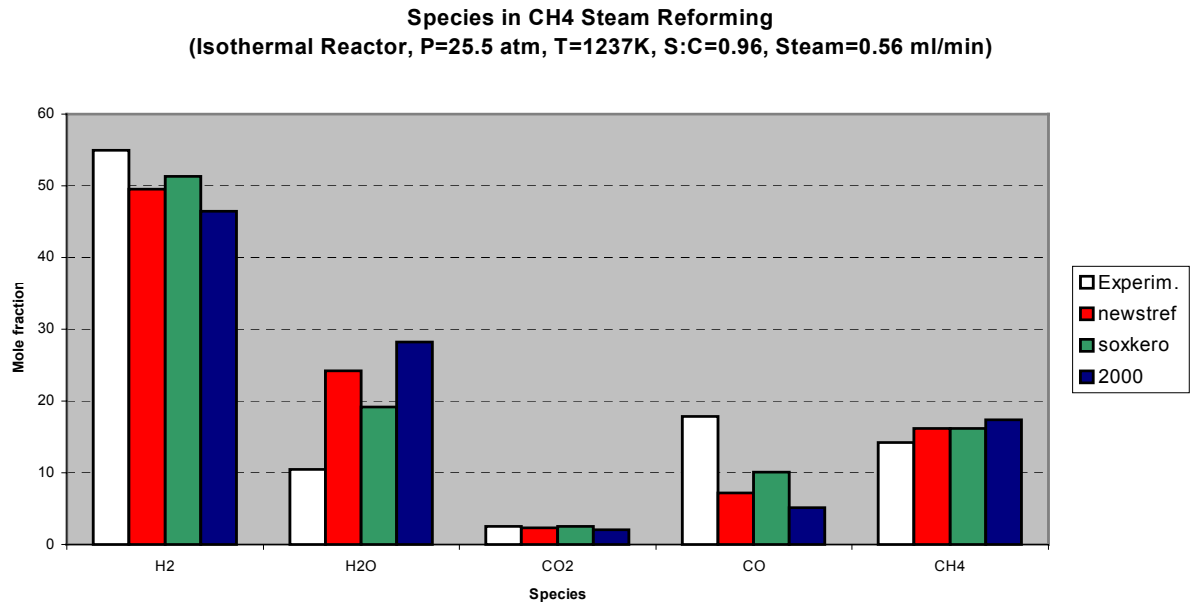

Figure 17: Results for isothermal reactor using three different kinetic model (P=25.5 atm)

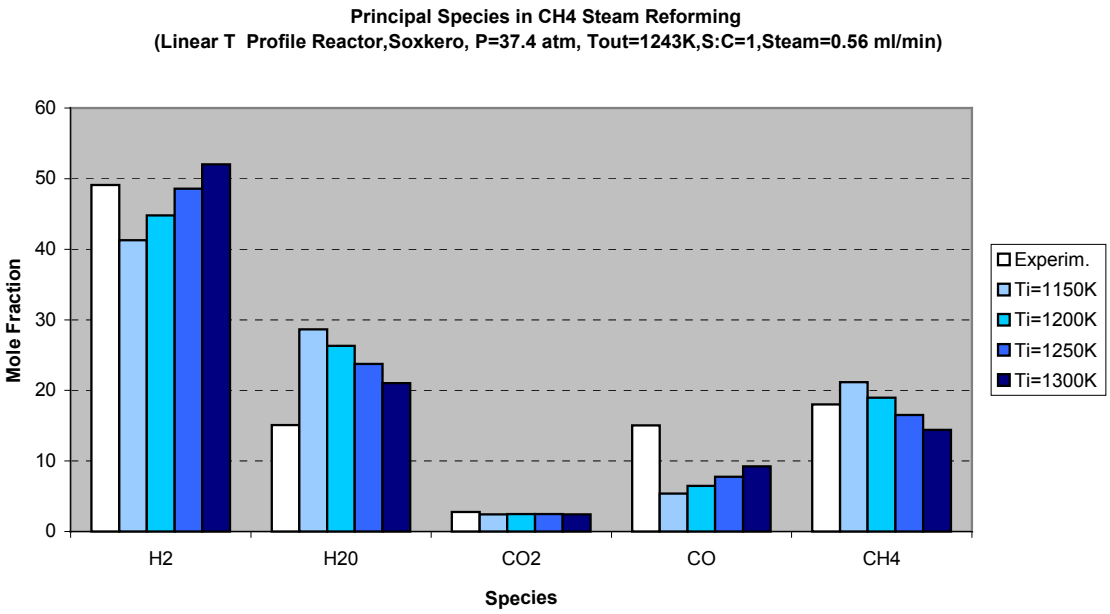

Figure 18: Results for linear T profile reactor (Soxkero, P=37.4 atm,Tout=1243K, S:C=1)

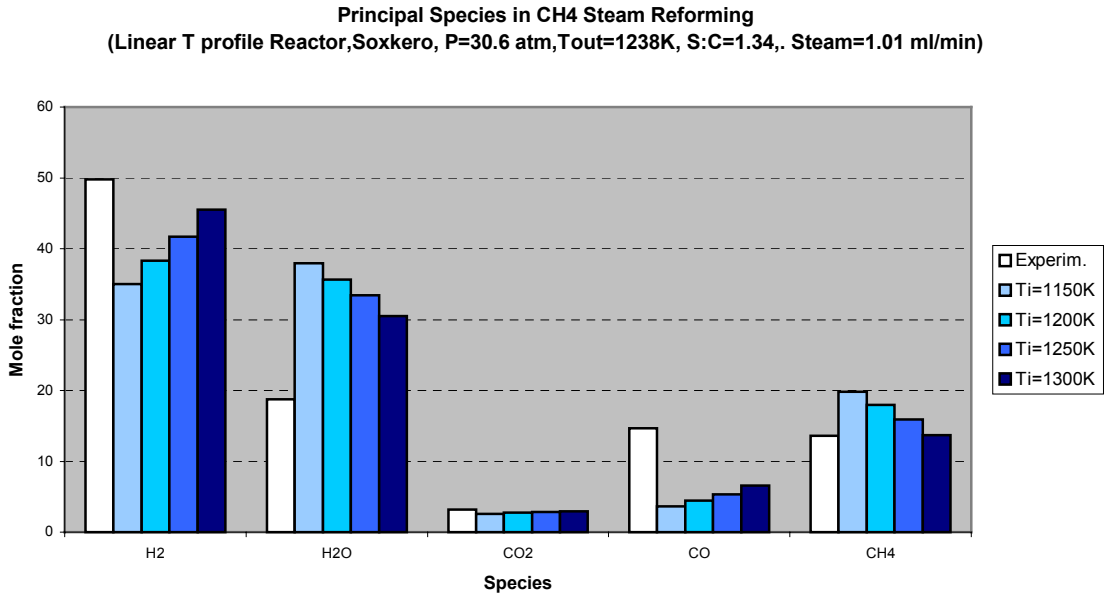

Figure 19: Results for linear T profile reactor (Soxkero, P=30.6, Tout=1238K,S:C=1)

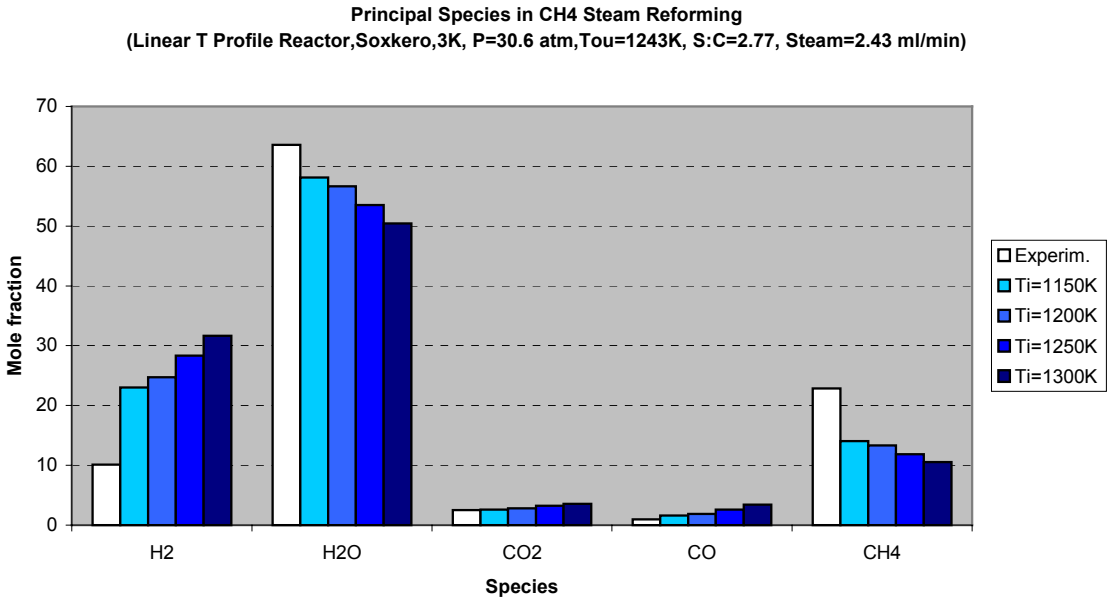

Figure 20: Results for linear T profile reactor (Soxkero,P=30.6 atm, S:C=2.77)

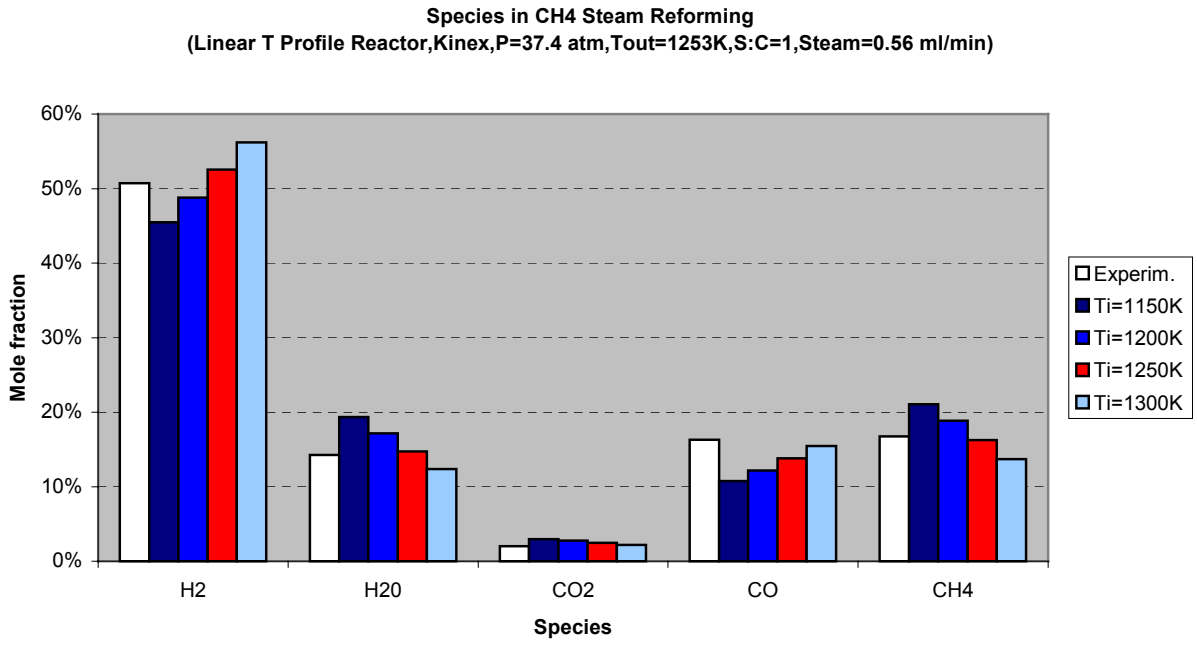

Figure 21: Results for linear T profile reactor (kinex, P=37.4 Tout=1253K,S:C=1)

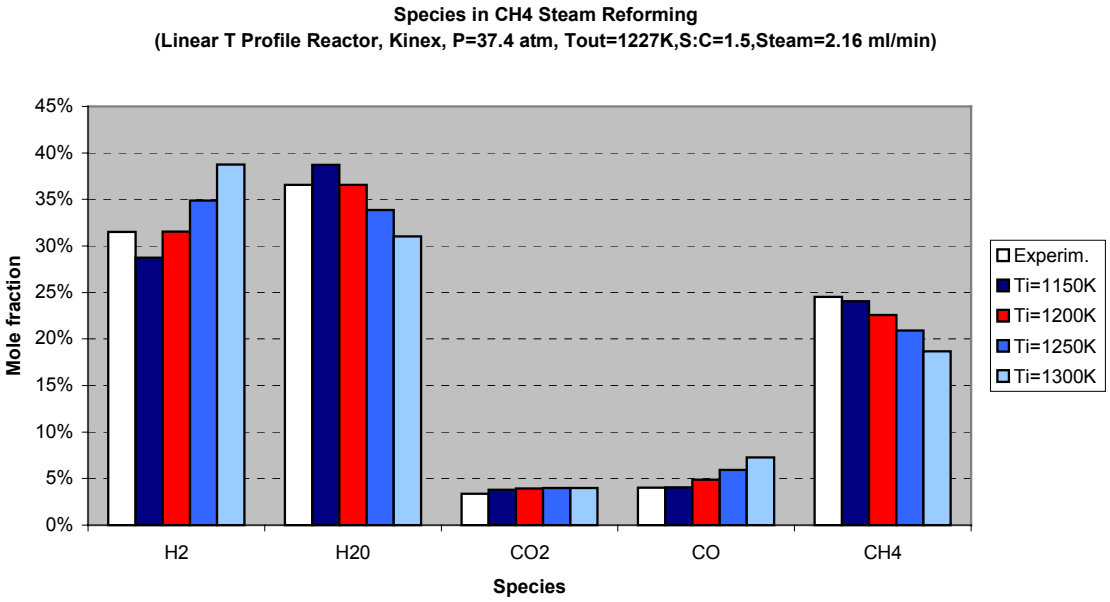

Figure 22: Results for Linear T Profile reactor (kinex, P=37.4, Tout=1227K,S:C=1.5)

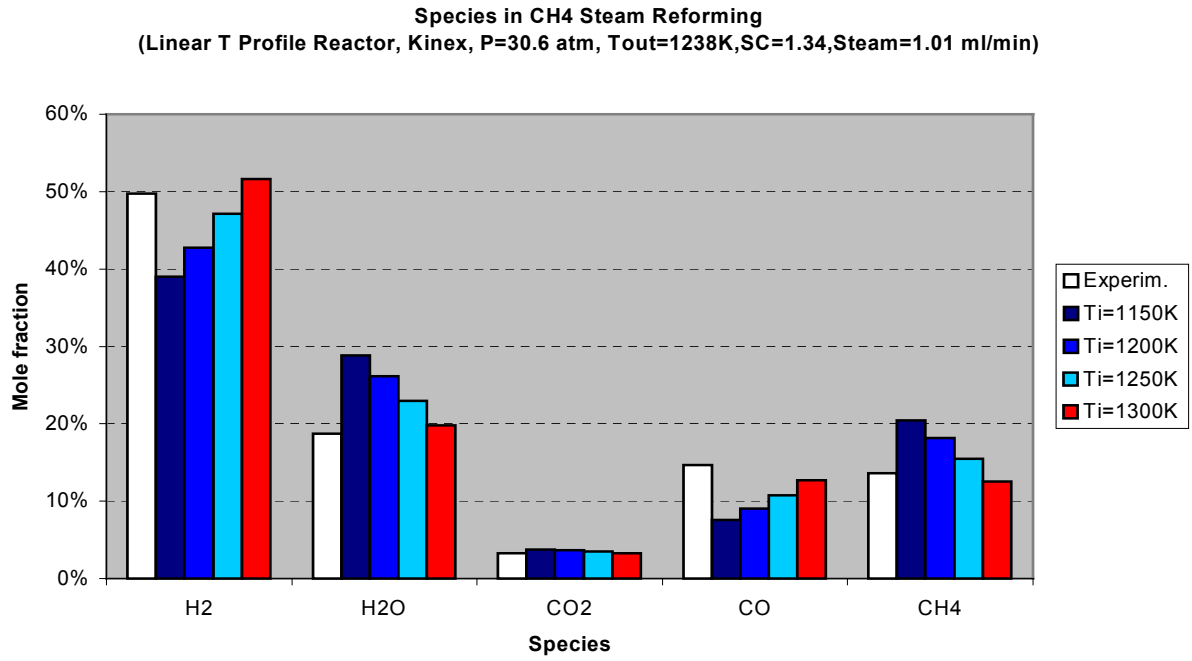

Figure 23: Results for isothermal reactor (kinex, P=30.6 atm, Tout=1238K, S:C=1.34)

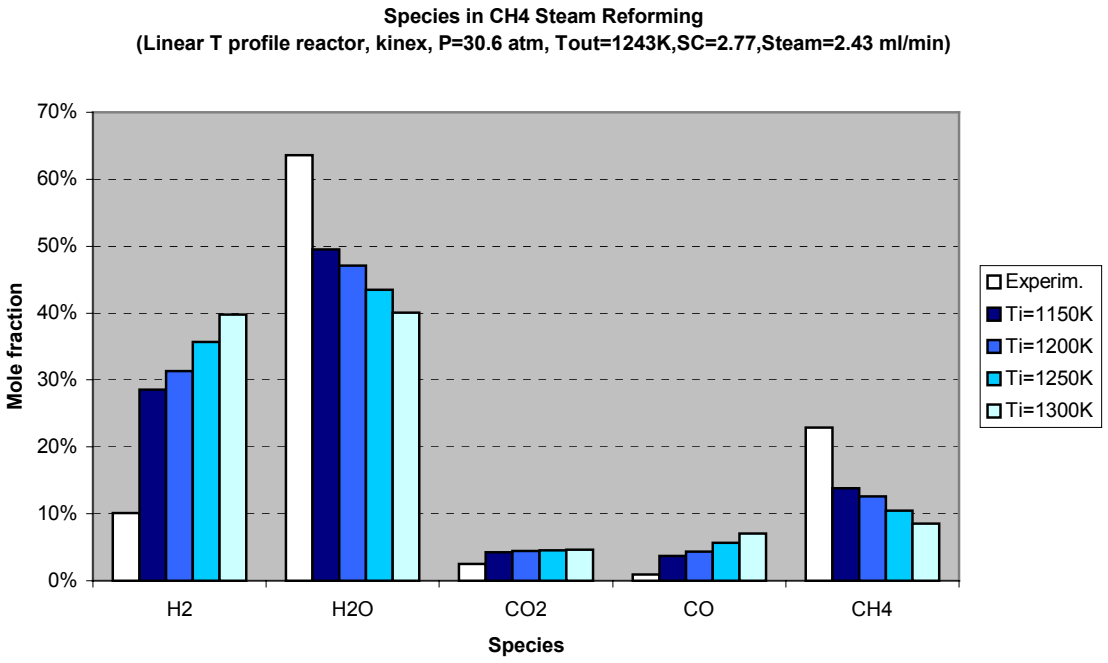

Figure 24: Results for linear T profile reactor (kinex, P=30.6 atm, S:C=2.77)

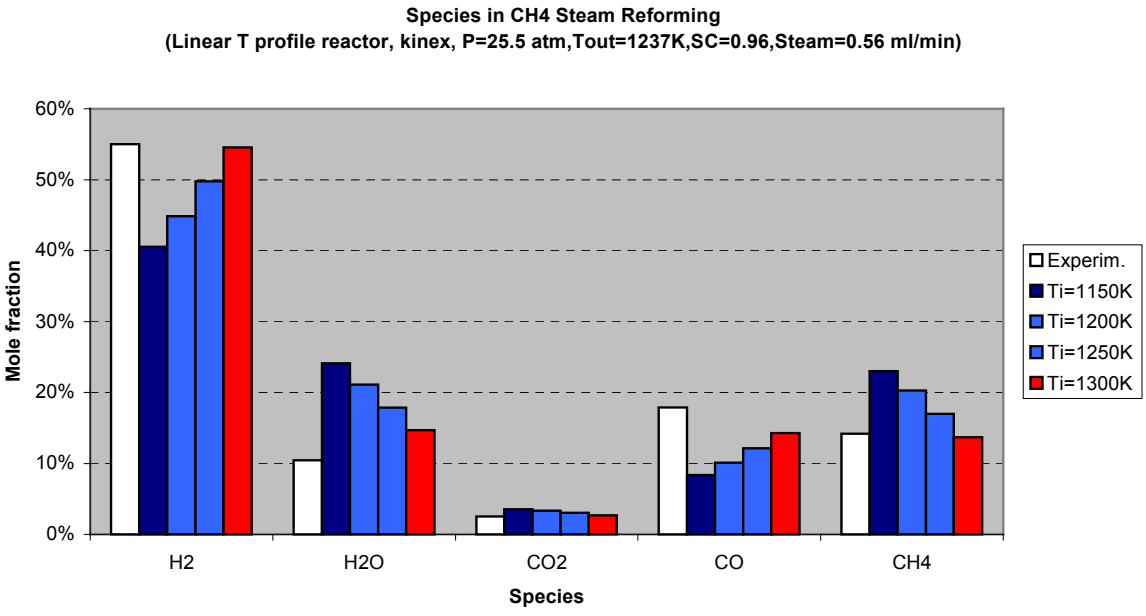

Figure 25: Results for linear T profile reactor (kinex, P=25.5, Tout=1237K,S:C=0.96)

2.5.9 PREDICTIVE TOOLS – CRACKING REACTIONS COMPUTATIONS

Above, results of a first batch of simulations of CH_4 steam reforming were presented. In order to assess the predictive capability of the simulation software tool (*DSMOKE*), results of these simulations were confronted with a set of experimental data, kindly supplied by TDA Research Inc. To perform the simulated tests, three different kinetics models were used. These models, with some extensions, have been used for cracking reactions. Briefly, the kinetics schemes used in the following simulations are:

CRACKING: Developed from the [default] general model in which some decomposition reactions of heavy hydrocarbons (like n-C_{12} or n-C_{14}) were added;

KINEX: Developed from the KINEX model (described above) by adding the decomposition reactions, as told before. KINEX model gave the best results in CH_4 steam reforming simulations, as we discussed in the previous report. As in the first step of the work, three different thermal reactors were considered: isothermal, adiabatic and with a linear T profile. Reactants considered here were JP-8 and n-octane, fed to the reactor at P=37.4 atm and different initial temperatures.

2.5.9.1 JP-8 CRACKING RESULTS

To simulate the cracking behavior of JP-8 in a reasonable time, a *surrogate* of the mixture was assumed. Hydrocarbons belonging to a particular class were combined and substituted with the head compounds of that class or with a species of mean properties (i.e., the $C_8 - C_{10}$ fraction with i-C_8). Figure 26 shows the results of this gathering. This method allows us to simplify the properties of the inlet stream and to develop rapidly a kinetic model. This was accomplished starting from the general [default] scheme and simply adding some missing decomposition reactions only related to the components of the JP-8 surrogate.

Figure 27 shows the experimental results for T=898K and P=37.4 atm. The reactor length is 101.6 cm and its internal diameter is 0.2 cm; the fuel residence time is 8-10 sec [29].

Figure 28 shows the results of the simulations made under the same conditions of the experimental data. In this case, the reactor is isothermal and the kinetics model used here is the general model CRACKING. Figure 28 clearly depicts low conversion of the n-C_{12} and m-xylene, a non-negligible quantity of tetraline and n-C14 and ethyl-cyclohexane, in other words, of those species, which are present in the inlet surrogate. This mean the overall kinetic ratio is quite low. Other species, like lighter gases (the target of the process) constitute only 25% of the total amount in the outlet gas.

Figure 29 shows, under the same conditions, the results obtained in an adiabatic reactor. In this case, C_{12} conversion (dodecane can be considered an essential species) decreases since the decreasing T profile soon freezes the endothermic cracking reactions. This trend is the same also for the other species present in the initial surrogate. Therefore, production of light gases is very low. Figure 30 shows the results obtained considering an infinite residence time. The great amount of CH_4 (over 33%) is counterbalanced by a great production of heavy cracking products (coke) like $C_{25}H_{20}$ or the radical $R_{20}H_9$, and a great production of C_{12} radicals (which can be regarded as unconverted fuel).

In conclusion, the code predicted low production of light hydrocarbons, just as recorded in the experimental tests (recall in Figure 27 species CH_4 and C_2H_6 are not present). DSMOKE simulations show the importance of the role played by the fuel residence time in order to optimize the production of light hydrocarbons. Although the agreement with the experimental data is not perfect, due to approximation of the inlet stream, we can conclude that DSMOKE, once again, seems to be a good predictive tool for this kind of phenomena.

2.5.9.2 N-OCTANE CRACKING RESULTS

Experimental results for this fuel are shown Figure 31. Physical conditions of these numerical tests are P=37.4 atm and Tout=500 °C. The reactor length is 30.5 cm and its internal diameter is 0.16 cm. In Figure 32, results obtained by simulations under the same experimental conditions are shown. This figure refers to a volumetric flow rate of 1.3 ml/min and to the three different thermal profiles. Simulations were performed fixing the outlet temperature at 500°C, as suggested by the experimental data. Thus, the highest conversion was found for the adiabatic case, because the average T inside the reactor is the highest. The lowest conversion was for the

isothermal case. The overall kinetics ratio seems to be faster than the real one (see in Figure 31 the low n-octane conversion). This trend was also observed increasing the flow rate to 4.8 ml/min (see Figure 33).

Finally, Figure 34 shows results obtained by using the KINEX model. The use of this scheme did not produce noticeable changes, since the generic abstraction reaction:

$R^*+H_2 \Rightarrow RH + H^*$

whose efficiency was enhanced in building the model, does not play a leading role in this cracking system, because of the low H2 production.

2.5.10 CONCLUSIONS

The DSMOKE software tool appears to work quite well in simulating cracking of hydrocarbons mixtures. However, results are affected by several approximations done in the simulations (i.e., JP-8 surrogate, ideal reactors, and no catalytic effects on the wall). In order for the code to yield more reliable results, future work will be focused in developing more detailed kinetics mechanisms, especially stressing reactions that involves heavy hydrocarbons.

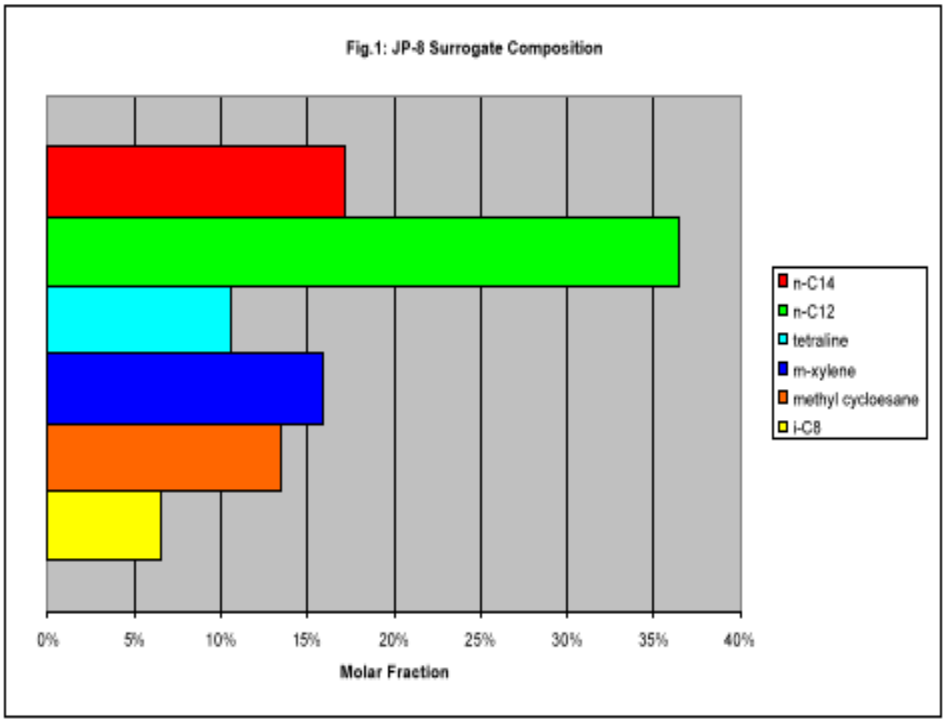

Figure 26: JP-8 Surrogate Composition

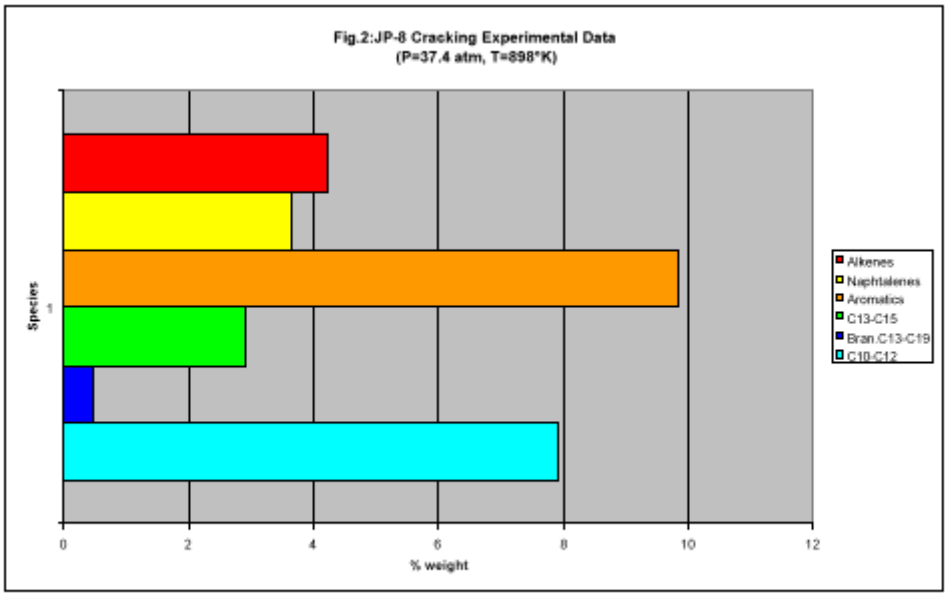

Figure 27: JP-8 Cracking Experimental Data

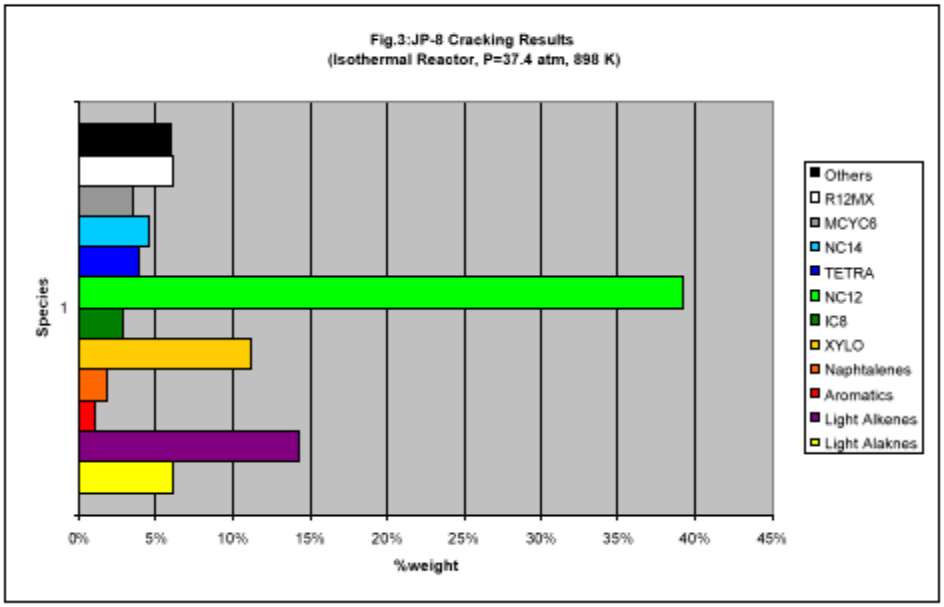

Figure 28: JP-8 Cracking Results

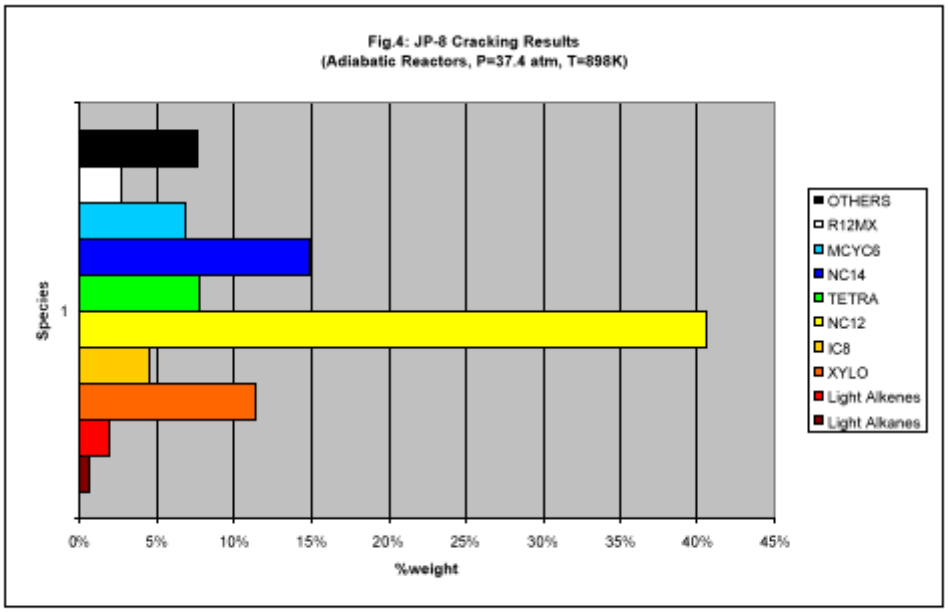

Figure 29: JP-8 Cracking Results

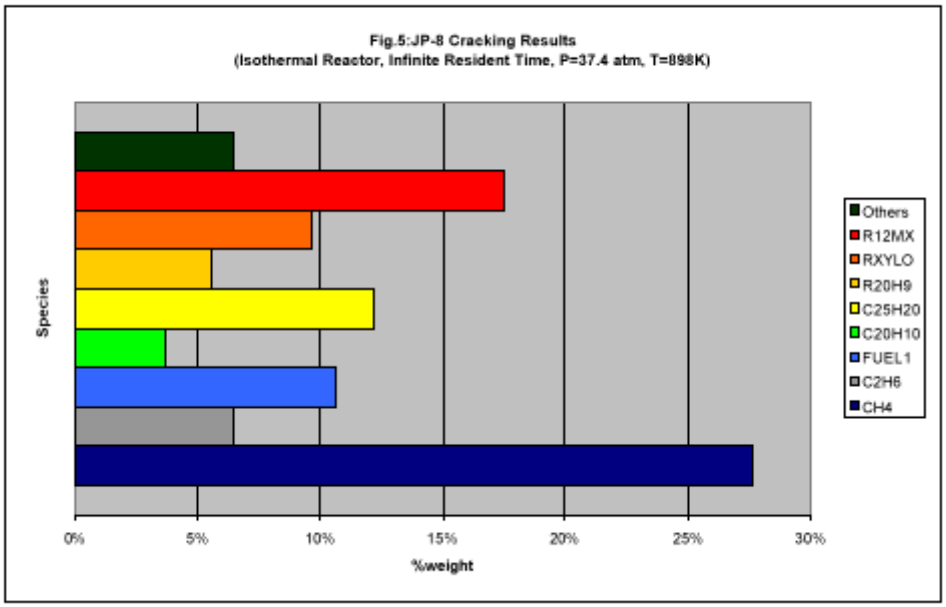

Figure 30: JP-8 Cracking Results

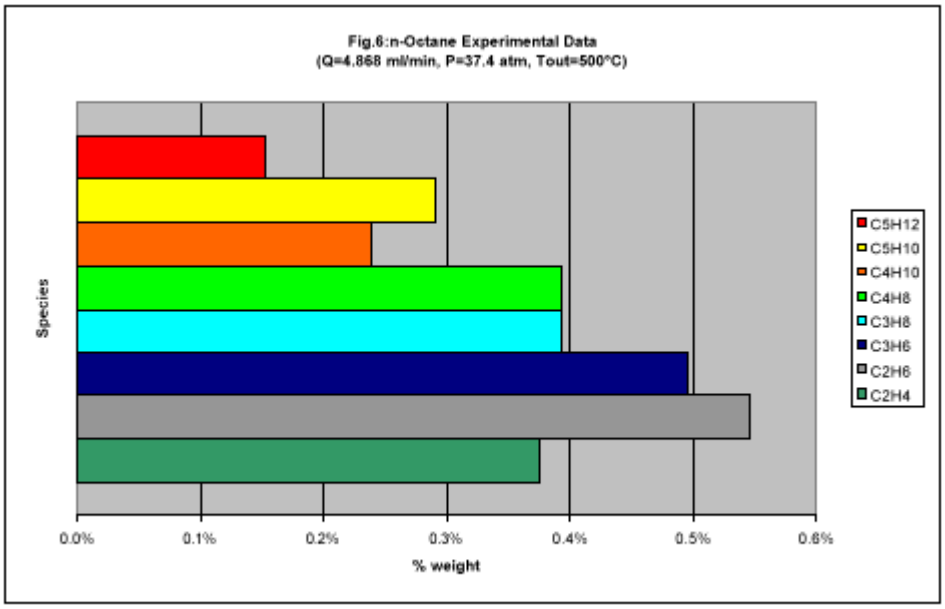

Figure 31: n-Octane Experimental Data

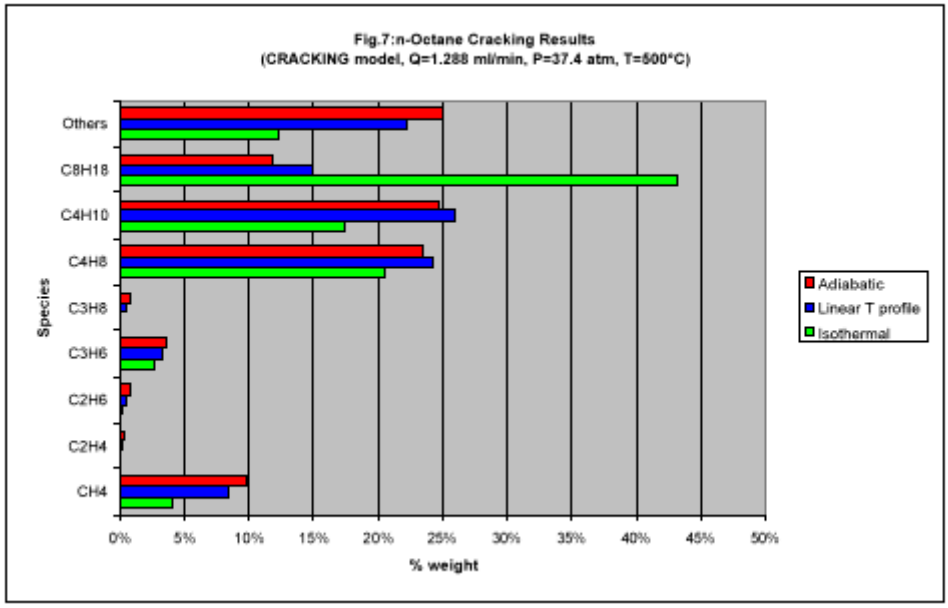

Figure 32: n-Octane Cracking Results

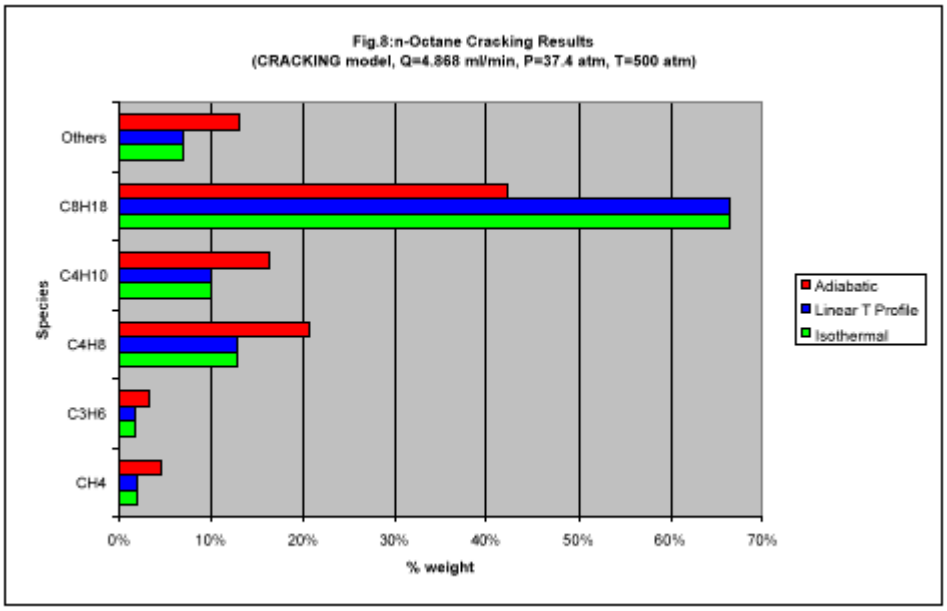

Figure 33: n-Octane Cracking Results

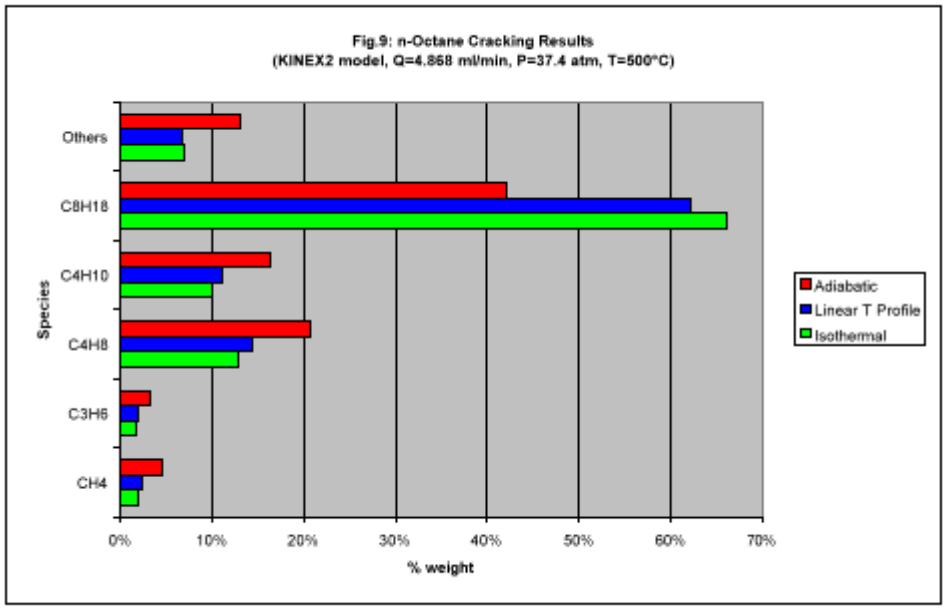

Figure 34: n-Octane Cracking Results

2.6 KINETIC CONSIDERATIONS.

Jet Fuels (JP) all belong to the general class of fuel called "kerosene". Detailed kinetic modeling combustion studies of kerosene aviation fuels are generally considered prohibitive due to their inherent chemical complexity. There have been studies of surrogates for "kerosene", which can serve as general examples. Aly and Salem [30] have predicted the laminar burning velocities of lean to stoichiometric laminar premixed kerosene flames using a single global kinetic step. As a first approximation, Guéret *et al.* [31] modeled kerosene oxidation via quasi-global models for *n*-decane, *n*-propylcyclohexane, tri-methyl benzene, xylene, toluene and

benzene. Concentration profiles of molecular species in the flow reactor were similar for the surrogate and kerosene; however, the need for further refinement of the aromatic models was recognized [31]. Dagaut *et al.* [32] later modeled kerosene combustion in low-temperature jet-stirred reactors using *n*-decane as a reference hydrocarbon while neglecting the aromatic components, and captured major species profiles adequately. Ranzi *et al.* [33] proposed a comprehensive reaction mechanism for higher order hydrocarbon fuels which only considers benzene in a semi-empirical manner. By contrast, Foelsche *et al.* [34] modeled the efflux composition of a rich JP-7/toluene-fueled gas-generator operating at intermediate temperatures (900-1300 K) using the toluene oxidation kinetic model of Emdee *et al.* [35] to describe the aromatic constituents; a surrogate could not represent the soot formation process. Vovelle *et al.* [36] studied low-pressure kerosene flames and modeled the aromatic component with a simplified toluene mechanism. Discrepancies between computations and experimental observations were attributed to uncertainties in the aromatic model. Leung [37] studied kerosene diffusion flames and modeled the aliphatic component with a quasi-global undecane sub-mechanism while assuming the aromatic component to be benzene. The above studies recognize the need to include an aromatic sub-mechanism, preferably considering mono-substituted aromatic molecules, in detailed kerosene kinetic modeling. Maurice [38] used a surrogate model of 89 mole % decane and 11 mole % of various aromatic surrogates: benzene, toluene, ethylbenzene, and ethylbenzene/naphthalene as an input to a detailed chemical kinetic model, which was compared to a number of experimental data sets for species profiles in kerosene flames. The n-decane/benzene surrogate captured major species profiles, but failed to predict benzene concentrations. By contrast, the major characteristics of the kerosene flame, including benzene profiles, were predicted accurately using *n*-decane/alkyl-substituted aromatic surrogate blends. No differences were noted amongst the various alkylbenzene surrogates. Addition of naphthalene did not affect major characteristics of the flame. However, if aromatics are used as inputs to a soot formation model [e.g. 39], individual aromatic concentrations in the parent fuel must be considered.

An outgrowth of the work of Lindsted and Maurice [38-40] was the comparison between NOx and CO emissions from combustion of Jet A in a well-stirred reactor and model predictions using a surrogate model of 78% n-decane and 22% ethylbenzene [41]. The comparison was generally good. A general conclusion from this work was that a detailed aromatic component needed to be added to the two-component surrogate model only to properly predict molecular growth/soot behavior.

Edwards and Maurice reviewed surrogate fuel options and recommended appropriate surrogates for various physical situations [28]. These recommendations are reproduced in Table 5.

Table 5. Recommendations on appropriate surrogate fuels

Physical Situation	Minimum complexity surrogate fuel recommendation
Single phase heat transfer w/o chemical reaction	Single component n-paraffin with approximately correct critical temperature
Higher precision heat transfer, including enthalpy effects	Use appropriate surrogate with correct chemical compound classes and representative mixture critical temperature
Fuel vaporization/injection/mixing (multi-phase, unreacted)	Use appropriate surrogate that matches distillation (boiling) curve
Fuel ignition	Use appropriate surrogate that matches the important chemical classes. If ignition improving additives present (e.g., nitrates), then will need to include additive chemistry
Fuel heat release, flame speed	Use appropriate surrogate to match important compound classes
NOx emissions during fuel combustion	Use appropriate surrogate that matches the major important chemical classes.
Aromatic and PAH emissions during combustion	Use appropriate surrogate that matches the major and minor important chemical classes that contribute to molecular growth.
General fuel thermal-oxidation behavior (inside fuel system)	Use surrogate that matches chemical class breakdown in fuel
Pyrolytic deposition from fuels	Use appropriate surrogate that matches the major and minor important chemical classes that contribute to molecular growth.
Thermal-oxidative deposition from fuels	No good surrogate, deposition levels driven by trace fuel species (heteroatomic species, dispersants)
Soot formation in combustion	No good surrogate--soot levels driven by trace fuel species (heteroatomic species, dispersants)

2.7 IMPACT OF FUEL SELECTION ON VEHICLE DESIGN

Very often, future airbreathing hypersonic vehicles now proposed are assumed to burn hydrogen fuel rather than hydrocarbons like methane or kerosene (e.g. JP-8). At a vehicle level, the fuel characteristics will therefore largely influence the engine performance and the design of the tanks.

Hydrogen fuel provides the largest amount of heat release per unit mass of fuel (Qc) (see table 6) and its low molecular mass is critical to realizing a high specific impulse (Isp). However, its high specific volume [1/ρ] is a problem to all airbreathing aerospace vehicles. At cryogenic storage temperatures, between 18 K and 25 K, hydrogen is liquid and its density varies from 70.8 kg/m³ to 89.9 kg/m³. Hence large tanks negatively impact vehicle weight and drag. For example, liquid methane is three to four times as dense as LH_2 while kerosene is about 10 to 12 times denser. This will be especially important for the cruise capability that can be characterized by the range factor (RF) also called the Specific Range (SR):

$$(SR =)RF = \theta.\frac{L}{D}.\ln\left[1-\frac{FW}{oew}\right].Qc$$

with $\theta = \frac{F \cdot V}{Qc \cdot \dot{m}_f} = \frac{ISP \cdot V}{Qc}(= TSFC)$, where FW = Fuel Weight, OEW = Operational Empty Weight, $\frac{L}{D}$ = Lift-to-drag ratio, ISP= specific impulse (in s), Qc = Heat of combustion, $\dot{m}_f$ = fuel massflow rate, F=thrust, V=vehicle velocity and TSFC is the thrust specific fuel consumption.

Table 6 Fuel Heating Values

Fuel	Qc (BTU/lbm)
H_2	51.570
CH_4	21.500
JP-4	18.400

As shown in figure 35 (where τ is Küchemann's parameter), the fuel density of the fuel impacts the factor $\frac{L}{D}$ as it influences largely the ''incompressible" zero lift drag coefficient $C_{Do}(M^2\text{-}1)^2$.

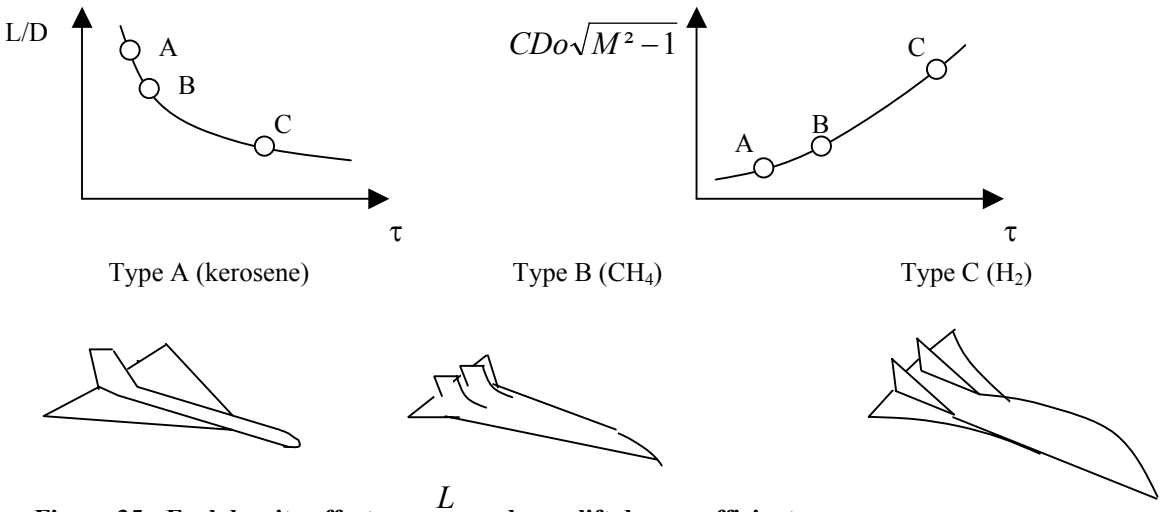

Figure 35: Fuel density effects on $\frac{L}{D}$ and zero lift drag coefficient

A possible law for airbreathing aerospace planes reaching hypersonic cruise speed in airbreathing mode for L/D is : $\frac{L}{D} = 0.998.\left[\sqrt{M^2-1}.Cdo\right]^{-0.564}$.

For a 72° sweep blended body vehicle at at Mach 5, $\left(\frac{L}{D}\right)_{max}$ is ~8 for a kerosene-fueled spaceplane, ~6 for a methane (CH_4)-fueled option, and ~4 for a LH_2-fuelled vehicle. However, when multiplying by the ISP factor θ, the negative effect of the fuel density on $\left(\frac{L}{D}\right)$ is more than offset by the large increase of the ISP (Figure 36). The net result is a much higher Range Factor RF with hydrogen as shown on Figure 37. However, the difference stagnates or even decreases above about Mach 5.

If the RF is translated into a Take-off-Gross-Weight (TOGW) and a Dry Weight (or Zero Fuel Weight), the hydrogen-fueled vehicle will always be much heavier for a given range. An example is given in Table 7 for a 3500 NM (NM=nautical miles) range at a Mach 4.0 cruise speed.

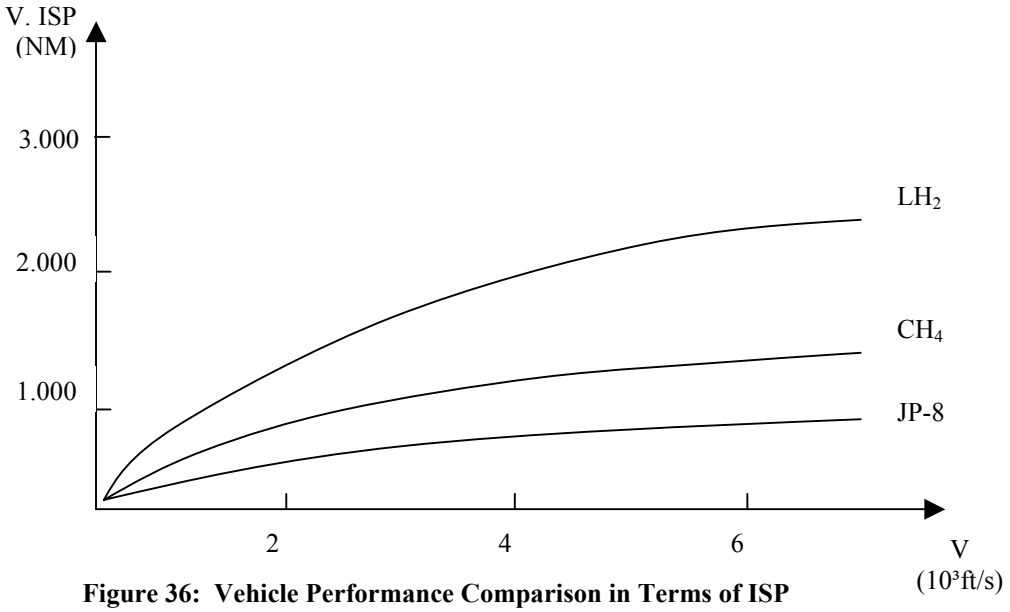

Figure 36: Vehicle Performance Comparison in Terms of ISP

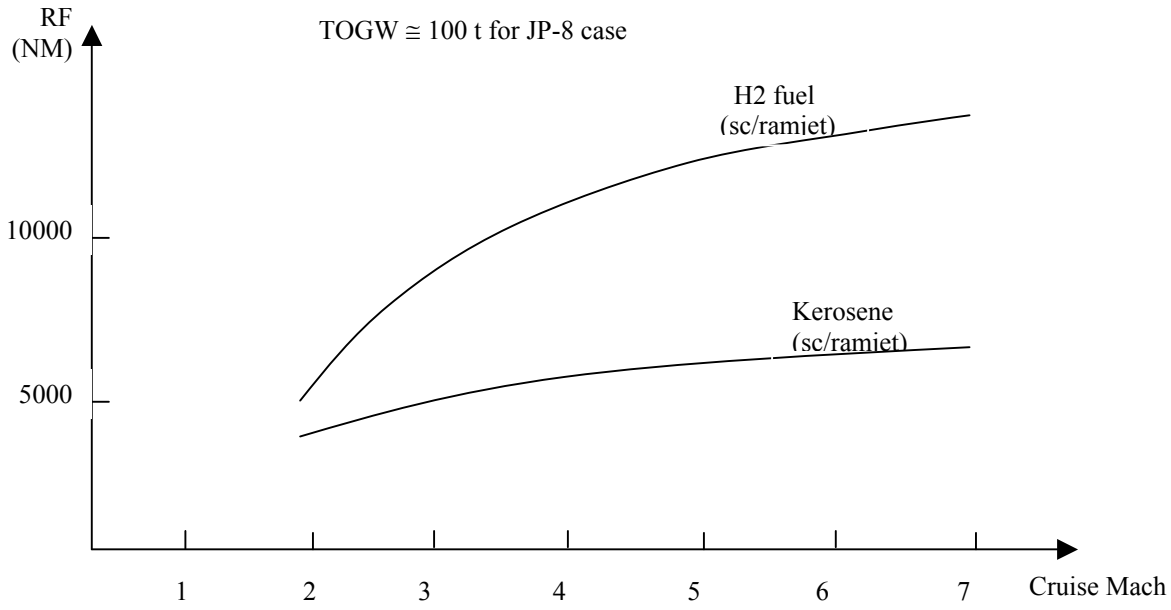

Figure 37: Vehicle Performance Comparison in terms of Range Factor

	LH2	*CH4*
ISP.V (NM)	1.700	1.300
TOGW (t)	45	30
W dry (t)	25	15
Fuel mass (t)	20	15

Table 7. Vehicle Performance Comparison

If a turbojet / turbofan is used for the low speed acceleration phase of the mission instead of, for example, an AirTurbo Rocket, hydrogen shows a clear advantage as it provides a much higher average transonic ISP (Figure 38).

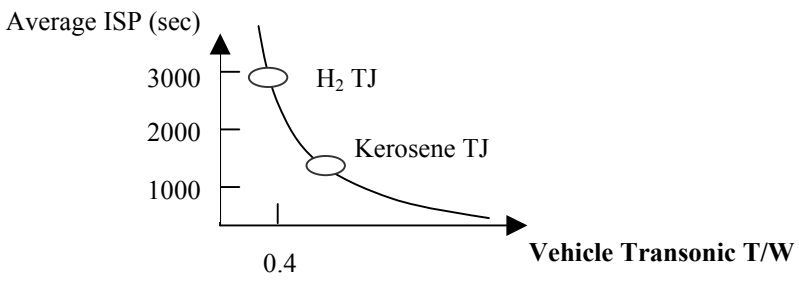

Figure 38. Vehicle Performance for Turbojet/Turbofan Powered Accelerator

Another candidate mission is the pure acceleration mission, where the primary issue is the specific delta velocity (delta ΔV).

$$Specific\ \Delta V = \frac{acceleration}{\dot{m} \cdot f} = \frac{ISP \cdot \left(\frac{T}{D} - 1\right)}{W \cdot \frac{T}{D}}$$

where W is the average vehicle weight over ΔV, and T is the thrust.
As different propellants of widely differing densities can be employed, it is evident that two equations are especially important for hypersonic vehicles. These equations are:

$$\text{Propellant density: } \rho_{propellant} = \frac{O/F + 1}{\frac{O/F}{\rho_{oxidizer}} + \frac{1}{\rho_{fuel}}}$$

and

$$\text{Oxidizer-to-Fuel ratio: O/F} = \frac{\frac{\rho_{propellant}}{\rho f_{uel}} - 1}{1 - \frac{\rho_{propellant}}{\rho_{oxidizer}}}$$

Select values for ρ_{fuel} are shown in Table 8:

Fuel	ρ_{fuel} (lb/ft^3)
Normal H_2	4.42
Subcooled H_2	4.66
Slush 50% H_2	5.13
Methane	26.0
JP-8	47.0

Table 8. Select fuel density values

These factors will, for example, largely influence the vehicle TOGW expressed as follows:

$$TOGW = WR \cdot \frac{\rho_{prop}}{(WR - 1)} \cdot \frac{Vp}{Sp} \cdot Sp$$

Where the $WR = \frac{TOGW}{OWE}$ and $TOGW = OWE + W_{prop}$, and OWE is overall weight empty, and the coefficient $\left(\frac{\rho prop}{WR - 1}\right)$ is often called the "technology input", depending on the fuel, the propulsion (also depending on the fuel) and the vehicle aerodynamics.

As noted before in this chapter, a potential solution to the negative effect of storing LH_2 on the vehicle weight and drag is chemical reforming, producing GH_2 – fuel from liquid hydrocarbon [LHC] and water. Reforming is also a strong endothermic process that can be used in an active cooling system for the most thermally loaded aerospace plane parts during the hypersonic flight (wing leading edges, inlet lips, aircraft nose).

It is therefore instructive to determine when reforming may become more advantageous than carrying LH_2 on board by reducing drastically fuel tank volumes.

A sample case considering methane is described in [43]. From a mixture of CH_4 and H_2O, a certain quantity of H_2 may be obtained as a function of the temperature, pressure and residence time.

The volume occupied on board by CH_4 and H_2O is :

$$V_{CH4} + V_{H2O} = \nu_{CH4} \,.\, M_{CH4} + \nu_{H2O} \,.\, M_{H2O}$$

Where M indicates the mass and ν the specific volume.

If the mass of H_2 obtained from reforming or catalysis would have been stored directly in liquid state, the hydrogen volume would have been then:

$$V_{LH2} = \nu_{LH2} \,.\, M_{LH2}$$

It becomes then obvious that the system becomes advantageous in terms of fuel tank volume if:

$$\mathrm{R} = \frac{V_{CH4+H2O}}{V_{LH2}} < 1$$

R is shown as a function of initial methane fraction and temperature for a reforming time *t=1* sec and at two pressures, 1 and 20 bar in Figures 38 and 39. It is important to note that if the fraction of CH_4 is equal to 0.5 and the temperature is higher than 3,000 K, carrying methane and water instead of LH_2 leads to a rather moderate tank volume reduction of ~30%. A larger reduction could be achieved if other combustible species are accounted in the calculation.

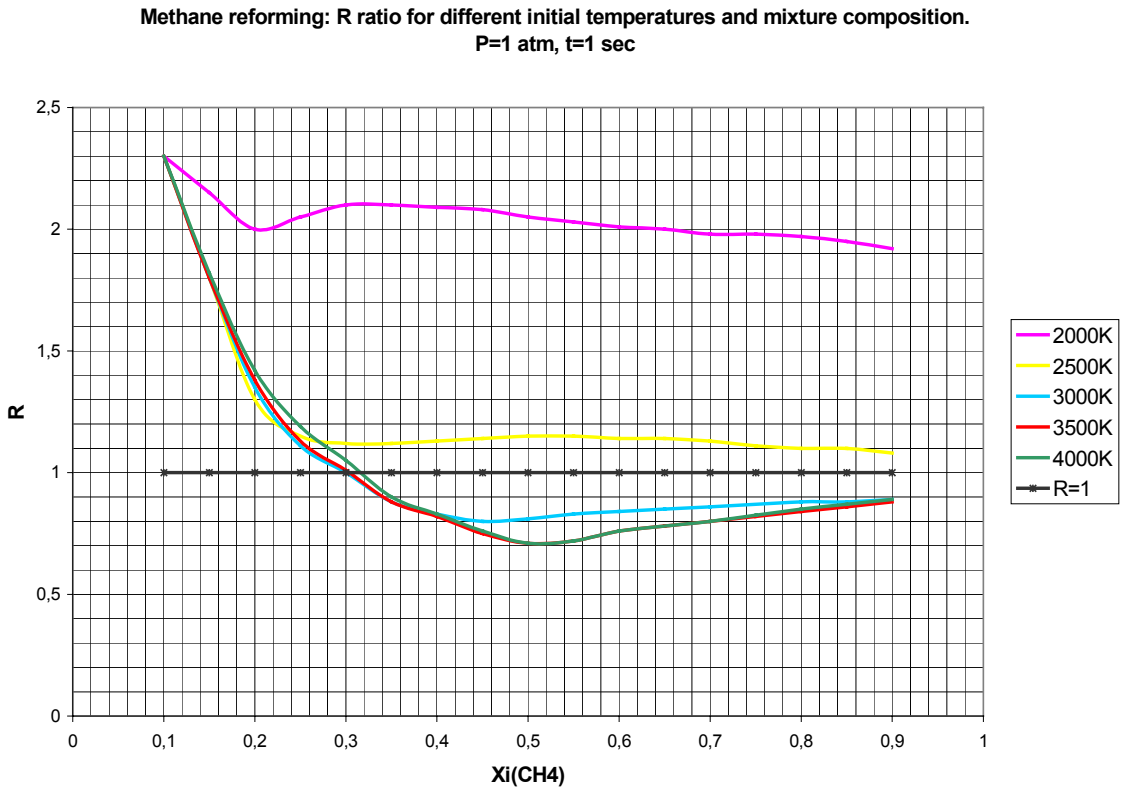

Figure 39. R as a function of CH_4 fraction

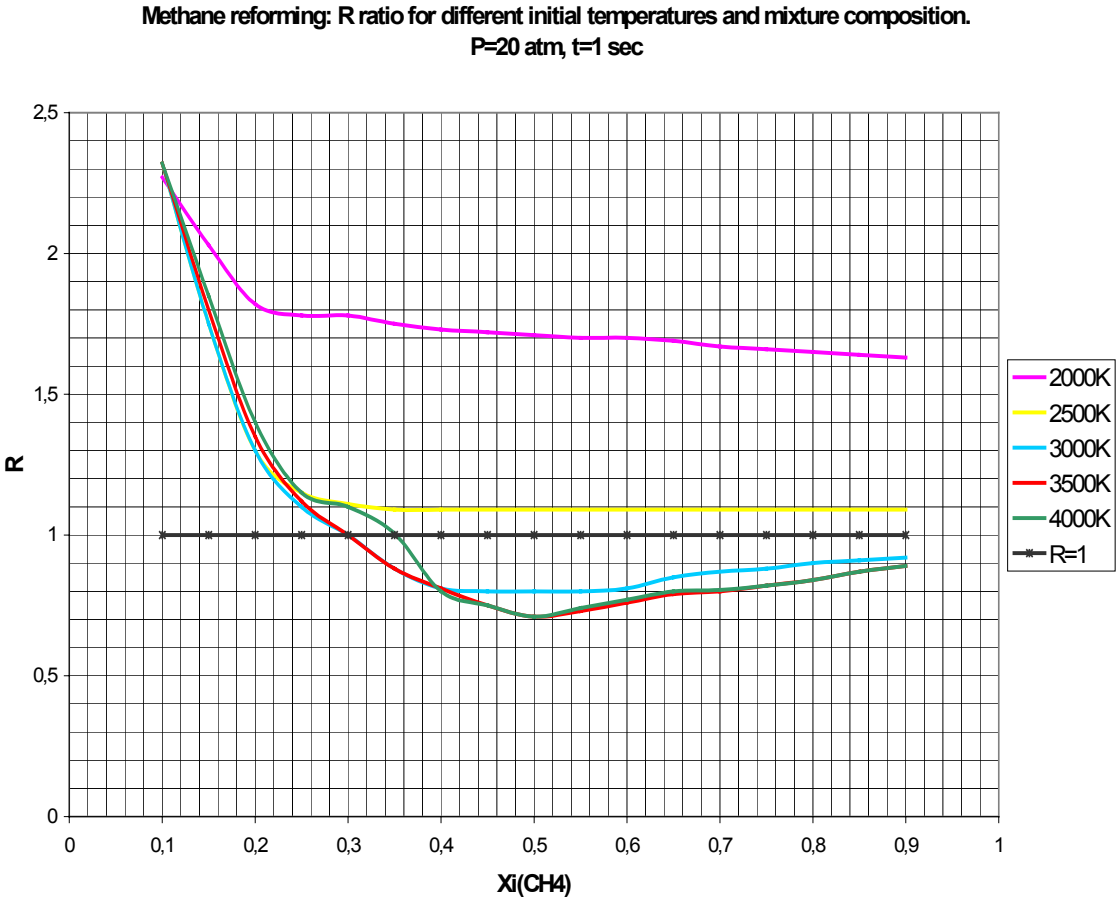

Figure 40. R as a function of CH_4 fraction

2.8 CONCLUSIONS AND RECOMMENDATIONS

This synthetic overview points to the following conclusions:

- most of future tactical SCRJ applications must rely on Kerosenes;
- cruiser, and especially accelerator applications benefit most from H_2. Because of its low ρ, onboard reforming (using so-called endothermic fuels) of conventional HC fuels is the fuel strategy of choice;
- simple but meaningful reforming calculations are already possible by using surrogate fuels. These calculations may pave the way toward preliminary analysis and design of effective and practical reforming systems;
- HC reforming by using convective heat transfer from hot parts (SCRJ engine walls, but also external aerodynamics surfaces) is probably the most energetically and exergetically efficient strategy for SCRJ applications ;
- Past work in the US and USSR has demonstrated the feasibility of reforming HC fuels for SCRJ. In fact, work at USAF, P+W and BOEING, as well as current plans for X-43C tests (see Chapter 1) indicate. HC will be the enabling technology of efficient SCRJ engines.

The main technology areas to explore in this context are:

- HC formulation/analysis, and their reforming kinetics
- reforming catalysts
- high temperature materials for SCRJ combustors, and their manufacturing
- energy/exergy budgets and their impact on overall vehicle design, operability, performance and cost.

2.9 REFERENCES

[1] Henderson, R. E. (ed.), "Hypersonic Air Breathing Missile," Chapter 1 in "Propulsion and Energy Issues for the 21st Century," AGARD Report 824, March 1997.

[2]. Final Report of Task Group 6/7 on Fuel Properties Report to the Fuel Tank Harmonization Working Group of the FAA Aviation Rulemaking Advisory Committee, Revised 7/15/98.

[3]. Maurice, L.Q., Edwards, J.T., and Griffiths, J.F., "Liquid Hydrocarbon Fuels for Hypersonic Propulsion," AIAA Progress in Aeronautics and Astronautics, S.N.B. Murthy and E.T. Curran, Editors, 2001.

[4]. Lewis, M. J. and Gupta, A. K., "Impact of Fuel Selection on Hypersonic Vehicle Optimization," ISABE 97-7200, September 1997.

[5]. Palaszewski, B., Ianovski (Yanovskii) L. S. and Carrick, P., "Propellant Technologies: A Persuasive Wave of Future Propulsion Benefits," 3rd International Symposium on Space Propulsion, Beijing, China, Aug 1997.

[6]. Leingang, J.L., Maurice, L.Q. and Carreiro, L.R., "In-Flight Oxidizer Collection Systems for Airbreathing Space Boosters," in Developments in High-Speed-Vehicle Propulsion Systems, Progress in Astronautics and Aeronautics, Vol. 165, eds. S.N.B. Murthy and E.T. Curran, 1996.

[7]. Gurijanov, E.P. and Harsha, P.T., "Ajax: New Directions in Hypersonic Technology," AIAA 96-4609, November 1996.

[8]. Maurice, L.Q., Lander, H.R., Harrison, W.E., and Edwards, J.T., "Advanced aviation fuels: a look ahead via a historical perspective" , Fuel, in press, 2001.

[9]. Lander, H. and Nixon, A. C., "Endothermic Fuels for Hypersonic Vehicles," Journal of Aircraft, 8(4), 200-207, 1971.

[10]. Dunnam, M.P., "Fluids For High Temperature Applications," Fifth AGARD Colloquium, High Temperature Phenomena, 87-110, 1962.

[11]. Lander, H. and Nixon, A. C., "Endothermic Fuels for Hypersonic Vehicles," Journal of Aircraft, Vol. 8(4), pp. 200-207, 1971.

[12]. Heiser, W. H. and Pratt, D. T., Hypersonic Airbreathing Propulsion, AIAA Washington DC, 1994.

[13]. Ianovski, (Yanovskii) L. S and Sapgir, G., "Heat and Mass Transfer to Hydrocarbon Fuels at Thermal Decomposition in Channels of Engines," AIAA 96-2683, July 1996.

[14]. Sobel, D. R. and Spadaccini, L. J., "Hydrocarbon Fuel Cooling Technologies for Advanced Propulsion," ASME Journal of Engineering for Gas Turbines and Power, Vol. 119, pp. 344-351, 1997.

[15]. Zubrin, R. M., "The Methane-Acetylene Cycle Aerospace Plane: A Promising Candidate for Earth to Orbit Transportation," AIAA-92-0688, January 1992.

[16]. Zhou, N. and Krishnan, A, "A Numerical Model for Endothermic Fuel Flows with Heterogeneous Catalysis," AIAA 96-0650, January 1996.

[17]. Chen, F., Tam, W.F., Shimp, N.R. and Norris, R.B., "An Innovative Thermal Management System for a Mach 4 to Mach 8 Scramjet Engine," AIAA 98-3734, July 1998.

[18]. Maurice, l.q., Corporan, e., Harrison, w.e., minus, d. Mantz, r., edwards, t., striebich, r.c., sidhu, s., graham, j., hitch, b., wickham, d., karpuk, m., "controlled" chemically reacting fuels: a new beginning," xiv isabe, florence, italy, september, 1999.

[19]. Coordinating Research Council, Handbook of Aviation Fuel Properties, CRC Report No. 530, 1983.

[20]. Defense Energy Supply Center, "Survey of Jet Fuels (1990-1996)," June 1998.

[21]. National Engineering Laboratory, PPDS2 physical property software, Glascow, Scotland, 1999.

[22]. Faith, L. E., Ackerman, G. H., and Henderson, H. T., "Heat Sink Capabilities of Jet A Fuel: Heat Transfer and Coking Studies," NASA CR-72951, July 1971,

[23]. TeVelde, J. A. and M. R. Glickstein, "Heat Transfer and Thermal Stability of Alternative Aircraft Fuels," NAPC-PE-87C, 1983 (AD 137404)

[24]. Nixon, A. C., et al, "Vaporizing and Endothermic Fuels for Advanced Engine Applications: Part III: Studies of Thermal and Catalytic Reactions, Thermal Stabilities, and Combustion Properties of Advanced Fuels," AFAPL-TR-67-114, Part III, Vol 1., Feb. 1970.

[25]. Sumey, I. E., "Fuels and Lubricants Influence on Turbine Engine Design and Performance," AFAPL-TR-73-54, Vol. II, November 1974.

[26]. Bucknell, R. L., "Influence of Fuels and Lubricants on Turbine Engine Design and Performance," AFAPL-TR-73-52, Volume II, June 1973.

[27]. Ely, J. F., and Huber, M. L., NIST Standard Reference Database 4 - NIST Thermophysical Properties of Hydrocarbon Mixtures, February 1990.

[28]. Edwards, T., Maurice, L. Q., "Surrogate Mixtures to Represent Complex Aviation and Rocket Fuels," AIAA 99-2217, July 1999.

[29]. Reid R.C., Prausnitz J.M, Poling B., "The Proprieties of Gases and Liquids", 4th Edition, McGraw-Hill Int. Series.

[30]. Aly, S.L. and Salem, H. "Prediction of Premixed Laminar Flame Characteristics of Commercial Kerosene Fuel," Fuel, 68:1203, 1989.

[31]. Guerèt, C. Cathonnet, M., Boettner, J.C. and Gaillard, F. Experimental Study and Modeling of Kerosene Oxidation in a Jet-Stirred Flow Reactor. Twenty-Third Symposium (International) on Combustion, The Combustion Institute, p. 211, 1990.

[32]. Dagaut, P., Reuillon, M., Boettner, J.C. and Cathonnet, M., "Kerosene Combustion at Pressures up to 40 Atm: Experimental Study and Detailed Chemical Kinetic Modeling," Twenty-Fifth Symposium (International) on Combustion, The Combustion Institute, p. 919, 1994.

[33]. Ranzi, E., Sogaro, A., Gaffuri, P., Pennati, G., Westbrook, C.K. and Pitz, W.J. "A New Comprehensive Reaction Mechanism for Hydrocarbon Fuels, " Combust. Flame, 99:201 (1994).

[34]. Foelsche, R.O., Keen, J.M., Solomom, W.C., Buckley, P.L. and Corporan, E., "Non-Equilibrium Combustion Models for Fuel-Rich Gas Generators," Journal of Propulsion and Power, 10:4:461, 1994.

[35] Emdee, J.L., Brezinsky, K. and Glassman, I., "A Kinetic Model for the Oxidation of Toluene Near 1200 K," J. Phys. Chem., 96:2151, 1992.

[36]. Vovelle, C., Delfau, J.L. and Reuillion, M., "Formation of Aromatic Hydrocarbons in Decane and Kerosene Flames at Reduced Pressures," in Soot Formation in Combustion: Mechanisms and Models, (H. Bockhorn, Ed.), Springer-Verlag, 1994.

[37] Leung, K.M., "Kinetic Modelling of Hydrocarbon Flames Using Detailed and Systematically Reduced Chemistry," PhD thesis, University of London, 1996.

[38]. Maurice, L. Q., "Detailed Chemical Kinetic Models for Aviation Fuels" PhD thesis, Imperial College, 1996.

[39]. Lindstedt, R.P. and Maurice, L.Q., "Detailed Chemical Kinetic Modelling of Toluene Combustion," Combustion Science and Technology, 120:119, 1996.

[40]. Lindstedt, R.P. and Maurice, L.Q., A Detailed Chemical Kinetic Model for Practical Aviation Fuels," Journal of Propulsion and Power, Vol. 16(2), pp. 187-195, 2000.

[41]. Maurice, L. Q., Blust, J. W., Leung, K. M., Lindstedt, R. P., "Emissions from Combustion of Hydrocarbons in a Well-Stirred Reactor," AIAA Paper 99-1038, January 1999.

[42]. Lewis M. J. and Chang J. S., "Joint Jet-A/Silane/Hydrogen Reaction Mechanism", AIAA Journal of Propulsion and Power, Vol. 16, No. 2, March-April 2000.

[43]. Bruno C., Filippi M. and Czysz P. A., "Hydrocarbon Fuels Reforming for Hypersonic Propulsion", ISABE 99-7237, Florence, 5-10 September 1999.

CHAPTER 3: PHYSICAL EFFECT OF VITIATION ON SCRAMJET DESIGN

1D-STUDY OF THE PHYSICAL EFFECT ON VITIATION OF THE INCOMING AIR IN AN EXPERIMENTAL SCRAMJET COMBUSTOR

Marc Bouchez, Rodolphe d'Incà
Propulsion Department
EADS - AEROSPATIALE – MATRA MISSILES
8, rue Le Brix / 18020 BOURGES CEDEX / France
marc.bouchez@missiles.aeromatra.com

3.1 INTRODUCTION

Many ground test facilities use combustion to heat the air up to scramjet flight conditions. Even after replenishment of oxygen, the incoming air has then part of its nitrogen replaced with combustion products.
When hydrogen burner is used in preheating air, the incoming flow contains typically 15% of water for Mach 6 flight conditions and up to 30% for Mach 8 conditions.
This vitiation has two effects:

- A chemical effect (H_2O, NO_X, OH, even in low concentration are changing the ignition delay, particularly in the vicinity of 600 to 1000 K static temperature)
- A physical effect : thermodynamics is changed by this composition change.

The applied Physics Laboratory of John Hopkins University (APL) has proposed to RTO to give available experimental results of a scramjet combustor. Aerospatiale Matra Missiles (AMM) has proposed to do on this example a simple analysis of the physical effect of vitiation.
This paper gives an example of the analysis of the flow in a scramjet combustor, where supersonic combustion leads to increase of pressure and slowing of the flow. This paper is mainly intended to contribute to the discussion of the effect of the water-vitiation of the incoming air by numerical simulations using simple tools (1D, 0D) and by performing several parametric studies.
While the effect on all the parameters can be investigated, the focus here is on static pressure, Mach number, and heat fluxes, assuming the same (constant) wall temperature.
The drag law and the combustion efficiency along the duct are generally taken constant whatever the composition of the incoming flow.

3.2 EXPERIMENTAL COMBUSTOR

3.2.1 COMBUSTOR SCHEMATIC

The combustion chamber is described below in figure 1 and 3. We must note that the fuel injection is normal to the flow. The injectors are located at X=23.4 in. They consist of six 0.156-in. diameter holes located on upper and lower surfaces.

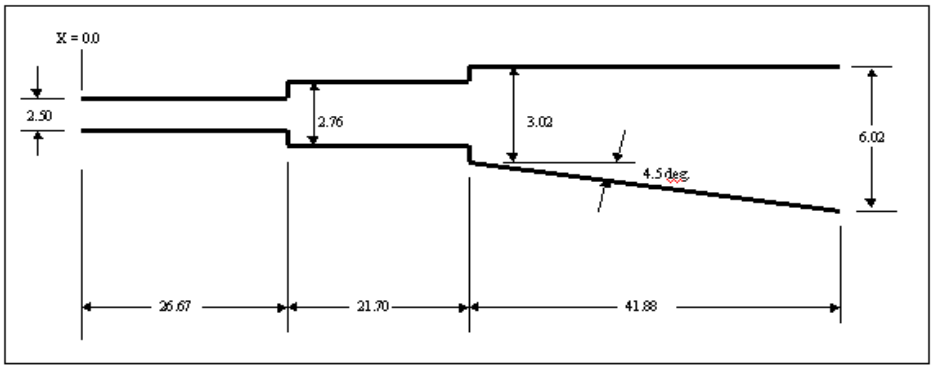

Figure 1: Combustor schematic. All dimensions in inches. It must be noted that the width of the chamber is supposed constant and equal to 12.25 in

INPUT DATA
The input data needed to achieve the simulations are presented in the following tables:

FLOW DATA

Characteristics	Value
Supply pressure	400 psia
Supply temperature	4200 °R
Combustor entrance Mach N.	3.3
Air mass flow rate	**10.8 lbm/s**
Heater H2 flow rate	0.4 lbm/s
Heater O2 flow rate	5.27 lbm/s

FUEL DATA

Characteristics	Value
H2 injection Mach number	1
H2 inject. Total pressure	217.4 psia
H2 inject. Total temp	550 °R

Experiments are carried out for the following equivalence ratios: ER=0.0, ER=0.51, ER=0.72 and ER=0.85. We assume a wall temperature of 550 °R along the whole duct.

EXPERIMENTAL RESULTS
The only data available after the test are the tap pressures along the combustor for the different equivalence ratios. An overview of all these data is presented in the graph below.

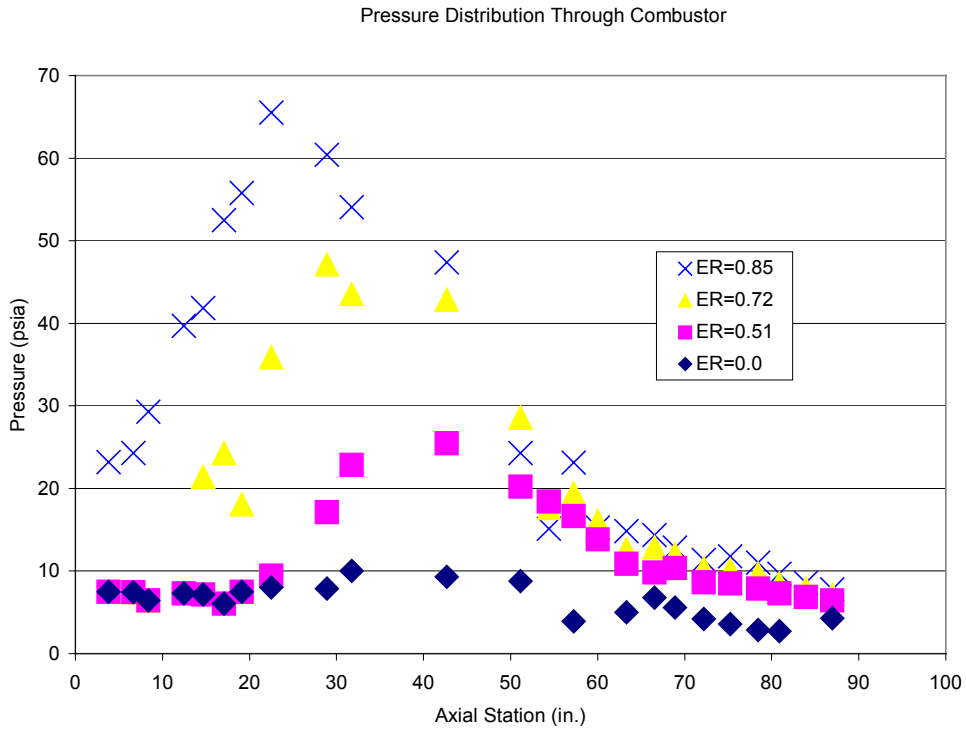

Figure 2: APL wall pressure measurement on the experimental combustor wall for different ER

It is interesting to note that the pressure sensors are not all located on the same face of the combustor. Given that the nature of the flow is quite different on each wall, we have to deal with these data very carefully.

3.3 1D ANALYSIS OF THE FLOW

3.3.1 1D ANALYSIS ASSUMPTIONS

The 1-D code PUMA (a French acronym meaning One-dimensional Program for Analysis of Aerothermochemistry), has been used to provide a first analysis of the results. This code has been extensively used by AMM for advanced studies of scramjets and to provide a first analysis of experimental results such as CHAMOIS ione (see Ref.1).

We must observe the limitations of this 1D study. Some effects that occur in the combustor, like shock waves or the recirculation zone behind the rear-facing step, are strongly 2D or 3D: we cannot directly integrate them into the program. That is why we must keep in mind that for, some cases (especially for high equivalence ratios), the results obtained are limited by the nature of the flow. Nevertheless, the 1D analysis is easy to be used in the frame of the present scope of this RTO report, and allows to perform parametric studies of the physical effect of the composition of the incoming air flow.

The heat release law is tuned until a reasonable agreement is reached between 1-D results and experimental results. To this purpose, the balance between the heat release, the effective geometry and the drag has to be identified, in order to decide the contribution of each term to the measured wall pressure increase.

In the present study, the choice is the following :

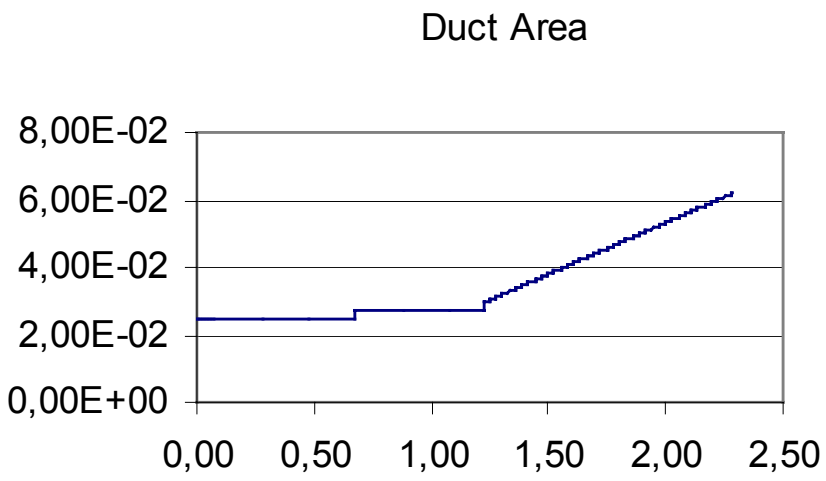

Figure 3: assumed duct area variation (geometry) of APL combustor (m²)

- To use the “geometrical geometry” as the flow boundary (no decrease due to boundary layer or subsonic zone), see Figure 3.
- To tune the drag with the non reactive case, and keep the same tuning constant for the reactive cases; the local skin friction coefficient is computed using semi-empirical laws and the 1D parameters of the flow, and sometimes increased by a factor in order to account for other types of drag. The multiplication factor is kept the same for any ER from 0 to 1.
- To derive from the pressure on the wall the heat release law, using simple combustion modeling and a single reaction. The combustion efficiency dependence along the duct is then kept the same during the vitiation parametric study.

The PUMA code is also able to estimate the heat fluxes along the combustor. The heat transfer coefficient is estimated using semi-empirical equations (Colburn law) in a duct. To take into account compressibility effects and non-adiabatic wall conditions, the Spalding and Chi equation has been used (see Ref.2).

Reference 2 reports a comparison of the method used here for another, more complex scramjet combustor, CHAMOIS. These fluxes had been computed for two different wall temperatures, 700 K and 1100 K, corresponding to the range of temperatures measured along the duct at its operating conditions. They have been compared with the post-processed results of the heat-flux-meters. Because CHAMOIS is a heat-sink facility, the wall temperature varies with time and spatially along the duct. Inverse methods are used to take into account the delay due to heat propagation between the two thermocouples of the heat flux meter. Figure 4 gives this comparison for the operating conditions investigated.

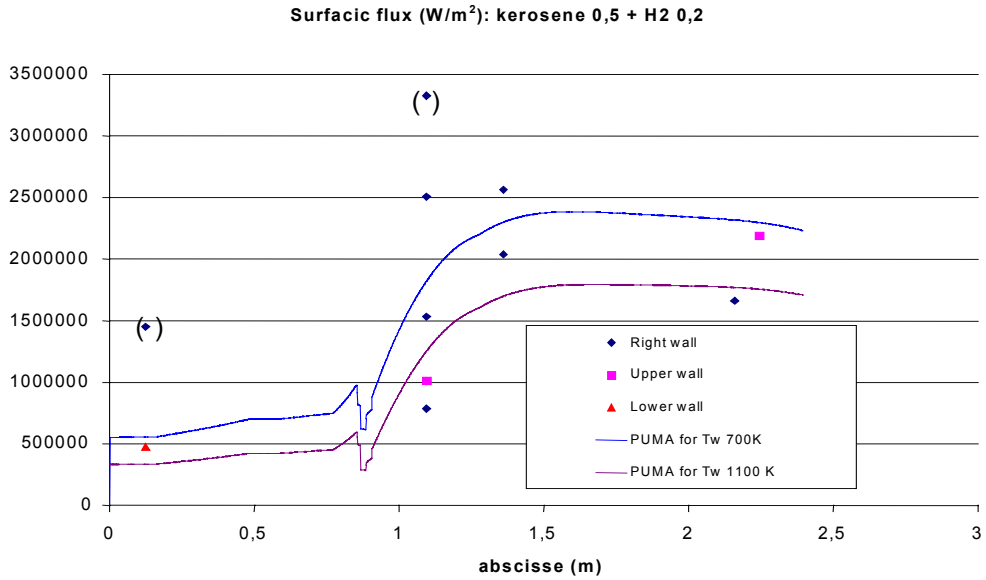

Figure 4: Heat flux (W/m²) along the CHAMOIS scramjet (experimental or PUMA data on another scramjet show sufficient accuracy for the formula used in the present study) .

For the first part of the present study, chemical kinetics is modeled as one irreversible reaction:
$H2 + ½\ O2 \rightarrow H2O$

3.3.2 NON REACTIVE COMPUTATIONS

These are the results obtained with ER=0. There are 2 cases: one where the drag coefficient is simply computed with Spalding's formula, the other with "corrected" drag coefficient. The purpose of this computation is, first, to see the difference between then computed results and the experimental results and, secondly, to see the effect of the drag coefficient on the shape of the pressure curves. Indeed, the experimental device is made of two steps and of a diverging part; the two steps can be responsible for strong 2D effects (like expansion and shock waves, recirculation zones) that cannot be easily computed with a 1D code like PUMA.

Two cases have been illustrated, with or without the correction (multiplication factor)
Case 1: ER=0. – Spalding's law of drag – vitiated airflow
Case 2: ER=0. – corrected Spalding's law of drag: the drag coefficient is increased by 20 for the first step and by 10 for the second one. This correction is supposed to simulate the effects of throttling or overexpansion on the wall pressure.

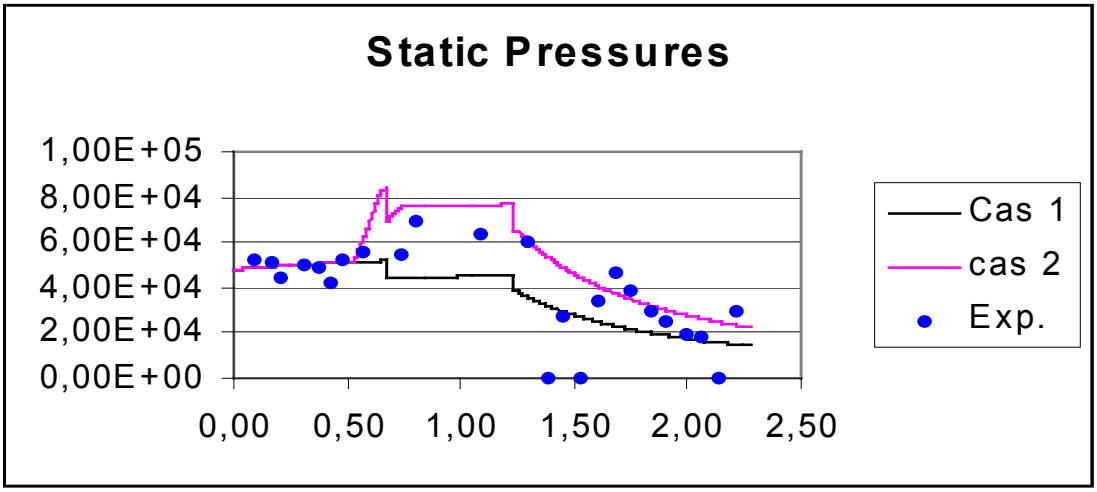

Figure 5: Non reactive computations : pressure (Pa)

For the case 1, the PUMA code computes only a quick expansion for the steps that is obviously not in agreement with experimental data.

The results are better with the case 2: the artificial increase of the drag coefficient improves the value of the pressure for the first step. However, there is a pike after the second step that cannot be simulated.
The corresponding Mach number is shown below :

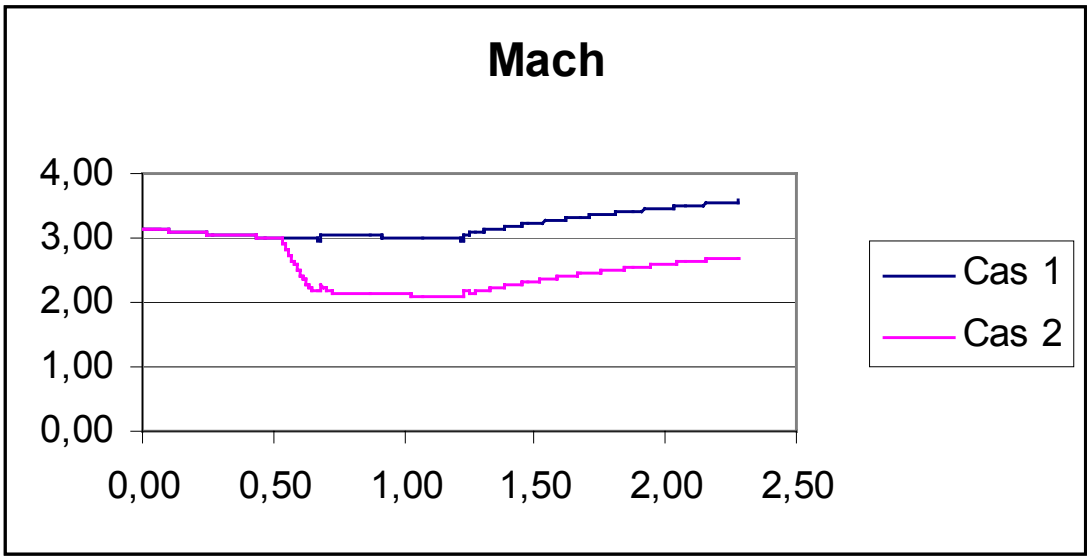

Figure 6: Non reactive computations (Mach number)

The static temperature has to be examined, in particular to see the ignition capability with the present flow.

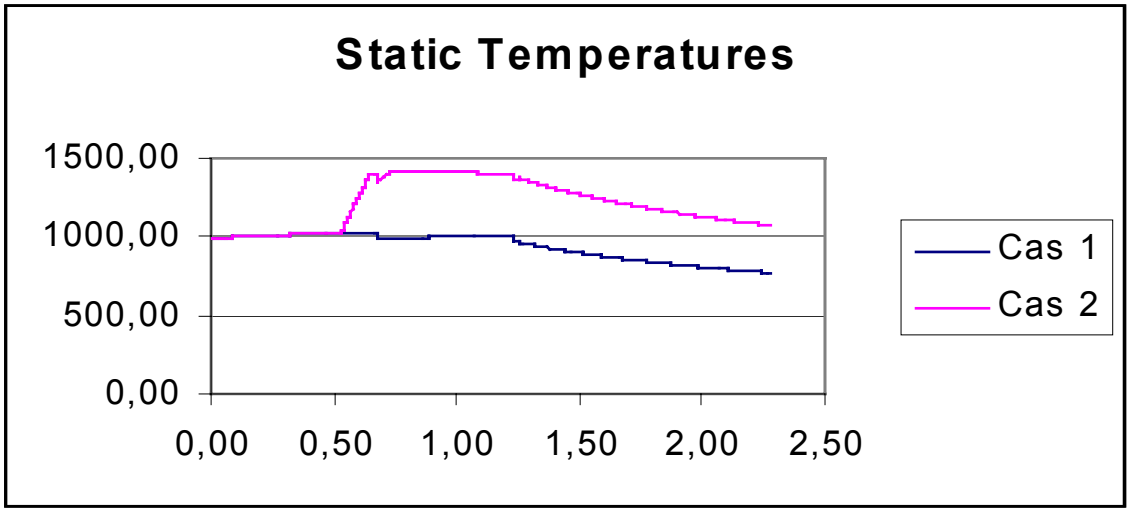

Figure 7 : 1D static temperature (K) before combustion

Self ignition of the hydrogen is expected at this air temperature. The chemical effect of water in the incoming flow is outside the scope of the present RTO subgroup task. Nevertheless, it is know that its effect on ignition delay is maximum in the vicinity of 1000/T=1: exactly the value at the present test conditions.

3.3.3 REACTIVE CASE (ER=0.51)

Now, we study the case of hydrogen injection with ER=0.51. The goal is to compute a combustion efficiency which yields the same pressure results as in the experiment.
Several cases have been computed, depending on the way to compute the drag, the composition of the incoming air (31%, 22% (reference) or 0% of water mass fraction in the incoming air).
Case 3b: ER=0.51 – vitiated airflow – Spalding's drag coefficient. We do not tune automatically the combustion efficiency ETAC(x) but assume a linear law. This approach predicts a computed maximum pressure which is too low in comparison with the experimental pressure (there are more shocks).
Case 4: ER=0.51 – vitiated airflow – Corrected Spalding's drag coefficient. Here the results are far better, since we have a good agreement between computed and experimental data.
Case 4b: ER=0.51 –vitiated airflow (composition YH2O=0.31). Corrected Spalding's drag coefficient.

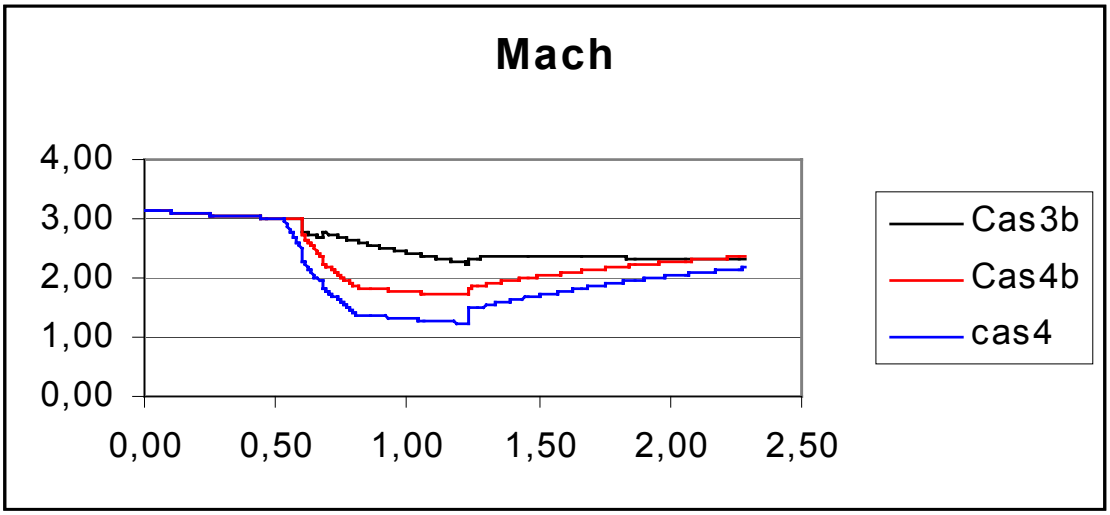

Figure 8 : Computed Mach number for several assumptions (ER=0.51)

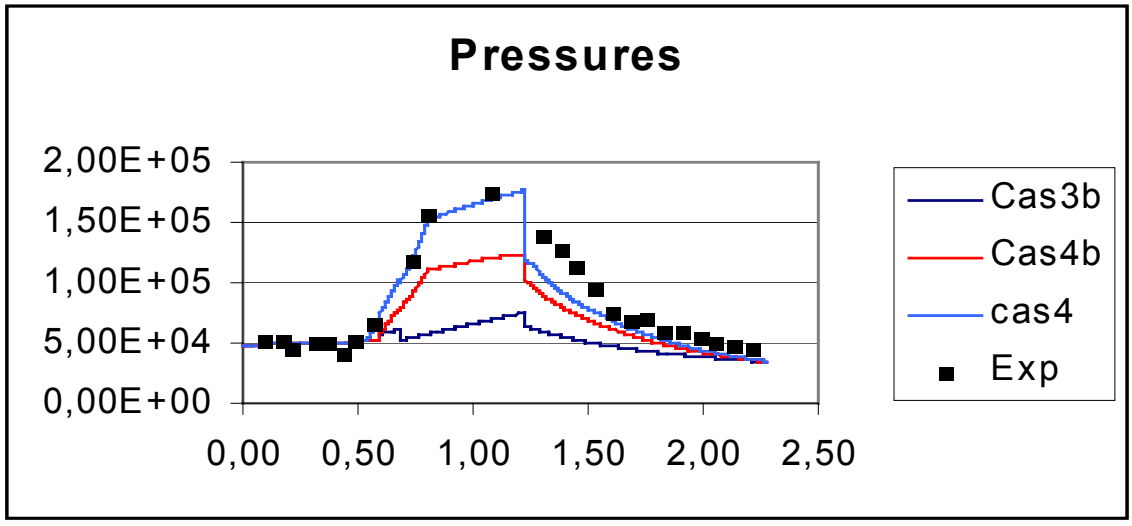

Figure 9: Pressure (Pa) for different assumptions (ER=0.51)

We clearly see here the differences between each case. The case 3b has a good x profile but its maximum pressure is too low: the Spalding's law alone cannot simulate the big shock effects occurring at the injection point (the flow strongly interacts with the fuel jet generating a shock wave). To integrate this

phenomenon in the simulation we locally multiply the drag coefficient by 20 (and by 10 for the steps). This is case 4, which is the reference for the following computations in order to study the physical effect of vitiation. The corresponding laws of combustion efficiency assumed along the duct are the following:

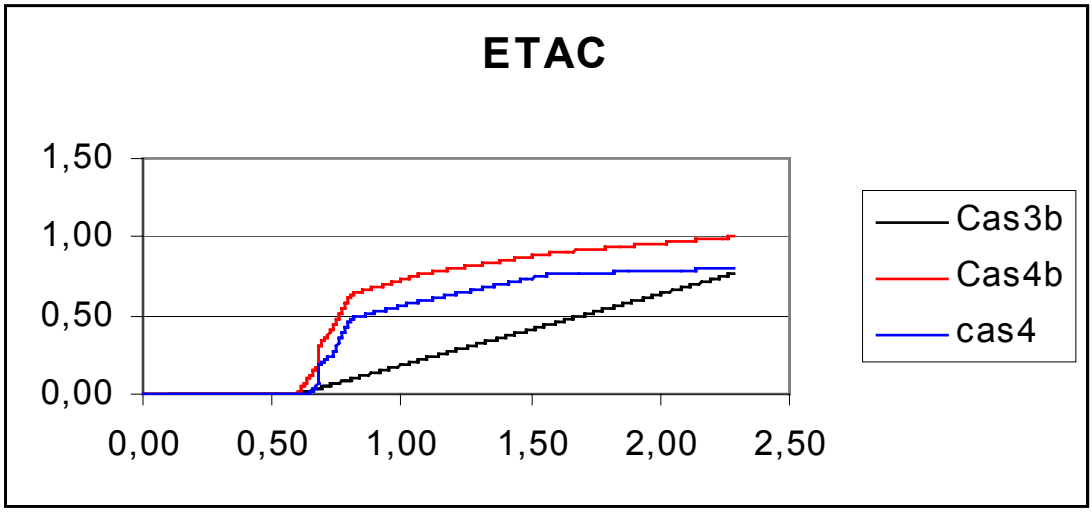

Figure 10: Combustion efficiency law along the duct (ER=0.51)

The heat transfer parameters at the wall can also be computed for the different cases, with the uniform wall temperature assumed constant at 305 K.

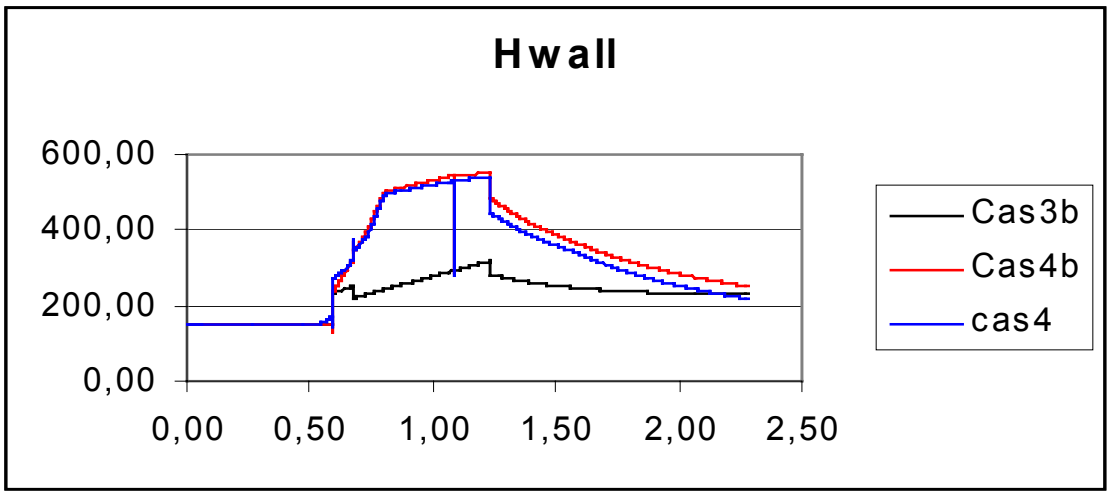

Figure 11: Heat fluxes along the duct at ER=0.51

This study illustrates also the uncertainty of the 1D analysis for such a 2D supersonic reactive flow. At this point, parametric studies of the effect of the composition of the incoming air can be performed, assuming the same combustion efficiency evolution along the duct, ETAC(x).

3.4 EFFECT OF VITIATION

A first 1D assumes the same combustion and drag laws, and has been performed with pure or water-vitiated air:

Case 4: ER=0.51 – Corrected Spalding's law of drag – vitiated airflow (22% of water)

Case 6: ER=0.51 – Corrected Spalding's law of drag – pure airflow – same ETAC(x) as for the case 4

Same Mach number, static temperature (for the same ignition environment), same static pressure (and same geometry)have been assumed at the entrance.

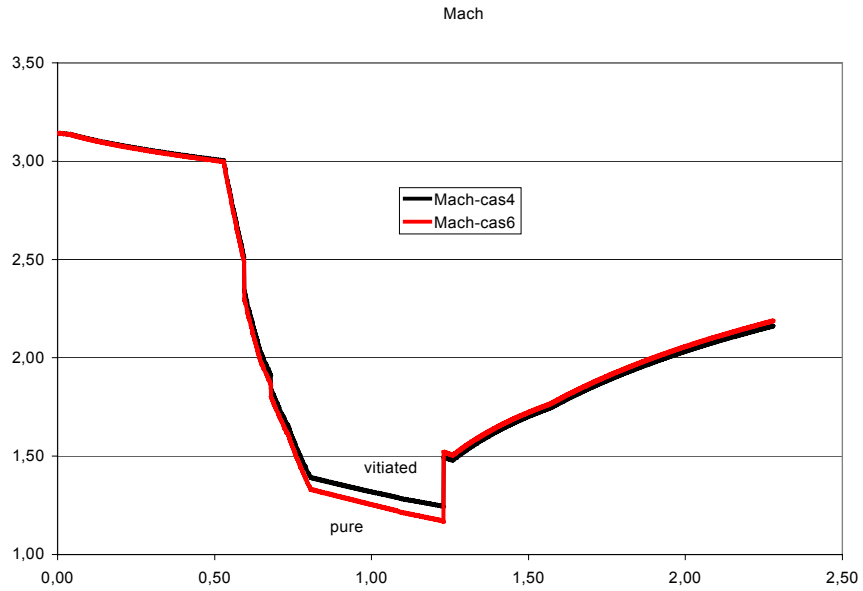

Figure 12: Computed effect of vitiation on Mach number

The computed effect is different after each step, probably because the 1D analysis is not appropriate in such a sudden expansion of the flow.

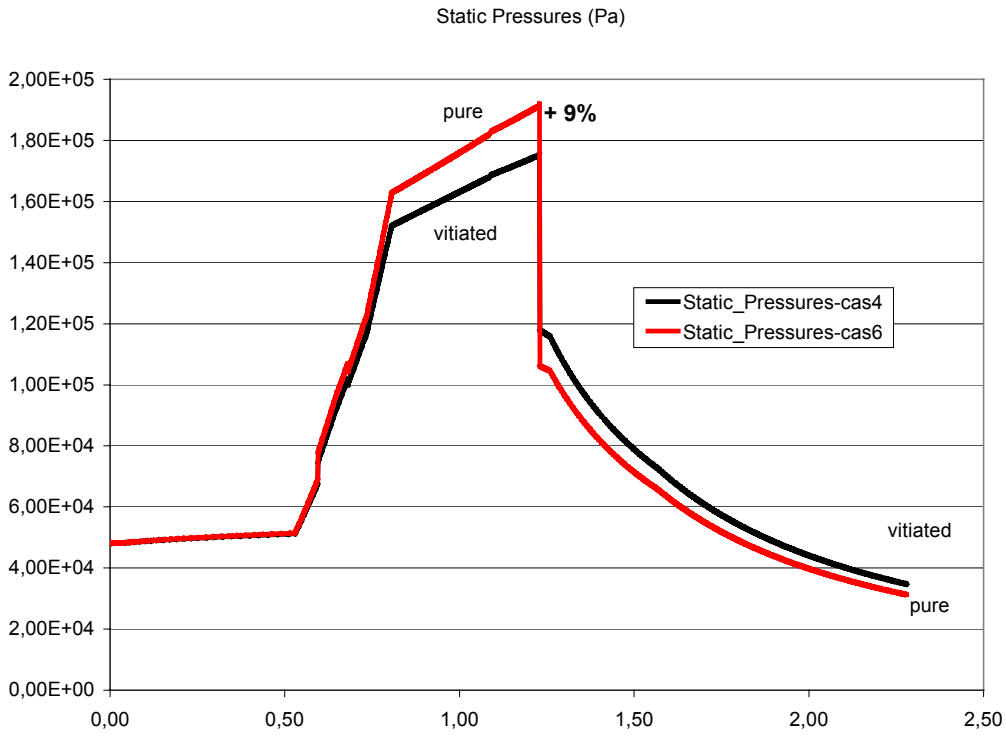

Figure 13: Computed effect of vitiation on pressure (Pa)

The opposite effect on Mach number and static pressure is visible in figures 12-13. The effect of vitiation on the computed heat flux (see figure 14) is note worthy: vitiation of the flow, within the assumptions made, leads to an increase of heat flux (about 5%). In this case, the check-out of a thermal protection or a cooling circuit should lead to a conservative design.

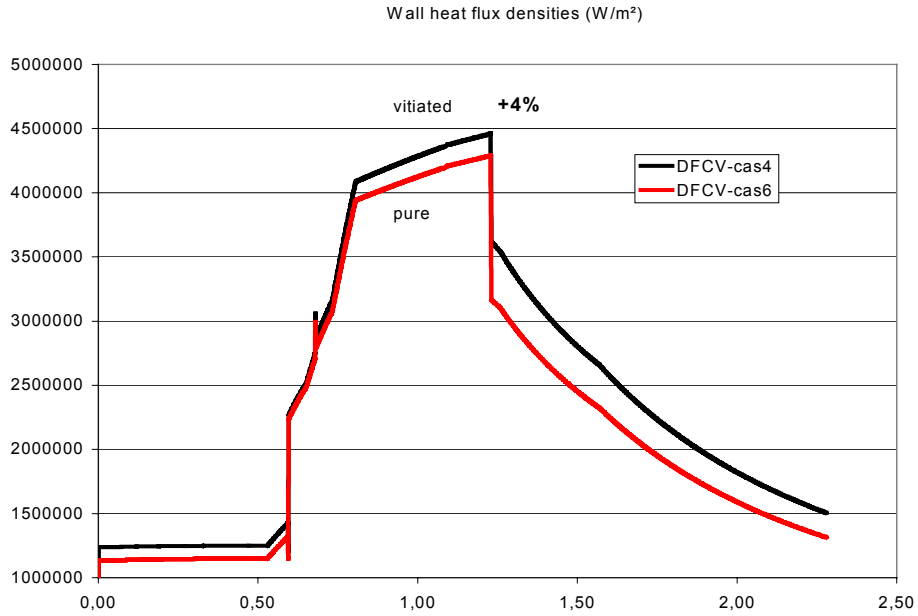

Figure 14: Computed effect of vitiation on heat fluxes

3.4.1 EFFECT OF COMBUSTION DISSOCIATIONS (EQUILIBRIUM MODELING OF COMBUSTION)

These first results have been extended, in particular to take into account the possible effect of incoming water on the combustion heat release (in the previous computations, only one reaction was considered). Combustion has been simulated using the same code but with equilibrium assumptions and more species (H2, O2, N2, H2O, NO, OH, H, O and N are considered). The Mach number, temperature, pressure and heat fluxes are very slightly modified.

Two new cases have been computed, with the same assumptions as cases 4 and 6, except the combustion modeling:

Case 8 : ER=0.51 – Corrected Spalding's law of drag – vitiated airflow– same ETAC(x) as for the case 4

Case 7 : ER=0.51 – Corrected Spalding's law of drag – pure airflow – same ETAC(x) as for the case 4

Equilibrium reduces the computed temperature, as shown for example on the static temperature profile of figure 15:

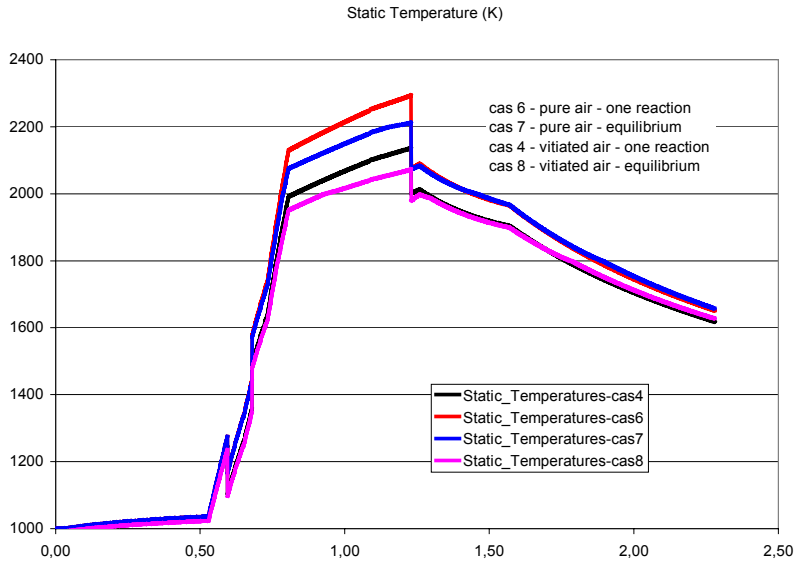

Figure 15: Effect of air vitiation and combustion modeling on static temperature

Some species computed are reported in figures 16-17, beginning with water:

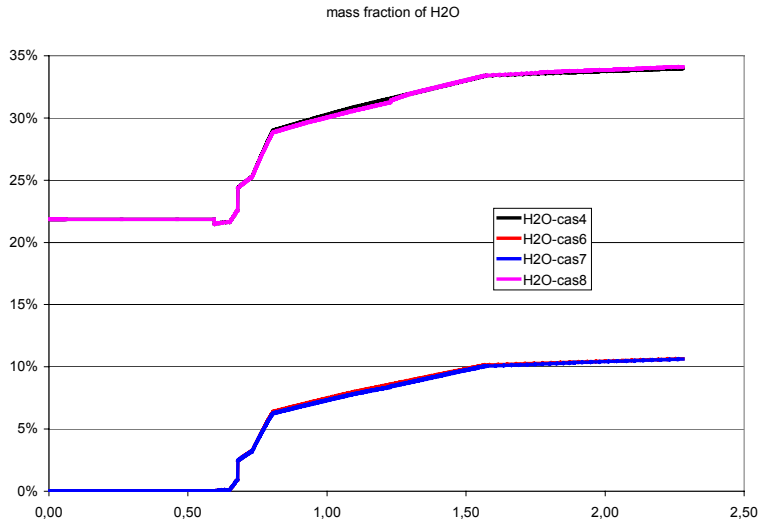

Figure 16: Water mass fraction computed along the duct

The equilibrium computations logically lead to 1% of NO in the hot gases, in the zone of the maximum static temperature (see figure 17):

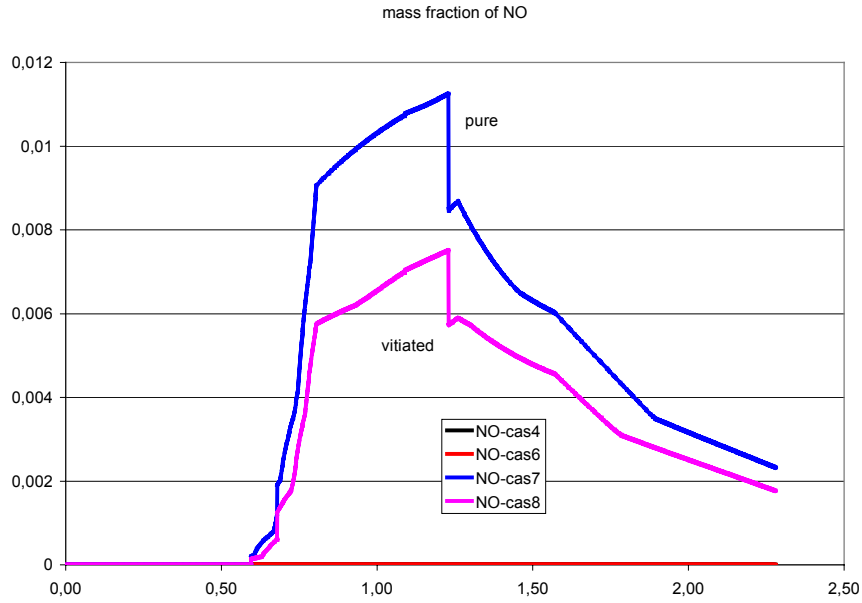

Figure 17: Computed NO along the duct

The angles of the shock and the expansion fans could be slightly different in pure and vitiated flow, as it can be derived from the specific heat ratio shown on Figure 18 ; 2D or 3D computations could provide interesting data but they are outside the scope of the present RTO subgroup task.

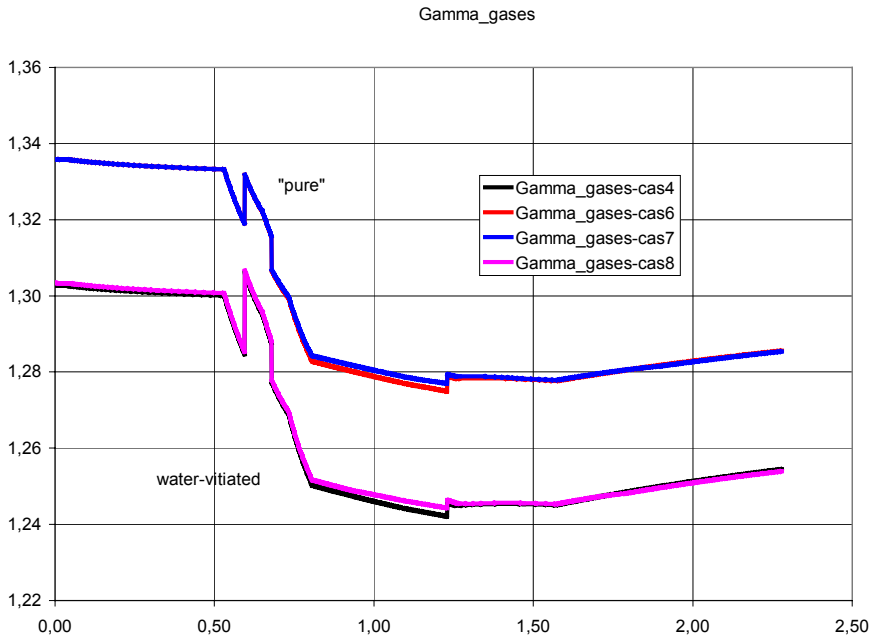

Figure 18: Specific heat ratio of the gases along the duct

Nevertheless, the effect of gamma on oblique shock at Mach 2.5 is very small (Mach after a 6° wedge varies from 2.27 to 2.28 and the deviation from 28.1 to 28.0°, static parameters change is less than 1%).

3.5 CONCLUSIONS AND RECOMMENDATIONS

A first analysis of the APL scramjet combustor has been carried on at AMM using 1-D codes.
Comparison of a scramjet operation with water or not in the incoming air has been performed. The present analysis is focused on the physical effect of the water-vitiation only: the combustion efficiency is assumed to be the same.
Vitiation, with these assumptions, leads to increase the heat fluxes (by 5%) and (generally) of the static pressure, in comparison with pure air.
Although the modeling in the simulations is somewhat crude, their results are suggestive of effects potentially important.
Therefore it is strongly recommended that this analysis could be profitably enhanced by 3D computations and by testing of the same combustor in two different test facilities (with or without water in the incoming flow).

3.6 REFERENCES

1 E. Dufour, M. Bouchez, “Post-Experimental computations of a kerosene-fuelled scramjet”, AIAA-2001-1817, Kyoto, Japan, April 2001
2 Handbook of Heat Transfer fundamentals, Mc Graw Hill editors, P.8.151 – table 14.

CHAPTER 4: AIR VITIATION EFFECTS ON SCRAMJET COMBUSTION TESTS

G.L. Pellett*, C. Bruno**, and W. Chinitz‡
G.L. Pellett
NASA Langley Research Center Hampton
Virginia 23681-2199 URL
g.l.pellett@larc.nasa.gov
C. Bruno
University of Rome "La Sapienza"
Via Eudossiana 18, 00185 ROMA – ITALY
c.bruno@dma.ing.uniroma1.it

W. Chinitz

GASL, 77 Raynor Avenue Ronkoma, N.Y.11779-6648

WChinitz@gasl-usa.com

4.1 OVERVIEW OF THE PHYSICS AND CHEMISTRY OF VITIATION EFFECTS

In ground tests, stored high-pressure air must be heated significantly, before expansion through a facility nozzle, to simulate hypersonic flight conditions. Resultants "vitiation effects" (using the term broadly) thus refer to particular chemical kinetic and thermodynamic effects on Scramjet (SCRJ) combustion caused by the use of artificially-heated (vitiated) air. Such heating may be accomplished in various ways. Two electrical techniques are by arc or by inductive electric (e.g., Plasmatron technology) heating. Both techniques are relatively expensive in terms of initial investment. A less expensive, simpler technology involves combustion preheating of beds of bricks or ceramic pebbles, followed by the input/heating of dry compressed air (as in Japan's NAL facility at Kakuda RC). Finally, an even lower cost air heating techniques is to burn fuel (e.g., H2, CH4, or C3H8) with a predetermined equivalence ratio, and then expands the resultant vitiated air, with or without oxygen makeup, through a facility nozzle. The question faced here is how to characterize and control the resultant effects on SCRJ test performance, since the vitiated air will differ from inlet-processed ambient air fed to a combustor in actual flight.

4.1.1 PHYSICAL-CHEMICAL EFFECTS DUE TO VITIATION

Several physical-chemical "facility processing effects" are currently recognized, starting with knowledge that species introduced to a typical test airstreams differ from those emerging from inlet-processed natural air. The classic paper by Edelman and Spadaccini in 1969 [1], entitled "Theoretical Effects of Vitiated Air Contamination on Ground Testing of Hypersonic Airbreathing Engines," discusses many of these effects and is an essential starting point for any serious study of air vitiation effects. A detailed summary of their findings and many others appears later in the "Detailed Review: Test Medium Effects on Ignition, Combustion and Flameholding Processes in Scramjet Combustors" portion of this paper. Below, we present an abbreviated general discussion of some key homogeneous gas phase effects.

* Hypersonic Airbreathing Propulsion Branch

NASA Langley Research Center, Hampton, VA 23681

** University of Rome, Rome, Italy. Chairman of

NATO-RTO-AVT-WG-10 Subgroup on Scramjets

‡ Allied Aerospace Industries, Inc., GASL Div., Ronkonkoma, NY

4.1.1.1 STEAM

At high altitude the air composition is extremely dry, whereas large amounts of steam are present in combustion-vitiated air. Analyses in [1] showed that such water vapor (and resultant HxOy radicals) could not only condense, which is clearly undesirable, but also spoil the duplication of flight conditions in SCRJs by changing important thermodynamic and chemical kinetic effects on ignition, flameholding, peak temperature, and energy release during radical recombination in a combustor and (especially) an exit nozzle.

Reference 1 deduced that large amounts of steam may exert strong kinetic effects, the reduced molecular weight will lower mass capture in an inlet, and thermodynamic heat capacity and steam-dissociation effects will cause loss of thrust. Quite recently, kinetic analyses of Scramjet combustion by Mitani at NAL [41,42,94] indicate that steam alone (without added HxOy radicals) inhibits ignition. Steam acts as a very efficient third body in recombining H + O2 + M → HO2 + M, and H + HO2 + M → H2 + O2 + M; and steam also reacts directly with H, namely H + H2O → OH + H2. Although steam from vitiation heaters can inhibit ignition at moderately low temperatures near atmospheric pressure, such inhibition is unimportant at reduced pressures. For example, for Mach 6 "simulated airs" at ~ 0.3 atm, variation of steam mole fraction from 0.0001 to 0.4 has essentially no effect because ignition delay is already much longer at this pressure, even at low steam contents [42]. Thus if T and P are such that (ignition delay) + (combustion time) > (mixing time), ignition will be suppressed; and this tends to occur at static T < 1100 K and 1-atm for H2/air combustion. Alternately, at static T > 1100 K there seems to be little effect of steam on ignition delay, because the critical kinetics are substantially faster than mixing rate. Thus the Damkoehler number (≡ mixing time/reaction time), which varies with T and P, may be used to characterize steam effects on ignition / flameholding-combustion (Damkoehler approach is developed in a section at the end of this paper, entitled "Scaling Air Vitiation Effects."

A complementary view of how HxOy radicals perturb H2/O2 ignition chemistry can be inferred through consideration of explosion limit behavior. Simulations of ignition delay times in H2/air mixtures [63,85] indicate ignition delays follow a pattern similar to the classical P vs T explosion limits of H2/O2 systems, i.e., delays become much longer at intermediate pressures between ~ 0.2 to 1 atm, such that H2/O2 mixtures do not explode at moderate temperatures between the second and the third (classical) explosion limits [93]. Although definitive SCRJ ignition tests that illustrate this behavior seem scarce, the now accepted kinetic explanation for ignition delay centers on the above-cited role of HO2 radical, both at 'low' T and P (scavenging H radicals) and 'higher' T (releasing OH radicals).

Even very small amounts of steam significantly catalyze O2 and N2 vibrational relaxation processes [92] that affect predictions of aerodynamic heating by clean air. For example, the larger the vibrational disequilibrium, the lower the resultant thermal load on a downstream external surface or on a SCRJ inlet surface, provided vibrational relaxation is relatively slow. Such relaxation effects may also play a role with short SCRJ test models and small tactical missiles. In these cases convective transport times may be comparable to "clean-air" vibrational relaxation times for O2 and N2, which effectively reduces "clean-air" thermal loads. Thus when steam shortens these relaxation times by orders of magnitude, wind tunnel tests can overestimate thermal loads. Calculations performed at DLR-Goettingen [83] show this effect is significant enough to warrant further investigation for high speed flight propulsion [84].

4.1.1.2 PRECOMBUSTION FREE RADICALS

Free radical species (from both well- and poorly-designed vitiation-combustion preheaters), such as H, O, and OH when H2 fuel is used, and also CxHyOz radicals if hydrocarbons (HC) are used, may significantly alter ignition delay times and flameholding/combustion in a SCRJ combustor [1]. Recent simulations indicate OH introductions may reduce ignition delay time by 10x or more [41, 42, 89, 90, 98], especially at typical low inlet temperatures and pressures (largest effect occurs at ~ 0.3 to 1 atm and ~ 900 K, i.e., at flight Mach numbers of order 3-4). Depending on vehicle type and mission profile, a switch from SRJ to SCRJ mode is often planned in this range, which further emphasizes the need to consider such possible effects of vitiated air-with-OH on ignition and flameholding. The effect of added H is similar, due e.g. to competition between the H + O2 --> OH + O chain branching reaction, and chain termination by H + O2 + M → HO2 + M, which are critical to ignition, flammability limits and flame propagation. Finally, O-atoms influence the symmetrical reaction, O + H2 --> OH + H, which is also very important for ignition and flame propagation.

Very rich H2 (or HC) precombustion in a rocket-based combined cycle SCRJ system may be an effective means to anchor flames in high speed flows, due to high fluxes of H-atoms (or HC radicals) injected into the leaner H2-air mixture of the main combustor [91, and others]. Resultant chain branching competes favorably with chain termination (above) that lengthens ignition times. Thus the increased presence of H and other radicals in vitiated air may enhance both ignition and flameholding in fuel-rich, combined cycle systems.

4.1.1.3 NITROGEN OXIDES, NO_X

Nitric oxide, NO, produced in amounts of 0.3 to 3 mole percent, can exert particularly strong effects on low-temperature ignition and flameholding processes. Nitric oxide results from any high-temperature combustion or (especially) arc heating process involving air. In addition, residual CxHyOz radicals stemming from incomplete preburning of HCs are not only very reactive with O2, but also N2, forming CN and excess NOx. Thus resultant NOx (estimated mostly in simulations, less from experiments) promotes ignition as a function of T, P, and equivalence ratio [9,17,18,80]. Note the percentage of NOx needed for significant effect on ignition delay approaches 1%, which is close to the upper 'thermal' NOx limit for a well designed HC-preheated wind tunnel. Note also, a theory of the effect of additives on HC combustion [101] defined families of NOx-releasing molecular species that act as very effective combustion promoters. Thus, despite our current lack of detailed NOx-effects data on SCRJ ignition and flameholding over a useful range of T, P, and input composition / flows, and considering the diffusive flame character typical of H2–air or (much more complex) HC–air flameholding, the NOx in HC-vitiated air may have particularly strong and unexpected effects on SCRJ combustion. Much further work is needed in the HC-fueled SCRJ area (see [49] for discussion of some known problems).

4.1.1.4 CO_2 AND STEAM

When large amounts of both CO2 and steam are present in vitiated air, their larger heat capacities, Cp, and molecular dissociation at high T will not only lower the maximum T and P of H2-fueled SCRJ combustion [1,38,47], but also decrease reflected shock angles [47]. These thermodynamic effects should be most pronounced at higher test Mach numbers, where temperatures are higher. Notably the effect of vitiation preheating with HC/air combustion is considered more 'neutral' in its effects on SCRJ combustor performance than preheating with H2/air, based on these dissociation effects [80; check this].

In opposition to the negative Cp-effects of CO2 and steam on flame temperature, steam has a positive third-body kinetic effect on H2-air flames at 1 atm and moderately lower T (say 1300 to 1400 K), where "non-robust" flameholding may occur, and intermittently fail. Both independent measurements and computations indicate steam (instead of N2) in air increases (1) non-premixed "flame strength," i.e. the aerodynamic strain rate limit for extinction of H2–air counterflow diffusion flames [24], and (2) the burning velocity of premixed flames over a range of equivalence ratios [6]. In these cases steam respectively strengthens the local temperature increase of flames near the airside edge or forward-flame edge, primarily via the enhanced third-body recombination, H + O2 + M → HO2 + M, which is followed by a series of exothermic reactions that overwhelm a negative "Cp effect." Under the same conditions CO2 weakens both diffusion and premixed flames via the Cp effect.

Thus an important set of controversial questions from the above concern whether heater-precombustion may improve or worsen the anchoring of turbulent diffusion flames in critical flameholding regions, which in turn can affect thrust performance. In practical ground-based testing, the promoting effect on ignition and flameholding of any excess CxHyOz radicals, downstream of a HC/air preheater, and the positive effect of steam on flameholding, would be opposed by cooling effects due to Cp at moderate temperatures, and dissociation of H_2O and CO_2 at higher temperatures. Clearly it is important to separate and account for the various competing effects. Russian practice at ITAM in Novosibirsk (where SCRJ combustion studies began in the mid-60s) was to use kerosene to produce high-temperature (vitiated) air. Whether or not this use reflected a deliberate technical judgment, to minimize possible vitiation effects, is not known by the authors.

4.1.1.5 CONDENSED SPECIES

Test facilities may also introduce metallic / condensed-oxide species in the airstreams. Arc heating typically releases copper oxide particles [39]. Even the stainless steel walls of shock tubes may release nickel-containing particles via shock tube erosion [96]. Fortunately, copper and nickel appear to be ineffective recombination catalysts in H2–air flames, based on a detailed study of metal oxide/hydroxide catalysts. A ranked listing (most efficient elements down to neutral ones) includes Cr, U, Ba, Sn, Sr, Mn, Ca, Mg, Fe, Mo, Co, and then Cu and Ni which are effectively neutral [102]. Air heating, by passing cold air over preheated ceramics (e.g. pebble heaters, as in the recent NAL-KRC facility) will release ceramic powder. Such "inert" particle effects on combustion were recently analyzed theoretically [41,95]. The heat sink effect was found negligible (dust must exceed 10% of total mass flow to exert an impact), but the effect on radical termination

(recombination) on particle surfaces became important at dust mass fractions > 0.001 and particle sizes < 3 microns. At sufficiently high temperatures this phenomenon may be alleviated by ceramic softening, that prevents particles from being eroded; such may occur with zirconia bricks [41,95]. Thus in planning SCRJ tests using ceramic heating facilities, one should estimate the potential magnitude of this problem.

4.1.1.6 CHARGED AND EXCITED SPECIES

Charged and electronically excited molecular species may also influence test results. In arc-heated wind tunnels oxygen and nitrogen ions can be present. Their concentrations should be relatively small because Coulomb forces are long-range, and recombinations of positive ions and electrons are very fast. However, there are electronically excited species that survive for long times. An example is O2 in the singlet delta state, a species observed during either homogeneous third-body or surface catalytic recombination of O. This state of O2 can persist for the order of seconds [103]. Relatively little is known about the possible effects of electronically excited species on combustion kinetics. However, if present in critical concentrations, they may reduce ignition delay time, because typical recombination / relaxation energies tend to be very high (of order 10 eV vs 1 eV for recombination of radicals). Finally, ions can be exploited locally to promote combustion and anchor a flame. An example of recent work in this area is by P.Tret'yakov at ITAM in Novosibirsk [100].

4.1.1.7 SOME PRACTICAL GENERALIZATIONS AND PROJECTIONS OF THE STUDY

Although the primary experimental goal of any facility should simply be to supply "air" with the thermodynamic and reactive properties of a “real” inlet, careful testing and analysis may reveal new ideas on stabilizing and anchoring flameholding/combustion modes. Thus, if variations of inlet air temperature and/or suspected radical concentrations cause unexpected improvements in flame anchoring and more efficient scramjet combustion, a good research plan should allow focused investigation of such internal free radical and inlet/combustor geometry effects.

Excess radicals in vitiated air may, for example, recombine catalytically on upstream inlet surfaces leading to the combustor. Heat released on the walls will alter expected surface heat flux and local wall temperatures. Specific tests for surface recombination on relevant materials, using reactive probes and measurement of wall temperatures and heat fluxes, may help reveal the effects of significant excess radical concentrations. Ideally, such tests should be performed prior to routine combustor testing to assess the presence of excess radical species in wind tunnel runs with vitiated air.

Looking ahead to the detailed review of scramjet combustion processes that follows, it should become apparent that possible homogeneous (and heterogeneous) air vitiation effects have not been adequately quantified to the point of being useful. Specific quantitative variations (e.g. partial derivatives) of key ignition, flameholding, and performance variables have not been mapped as a function of temperature, pressure, and fuel/air inputs. Thus realistic and functional “vitiation-compensation” offset procedures are simply not available to assess and compare data from different facilities, and hypothetical relationships between ground-based and free-flying SCRJ tests remain very uncertain and untested. Better information is needed on the merits of H2 vs. HC combustion preheating, and refined methodology should be developed and certified to enable improved testing and utilization of test facilities.

4.2 DETAILED REVIEW OF EFFECTS ON IGNITION, FLAMEHOLDING AND COMBUSTION

4.2.1 INTRODUCTION

The total temperatures (enthalpies) required to ground-test air-breathing (aero-propulsion) engines at high Mach number flight conditions can be achieved in a number of ways. Among these are:

- heat exchangers, including pre-heated ceramic beds,
- direct electrical heating, e.g., arc discharge and resistance heaters,
- compression heating,
- shock heating, and
- in-stream combustion, with oxygen replenishment to match air content.

Each method has distinct advantages, disadvantages and limitations. All have a common characteristic of being designed for intermittent flow, due to the extreme energy required for continuous operation at simulated Mach numbers above about 3. All also distort the composition of atmospheric air to some degree, due to the high temperatures that occur in a plenum section prior to expansion of the flow to simulated flight conditions. In the case of in-stream combustion, the resulting test medium is commonly referred to as "combustion-vitiated air," being composed of oxygen, nitrogen and some fraction of combustion products.

Table 1 lists mole percentages of several gaseous air contaminants in wind tunnels due to typical methods of generating high enthalpy supersonic flow. The presence of very large amounts of steam, and much smaller but potentially reactive quantities of nitric oxide (NO) and free radicals, e.g. OH and O, are of concern for both hydrogen- and hydrocarbon-vitiated air. Nitric oxide formation with attendant O2 depletion is major contaminant "sources" in facilities using arc heaters. Carbon dioxide, CO, and residual CxHyOz molecular/radical species are additional air contaminants in hydrocarbon-vitiated air. Furthermore, deviations in the control of O2 makeup, departures from complete mixing and combustion in a facility heater, and incomplete recombination in a facility nozzle, may cause significant deviations in downstream test simulations. Finally, methods for producing very high enthalpy flow, e.g. a piston-driven reflected shock tunnel or a shock/detonation-driven expansion tube, may alter the test gas drastically. Significant O-atom production may profoundly affect ignition/combustion kinetics. Also, relaxation rates of vibrationally-excited O2 and N2 are greatly accelerated by steam. Thus various generated air contaminants introduce uncertainty in scramjet testing, and may even require compensation to achieve "clean air performance."

Table 1. Mole Percentages of Contaminants in High Enthalpy Vitiated Air Simulated* for Mach 4-7 and 1-atm Static Pressure

		Method / Fuel for Producing High Enthalpy Air				
SPECIES	FLIGHT	AIR+ARC HEATER	H_2 + AIR/O_2	CH_4 + AIR/O_2	C_3H_8 + AIR/O_2	$CH_3N_2H_3$ + N_2O_4 + O_2
H_2O	<< 1	.1	5 - 33	3 - 21	2 - 15	3 - 21
CO_2	.03	.03	.03	1.4 - 10	1.7 - 11	1.1 - 7
C O	0	0	0	≤ 0.2	≤ 0.3	≤ 0.1
N O	< .01	.2 - 3.5	≤ 1.4	≤ 1.6	≤ 1.8	≤ 1.5
O_3	<.001					

*Calculated using equilibrium combustion and frozen expansion from 8 atm.

CH_4 ----------methane
C_3H_8 ---------propane
$CH_3N_2H_3$ -------- monomethyl hydrazine
N_2O_4 ---------- nitrogen tetroxide

4.2.1.1 ADVANTAGES OF IN-STREAM COMBUSTION HEATING

The ubiquitous use of combustion-vitiated air facilities warrants special attention to the advantages and disadvantages of this method for achieving high total enthalpies. These facilities have a number of very important advantages relative to other methods for achieving comparable total temperatures:

- Low capital investment
- Low technical risk
- Low operating costs
- High productivity
- Wide operating range
- Long run duration
- High versatility

Paramount among these is the relatively low capital investment required to design and build the heater component of a test facility - often the most expensive component. The cost of an in-stream combustion heater is lower than for any other method of achieving comparable temperatures in large masses of air, by a factor of four or more.

The most commonly used fuel for in-stream combustion heating is hydrogen, because there is relatively low technical risk associated with designing an efficient hydrogen burner that operates over a wide range of conditions (i.e., temperatures, pressures, mass flow rates). Burners developed some thirty years ago at GASL have been operated over simulated mach 2 through 8 conditions (444 k< tt < 2500 k). Although higher temperatures are also possible, pressure constraints on the burner vessels (p < 12,400 kPa) bound the practical limit of higher temperature operation.

Use of chemical heat release also contributes to relatively low cost. Typical combustion heaters are equivalent to 200MW arc heaters in terms of heat transferred to the test medium, but with far lower direct operating costs per heating unit. Although shock heating can have even lower operating cost per run, run times may be unacceptably short for full development of ignition and flameholding in recirculation regions, and for applications such as engine durability testing.

Run times for heaters employing in-stream combustion are typically limited only by the supplies of air, fuel, replenishment oxygen and cooling water. Other factors, such as model survival, vacuum/exhauster capability, etc., usually cause limitations on run time.

In-stream combustion heaters also offer high facility productivity, although factors such as the replenishment of gas supplies and vacuum, model changes, data reduction and analysis, etc., limit turnaround time. The heaters typically attain operating conditions in tens of seconds, and turn off almost as quickly. Direct electrical heaters offer comparable productivity, but storage heaters typically require several hours to heat up prior to run.

Finally, the versatility of in-stream combustion heaters should be recognized. The heater-mixer-plenum chambers are quite compact and relatively lightweight compared to other systems. Pressure and temperature in the plenum can be varied in real time during a run by scheduling the mass flow rates of the gas supplies. This permits real-time simulation of flight total pressure and total temperature corresponding to a segment of a flight trajectory (or even an entire flight trajectory, in principle). Furthermore, gas supplies can also be brought into a unit by flexible hoses, enabling relatively easy movement of the heater-mixer-plenum-nozzle assembly for real-time simulation of the flight Mach number approaching a stationary engine model, in concert with variations in total pressure and total temperature. (Movement of the engine model is seldom practical due to problems with ducting the hot exhaust stream from the engine into a diffuser/exhauster system, and with moving the force measurement system).

4.2.1.2 DISADVANTAGES OF IN-STREAM COMBUSTION HEATING

Given these compelling advantages of in-stream combustion heating, one must ask what price is paid in terms of the fidelity of the resulting simulations and engine data. Whereas high speed aeropropulsion test facilities should at least duplicate the flight environment (speed, total temperature, total pressure), matching all the non-dimensional simulation parameters required for complex chemically reacting, supersonic or hypersonic flow through an engine, is virtually impossible. The first and most obvious disadvantage posed by the use of vitiated air is that it requires selection of the most appropriate thermodynamic parameters to duplicate, since not all can be matched due to the differences in gas composition. Although 21 molar percent oxygen content is presumably "correct" from the reactivity standpoint (to be examined), a portion of the nitrogen content is displaced by water vapor and (if a hydrocarbon fuel is used) carbon dioxide, and the molecular weight is altered, so that mass capture and thrust may be affected by gas properties (discussed below). Other variations in chemical species/distributions may also occur, depending on the fuel or propellants employed (Table 1), the degree to which complete combustion is achieved, and the degree to which chemical recombination occurs in the nozzle expansion process.

Consequently, the molecular weights and specific heats of test gas mixtures will not match those of air. Thus, selections must be made about which properties of the flight environment will be duplicated and which will be relaxed to some extent. Given the importance of chemical reactions in an engine, duplication of static temperature and pressure (or density) is almost always selected, while some degree of relaxation is accepted in the local Mach number or sound speed and (sensible) enthalpy. Unfortunately, attempts to examine the effects of vitiation by comparing data between two types of facilities invariably run into the problem of selecting a proper basis for comparison. Can the effects of "vitiation" per se be separated from the effects of inherent or inevitable differences in test conditions? How are the data to be extrapolated to flight?

With regard to the definition of a “correct” oxygen content, it is not possible to match both the mass and mole fractions of oxygen in air due to differences in molecular weight between vitiated air and real air. Maintaining 21 molar percent of oxygen permits proper stoichiometry and reactivity with the fuel on a molar basis, but the fuel-air mixture ratio (on a mass basis) changes as the vitiated air temperature (and distribution of vitiation-combustion gases) is changed. On the other hand, maintaining 0.23 mass fraction of oxygen requires smaller changes in fuel-air mixture ratio with changes in air temperature, but the mole fraction of oxygen

changes. This is a dilemma that, although generally minor in its practical consequences, must be recognized, and the implications of the selection must be resolved during data reduction and interpretation.

The second disadvantage of in-stream combustion heating is that important thermochemical and chemical kinetic processes associated with combustion heat release in the engine may be affected by chemical species present in vitiated air "contaminants," but not in atmospheric air. The key thermo-chemical processes are auto-ignition/flameholding and the formation of near-equilibrated combustion products, which subsequently expand and recombine in the engine nozzle. For example, auto-ignition and flameholding may benefit significantly from the presence of trace amounts of free radicals in the test medium, due to incomplete combustion in the heater and/or some degree of dissociation in the heater that is not followed by near-complete recombination in the facility nozzle (the "freezing" phenomenon). A similar problem can also occur in other high temperature heaters due to the formation of nitric oxide, and sometimes even atomic oxygen, which remain frozen in the test gas. If auto-ignition and flameholding are marginal, the benefit obtained by testing in vitiated air may be decisive (and misleading). On the other hand, if auto-ignition and flameholding are vigorous, the benefit may be inconsequential. From a thermodynamic standpoint, the final state reached after complete combustion will be affected by the difference in specific heat between dry air and vitiated air. In general, the excess water vapor (and CO2) in vitiated air will tend to absorb more enthalpy and thereby suppress the pressure rise produced by combustion. Finally, vibrational relaxation (of N2) and chemical recombination (of H, O, and OH) processes in a nozzle expansion are very efficiently catalyzed by water vapor. This is a positive benefit in the facility nozzle, but in an engine nozzle the excess water vapor in vitiated air may produce misleading effects. The latter effect will clearly be dependent on the amount of water vapor produced by the engine as compared to that in the vitiated airstream.

The third disadvantage is that condensation of the combustion products may occur in the facility nozzle or test cell, at the simulated altitude-temperature. Condensation to a liquid (or solid) releases heat, produces a corresponding static pressure rise, and reduces total pressure. Expansion of the flow to atmospheric flight conditions invariably drops the temperature below the equilibrium saturation line for water vapor. (At Mach 8 conditions, about 33% of the test gas may be water vapor in a hydrogen-fired combustion heater.) Fortunately, there are two mitigating circumstances that must be recognized. First, condensation is a finite-rate process. Studies of condensation in early supersonic and hypersonic tunnels employing humid atmospheric air showed that up to 111 K (200 R) of supercooling (or supersaturation) could occur before the first signs of condensation, if the rate of expansion exceeded about 1 million degrees per second. This supercooling limit is more than sufficient for simulation of typical atmospheric air temperatures; facility nozzles having an exit area of one or two feet in diameter readily exceed the required expansion rate to avoid condensation (although much larger nozzles may not). Thus, if an engine inlet is at or very near the facility nozzle exit plane, condensation will not ordinarily occur under most conditions. Second, the compression process in the inlet quickly raises the temperature (and pressure) above the condensation line. Finally, airframe-integrated engines are typically tested at conditions simulating those downstream of the vehicle bow shock, which are also usually above the condensation line.

Therefore, for a wide range of practical test conditions, condensation should not occur in a vitiated airstream ingested by an engine. Nevertheless, it may occur in the external flow further downstream in the test cell, or in the diffuser, resulting in a higher back-pressure and poorer diffuser performance than with dry air.
Finally, hot water vapor or carbon dioxide may react with hot structural materials (e.g., carbon) differently than with either hot oxygen or nitrogen. This may or may not have consequences for materials testing, and ultimately engine durability testing, in facilities heated by in-stream combustion. Although there are no known indications of a problem of this type, it should not be dismissed out-of-hand for new flight-weight, high-temperature materials.

In the following sections, prior studies of vitiation effects on (mostly) H2–air ignition, flame-holding and related modes of combustion, and high-speed engine model testing are reviewed.

4.2.2 EARLY STUDIES OF FACILITY/VITIATION EFFECTS ON IGNITION, FLAMEHOLDING / COMBUSTION

4.2.2.1 BRIEF OVERVIEW OF VITIATION-CONTAMINATION STUDIES UP TO 1990

Early studies of vitiated-air contamination effects on engine combustion processes employed various techniques. A pioneering study included analytical assessments of equilibrium, vibrational and chemical relaxation, finite-rate condensation, combustion and mixing efficiency, and overall scramjet engine performance [1]. Early measurements and analyses of contaminant effects under a variety of premixed combustion conditions involved: Laminar burning velocities from conical flames [2-6]; ignition delays for H2/O2 explosions sensitized

by NOx in batch reactors [7]; ignition delays in reflected shock tubes, shortened by H2O at 1000 to 1500 K and unaffected by CO2 [8], and sensitized by NOx [9]; blow-out residence times from well-stirred reactors [10]; calculated ignition and reaction times (5% and 95% of steady-state) from plug-flow reactor models [11-16], in which [13] used a global model to assess ignition for several complex scramjet flameholding geometries, [15,16] used detailed kinetics to assess effects of NO, H2O, temperature and pressure, [15] also included O3 and H2O2 air additives, and [16] included analyses of well-stirred reactor and premixed supersonic ignition/combustion cases; and finally, [17,18] provided refined kinetic analyses of effects of NOx, H2/O2 equivalence ratio, temperature, and pressure on the catalytic NO, and non-catalytic NO2, autoignition of H2/air mixtures. Notably, none of the above contamination studies relate to nonpremixed turbulent ignition and flameholding, which are particularly important when H2 and H atom are major reactants. Although some very recent studies of diffusion-influenced combustion processes have appeared, relevant information is still lacking.

In one area of non-premixed combustion, one of the authors (GLP) has conducted experimental studies of NO, CO, CO2, H2O and O2 air-contaminant effects on aerodynamic extinction limits of laminar H2/N2 vs "air" counterflow diffusion flames, using an axisymmetric tube-based Opposed Jet Burner (OJB) [19-24]. The results provide quantitative flame-strength offset data on highly-strained nonpremixed flames, which apply at density-weighted input flow conditions (nominally 1-atm) and relatively-low peak temperatures (~1300-1400 K) that fall between those typically needed for ignition and those in adiabatic flames. The resultant flame strength (equivalent to airside strain rate at extinction) offsets for steam, CO2, and O2 are significant [22,24]. For example, increasing O2 from 21 to 22 molar % increases flame strength by 7.5%, which compares (interestingly) with a 7.4% increase in the burning velocity of a stoichiometric H2 –"air" flame (GLP analysis of Ref. 35 data). Respective near-linear offsets, at 21% O2, for 33% steam and 10.5% CO2 are +4.8% and –9.9%. These [24] results have recently been generalized (unpublished manuscript) in light of a comprehensive summary of "clean air" baseline data [25] derived from five sets each of tube- and nozzle-OJBs. To date, only limited numerical simulations of CO2 and H2O effects on H2–air counterflow diffusion flame structure and extinction limits have been available using detailed chemistry [26]. These numerical results are being supplemented by new 1-D and 2-D simulations.

4.2.2.2 DETAILED REVIEW OF VITIATION CONTAMINATION EFFECTS STUDIES UP TO 1990

Edelman and Spadaccini were first to address the high-speed-combustion problem in a study of "Theoretical Effects of [hydrogen- and propane-] Vitiated Air Contamination on Ground Testing of Hypersonic Airbreathing Engines" [1]. Using 1-D analyses for a Mach 7-10 flight regime, they concluded scramjet thrust levels in H2-vitiated air with O2 makeup would be lower than for clean air due to (steam) heat capacity and dissociation effects; and the presence of free radicals such as OH, O, and H would accelerate flameholding and subsequent combustion in a test engine, while H2O and CO2 would either increase or decrease reaction time, depending upon initial temperature, pressure and concentration level.

Kuehl, in a 1962 pioneering study, found that steam (anomalously) enhanced the laminar burning velocity, Su, of H2-air flames at 1/4 atm, 700 K (input), when substituted for part of the N2 in air [2]. He postulated internal thermal radiation transfer was the major contributing factor (now considered incorrect even for 1-atm flames; discussed later). Later, Reed et al. measured effects of air vitiation on burning velocities and flammability limits of methane/air/diluent mixtures [3,4], Erickson and Klich conducted analytic chemical kinetic studies of water vapor and CO2 effects on H2-air constant-pressure combustion [11], and Carson analytically assessed effects of O, H, and OH on H2–air combustion [12].

Slack and Grillo investigated the sensitization of H2-air ignition by NO and NO2 using a reflected shock tube technique [9]. They found an order-of-magnitude reduction of the ignition-delay induction period with ~ 0.5 mole-% NO or NO2 at < 1000 K and 2 to 1 atm. Sensitization occurred via the Ashmore and Tyler mechanism [7]: Initiated by HO2 + NO --> OH + NO2 , H + NO2 --> OH + NO, and also H2 + NO2 --> HNO2 + H when NO2 is present; supported by H2 + OH --> H2O + H; and terminated by OH + NO + M --> HNO2 + M and OH + NO2 + M --> HNO3 + M. Sensitization was most pronounced in the vicinity of the second explosion limit for H2-air, where rates of H + O2 + M --> HO2 + M, and H + O2 --> OH + O are balanced (exactly, at the crossover temperature; e.g. 925 K at 1 atm).

Jachimowski and Houghton employed a reflected shock tube to investigate the respective effects of CO2 and H2O vapor on the induction period of the H2-O2 reaction, using up to 1:1 H2 vs CO2 or H2O in Ar diluent at 1000 to 1500 K and ~ 1 atm [8]. Experimentally, CO2 did not produce a noticeable effect, whereas H2O appeared to shorten the induction period. However, their kinetic analysis for H2O depended upon assumed adjustments of two rate coefficients, and was inconclusive at both low and high temperatures.

Subsequently, Jachimowski [27] analyzed Slack and Grillo's shock tube ignition data [9] (based on "real" H2-air mixtures instead of "simulated" mixtures containing Ar) to deduce a refined set of rate coefficients that fit both the ignition data, and also some H2-air burning velocity data [28,29]. Using the refined mechanism, [27] concluded that chemical kinetic effects can be important at representative scramjet combustion conditions

(up to Mach 16) and that combustor models which use nonequilibrium chemistry are preferable to models that assume equilibrium chemistry. Also, for Mach numbers up to 16, [27] concluded "an ignition source will most likely be required to overcome the slow ignition chemistry."

Huber et. al. examined the "Criteria for Self-Ignition of Supersonic Hydrogen-Air Mixtures" [13]. They derived a correlation of available self ignition data (64 runs) obtained in representative scramjet combustors. Their correlation was based on a pressure-scale product as a function of combustor-entrance stagnation temperature, and a global reaction rate to approximate finite rate chemistry. Their principle findings are quoted as follows.

> " (1)For the typical case of fuel stagnation temperature much less than air stagnation temperature, the ignition very likely occurs in those regions where the mixture equivalence ratio is approximately 0.2. (2) Self-ignition is extremely sensitive to the mixture temperature at the pertinent ignition locations. As a result, wall temperature and recirculation-zone temperature recovery factor have dominant influence on the phenomenon, and it is desirable for both to be as high as possible. (3) For the typical case of highly cooled walls, the ratio of boundary-layer thickness to jet penetration height, step height, or base half-height has strong influence on ignition since it directly influences recirculation-zone recovery temperature. (4) The likely regions for self-ignition in the combustor seem to have an order of merit as follows: (a) strut bases and steps where the fuel is injected well upstream, (b) the upstream recirculation regions of strong transverse jets on plane surfaces, (c) behind steps with transverse fuel injection, and (d) bow-shock regions of transverse fuel jets."

Odgers and Kretschmer, in their paper "Considerations of the Use of Vitiated Preheat", reviewed available combustion data, assessed applications in gas turbine development [14], and concluded for a gas turbine combustor "no model currently available in the literature has been established which will describe the combustion behavior with an accuracy sufficient for vitiated preheating to be used to assess unvitiated performance at the same nominal conditions."

Rogers and Schexnayder performed a "Chemical Kinetic Analysis of Hydrogen-Air Ignition and Reaction Times" in the presence of contaminants [15]. They found "for mixture equivalence ratios between 0.5 and 1.7, ignition times (5% of temperature rise) are nearly constant; however, the presence of H2O and NO can have significant effects on ignition times, depending on the mixture temperature. Reaction time (95%) is dominantly influenced by pressure but is nearly independent of initial temperature, equivalence ratio, and the addition of chemicals" (e.g. H2O, NOx, H2O2, and O3).

Later, Rogers numerically examined several important aspects of "Effects of Test Facility Contaminants (NO and steam) on Supersonic Hydrogen-Air Diffusion Flames" [16]. Static input temperatures ranged 850 to 1250 K, and static pressures 0.2 to 2.5 atm. A plug flow reactor (PFR) model was used to determine temperature vs time for ignition (5%) and reaction (95%), and a well-stirred reactor (WSR) model was used to assess overall flame stability (blow-off) at 1-atm. Rogers concluded: (a) 0.5 to 1 mole-% NO enhanced PFR ignition for stoichiometric ($\phi = 1$) H2/air mixtures, and increased WSR flame stability for $\phi > 0.3$ at < 1100 K and ≥ 1-atm; and (b) H2O retarded PFR ignition for $\phi = 1$ at < 1100 K and < 1.5 atm, and slightly enhanced PFR ignition and combustion at > 1100 K. However, for WSR inputs at 1000 K and ϕ of 0.3 to 2 at 1-atm, H2O progressively enhanced WSR flame stability (to 14% less residence time, for 25 mass-%), both with and without 1% NO.

Finally, Rogers numerically simulated diffusive supersonic combustion of a central core of H2 flow (240 K, Mach 2) and coaxial air (1000 K, Mach 2.2), at 1-atm [16]. Most cases were synthetically pre-seeded with a H2/air ignition source near the H2 tube lip, and all required a small initial turbulent intensity (0.01 or 0.02) for the "k-epsilon" model. After the ignition seed cooled from 1800 to nearly 1000 K, onset of significant downstream combustion occurred: (a) sooner with 1% NO in the air, and (b) later with 8 mass-% H2O, compared to clean air. Combustion onset always moved upstream with increasing turbulent intensity; and unseeded autoignition with H2O-contamination occurred later than in clean air. These retarding effects of H2O were consistent with the PFR ignition studies at < 1100 K.

Twenty-four years after Kuehl reported a positive effect of added steam on Su relative to N2 [2], Koroll and Mulpuru conclusively confirmed that steam has an anomalous and extraordinary chemical kinetic effect on flame structure and Su of H2/O2 mixtures when steam replaces N2-diluent [6]. Notably, before Kuehl, steam was considered an inert heat sink that lowered Su by reducing flame temperature [30,31]. Sometime after Kuehl, but before [6], Liu and MacFarlane [5] reported detailed Su measurements as a function of input temperature (296-523 K) and composition (18 to 65 mole-% H2-air plus 0 to 15% steam), using a 3 mm Mache-Hebra nozzle. They found a doubling of input temperature from 300 to 600 K tripled Su. They also reported Su decreased with steam addition (which consequently decreased O2). A normalization (by GLP) of their Su data correlation by resultant X(O2) showed a net "apparent neutral effect" of steam addition. Despite this "neutral" finding for a 3 mm nozzle, Koroll and Mulpuru's comprehensive experimental / theoretical study [65], which

used a larger (5 mm) more-ideal nozzle and included O2 make-up, decisively showed that progressive reductions in Su due to steam addition were not commensurate with changes in the heat capacity of the mixture. In fact, steam enhanced Su by up to 16% when it replaced N2 diluent in a mixture at fixed O2 concentration.
Although the Su results offer important chemical kinetic insight on the effect of steam in premixed H2/O2 flames (third body effect; discussed later), measured "strengths" of H2–(air + steam) diffusion flames are also important [24]; i.e., because early stages of flameholding are essentially non-premixed, and significant differences in flame structure exist which effectively control the respective effects of air contaminants on H2 + air burning velocity and H2–air flame strength [25].

4.2.3 DETAILED REVIEW OF CONTAMINATION EFFECTS STUDIES SINCE 1990

During the 1990's several detailed studies of non-premixed / premixed flame systems significantly advanced our understanding of ignition and combustion processes, and possible air contamination effects relevant to testing of high-speed (mainly) hydrogen-fueled airbreathing propulsion devices.

In what follows, we first highlight a fundamental basis of scramjet efficiency. Second, we briefly review two representative studies of highly-complex non-premixed flames with vortex and turbulence interaction, and four studies of premixed flames affected by pressure, composition, stretch and diffusion. We then focus on eleven detailed studies of facility-based contamination effects on Scramjet ignition and flameholding/combustion, and seven experimental flame stabilization studies with bluff bodies and cavities. Next, we review a study of chemical reaction effects on numerical simulation of supersonic combustion flows, in which at least 8 reactions were required to properly simulate the transverse injection of H2 in a generic scramjet configuration. We also identify some results on O2 dissociation and O-atom and NO production in very-high-speed pulsed facilities. Near the end of the review, we examine several detailed ignition studies involving non-premixed diffusion and turbulence. We also review a premixed high-pressure ignition study, two catalytic ignition studies, and numerical simulations of ignition and combustion in high-speed shear layer flows. These recent ignition studies offer several new and important insights. Finally, we attempt to summarize the principal findings of this review.

4.2.3.1 ON THE FUNDAMENTAL BASIS OF SCRAMJET EFFICIENCY

In contrast to rocket combustion at relatively high pressures, Harradine et al. point out that due to inherently-low gas densities, three-body recombination kinetics remain important during ignition, flameholding, supersonic combustion, and nozzle expansion [32]. Their study on the chemical basis of scramjet efficiency compared equilibrium assumptions with detailed finite-rate kinetics for premixed combustion, and then conducted a sensitivity analysis. They concluded slow three-body recombinations of H_2O dissociation products (H, OH, and O) during combustion and nozzle-expansion represent a major obstacle towards achievement of high efficiency.

4.2.3.2 NON-PREMIXED H2–AIR DIFFUSION FLAMES W/VORTEX, TURBULENCE INTERACTION

Ref. [33] describes an experimental / numerical investigation of vortex interaction and flame quenching patterns that occur when a pulse of air is injected, from a 5-mm diameter syringe tube, to generate a vortex that passes coaxially through a steady opposed-jet (25-mm diameter) H2/N2–air counterflow diffusion flame. Changes in flame structure due to various vortex normal velocities were followed using OH PLIF. When an air-side vortex was forced toward the flame at relatively high speed, point-quenching of the flame occurred at the stagnation point. At moderate speeds, the flame surface deformed and quenching developed in an annular ring away from the stagnation surface; here, extinction was not caused by a strain rate mechanism per se, but from the combined effect of preferential diffusion and flame curvature.

Ref. [34] applied an unsteady laminar-flamelet model in numerical simulations of a steady, turbulent, H2/N2–air jet diffusion flame. Differential diffusion was neglected, and unity Lewis numbers were assumed. Transient effects were considered in terms of relevant timescales. Radiation effects were unimportant, and flame structure was hardly affected by transient effects, but slow processes like NO formation were affected. Predictions by the unsteady model agreed reasonably with experimental data for temperature and concentrations of major species, OH, and NO. In contrast, while steady flamelet libraries yielded good results for flame structure and OH concentrations, NO was overpredicted by an order of magnitude. However, reasonable NO results were obtained by solving an unsteady flamelet in a postprocessing mode. A needed step is to include nonequal Lewis numbers to explore wide ranges of scalar dissipation rates.

4.2.3.3 PREMIXED H2/O2/N2 FLAMES: EFFECTS OF PRESSURE, COMPOSITION, STRETCH, DIFFUSION

A comprehensive experimental / numerical study of laminar premixed H2/O2/N2 flames (spherical, outwardly propagating) examined effects of pressure and composition on flame / stretch interactions [35]. Fuel equivalence ratios ranged 0.45 to 4.0; pressures 0.35 to 4.0 atm; volumetric O2 12.5 to 21%; and Karlovitz numbers 0 to 0.6. Both measured and predicted ratios of laminar burning velocities, for large-radius nearly-unstretched (S'u) flames to stretched (SL) cases, varied linearly with Karlovitz numbers (= flame stretch * mass diffusivity / SL2). Resultant Markstein numbers (slopes) varied from -4 to 6 with equivalence ratio (and pressure). These results implied that flame stretch and preferential diffusion interacted strongly with burning velocity.

Ref. [36] computationally examined inward-propagating laminar spherical flames, in both lean and rich H2/air mixtures, to investigate the extinction of fuel pockets and formation of unconsumed reactants through flame-vortex interaction in turbulent flames. The first set of results, assuming quasi-steady propagation, showed the lean (Le < 1) flame becomes progressively weaker such that extinction is stretch-induced and accompanied by substantial unconsumed H2 and O2. In contrast, the burning intensity of a rich (Le > 1) flame is so enhanced by stretch that the flame can survive to a much smaller radius -- where extinction is caused by depletion of O2 ahead of the flame, and practically no unconsumed O2 remains. Second, for the more realistic case of transient propagation, a flame can persist almost to the center for both lean and rich flames, and all deficient reactants are consumed upon flame extinction. The authors extended the transient results to hydrocarbon flames, within the context of stretch and nonequidiffusion, and suggested that formation of unreacted fuel pockets may also be of limited importance here because complete consumption of the deficient reactant may occur upon extinction of the inwardly propagating flame.

Ref [37] numerically computed the effects of stretch and preferential diffusion on the structure and extinction of a laminar counterflow, premixed H2/air, symmetric double-flame system. They demonstrated use of local adiabatic equilibrium temperature as a basis for measuring energy loss and gain in stretched flames, caused by preferential diffusion (mass and thermal) and reaction incompleteness (quantified by the difference between actual flame temperature and local equilibrium temperature). Energy gain was quantified by the difference between local free stream and burned gas equilibrium temperatures. With increasing stretch, lean hydrogen flames gained energy through preferential diffusion; and continuously lost energy through reaction incompleteness, which finally caused extinction (e.g. 3400 s-1 at ϕ = 0.3). For rich mixtures, energy loss through reaction incompleteness leveled off at high stretch rates; thereafter, energy loss by preferential diffusion led to extinction (e.g. 30,600 s-1 at ϕ = 1.3). Note the latter extinction limit is roughly double that for extinction of a H2–air counterflow diffusion flame (which resides on the airside).

A recent numerical study of air contamination effects examined premixed combustion in a plug flow reactor [38]. The authors used 50 plots to illustrate the effects of NO, CO2 and H2O contaminants on effective ignition and reaction times, for 21% O2 and respective H2, CH4 and C2H6 fuels, at pressures from 0.1 to 100 atm and initial premix temperatures from 800 and 1200 K. Findings included: NO > 0.2% exhibited pronounced sensitizing effects; 0 to 20% H2O inhibited ignition monotonically below 1100 K, but slightly accelerated combustion above 1000 K; and H2O + CO2 (in 2:1 ratio) had very little additional effect over H2O on either ignition or reaction times.

4.2.3.4 FACILITY-BASED CONTAMINATION EFFECTS, H2 SCRAMJET COMBUSTION STUDIES

Facility-based studies have addressed some of the more obvious contamination issues. In the following review of recently studied H2-fueled SCRJ configurations, it should be apparent that even "well-controlled" experiments are frequently compromised with respect to important controlled conditions, ranging e.g. from undesired boundary layer phenomena to the generally assumed tight control of O2 level. Also, they often lack the singular cause and effect relationships we seek to pinpoint.

Nitric oxide (NO) production in air attained ~3 mole-% in an arc-heated supersonic tunnel during Mach 8 flight simulations [39]. The combined effect of 3% NO production (with destruction of 1.5% O2 and N2) was then assessed analytically. A 1-D finite-rate kinetics code, coupled with a 3-stream mixing code, revealed a very slight net enhancement of calculated thrust performance [39]. Notably, NO is predicted to cause a significant increase in calculated performance due to enhanced nozzle recombination kinetics [40], that is partially "compensated-for" by decreased O2 and combustion heat release [39].

Scramjet ignition difficulties related to heated air containing H2O, radicals, and dust were assessed theoretically by Mitani using a reduced kinetic model [41], and experimentally at Mach 6 by Mitani et al. [42].

In [41] an analytic expression was developed based on steady-states for HO2 and O atom. It predicted ignition delay in terms of O2 and H2O concentrations, and three rate coefficients: i.e. for H + O2 + M --> HO2 + M and H + O2 --> OH + O, which have equal rates at the crossover temperature, Tc, that defines the "second explosion limit" for H2-air; and for H + H2O --> OH + H2, which has steam as a reactant. The retarding effect of high steam concentrations (15-30 mole %) on ignition increased significantly with higher pressure and (of course) lower temperature [41,42]. Also, synthetic addition of O atoms was 1.5 times more effective for ignition than addition of H atoms [41]. With respect to dust effects, radical termination on surfaces mimics heat loss, but can become significant when dust mass fraction exceeds 0.001 and particles are < 3 μm and chemically active, whereas the heat sink effect only becomes important after mass fraction exceeds 0.1 [41].

Mitani's experimental assessment [42] featured tests of a H2-fueled scramjet at Mach 6 flight conditions, with air from both a vitiation-combustion heater (V mode) and a storage heater (S mode). Although steam from V can have a strong third-body effect in retarding ignition at ≥ 1 atm, via third-body recombination of H + HO2 to H2 + O2, steam effects on ignition were irrelevant in their engine tests because ignition delay at low pressure (0.03 M Pa) was already 5x larger, and thus not further affected by steam. Furthermore, some "compensating ignition enhancement" was promoted by transport of equilibrated HxOy radicals from the steam-containing V mode.

Post-ignition combustion behavior in Mitani's (et al.) engine was also affected by the test air [42]. Gas sampling showed that, as fuel flow increased, combustion changed from a weak boundary-layer mode along the engine walls, to an intensive mode where flame anchored near the backward-facing step. Because a detached flame coexisted with the weak-mode "semi-anchored" flame, the detached flame appeared to promote overall kinetic-control with enhanced sensitivity to test air composition.

Kanda, in a follow-up paper [43], refined his assessment of the [42] intensive combustion mode, which produced a much larger thrust than the weak mode after a sufficient increase in primary fuel was injected normally downstream of the backward-facing step. Note pilot fuel was always injected just upstream of the step, and parallel injection was also used with any short-isolator model. Kanda concluded the boundary layer downstream of the step interacted with the fuel jet (aided by a strut at Mach 6). Thus recirculation between the step and primary fuel jet, and particularly recirculation downstream of the jet, appeared to cause significant heat release near the fuel injector, which greatly enhanced combustion efficiency (90% vs. 5%).

Ref. [44], in a collaboration with Japan's NAL, also investigated experimentally and numerically the effects of combustion on the change of flowfield in a similar model SCRamjet combustor with a backward-facing step. The main airflow was at Mach 2.0, and the total temperature was 1000 K for cold flow and 1800 K for hot flow (H2-O2-air vitiation heater). Parallel injection of hydrogen was through a slit on the backward step face. The weak combustion (WC) mode was not accompanied by a shock wave, and the flowfield was similar to that for cold flow. The intensive combustion (IC) mode was accompanied by a precombustion shock wave, a large separation region generated just behind the step by the shock wave, and a resultant vortex that rolled the fuel up. The main reacting region was the shear layer just behind the shock wave, where the main airflow bumped the rolled-up fuel, and the temperature was elevated by the shock wave. This IC flowfield, controlled by the rate of mixing, led to a comparatively fast heat release and a raised pressure level in the combustor, which supported the shock wave. Thus a passive feedback occurred, and both the mixing efficiency and combustion efficiency became high. Alternately, in the WC mode, the reacting region spread more gradually over the thin shear layer downstream of the step, the heat release was lower, the flowfield was controlled by the lower reaction rate, and the combustion efficiency was lower.

To improve measurements of the combustion performance of scramjet engines using gas sampling, Mitani et al. [45] constructed four kinds of probes and quantified their degrees of reaction quenching in a Mach 2.5 supersonic combustor. They included freezing-oriented pitot probes (0.3 and 0.7 mm orifices), a freezing-type static probe, and a reaction-oriented pitot probe (1.0 mm orifice, heated nickel). The probes were tested in a slightly-diverging supersonic flow reactor duct that contained two swept-ramp H2 injectors, and was directly connected via a contoured nozzle to a H2-O2-air vitiation heater. The heater and nozzle produced a Mach 2.5 "airflow" (containing 20% H2O, and HxOy radicals), with airflow total temperature Tt from 750 to 2200 K. Autoignition was observed in the reaction-oriented probe for Tt > 910 K. The freezing-oriented probes yielded gas compositions having partially burned H2 and O2, even at Tt = 2190 K. The calculated combustion efficiency increased from 0% to 100% as Tt increased with the freezing-oriented probes. The pitot pressure measurements indicated combustion actually occurred in the supersonic combustor, not in the 0.3 mm freezing-oriented probe. They concluded, by comparing with static pressure measurements, that the 0.3 mm freezing-oriented pitot probe indicated the correct combustion efficiency for scramjet engine conditions. The similar 0.7 mm probe failed to quench H2-O2 reactions, misled the occurrence of combustion at Tt = 1000 K, and yielded an incorrect higher combustion efficiency at Tt = 1200 K.

Takahashi et al. [46] tested active control of flameholding by secondary air injection downstream of a rearward-facing step, and effectively reduced pressure oscillations from unstable flameholding and/or blowoff in

a fixed-geometry, rectangular scramjet combustor at an off-design point. Injected air controlled the effective cross-sectional area of the combustor, and also improved self-ignition at low total temperatures.

A numerical assessment of H2O and CO2 vitiation effects on mixing and combustion efficiency, at Mach 7 flight conditions, involved simulations of a premixed diverging-duct combustor flow-field, using a single 30º angled injection of H2 for both a hydrocarbon-vitiated air stream and clean air [47]. The temperature rise due to combustion was lower in the vitiated air case, due to the higher heat capacity and more extensive dissociation of H2O and CO2. Also, both combustion-induced pressure rise and reflected shock angles were lower, due to the same cause. Finally, only small differences in overall mixing efficiency and combustion efficiency were found, both in the near and far field. Thus [47] concluded observed differences were mainly due to thermodynamics; and whereas vitiation-combustion facilities are useful in simulating scramjet flow fields, appropriate analysis is necessary.

4.2.3.5 CONTAMINATION EFFECTS, HYDROCARBON-FUELED SCRAMJET COMBUSTION

Chinitz and Erdos examined the effects of NO and steam contaminants on ignition and combustion, with 1-atm "air," of several neat hydrocarbon fuels [48] and the simulated products of Norpar-12 endothermic-decomposition [49]. Ref. [48] used pure steam and NO, and also assessed possible chemistry effects on detonations. Because the respective effects of NO and steam on neat hydrocarbon fuels in [48] were too variable in magnitude and direction to permit generalizations, the principal conclusion from that study was that "careful pre- and post-test analyses, using validated chemical kinetic mechanisms, will be required to ensure that wind tunnel experiments using hydrocarbon fuels achieve the result desired and that the data obtained are correctly interpreted."

In [49], the authors adopted a recommended surrogate fuel mixture of H2, CH4, C2H4, C2H6, C3H6, and C3H8 to represent the typical catalytic decomposition products of Norpar-12 at 867 K. Next, they calculated heater-vitiate at 500-psi, and expanded it through a 10o half-angle nozzle (7.3 area ratio), assuming frozen composition to the nozzle throat and finite-rate recombination in the expansion. The resultant vitiate was assumed to enter an engine model and process to combustor conditions at constant composition, with initial temperatures of 800 to 2000 K.

First, [49] examined the effects of NO concentration and initial temperature on ignition delay and (95%) combustion times. Unlike with the neat fuels, the enhancing effect of NO on ignition delay was greatest at 800 K, but otherwise was relatively slight and somewhat complex. Second, [49] examined the effects of steam and its HxOy dissociation products on ignition delay and combustion times as a function of initial temperature and Mach number based on total enthalpy. Notably, both ignition and combustion times were dramatically increased at initial temperatures below 1200; e.g., at 800 K these delay times were longer by two (or more) orders of magnitude. This suggested "combustion may not occur at these temperatures in vitiated air wind tunnel tests, whereas combustion would occur in flight." Third, [49] examined the effect of atmospheric ozone on ignition and combustion times, and showed the effects were relatively small. Finally, [49] showed some moderate effects of excess steam on species recombination in nozzle expansions, to form CO and CO2 and to affect the axial temperature and pressure distributions. Thus the steam "may also enhance recombination in the exhaust nozzle, thereby augmenting the measured thrust in a vitiated air facility."

4.2.3.6 EXPERIMENTAL FLAME STABILIZATION STUDIES WITH BLUFF BODIES AND CAVITIES RECENTLY

Several flame stabilization studies involving bluff bodies, fueled struts, cavity flameholders, and trapped vortex combustors have appeared in the literature. In one well designed parametric study, the flame stabilization characteristics of a separated strut were examined at Mach 1.5 [50]. Two opposing triangular prisms (with 15 and 10 mm bases) were configured as if a single stepped-strut was sliced at the backward-facing wall. With parallel injection of H2 from the larger base, shadowgraph and schlieren imagery demonstrated no shocks or expansion waves existed within the gap. Variations of the airflow total temperature, H2 flow rate, and gap length were examined in conjunction with LDV measurements. Flame stabilization characteristics changed drastically with gap length, and were controlled by competition between reaction rates and mass transfer rates (residence time), as measured by local Damköhler number. Progressive widening of the gap increased residence time, altered air entrainment and effective equivalence ratio, and eventually created two stable flameholding regions. The technique has merit as a parametric research tool for the development of flame stabilization approaches.

A trapped-vortex combustor concept has been used to assess flame stabilization in a cavity between two axisymmetric disks mounted in tandem [51,52]. Fuel and air injection into the cavity stabilized vortex combustion and increased residence time, despite outside unsteadiness and restricted entrainment of excessive

air into the cavity [52]. This technique is also noteworthy as a research tool for the assessment and refinement of flame stabilization methodology.

In a simple basic study of subsonic CH4–air diffusion flames stabilized behind a backward-facing step, a halon fire supressant was pulse-injected into the air flow while CH4 issued from a porous plate downstream of the step [53]. The critical mole fraction of agent needed for flame extinction varied strongly with injectant period, air input velocity and step height. Also, two distinct regimes of flame stabilization were observed, i.e., a rim-attached wrinkled laminar flame, and a wake-stabilized turbulent flame. This simple device allows the characterization of air contaminant residence time and flame structure on subsonic flame stability.

An excellent review and initial assessment of cavity flameholders, for ignition and flame stabilization in high speed flows, describes previous scramjet research, present concepts for flame stabilization, and the use of ultra-high-speed schlieren imaging to identify two basic flow regimes [54]. The authors' phenomenological assessment includes the following. For open cavities (L/D < 10) the turbulent shear layer separates from the upstream lip and reattaches to the back face, and small cavity drag results. For closed cavities (L/D > 10) the free shear layer reattaches to the lower wall, resulting in significantly increased drag. Self-sustained cavity oscillations depend on both L/D ratio and Mach number. In a short cavity, transverse oscillations may dominate, but longitudinal oscillations may be present. In a long cavity, longitudinal oscillations dominate, but these may be caused either by reflected acoustic waves or shedding vortices. Finally, [54] discusses some key fundamentals of resonant frequencies, fluid injection, exchange of heat and mass, use of passive and active control methods, and the adequacy of short duration pulse facilities.

Following the above [54] review and initial study, [55] describes an experimental effort to characterize the flameholding process of an underexpanded H2 jet injected into a supersonic cross flow of air, for different jet-to-free-stream momentum flux ratios. An expansion tube was used to accelerate "radical-free air" to flight Mach 10 and 13. Schlieren images showed the shock structure around the jet, and periodic coherent structures in the jet/free-stream interface. Overlaid OH-PLIF (side and top view) and schlieren images showed that initial OH signals appeared in the recirculation region upstream of the jet exit, and in the bow shock region, compared to previous experiments at lower total enthalpy where no strong OH signal was observed within 10 jet diameters. At Mach 10 the OH signal decreased significantly as the mixture expanded around the jet flow field, indicating a partial quenching of ignition. The authors concluded combustion of hydrogen and air at high enthalpy conditions was a mixing limited process, and that improved injection schemes would be required for practical applications in scramjets.

Ref. [56] used OH PLIF and schlieren imaging to investigate shock-induced combustion phenomena on a 40° wedge in an expansion-tube flow. Stoichiometric H2/O2 mixtures, with N2 dilutions of 75, 80, and 85%, were tested at two different flow conditions. "Three test cases yielded shock-induced combustion behind an attached shock at the tip of the wedge. Depending on the sensitivity of the mixture, the flame front either rapidly converged with the shock or slowly diverged away from it. Measured wave angles and surface pressures were, in general, well modeled by shock-polar theory using frozen thermochemistry. Two other test cases, using the most sensitive gas mixtures, produced a closely coupled flame front behind a detached shock wave near the wedge tip. In this case surface pressure was better modeled using equilibrium chemistry. And finally, simple finite-rate chemistry modeling of the ignition zone agreed well with the experimental results in all cases.

4.2.3.7 COMPUTATIONAL FLAME STABILIZATION STUDIES

Ref. [57] investigated the effects of certain chemical reaction sets (0, and 7 vs 8) on numerical simulation of supersonic combustion flows. The generic configuration included transverse injection of a 1.5-mm under-expanded jet of H2, at 300 K total temperature, three step-heights downstream of a 5-mm rearward-facing step. Air inlet conditions were 800 K and 0.5 atm static pressure at Mach 2. Results from the 3-D version of SPARK, which simulated turbulence using the Baldwin-Lomax model, compared favorably with experimental wall pressure distributions. Deletion of the eighth reaction, H + O2 + M --> HO2 + M, strongly induced thermal choking. Thus "the oblique shock generated at the step became stronger, the pressure constantly increased, and the flow became subsonic in a continuously larger region." Once the eighth reaction was included, "the flow reaccelerated back, the upstream interaction disappeared, and the solution marched towards the characteristic supersonic flow bounding the subsonic reacting region" near the injection wall. Transition from a nonreacting to an 8-reaction case increased the size of the circulation zone, decreased local velocities, and thus increased flameholding residence times. Also, the fuel jet expansion changed significantly, the usual barrel shock disappeared, and the jet penetrated (80 %) deeper into the main flow. Finally, an oblique shock wave system was created that was characteristic of a weaker expansion and significantly higher (70 %) back pressure in the test section.

4.2.3.8 VERY HIGH-SPEED PULSED FACILITIES

Various hypersonic pulsed-flow shock facilities have also been used. Effects of test gas composition on combustion of injected H2 were examined using simplified scramjet combustor models in both the T4 free-piston reflected-shock tunnel, where 50 mass-% of O2 is dissociated to yield O-atom and NO, and in the HYPULSE shock expansion tunnel, where < 3% of O2 is dissociated [58]. Ref. [58] found the static pressure rise upon combustion was significantly greater when dissociated oxygen was present (T4 free-piston RST), and "this is attributed principally to the heat of formation of the oxygen adding to the combustion heat release of the fuel at these test conditions." Approaches for reducing and compensating the O2 dissociation effect are discussed. It seems the influence of high (to very high) O-atom concentrations on combustion kinetics need to be more thoroughly assessed.

In an independent study [59], transverse jet mixing and combustion in a duct model were compared in both the T5 free-piston shock tunnel and the HYPULSE tunnel. Here, test results agreed closely, and "no significant effects of the dissociated oxygen and NO production in the T5 flow have been detected compared to the clean-air HYPULSE expansion tube flow." Notably, H2 combustion efficiencies were very low in these tests, ranging from 25% in a high pressure case with $\phi = 2$, to 10% with $\phi = 1$. Thus the conclusion seems quite conditional.

Finally, [60] performed an analysis of H2–air combustion in the respective high-speed tunnels, using a one-dimensional quasi three-stream-mixing combustor code (SCRAM3) with finite chemistry. For a simulated Mach 17 flight condition, the results indicated "the combustion process is kinetically controlled in experiments in both tunnels and that the presence of the nonequilibrium partially dissociated oxygen in the reflected shock tunnel enhances the combustion. Similarly, methods of compensating for the dissociation effect are also discussed in [40].

4.2.3.9 DETAILED IGNITION STUDIES, NONPREMIXED DIFFUSION

There have been several recent detailed ignition studies that significantly increase our understanding of the nonpremixed ignition of H2-air systems.

Recently, critical conditions for ignition in steady laminar counter flowing H2/N2 vs air were determined at temperatures larger than Tc , using linear bifurcation and numerical techniques [61]. Analysis of the radical pool at ignition revealed that, regardless of dilution, the steady-state assumption for O-atom fails before that for OH on the airside of the mixing layer. Thus after neglecting initiation, and assuming steady state for HO2 and OH, an earlier seven-step scheme was reduced to a minimum of three global steps needed to describe ignition. These were: H2 + O2 --> O + H2O; O + 2H2 --> 2H + H2O; and 2H + M --> H2 + M. Excellent agreement was obtained at all fuel dilutions with numerical solutions based on detailed chemistry.

Very recent experimental and computational ignition studies of 6 to 38% H2/N2 vs heated-air laminar counterflowing jets showed the existence of mild oxidation regimes, and multiple ignition and extinction states, at pressures between 0.3 and 8 atm [62]. Experimentally, LDV, thermocouple, and Spontaneous Raman Spectroscopy measurements of H2O showed up to three stable stationary states could be achieved for identical boundary conditions! For example, measurements of steam for 9% H2 at 4 atm, with a density-weighted input strain rate of 300 1/s, identified a frozen lower branch of the Damköhler S-curve, a mild oxidation regime, and a flame. Computationally, strain rates ranged 10 to 40000 1/s, and air input temperatures varied 950 to 1100 K. Moreover, by changing input strain rate, up to five steady-state multiplicities and up to two ignition and extinction states resulted from thermokinetic and transport effects.

Additional computational [63] and experimental [64] studies of inhomogeneous ignition in turbulent counterflowing hydrogen versus heated air provide further valuable insight. First, Kreutz and Law [63] derived a number of "skeletal" and "reduced" reaction mechanisms to simplify a detailed kinetic mechanism having 9 species and 19 bidirectional elementary steps. They found use of homogeneous approximations, such as steady-state or partial equilibrium, can lead to significant errors in the inhomogeneous system when deriving reduced reaction mechanisms. Typically, ignition is controlled by processes occurring within a localized ignition kernal, where H2 mixes and reacts rapidly with air. Kreutz and Law demonstrate H + HO2 --> 2OH is a critical step in kinetically-controlled ignition. A 6-step skeletal mechanism is presented to represent the smallest set of elementary reactions that provides proper turning point behavior in the first and second inhomogeneous ignition limits. Resultant density-weighted strain rate limits for diffusion flame ignitions are shifted in pressure and temperature (as displaced Z curves) along the classic crossover temperature, which defines the first and second homogeneous explosion limit. Transition to the third ignition limit involves additional propagation (2HO2 --> H2O2 + O2 --> 2OH + O2) and branching (HO2 + H2 --> H2O2 + H --> 2OH + H) pathways that compete with chain termination. This 9-step skeletal mechanism appeared to capture all three limits very well over 3 orders of magnitude in strain rate.

Based on the above, Kreutz and Law drew several conclusions [63], paraphrased as follows. Mass transport of radicals out of the ignition kernel affects the ignition process, particularly in the first and third limits where the dominant chemistry is relatively slow. Thus ignition temperatures in these limits are sensitive to aerodynamic straining. An important feature of nonpremixed ignition is the radical pool is extremely small at the ignition turning point. Thus heat release from chemical reactions is so small that essentially no "thermal feedback" occurs in the system at the ignition turning point, and concentrations of major species are effectively unperturbed. In summary, [63] developed a new view of the ignition turning point as a "decoupled ignition environment" in which major species and temperature are "totally frozen" just before ignition, and the chemistry of minor species controls the process. They also developed a new "Steady-State-Ratio" sensitivity analysis that, used in conjunction with a previous flux analysis, quantifies system response near the ignition turning point to important parameters in the conservation equations.

Next, the experimental ignition measurements of turbulent nonpremixed H2 by heated counterflowing atmospheric air [64] showed that, for fuel approaching 15% H2/N2, ignition temperature was no longer sensitive to turbulent intensity. This was consistent with earlier laminar counterflow results, where the dominant (second-limit) chemistry was rapid enough compared to transport rates that ignition temperature was insensitive to local strain rate. Below 14% H2, ignition was intermittent in that flows repeatedly ignited and extinguished over a range of input temperatures, and the range of intermittency widened with decreasing fuel, increasing turbulent intensity, or increasing global strain rate. Thus local strain rate in the ignition kernal "...can alternately traverse beyond the ignition and extinction turning points [in Damköhler S-curves], causing the flow to intermittently ignite and extinguish."

Ref. [65] performed some very revealing 1-D and 2-D direct numerical simulations of the autoignition of counterflowing N2-diluted-H2 vs heated-air, in mixing layers with both laminar and homogeneous turbulent flows. The air temperature (1100 K) was higher than the crossover temperature (e.g., 925 K at 1-atm), and simulations were performed with and without heat release. Three turbulent intensities were used: weak, moderate, and strong, with characteristic timescale ratios ($\tau turb/\tau ig$) of 3, 1, and 0.3. Peak concentrations of radicals increased by more than 7 orders of magnitude before the temperature showed any noticeable change due to reaction; then temperature rose substantially (by ~200 K) to ignition, while radical concentrations changed by ~2x. As a result, the ignition delay w/ and w/o heat release was almost identical up to the ignition point for laminar flow (137 & 126 μs), and for all three turbulence levels (129 & 121; 130 & 122; and 139 & 130 μs, respectively). The authors concluded (a) for weak to moderate turbulence, ignition was only slightly facilitated by turbulence due to enhanced mixing; (b) for stronger turbulence, ignition was retarded due to excessive scalar dissipation and diffusive loss at the ignition location; (c) ignition of nonpremixed hydrogen and air in turbulent flow fields can be characterized purely by radical runaway as opposed to thermal runaway; and (d) ignition delays are quite insensitive to a wide range of initial turbulent fields. Note that (d) agrees with recent experimental measurements using a counterflow technique [64]. In addition, the ignition kernal always occurred where hydrogen was "focused;" peak HO2 was aligned closely with scalar dissipation rate; and the peak HO2 shifted toward the cold fuel stream, and eventually vanished with onset of intensive burning. Thus the study "confirmed the important role of the branching reaction, HO2 + H --> OH + OH for chemical ignition" which became increasingly important as the ignition point was approached. Finally, it was shown "that the ignition kernal tends to be located where the mixing layer is convex toward the fuel side, due to the high diffusivity of the hydrogen molecules."

The extinction limits of stoichiometric H2–O2 and H2–air counterflow diffusion flames at elevated pressures (1 to 100 atm) were numerically evaluated to determine the effects of pressure and O2 content. Also, the effects of acoustic-pressure oscillation on peak temperature and strain rate were determined [66]. The extinction strain rate for H2–O2 increased linearly with pressure to 100 atm, whereas for H2–air it became asymptotic around 50 atm. Similar behavior was retained with four-, three-, and two-step mechanisms. Finally, a sensitivity analysis showed that (a) H + O2 --> OH + O and OH + H2 --> H2O + H control extinction strain rate at 50 atm, and (b) a (hypothetical) depression of the recombination rate for H + O2 + M --> HO2 + M would favorably stabilize local acoustic oscillations.

4.2.3.10 IGNITION OF PREMIXED H2/O2/INERT MIXTURES

Autoignition of H2/O2/He mixtures at high pressure (3.5 to 7 M Pa) was investigated using a free-piston compressor to rapidly increase temperature and pressure [67]. Measurements of a so-called dynamic-ignition temperature (~1150 K) were independent of pressure. A fundamental difference was cited between (a) ignition delay in the author's new analytic "dynamic third-limit" simulation, where rapid breakdown of accumulating H2O2 occurs via H2O2 + M --> 2OH + M, and (b) the classic third explosion limit characterized by a quasi-steady chain-breaking mechanism. The latter did not correctly predict radical concentrations on the

non-explosive side of the ignition limit. The author argues the quasi-steady limit doesn't apply to the dynamic experimental conditions, and furthermore is based on data from a reaction vessel technique that "is notoriously unreliable and completely unsuited to determining the third limit." Expressions for the new dynamic third limit, derived in terms of critical OH concentrations ranging 0.5 to 5 x10-9 mole/cm3, were consistent with the data, which were located at temperatures (~1150 K @ 50-atm) well above (into) the classic third explosion limit (that varied from ~840 K @ 0.5-atm to 740 K @ 50-atm). Finally, the author contends (personal communication) the correct third limit is an extension of the second limit that does not turn back on itself until temperatures approach 1200 K.

Ref. [68] examined the catalytic ignition of H2/O2 mixtures at 1-atm with emphasis on dynamic behavior. The authors measured (using a Pt wire technique that served as both thermometer and calorimeter) and simulated the temporal evolution, from a kinetically-controlled regime before ignition, to a post-ignition state controlled by mass transport. Good agreement was obtained between experimental results and simulations. Early on, the surface is considered covered by H atoms which poison the surface by preventing dissociative adsorption of O2. Increasing temperature promotes desorption of H2 and creates more free sites for O2 dissociation, which eventually leads to ignition. The authors conclude catalytic ignition is "primarily governed by coupling between (i) the heat balance, (ii) the kinetics of adsorption of H2 + O2, and (iii) the desorption kinetics of H2." Their model is offered for application to coupled gas-phase/heterogeneous ignition/combustion processes.

Ref. [69] studied the catalytic ignition of H2/O2 mixtures, diluted by N2, on a small platinum sphere at 1-atm. Temperature-time histories were measured using a thermocouple junction which supported the sphere. A "well known" significant difference in reactivity was observed between the first exposure of a catalyst and subsequent exposures. Plots of ignition temperature vs. relative hydrogen, H2/(H2 + O2), showed evidence of a minimum ignition temperature not seen by other investigators, including those who used H2–air mixtures. A simple overall reaction model with an Arrhenius expression was used with modest success to relate ignition temperature to reactant concentration (dilution ratio).

4.2.3.11 IGNITION AND COMBUSTION IN SHEAR LAYER FLOWS

Ref. [70] analyzed thermal ignition in a supersonic mixing layer, using a numerical model that employed a single reaction with Arrhenius temperature dependence, constant gas properties for specific heat and density-weighted viscosity, and unity values for the Lewis and Prandtl numbers. A large-activation-energy asymptotic analysis was also performed. The study demonstrated that "for small values of viscous heating, the ignition distance scales approximately linearly with the freestream Mach number, whereas for large viscous heating, it decreases rapidly due to the temperature-sensitive nature of the reaction rate." These results illustrated the "potential of using local flow retardation to enhance ignition rather than relying solely on external heating." The effects of flow nonsimilarity were also assessed and found to be more prominent for the mixing layer flow in comparison to a previously studied flame-plate configuration.

Ref. [71] followed [70] with detailed numerical simulations of supersonic laminar-shear-layer flows, using finite-rate kinetics to characterize diffusive ignition/reaction to examine the roles of viscous heating, radical proliferation, and thermal runaway relative to the H2/O2 second explosion limit. Results showed that "the state of the H2/O2 second explosion limit has the dominant influence in the system response in that, for all practical purposes ignition is not possible when the air stream temperature is lower that the crossover temperature, even allowing for viscous heating. On the other hand, when the air stream temperature is higher than the crossover temperature, the predicted ignition distance indicates that ignition is feasible within practical supersonic combustion engines." "Furthermore, for the latter situations, the ignition event is initiated by radical proliferation (runaway),"…"instead of thermal runaway." Finally, while these results agreed qualitatively with the [70] results above, the "analytically-predicted ignition distances (asymptotic analyses) are much shorter that the (detailed) computed values because the [70] analysis overemphasized the viscous effect through the constant $\rho\mu$ and unity Prandtl number assumptions."

Thus the limited theoretical studies of hydrocarbon fuels in [48,49] suggest the effects of steam and its dissociation products may be highly significant below model-engine combustor entrance temperatures of ~ 1100 K. Steam's effect is to increase ignition and reaction times several orders-of-magnitude, giving the appearance of a poorly functioning, or non-functioning engine configuration. Above about 1100 K, little effect of steam contamination was observed.

With regard to the chemical kinetic effects of NO on ignition of hydrocarbon fuels, it is essential to note that in computationally assessing the effects, an adequately complete and properly-optimized (for ignition) kinetic mechanism must be utilized. That is, a mechanism wherein all potentially important reactions between NO and the remaining constituents are included, and the rate coefficients have been validated under ignition conditions. The size of such a mechanism is considerable when hydrocarbon fuels are used. In the absence of a relatively complete and properly validated mechanism, erroneous conclusions are easily drawn regarding predicted effects of NO in ground tests designed to replicate hypersonic flight. Clearly, supporting analytical

studies using proven mechanisms are required to either "correct" the SCR test data for the effects of flow contaminants if they are minor, or flag the data if they are profound.

4.3 SCALING OF AIR VITIATION EFFECTS ON SCRAMJET COMBUSTION

4.3.1 OVERVIEW OF SCALING

In this paper the initial overview of air vitiation effects on ignition, flameholding and SCRJ combustion processes, backed by a detailed technical survey (main body of paper), shows that effects on ignition delay and flameholding/combustion chemistry may differ substantially, depending on the type and operational mode of a particular facility.

In the context of this NATO Subgroup, a major goal is to provide technical bases for extrapolating ground test data to predict flight performance. The extrapolation process consists in identifying, deriving and applying appropriate scaling procedures. Scaling in the SCRJ context means to characterize the essential physics and chemistry of inlet compression, ignition, and flameholding / combustion when the key parameters of vitiation are varied (air composition, temperature, pressure, and test section geometry). Thus our overall scaling goal is to: (1) Assess the magnitude of vitiation effects on combustor performance; and (2) deduce feasible compensatory effects involving deliberate variations of vitiation/test parameters.

4.3.2 SCALING OF COMBUSTION FLOWS IN SCRAMJETS

Although aerodynamicists are familiar with the scaling of external flows in wind tunnels, scaling tasks become vastly more complicated when combustion is occurring. Logically, SCRJ scaling should at least include the effects of vitiation processes on classic Damkoehler, Reynolds and Mach numbers, and scaling might follow some conventional similarity-law investigations in designing combustors (except those at very low pressure) [82]. For gas phase kinetic effects (e.g., due to H2O, CO2, NOx and HxOy radicals) scaling laws seem quantifiable for H2-air combustion [97]. However, for particulate effects (soot, ceramic particles, droplets) scaling is much more complex because two-phase processes are involved [41]. Despite all the complexities introduced by combustion, an attempt at scaling may still be a reasonable initial approach to assess vitiation effects during SCRJ testing.

Such an approach begins with trying to maintain all the major similarity parameters between a subscale model and its subsequent flight application. For combustors, dimensionless parameters might include Re, M, Pr, Sc, Dai, Le, and St numbers. However, a cursory analysis indicates using all seven parameters represents an impractical requirement, e.g. [82]. Variations in temperature and pressure impact both chemistry and gasdynamics, which pose impossible constraints on the problem. This dilemma was recognized early by Sedov in Russia [104]. The question thus becomes, which parameters to fix and which to float?

Notably, some engine and/or vehicle designers take a dim view of “parameter selection processes.” Faced with the unknown consequences of preferentially relaxing similarity requirements, it sometimes “seems safer” to fix certain well-known physical quantities. Among the major choices for Scramjets are stagnation temperature, To, Mach number, M, and stagnation enthalpy, ho. Such an approach appears more intuitive than technically driven; i.e., it is tacitly assumed that chemistry and turbulence will be the same at fixed total temperature, or combustor entrance velocity. In fact, the analytic reason for using Da, Re or M similarity is based on the opposite assumption – namely, one maintains relevant time ratios, not absolute time. Thus faced with the unpredictability of flight performance, at least a simplified similarity approach seems justified if nothing else can be developed.

4.3.2.1 SIMPLIFYING ASSUMPTIONS

We now attempt to delineate which similarity parameters should be maintained in the simplified analysis of an entire SCRJ combustor. First, we assume both key combustion kinetics for flameholding, and overall heat release for thrust, are of paramount importance. For a well-designed combustor, we also assume (at 0-th order!) friction is less critical than choking, and vorticity due to turbulence will be mostly streamwise. In agreement with experimental data at M >>1, turbulence intensity should be relatively small in most of the combustor space, with exceptions in regions where (1) supersonic mixing is purposefully enhanced in some way (e.g., by shock trains, or induced unsteadiness), and (2) flameholding is aided and sometimes accomplished in cavity flows and blunt body wakes. Thus considering gross supersonic transport of species, the primary balance

will occur between convection and chemical kinetics, and this leads to a single Damkoehler similarity parameter, the Dai number of first kind, associated with species i.

In a rigorous consideration of turbulent mixing, one might define a spectrum of convective times, each relative to a turbulent scale. This would produce a spectrum of DaI, and require a matrix of Dai with size equal to the number of species times the number of turbulent scales. In our 0-th order analysis we neglect this multiplicity, and assume the turbulent spectrum is very limited (unlike for subsonic flows!). The above limitations imply we are considering "true" SCRJ configurations, where ignition and flameholding occur without a purposely designed subsonic recirculation region. These are strong and perhaps unacceptable assumptions for some applications, but they may be adequate for certain advanced combustors in high M-vehicles.

As for energy release, the same rough assumptions lead to a rate balance between chemical heat release and both convection and enthalpy change; thus a single Dai number also applies. Finally, similarity also occurs between the molecular transport of energy and species, so local transport rates are scaled by a Lewis number.

Perhaps a weak point in this similarity approach is the assumption that mixing occurs without strong interaction with kinetic effects, which are influenced by vitiation. Most experimentalists would take strong exception to such an assumption; after all, SCRJ combustion is precisely a case where reaction times are similar to convection times, and heat addition enhances mixing. The justification in making such an assumption is that strong interaction will be unlikely inside the shear layer immediately downstream of fuel injection, but will occur once air and fuel are mixed further downstream. When such mixing has occurred, the correct quantity to observe is not absolute ignition (or combustion) time, but the ratio between available convection time and reaction time (Damkoehler number, related to combustor size).

Notably, the above Damkoehler approach is frequently used in assessing nonequilibrium effects within shock waves, or surface catalytic effects over re-entry vehicles [99]. Thus either the characteristic vibrational relaxation time, or surface catalytic recombination time, is less important than the relevant Da (ratio) number [81]. For example, in a small (a few cm long) subscale model inside a wind tunnel, vibrational relaxation past the bow shock may occur downstream over the entire model; during a Shuttle re-entry, this takes place only a few centimeters downstream of the bow shock. Thus if we maintain the same Mach number and stagnation temperature in both situations, the absolute times are the same, but the effects on flowfield will be very different.

4.3.2.2 SIMPLIFIED DAMKÖEHLER NUMBER (*DA*) SCALING

Based on the species equation for a SCRJ combustor and using the above assumptions, the balance between the transport rate of reacting/convecting species i (e.g. OH) and its rate of formation, wi, can be written by

$$\rho Yi U / L \sim wi \qquad (1)$$

where U is the axial velocity, L the combustor length scale, Yi the mass fraction of species, and ρ the density. Arrhenius kinetics for wi are given (for a single reaction) by wi ~ Ai ρn exp(-Ea/RT), where n=2 for chain propagating or branching reactions, n=3 for recombination reactions, and Ai is the pre-exponential factor (A*i includes the Tb factor for simplicity).

By letting U = M c (where c, the speed of sound, is ~ T1/2), the Dai number is obtained for a single reaction as the ratio between wi and the transport rate. Substituting,

$$Dai \sim Ai\ \rho n\text{-}1\ [L / (YiM\ T1/2)] \exp[-Eai/RT] \sim A^*i\ \rho n\text{-}1\ L / (YiM\ T1/2) \qquad (2)$$

This indicates, for bimolecular (n=2) radical pool formation reactions typical of the ignition delay period, Dai scales as ρL for the “conventional” binary or pressure-length scaling law; whereas for radical-termination/recombination heat-release kinetics, dominated by termolecular (n=3) reactions, Dai will scale as ρ2L. This is also the conclusion of [97].

4.3.2.3 INTRODUCTION OF KEY OH FORMATION KINETICS FOR IGNITION

One can proceed a step further by looking at representative SCRJ ignition kinetics. A key indicator is the rapid rate of OH formation via the early bimolecular chain branching H2/air reactions [88,63],

$$H2 + O \rightarrow OH + H \qquad (-\ 8\ kJ/mol) \qquad [R1]$$
$$O2 + H \rightarrow OH + O \qquad (+\ 66\ kJ/mol) \qquad [R2]$$

For the initiation of H2-air combustion, the most accredited step is $H2 + O2 \rightarrow HO2 + H$, which provides the needed H for the chain branching reaction [R2]. Note the effect of vitiated air containing O is to bypass this slow reaction, [R2], and "jump-start" chain branching via [R1].

If OH is also present in vitiated air, its effect is felt via the chain propagating reaction,

$$H2 + OH \rightarrow H2O + H \qquad [R3]$$

that provides H radicals for [R2]. All the above OH formation reactions are 2nd order, so the multi-reaction Dai scaling suggested in Eqs. 1 and 2 leads to the pressure-length scaling expression,

$$DaOH \sim (\rho L / U) [A*1YH2YO/YOH + A*2YO2YH/YOH + A*-3YH2OYH/YOH - A*3YH2] \quad (3)$$

The reverse of the branching reactions [R1-R2] have been neglected due to the small radical concentrations. At early times the rate of OH formation will be fast. Subsequently it slows down, and OH is consumed by [R3]. In this first attempt at using similarity, none of the other H2-air reactions are included, including termination reactions by third body recombinations.

Some effects of air vitiation on ignition processes can now be approximated. For similar ignition performance in ground testing and in flight, the Da number should be the same. Thus for ground tests, e.g. at 1 atm pressure, the test combustor length scale L must be increased if the inlet of the real vehicle supplies the engine with air at $P > 1$ atm.

Using vitiated air, where the initial O, H, H2O and OH concentrations can be estimated, ignition kinetics start with YO, YH, YH2O and YOH different from zero. Thus an initial "effective" Dai in a particular ground testing condition / facility can be deduced.

For the much smaller initial values of radical concentrations under flight inlet conditions, a different initial flight Dai will be predicted. Thus if we wish to achieve the same flight ignition performance on the ground, the respective initial Dai should be equal. This means increasing the ($\rho L/U$) factor, or the initial YH2, YO2 concentrations, accordingly. The maintenance of both initial and later stages of flameholding becomes much more complex, using the Dämkoehler scaling approach, because radical concentrations change rapidly once combustion is initiated.

Likewise, one may start with an achievable, functional ground test (initial) Dai for ignition, and then scale a flight test article so the target flight (initial) Dai is reproduced. Such an exercise may suggest flight test conditions should be "modified" to achieve the flight Dai by using a silane, plasma or photolytic ignition aid. Finally, high-recombination-rate coatings might be employed for thermal protection system models to assess catalytic recombination effects during an actual re-entry [81].

4.4 CONCLUSIONS AND RECOMMENDATIONS

4.4.1 OVERVIEW SUMMARY OF AIR VITIATION EFFECTS

The results detailed in this paper make clear that test medium effects on ignition, combustion and flameholding in a SCRJ test article continue to be a moving target. On the experimental front, uncertainties stem from differences in: Methods of achieving high total enthalpies; test facility configurations; nature of test article configurations including relative scale; nature of preheating combustion processes (e.g. premixed or non-premixed); geometric aids to ignition, combustion and flameholding (e.g., bluff bodies, cavities, steps, etc.); simulated-flight inlet conditions (static pressure and temperature, velocities); relative velocities in downstream shear layer combustion; and possible effects of associated factors such as turbulence, skin friction and heat loss. In addition, measurement fidelity is a question hanging over all experimental studies.

Theoretical studies of test medium effects are clouded by questions of definitive chemical kinetic mechanisms and associated reaction rate coefficients, especially for hydrocarbon-fueled test articles. Additional questions arise in connection with detailed theoretical modeling of actual test conditions. For example, in the majority of hypersonic test facilities, the "air" passes through a facility nozzle, with an exit-flow chemical composition somewhere between that of a "frozen" expansion and that for a "shifting equilibrium" expansion. Even refined 2-D computational studies that start at the facility nozzle throat entrance, and proceed through the test article, are still suspect (until established otherwise). This is because of methodological questions surrounding chemical kinetic mechanisms for the SCRJ nozzle expansion process, "accurate" turbulence modeling, assorted viscous and shock wave effects, and other phenomena which are extraordinarily difficult to deal with computationally (e.g., separation-reattachment effects).

It seems fair to conclude that the presence of "extra air species" can affect both the chemistry and flow properties in test articles meant to simulate flight conditions. Test media having thermodynamic and transport

properties (e.g., average specific heat, viscosity, thermal conductivity and diffusivity) that differ from those derived from inlet-processed ambient air will certainly impact attempts to replicate flight conditions for a test article.

At high plenum temperatures, dissociation of the test medium, whether combustion-vitiated or not, becomes a potential problem. Nitric oxide is the first product of concern. Atomic oxygen may also be produced, which even in minute quantities (e.g. 1012 atoms/cm^3) can significantly reduce ignition delay times. In-stream combustion will produce hydroxyl radicals at equilibrated or superequilibrated concentrations, which are as active (or more so) as atomic oxygen. The importance of such contaminants is, again, dependent on the test conditions, engine conditions and configuration. One generalization that can be drawn is that, if auto-ignition and flameholding-combustion are marginal, due to some combination of local temperature and pressure and mixing time/length, the presence of free radicals may dramatically improve engine performance in ground tests. But, on the other hand, if autoignition and combustion are vigorous, the effects of free radical seeding in the flow may be insignificant.

4.4.2 REQUIRED FUTURE RESEARCH

The many years of study of test medium effects on ignition, combustion and flameholding processes, in test articles designed to replicate hypersonic flight, have yielded only a few definitive answers, as discussed earlier. It seems clear that many attempts to sort out the complex phenomena occurring within test articles, while perhaps providing some information relevant to the specific model and test configuration, often fail to supply definitive answers to the questions raised herein. What is required are unit-process experiments that separate, to the maximum extent possible, the chemical kinetic effects associated with "contaminant" species from the complicating thermo-fluid dynamics.

As an example, benchmark-quality ignition experiments in pulse facilities (e.g. shock tube/tunnel and expansion tube/tunnels at thermodynamic conditions corresponding to hypersonic flight), that focus on the effects of NO (and O-atom) on the ignition of hydrocarbon fuels premixed in air, might help to resolve the nitric oxide question. Definitive chemical kinetic mechanisms must be developed, validated and used for key fuel-air reactions as more detailed kinetic mechanisms and computational power become available. Such attempts have been made in the recent past, but disagreements and inconsistencies persist.

Key reaction rate coefficients, associated with elementary reactions in "definitive" mechanisms, must be determined using assessment techniques such as those employed by Baulsch [77], Warnatz [78], Kreutz and Law [63], and Yetter, Dryer and Rabitz [79]. Furthermore, applications of reduced models should be preceded by careful kinetic sensitivity studies under relevant conditions (e.g. tested near ignition turning points for ignition studies). Where the scatter of available data is unacceptably large, modern approaches based on quantum-mechanical theory should be used to resolve such discrepancies.

In a climate of austere budgets and insecure support for hypersonics, the above recommendations will likely seem impractical by many in this community. The price to be paid is continuing uncertainty on what will in fact be achieved during actual flight. Efforts to reduce or eliminate these uncertainties could be carried out systematically at modest cost over a reasonable amount of time. To ignore such uncertainties is to compromise the promise of airbreathing hypersonic flight.

4.5 REFERENCES

1. Edelman, R.B., and Spadaccini, L.J., "Theoretical Effects of Vitiated Air Contamination on Ground Testing of Hypersonic Air Breathing Engines, *J. Spacecraft*, **6**, No. 12, Dec., 1969, pp. 1442-1447. See also, AIAA Paper 69-338, April 1969, 32 pp.; and AIAA Paper 69-456, June 1969.

2. Kuehl, D.K., "Effects of Water on the Burning Velocity of Hydrogen-Air Flames," *ARS Journal*, **32**, 1962, pp. 1724-1726.

3. Reed, S.B., and Wakefield, R.P., "Vitiation of Combustion Air," *I.G.E. Journal*, Vol. , Feb. 1970, pp. 77-92.

4. Reed, S.B., Mineur, J., and McNaughton, J.P., "The Effect on the Burning Velocity of Methane of Vitiation of Combustion Air," *J. of Institute of Fuel*, 44, 1971, pp. 149-155.

5. Liu, D.D.S., and MacFarlane, R., "Laminar Burning Velocities of Hydrogen-Air and Hydrogen-Air-Steam Flames," *Combustion and Flame*, 49, 1983, pp. 59-71.

6. Koroll, G.W., and Mulpuru, S.R., "The Effect of Dilution with Steam on the Burning Velocity and Structure of Premixed Hydrogen Flames", *Twenty-First Symposium (International) on Combustion*, 1986, pp. 1811-1819.

7. Ashmore, P.G., and Tyler, B.J., "The Nature and Cause of Ignition of Hydrogen and Oxygen Sensitized by Nitrogen Dioxide," *Ninth Symposium (International) on Combustion*, 1963, pp. 201-209.

8. Jachimowski, C.J. and Houghton, W.M., "Effect of Carbon Dioxide and Water Vapor on the Induction Period of the Hydrogen-Oxygen Reaction," NASA TN D-4685, 1968, 15 pp.

9. Slack, M., and Grillo, A., "Investigation of Hydrogen-Air Ignition Sensitized by Nitric Oxide and by Nitrogen Dioxide," NASA CR-2896, 1977, 38 pp.

10. Clark, A.E., Odgers, J., Stringer, F.W., and Harrison, A.J.: "Combustion Processes in a Spherical Combustor." *Tenth Symposium (International) on Combustion,"* The Combustion Institute, 1965, pp. 1151-1166.

11. Erickson, W.D., and Klitch, G.F.: Analytical Chemical Kinetic Study of the Effect of Carbon Dioxide and Water Vapor on Hydrogen-Air Constant-Pressure Combustion. NASA TN D-5768, 1970.

12. Carson, G.T: Analytical Chemical Kinetic Investigation of the Effects of Oxygen, Hydrogen, and Hydroxyl Radicals on Hydrogen-Air Combustion. NASA TN D-7769, 1974.

13. Huber, P.W., Schexnayder, C.J. Jr., and McClinton, C.R., "Criteria for Self-Ignition of Supersonic Hydrogen-Air Mixtures," NASA TP-1457, 1979, 54 pp.

14. Odgers, J., and Kretschmer, D., "Considerations of the Use of Vitiated Preheat," *J. Energy*, 4, Nov.-Dec. 1980, pp. 260-265.

15. Rogers, R. Clayton, and Schexnayder, Charles J., Jr., "Chemical Kinetic Analysis of Hydrogen-Air Ignition and Reaction Times," NASA TP-1856, 1981, 51 pp.

16. Rogers, R. Clayton, "Effects of Test Facility Contaminants on Supersonic Hydrogen-Air Diffusion Flames," presented at 23rd JANNAF Combustion Meeting, Hampton, VA, Oct., 1986. CPIA Publication 457, Vol. 1, Oct. 1986, pp. 377-390.

17. Laster, W.R. and Sojka, P.E., "Autoignition of H_2-Air: The Effect of NO_2 Addition," *J. Propulsion and Power*, 5, No. 4, 1989, pp. 385-390.

18. Laster, W.R. and Sojka, P.E., "Autoignition of H_2/Air/NO_x Mixtures: The Effect of Temperature and Pressure," Technical Note, *J. Propulsion and Power*, **5**, No. 4, 1989, pp. 510-512.

19. Guerra, Rosemary, Pellett, G.L., Wilson, L.G., Northam, G.B., "Opposed Jet Burner Studies of Hydrogen Combustion with Pure and N_2, NO Contaminated Air," AIAA Paper 87-0090, Jan., 1987, 11 pp.

20. Guerra, Rosemary, Pellett, G.L., Wilson, L.G., Northam, G.B., "Opposed Jet Burner Studies of Effects of CO, CO_2 and N_2 Air Contaminants on Hydrogen-Air Diffusion Flames," AIAA Paper 87-1960, July, 1987, 14 pp.

21. Pellett, G.L., Jentzen, M.E., Wilson, L.G., and Northam, G.B., "Effects of Water-Contaminated Air on Blowoff Limits of Opposed Jet Hydrogen-Air Diffusion Flames," AIAA Paper 88-3295, July, 1988, 10 pp.

22. Pellett, G.L., Wilson, L.G., Northam, G.B., Guerra, Rosemary, "Effects of H_2O, CO_2, and N_2 Air Contaminants on Critical Airside Strain Rates for Extinction of Hydrogen–Air Counterflow Diffusion Flames," Presented at 26th JANNAF Combustion Meeting, Pasadena, CA, Oct., 1989.

23. Pellett, G.L., Northam, G.B., Wilson, L.G., "Counterflow Diffusion Flames of Hydrogen, and Hydrogen Plus Methane, Ethylene, Propane, and Silane, vs. Air: Strain Rates at Extinction," AIAA Paper 91-0370, Jan., 1991.

24. Pellett, G.L., Northam, G.B., Wilson, L.G., "Strain-Induced Extinction of Hydrogen–Air Counterflow Diffusion Flames: Effects of Steam, CO_2, N_2, and O_2 Additives to Air," AIAA Paper 92-0877, Jan., 1992.

25. Pellett, G.L., Isaac, K.M., Humphreys, W.M., Jr., Gartrell, L.R., Roberts, W.L., Dancey, C.L., and Northam, G.B., "Velocity and Thermal Structure, and Strain-Induced Extinction of 14 to 100% Hydrogen-Air Counterflow Diffusion Flames," *Combust. Flame* 112, No. 4, 1998, pp. 575-592.

26. Chelliah, H.K., Krauss, R.H. and McDaniel, J.C., Jr., "Modeling of Vitiation Effects on H_2-O_2 Combustion Using Reduced Reaction Mechanisms," AIAA Paper 94-2577, June 1994, 8 pp.

27. Jachimowski, C.J., "An Analytical Study of the Hydrogen-Air Reaction Mechanism with Application to Scramjet Combustion," NASA TP 2791, 1988.

28. Warnatz, J. "Concentration-, Pressure-, and Temperature-Dependence of the Flame Velocity in Hydrogen-Oxygen-Nitrogen Mixtures. *Combust. Sci. Technol.,* 26, nos. 5 and 6, 1981, pp. 203-213.

29. Milton, B.E., and Keck, J.C., "Laminar Burning Velocities in Stoichiometric Hydrogen and Hydrogen-Hydrocarbon Gas Mixtures. *Combust. Flame*, 58, 1984.

30. Drell, I.L., and Belles, F.E., "Survey of Hydrogen Combustion Properties," NACA Report 1383, 1958.

31. Dugger, G.L., Simon, D.M., and Gerstein, M., "Basic Considerations in the Combustion of Hydrocarbon Fuels with Air," NACA Report 1300, 1959.

32. Harradine, D.M., Lyman, J.L., Oldenborg, R.C., Schott, G.L., and Watanabee, H. H., "Hydrogen/Air Combustion Calculations: The Chemical Basis of Efficiency in Hypersonic Flows," *AIAA Journal*, 28, No. 10, 1990, pp. 1740-1744.

33. Katta, V.R, Carter, C.D., Fiechtner, G.J., Roquemore, W.M., Gord, J.R., and Rolon, J.C., "Interaction of a Vortex with a Flat Flame Formed Between Opposing Jets of Hydrogen and Air," *Twenty-Seventh Symposium (International) on Combustion*, 1998, pp. 587-594.

34. Pitsch, H., Chen, M., and Peters, N., "Unsteady Flamelet Modeling of Turbulent Hydrogen-Air Diffusion Flames," *Twenty-Seventh Symposium (International) on Combustion*, 1998, pp. 1057-1064.

35. Aung, K.T., Hassan, M.I., and Faeth, G.M., "Effects of Pressure and Nitrogen Dilution on Flame/Stretch Interactions of Laminar Premixed H2/O2/N2 Flames," Combust. Flame, 112, 1998, pp. 1-15.

36. Sun, C.J. and Law, C.K., "On the Consumption of Fuel Pockets vis Inwardly Propagating Flames," *Twenty-Seventh Symposium (International) on Combustion*, 1998, pp. 963-970.

37. Lee, S.D., Chung, D.H., and Chung, S.H., "Local Equilibrium Temperature as a Measure of Stretch and Preferential Diffusion Effects in Counterflow H_2/Air Premixed Flames," *Twenty-Seventh Symposium (International) on Combustion*, 1998, pp. 579-585.

38. Lai, H. and Thomas, S., "Numerical Study of Contaminant Effects on Combustion of Hydrogen, Ethane, and Methane in Air," AIAA paper 95-6097, April, 1995, 12 pp.

39. Fischer, K. and Rock, K, "Calculated Effects of Nitric Oxide Flow Contamination on Scramjet Performance," AIAA Paper 95-2524, July, 1995, 12 pp. Also, proposed NASA TP, 2001.

40. Hussaini, M.Y., Kumar, A., and Voigt, R.G., editors, In Sections on Flameholding/Extinction, and Chemical Kinetics, Major Research Topics in Combustion, Springer-Verlag, New York, NY, 1992, 650 pp.

41. Mitani, T., "Ignition Problems in Scramjet Testing," *Combust. Flame*, 101, 1995, pp. 347-349.

42. Mitani, T., Hiraiwa, T., Sato, S., Tomioka, S., Kanda, T., and Tani, K., "Comaprison of Scramjet Engine Performance in Mach 6 Vitiated and Storage-Heated Air," *J. Propulsion and Power*, 13, No. 5, 1997, pp. 635-642.

43. Kanda, T., "Study of the Intensive Combustion in the Scramjet Engine," AIAA paper 98-3123. July 1998.

44. Takahashi, S., Wakai, Kazunori, Tomioka, Sadatake, "Effects of Combusion on Flowfield in a Model Scramjet Combustor," *Twenty-Seventh Symposium (International) on Combustion*, 1998, pp. 2143-2150.

45. Mitani, T., Chinzei, N., and Masuya, Goro, "Mach 2.5 Experiments of Reaction Quenching in Gas Sampling for Scramjet Engines," *Twenty-Seventh Symposium (International) on Combustion*, 1998, pp. 2151-2156.

46. Takahashi, S., Sato, N., Tsue, M., and Kono, M., "Control of Flame-Holding in Supersonic Airflow by Secondary Air Injection," *J. Propulsion and Power*, 14, No. 1, 1998, pp. 18-23.

47. Srinivasan, S., Erickson, W.D., "Interpretation of Vitiation Effects on Testing at Mach 7 Flight Conditions," AIAA Paper 95-2719, July, 1995.

48. Chinitz, W., and Erdos, J.I., "Test Facility Contaminant and Atmospheric Ozone Effects on Hydrocarbon Flames and Nozzle Expansions." AIAA Paper 96-2917, July, 1996

49. Chinitz, W., and Erdos, J.I., "Test Facility Chemistry Effects on Hydrocarbon Flames and Detonations," AIAA Paper 95-2467, July 1995.

50. Niioka, T., Terada, K, Kobayashi, H., and Hasegawa, S., "Flame Stabilization Characteristics of Strut Divided into Two Parts in Supersonic Airflow," *J. Propulsion and Power*, 11, No. 1, 1995, pp. 112-116.

51. Hsu, K.-Y., and Goss, L.P., and Roquemore, W.M., "Charactristics of a Trapped-Vortex Combustor," *J. Propulsion and Power*, 14, No. 1. 1998, pp. 57-65.

52. Katta, V.R., and Roquemore, W.M., "Study on Trapped-Vortex Combustor—Effect of Injection on Flow Dynamics," *J. Propulsion and Power*, 14, No. 3. 1998, pp. 273-281.

53. Takahashi, F., and Schmoll, W.J., "Suppression of Bluff-Body Stabilized Diffusion Flames," AIAA Paper 98-3529, July, 1998.

54. Ben-Yakar and Hanson, R.K., "Cavity Flameholders for Ignition and Flame Stabilization in Scramjets: Review and Experimental Study," AIAA Paper 98-3122, July 1998.

55. Ben-Yakar, A. and Hanson, R.K., "Experimental Investigation of Flame-Holding Capability of Hydrogen Transverse Jet in Supersonic Cross-Flow," *Twenty-Seventh Symposium (International) on Combustion*, 1998, pp. 2173-2180.

56. Morris, C.I., Kamel, M.R. and Hanson, R.K., "Shock-Induced Combustion in High-Speed Wedge Flows," *Twenty-Seventh Symposium (International) on Combustion*, 1998, pp. 2157-2164.

57. Segal, Corin, Haj-Hariri, Hossein, and McDaniel, James C., "Effects of the Chemical Reaction Model on Calculations of Supersonic Combustion Flows," *J. Propulsion and Power*, 11, No. 3, 1994, pp 565-568.

58. Morgan, R.G., Stalker, R.J., Bakos, R.J., Tamagno, J., and Erdos, J.I., "Scramjet Testing-Ground Facility Comparisons," Paper No. ISABE 91-194(L), Nottingham, UK, Sept. 1991.

59. Belanger, J. and Hornung, Hans G., "Transverse Jet Mixing and Combustion Experiments in Hypervelocity Flows," *J. Propulsion and Power*, 12, 1996, pp.186-192.

60. Jachimowski, C.J., "An Analysis of Combustion Studies in Shock Expansion Tunnels and Reflected Shock Tunnels." NASA TP-3224, 1992, 10 pp.

61. Sánchez, A.L., Balakrishnan, G., Liñán, A., and Williams, F.A., "Relationships between Bifurcation and Numerical Analyses for Ignition of Hydrogen–Air Diffusion Flames," *Combustion and Flame*, 105, 1996, pp. 569-590.

62. Fotache, C.G., Sung, C. J., Sun, C.J., and Law, C.K., "Mild Oxidation Regimes and Multiple Criticality in Nonpremixed Hydrogen–Air Counterflow," *Combust. Flame*, **112**, 1998, pp. 457-471.

63. Kreutz, T.G., and Law, C.K., "Ignition in Nonpremixed Counterflowing Hydrogen Versus Heated Air: Computational Study with Skeletal and Reduced Chemistry," *Combustion and Flame*, 114, 1998, pp. 436-456.

64. Blouch, J.D., Sung, C.J., Fotache, C.G., and Law, C.K., "Turbulent Ignition of Nonpremixed Hydrogen by Heated Counterflowing Atmospheric Air," *Twenty-Seventh Symposium (International) on Combustion*, 1998, pp. 1221-1228.

65. Im, H.G., Chen, J.H., and Law, C.K., "Ignition of Hydrogen-Air Mixing Layer in Turbulent Flows," *Twenty-Seventh Symposium (International) on Combustion*, 1998, pp. 1047-1056.

66. Sohn, C.H., and Chung, S.H., "Structure and Acoustic-Pressure Response of Hydrogen–Oxygen Diffusion Flames at High Pressure," *Combust. Flame*, 115, 1998, pp. 299-312.

67. Cain, T.M., "Autoignition of Hydrogen at High Pressure," *Combust. Flame*, 111, 1997, pp. 124-132.

68. Rinnemo, M., Deutschmann, O., Behrendt, F., and Kasemo, B., "Experimental and Numerical Investigation of the Catalytic Ignition of Mixtures of Hydrogen and Oxygen on Platinum," *Combust. Flame*, 111, 1997, pp. 312-326.

69. Enomoto, H., Kato, H., Tsue, M., and Kono, M., "Catalytic Ignition of Hydrogen-Oxygen on Platinum," *Twenty-Seventh Symposium (International) on Combustion*, 1998, pp. 2259-2266.

70. Im, H.G., Chao, B.H., Bechtold, J.K., and Law, C.K., "Analysis of Thermal Ignition in the Supersonic Mixing Layer," *AIAA Journal*, 32, 1994, pp. 341-349.

71. Nishoka, M. and Law, C.K., "A Numerical Study of Ignition in the Supersonic Hydrogen/Air Laminar Mixing Layer," AIAA paper 95-0377, Jan. 1995.

72. Jachimowski, C.J., "Chemical Kinetic Reaction Mechanism for the Combustion of Propane," *Combustion and Flame*, v. 55, 1984, pp. 213-224.

73. Warnatz, J., "The Mechanism of High Temperature Combustion of Propane and Butane," *Combustion Science and Technology*, 34**,** 1983, pp. 177-200.

74. Westbrook, C.K. and Pitz, W.J., "A Comprehensive Chemical Kinetic Reaction Mechanism for Oxidation and Pyrolysis of Propane and Propene," *Combustion Science and Technology*, 37, pp. 117-152 (1984).

75. Chinitz, W., Cresci, D., Tsai, C.-Y. and Aradi, A.A., "Theoretical and Wind Tunnel Experimental Studies of Diesel Ignition and Ignition-Enhancing Additives," SAE Paper No. 961162, May 1996.

76. Radhakrishnan, K. and Bittker, D.A., "LSENS, A General Chemical Kinetics and Sensitivity Analysis Code for Gas-Phase Reactions: User Guide," NASA TM 105851, Jan. 1993.

77. Baulch, D.L., Drysdale, D.D., Horne, D.G. and Lloyd, A.C., *"Evaluated Kinetic Data for High Temperature Reactions, Vol. 1,"* CRC Press, Cleveland, OH, 1972.

78. Gardiner, W.C., ed., *"Combustion Chemistry,"* Springer-Verlag, New York, 1984.

79. Yetter, R.A., Dryer, F.L., and Rabitz, H., "A Comprehensive Reaction Mechanism for Carbon Monoxide/Hydrogen/Oxygen Kinetics," *Combustion Science and Technology*, 79, 1991, pp. 97-128.

80. Baranovskii, S.I., Nadvorskii, A.S., and Romashkova, D.D., (1989), "A Simple One-Dimensional Model of the Air Contamination Effect on Supersonic Combustion," Comb., Detonation and Shock waves, Plenum Press, 1989, 24, pp. 677-685 (translation of Fizika Goreniya i Vzryva, 24, No. 6, pp. 42-51, 1988).

81. Barbato, M., Reggiani, S., Bruno, C., and Muylaert, J., (2000) "Model for Heterogeneous Catalysis on Metal Surfaces with Application to Hypersonic Flows," J. Thermophysics and Heat Transfer, Vol. 14, No.3 , July-September 2000, pp. 412 - 420.

82. Benelli, G., Bruno, C., and Marcolongo, V., (1992), "Scaling Laws for Industrial Gas Turbines," in Proc. of the Joint French, Italian and Swedish Sections of the Combustion Institute, Capri, 21-24 Sept. 1992, CUEN Publishers, Naples, section III-7.

83. Bertolotti, F., (1997), "The Influence of Rotational and Vibrational Energy Relaxation on the Instability of Boundary Layers in Supersonic Flows," DLR Forschungbericht 97-18, Goettingen. See also, "The Influence of Rotational and Vibrational Energy Relaxation on Boundary-Layer Stability," J. Fluid Mech., 372, 1998, pp. 93-118.

84. Bogdonoff, S.I., (1998), personal communication, 1998.

85. Deshaies, Figueira Da Silva, L.F., and René-Corail, M., B., (1997), "Some Generic Problems Related to Combustion of H2 and Air in Supersonic Flows," in Combustion and Supersonic Flows, ed. by M. Champion and B. Deshaies, Kluwer Publishing, Dordrecht, 1997, pp. 15 - 42.

86. Guy, R.W., Rogers, R.C., Puster, R.L., Rock, K.E., and Diskin, G.S., "The NASA Langley Scramjet Test Complex," AIAA Paper 96-3243, July, 1996.

87. Krauss, R.H., et al., "Experimental and Numerical Investigation of Steam-Vitiated Combustion," AIAA Paper 96-0856 1996.

88. Glassman, I., (1996), Combustion, 3rd ed., J. Wiley and Sons, New York, Ch. 2, 1996 pp. 35-54

89. Golovitchev, V.I., and Bruno, C., (1993), "Ignition Delay Times Studies for H2- and CH4-Air Mixtures," in Proc. Joint Meeting of the Italian and Spanish Sections of the Comb. Institute, June 28-July 1, 1993, Citta' Studi Edizioni, Milan, pp. VIII-2.1 – VIII-2.4.

90. Golovitchev, V.I., Pilia, M.L., and Bruno, C., (1996), "Autoignition of Methane Mixtures: The Effect of Hydrogen Peroxide," J. Propulsion Power, 12, No. 4, 1996, pp. 699-707.

91. Guerra, R., Waidmann, W., and Laible, C., (1991), "An Experimental Investigation of the Combustion of a Hydrogen Jet Injected Parallel in a Supersonic Air Stream," AIAA Paper 91-5102 Dec. 1991.

92. Meador, W.E., Townsend, L.W., and Miner, G.A., "Effects of H2O Vapor on Vibrational Relaxation in Contracting and Expanding Flows," AIAA Paper 96-0105, Jan., 1996.

93. Lewis, B., and von Elbe, G., (1987), Combustion, Flames and Explosions of Gases, 3rd ed., Academic Press, New York, 1987, Chapter II, p. 25.

94. Mitani, T., (1992), "Chemical Reactions in Scramjet Engines," NAL Technical Report TR-1184, 1992.

95. Mitani, T., (1994), "Effects of Dust from Storage Heaters on Ignition of Scramjets," NAL Technical Report TR-1234, 1994.

96. Park, C., in: "Review of Finite-Rate Chemistry Models for Air Dissociation and Ionization," Molecular Physics and Hypersonic Flow, ed. by M.Capitelli, Kluwer Academic Publishers, Dordrecht, 1996,pp. 581-596.

97. Pulsonetti, M., and Stalker, R.L., (1995), Paper presented at Workshop on Supersonic Combustion, University of Queensland, Brisbane, Sept. 18-20, 1995.

98. Ramohalli, K., Yang, Y. and Cort., A., (1990), "Further Results from Free Radicals-Augmented High Speed Turbulent Combustion," AIAA Paper 90-2097, July 1990. pp12.

99. Sarma, G.S.R., (2000), "Physico-Chemical Modeling in Hypersonic Flow Simulation," Prog. in Aerosp. Sci., Vol. 36, No. 3-4, 2000, pp. 281-349.

100. Zabaikin, V.A., Perkov, E.V., and Tret'yakov, P., (1992) "Effect of additive H2O2 on the Ignition and Combustion of Hydrogen in a Supersonic Air Flow", Paper presented at the 6th ICMAR, Siberian Academy of Sciences Publishers, Novosibirsk, Russia.

101. Zamansky, V.M., and Borisov, A.A., (1992), "Promotion of High Temperature Self-Ignition, " Prog. Eng. Comb. Sci., Vol. 18, 1992, pp. 297-325.

102. Bulewicz, E.M. and Padley, P.J., Thirteenth Symposium (International) on Combustion, 1971, pp. 73-80.

103. Candler, G.V., "Effect of Internal Energy Excitation on Supersonic Air Flow," AIAA paper 99-4964, Nov. 1999.

104. Sedov, L.I., (1972), "A Course in Continuum Mechanics", Vol. II, Sections 7.7 to 7.9, Walters-Noordoff Publishing, Groningan, pp.226-272

105. Pulsonetti, M.V. "Scaling Laws for Scramjets", Ph. D. Thesis, Department of Mechanical Engineering, University of Queensland, Australia, 366 pp.

CHAPTER 5: REVIEW OF EXPERIMENTS ON IGNITION AND FLAMEHOLDING IN SUPERSONIC FLOW

T. Cain and C. Walton
QinetiQ, Ively Rd., Farnborough, GU14 0LX, United Kingdom
tcain@taz.qinetiq.com

5.1 ABSTRACT

Supersonic combustion data obtained at the low static temperatures appropriate for an efficient scramjet engine are reviewed. Attention is directed at the methods by which the fuel was ignited and combustion maintained. The cited supersonic combustion experiments are grouped under the six headings: chemical intiators; non-uniform flows; turbulent flameholding; combustion induced compression; partial subsonic combustion and plasma sources. The paper is drawn from the NATO RTO AVT WG10 report on technologies for propelled hypersonic flight which aims to summarise the state of the art, identifying the key issues still hindering scramjet development.

5.2 INTRODUCTION

Studies of engine components done in isolation run the risk of having little applicability to the design of a complete engine. This is particularly common for supersonic combustion experiments and many examples are found in the literature of experiments conducted with inlet temperatures much higher than practical in flight. There is a good reason for this: it is difficult to sustain a hydrogen or hydrocarbon flame in a low temperature supersonic flow. A well designed combustor makes this possible, a less effective combustor can be made to function simply by elevating the static temperature until spontaneous ignition is achieved. In this paper we have endeavoured to identify published supersonic combustion data obtained at the low static temperatures appropriate for an efficient scramjet engine. The methods by which the fuel was ignited and combustion maintained are then examined. The reader looking for a wider perspective on scramjet development and testing is referred to the comprehensive articles by Waltrup,[1,2] Northam and Anderson[3] and Curran[4] who also reference earlier authoritative reviews.

The paper begins with a brief look at hypersonic intake compression limits and the ignition delay of hydrogen and hydrocarbon at the preferred intake exit conditions. Supersonic combustion experiments are then discussed under the six headings: chemical intiators; non-uniform flows; turbulent flameholding; combustion induced compression; partial subsonic combustion and plasma sources.

5.3 COMBUSTOR INLET CONDITIONS

Low combustor entry temperature is desirable/essential due to intake and nozzle limitations.
Shocks and skin friction result in a decrease in total pressure in the intake and when this loss is considered for flight Mach numbers greater than about 7, the temperature at which heat should be added for maximum cycle efficiency is much less than the stagnation temperature. This discontinuous transition in optimum temperature from *stagnation* to *much less than stagnation* is associated with the absence of a normal shock in a scramjet intake. Excessive entropy increase associated with the normal shock is one reason for the need for supersonic combustion in hypersonic ramjets. An equally important factor is that the post combustion temperature must be kept sufficiently low to avoid excess dissociation of the combustion products. Dissociated species will generally have insufficient time to recombine as the exhaust expands within the nozzle and therefore the chemical energy will not be fully extracted. To keep the combustor exit temperature to less than 2400K (say) requires an engine to be run at a low equivalence ratio and this exacerbates the need to minimize compression losses (since the ratio of heat input to air stream kinetic energy decreases) as well as applying a direct constraint on the optimum combustor entry temperature.

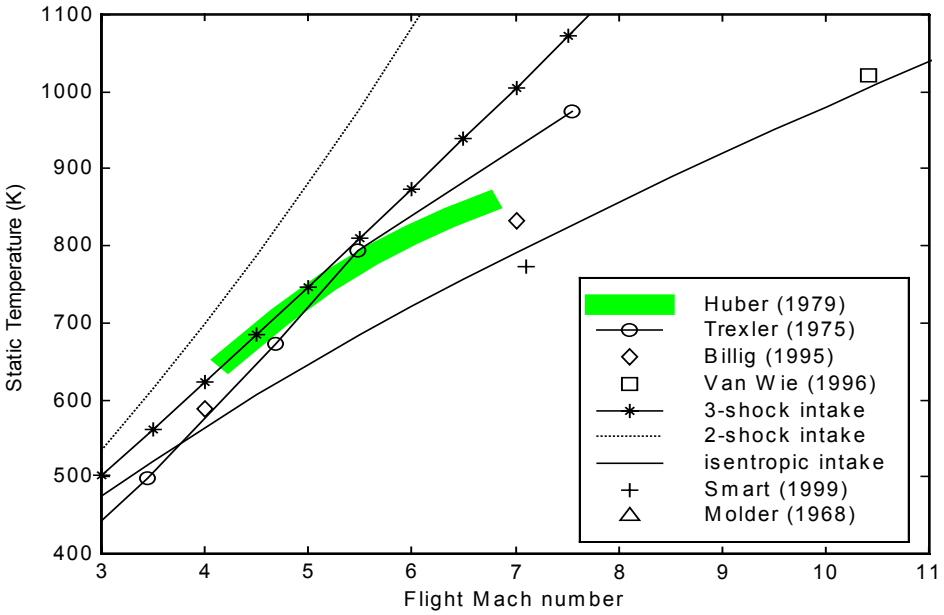

Figure 1: Intake exit temperature

Figure 1 shows intake-exit/combustor-entry temperature as a function of flight Mach number for various theoretical and actual intakes. The free stream static temperature is assumed to be 220K. Huber's curve[5] for a "typical intake" corresponds closely with Trexler's Airframe-Integrated engine[6] and Billig's SCRAM[7]. The theoretical curves are obtained by considering compression to a pressure that is twice the dynamic pressure, q, as that is close to the limit for a self starting intake. These theoretical curves do not include skin friction losses (always significant for hypersonic intakes) and are presented only to aid appreciation of the measured performance.

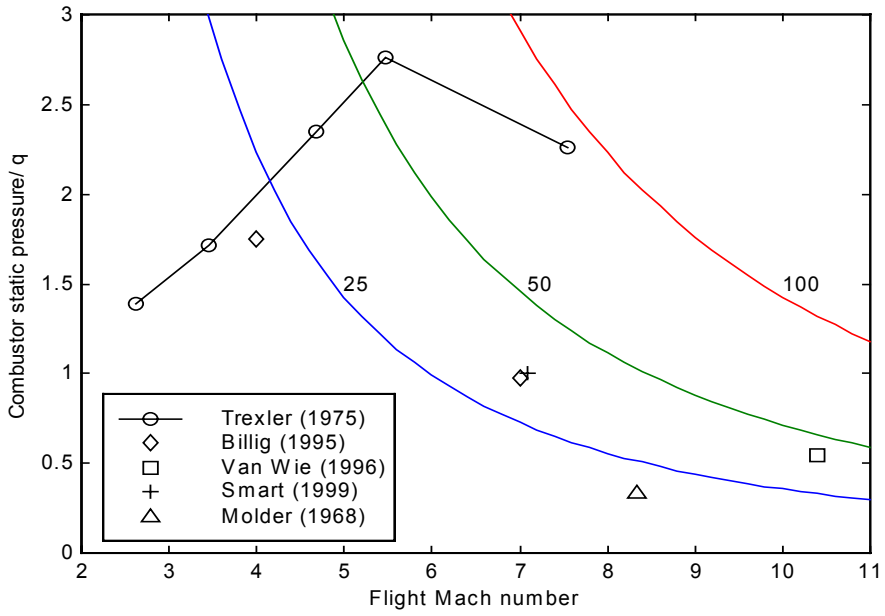

Figure 2: Intake exit pressure normalized by free stream dynamic pressure. Combustor to free stream static pressure ratio contours are labelled with their value.

Figure 2 shows the combustor entrance pressure, p_c, normalized by q as a function of flight Mach number. Trexler's intake was able to exceed the $2q$ limit by spilling flow even at the cruise condition. Compression of air not entering the combustor results in "pre-entry drag" on the intake and of course has an adverse effect on the net engine thrust.

Consideration of Lift on Drag ratio, airframe heating, wing loading, and combustor pressure tends to result in a q=0.5 to 1bar flight trajectory. Thus combustor pressures near 1atm are to be expected up to Mach 7, possibly decreasing to 0.3bar by Mach 10.

The reason high Mach number intakes are designed with lower p_c/q can be understood by reference to the lines of constant combustor-to-freestream static pressure ratio in figure 2. Van Wie's Mach 10 intake[8] provides a pressure ratio above 40 which is adequate to extract the heat energy in the subsequent exhaust expansion. Due to intake losses it is better not to compress the flow more than necessary to obtain good combustor/nozzle performance. Intake boundary layers provide a second reason for restricting pressure ratio at high Mach numbers. High Mach number intakes have long ramps to limit shock losses and this combined with the decrease in Reynolds number (for constant q) results in a high fraction of the captured air being within the boundary layer. The adverse pressure gradient must be limited to prevent boundary layer separation.

It is worth noting that maximum cruise efficiency (the product of propulsive efficiency and lift on drag) of an integrated airframe/engine was found to occur at still lower combustor temperatures than the optimum for propulsive efficiency in Townend's preliminary studies[11]. This together with the very viscous nature of flows within ducts naturally led to consideration of hypersonic aircraft with external burning for propulsion at Mach numbers greater than 10.

5.4 CHEMICAL KINETIC LIMITATIONS

Optimum combustor inlet temperature and pressure are in regions in which ignition delay for both hydrogen and hydrocarbon is very sensitive to temperature, varying from 0.1ms to >>10ms.

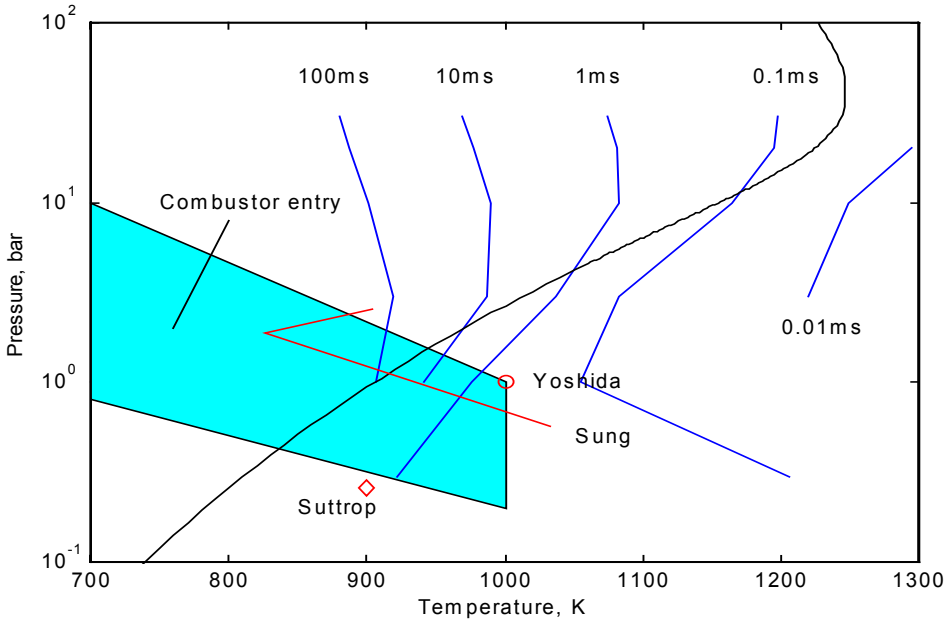

Figure 3: Approximate ignition delay in stoichiometric hydrogen air calculated by Cuoco and Bruno (RTO WG10, 2001). The diagonal line separating the explosive states (lower right) from the non-explosive (upper left) is the explosion limit from Cain[12].

Figure 3 presents approximate contours of ignition delay for stoichiometric hydrogen air on the temperature/pressure plane. In all cases, just as in the near totality of experiments performed to-date, hydrogen is assumed, or injected, at room temperature, thus effectively cooling any mixture being formed. Ignition of mixtures at pressures greater than the explosion limit occurs after self heating in the induction phase causes the mixture to cross the limit.

For typical hydrocarbons at atmospheric pressure, the ignition delays are not less than 1ms until temperatures above 1300K. Thus for both hydrocarbon and hydrogen fuel, it is immediately apparent that autoignition will not occur in scramjets under the preferred operating conditions, except perhaps in local hot spots as will be discussed. Thus we are forced to look for methods of igniting and sustaining a flame.

5.5 CHEMICAL INITIATORS

Chemical initiators such as silane, Fluorine and OTTO can be used but there may be penalties in specific impulse, system complexity and handling hazards.

For hydrogen, the rapid increase in ignition delay with increasing pressure (at temperatures below 1000K) or decreasing temperature is due to increasing dominance of a chain breaking reaction in which the H radical combines with molecular oxygen to produce the relatively unreactive HO2 molecule.

$$H + O_2 + M \Rightarrow HO_2 + M$$

Without the third body M, the collision between H and O_2 could produce O and OH and it is the competition between these two elementary processes, one chain breaking the other chain branching, that determine the explosion limit.

The fact that it is not a single activation energy that controls the reaction rate, but instead it is the complex interplay between a series of elementary processes promises the possibility of modifying this mechanism by the addition of another species in small quantity. The species does not necessarily have to have a significant thermal effect but might instead provide parallel pathways for the reaction to proceed.

Promoters that have been studied for hydrogen include: SiH_4, H_2O_2, NO and NO_2. For hydrocarbons the list expands to include: H_2, SF_6, ClF_3, B_5H_9 and OTTO (a nitrate ester). According to Waltrup[13], promoters that did perform well in engine tests contained toxic, pyrophoric or carcinogenic components that were unacceptable. References to US work with chemical ignition promoters can be found in Waltrup's article, that by Hunt et al.,[14] and Northam and Anderson's review of the work at Langley[3].

A major role of promoters is their use to ignite and maintain flames in combustor tests at smaller scale and lower pressure than encountered in flight. To keep the reaction timescale in correct proportion to the flow timescale it is important for experiments to be done with the same Damkohler number L/ut_c as that in flight. With small scale model tests, the time for combustion has to be reduced and this has been done for hydrogen by adding silane. In practice the combustion timescale, t_c, has been taken as the ignition delay but the choice of temperature at which ignition delay is calculated is not much better than arbitrary. The problem of finding the appropriate temperature can be converted to a problem of finding an appropriate recovery factor as done by Huber et al.[5] but it makes the problem no more quantitative. When testing sub-scale versions of the X22A engine for NASP, Voland and Rock[15] assumed that in flight, combustion would be limited by mixing. This greatly simplifies the problem of sub-scale simulation since one need only ensure that the reaction timescales in the ground tests are sufficiently short that the sub-scale engine performance is also mixing limited. In the case of the 12.5% scale Parametric Engine this was done by using a continuous silane/hydrogen pilot. It seems that the mixing-limited assumption was justified by subsequent tests of a 30% scale version of the X22A known as the Concept Demonstration Engine for which silane was used as an ignition source but not needed as a pilot.

A study in which static temperature and silane concentration were varied and combustion efficiency was measured would be very useful in understanding the true role of kinetics in low temperature flame holding.

5.6 NON-UNIFORM FLOWS

The flowfield within combustors is always non uniform with boundary layers, fuel jets, and often disturbances from geometric variations such as struts, steps and cavities. Chemistry is strongly coupled to the spatial and temporal variations in fuel/air concentrations and temperature. The temperature variations are very significant in comparison to those in subsonic flows.

Given the non-linear nature of chemical kinetics it is very important to distinguish the local instantaneous value of temperature from the mean value one might compute or infer from averaged measurements. The fact that the fuel/air shear layers are non-uniform and turbulent means that it may be possible to spontaneously ignite and burn fuel at mean conditions that could not otherwise support combustion.

The hydrogen auto ignition limits obtained by Sung et al.16 with a rectangular Mach 2.5 combustor and a central strut containing a slot injector is plotted on figure 3. Combustor entrance conditions had to be to the right of the line for autoignition to occur. At the ignition limit, the fuel ignited downstream and the flame propagated up to the base of the strut, so the base flow was not the source of ignition.

The limit found by Yoshida and Tsuji[17] with hydrogen injected normal to a Mach 1.8 flow from a wall slot is also plotted on figure 3. Again, at the ignition limit, the flame was first observed far downstream of the jet.

Cookson et al.[18] experimented with parallel injection from a circular orifice into an open Mach 2 co-flow at atmospheric pressure. With air static temperatures less than 1050K they found the diffusion flame became ragged and small detonations could be heard. It is interesting to note that when Cookson enclosed the airflow in a conical tube with 0.75° degree wall divergence, combustion was observed to occur after the Mach disc formed at the tube exit and it did not propagate upstream. This clearly demonstrates the 1050K static temperature was very close to the limit for auto-ignition. By adding a short length of constant area prior to the divergent section, combustion was restored - a technique that is now common practice.

So it is clear that boundary layers, base flows, and upstream separated regions are not guaranteed to work as ignition sources. Figure 4 presents results compiled by Huber et al.5 from a wide survey of hydrogen supersonic combustors. The static temperatures have been calculated from the tabulated Mach number and total temperatures, allowing for variable specific heat and the presence of water vapor in the vitiated facilities. Also plotted on the figure are the thermal choking limits for equivalence ratios of 0.2 (leftmost), 0.4, 0.6, 0.8 and 1 for constant area (dashed) and constant pressure (solid) combustion. The combustor initial conditions must be to the right of these curves to avoid thermal choking.

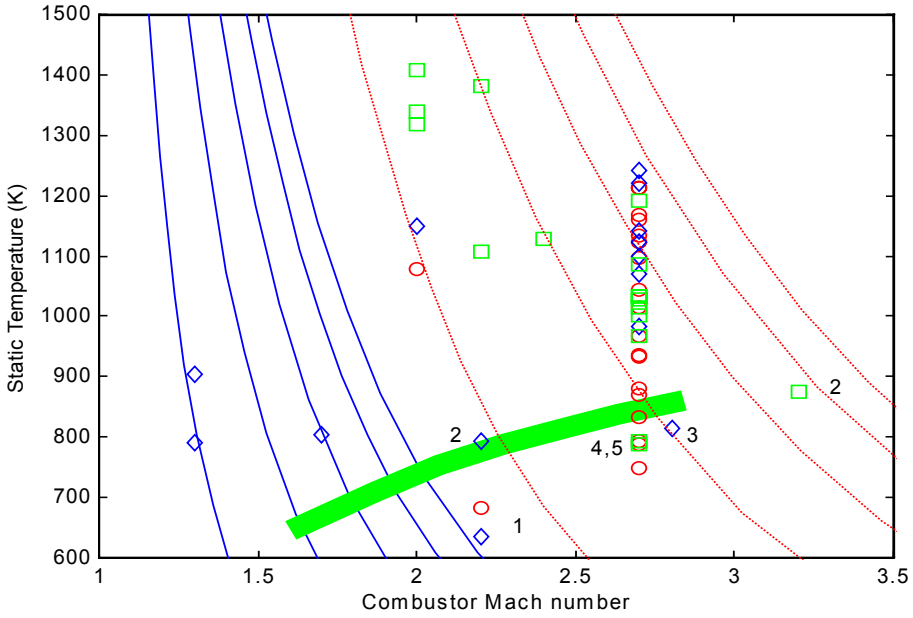

Figure 4: Hydrogen ignition results and "typical intake" as compiled by Huber et al (1979). Thermal choking limits for equivalence ratios of 0.2, 0.4, 0.6, 0.8 and 1 are drawn for combustion at constant area (red dashed) and constant pressure (blue solid).

The point being made with the curves is that all practical combustors must incorporate divergence to allow complete combustion without unstarting the engine. We have seen from Cookson's experiment and many others since that small divergence can result in flame-out or very poor combustion efficiency. Takahashi et al.[19] used air injection from the combustor wall to control the divergence and maintain the flame, as did Guy and Mackley for the Airframe-Integrated scramjet[20]. The advantage of Takahashi's system was that it was automated, with the bleed air flow rate linked via a control system to combustor pressure measurements.

Huber's intake curve is also plotted on figure 4 and reveals that the majority of the combustor experiments are at temperatures far higher than an intake should deliver. The circles correspond to cases for which auto-ignition did not occur, the diamonds are at an ignition limit and the squares correspond to cases where ignition was observed but the lower temperature limit was not established.

There are a few cases sufficiently cold to be of interest and these are labelled from 1 to 5.

Case:

1. Northam et al.[21]. The combustor was a section of the NASA Langley Airframe-Integrated scramjet. In this direct connect test, a centre strut was contoured to produce Mach 2.2 flow either side of the strut. The authors concluded from the measured pressure distributions that the combustion at low total temperatures was occurring in a shock induced separated region near the base of the strut. No measurements of combustion efficiency are reported and so it is not clear how effective this subsonic combustion zone was in promoting supersonic combustion downstream.

2. Guy and Mackley20. The paper presents free jet test results of the Airframe-Integrated engine. The Mach 2.2 result, tabulated by Huber et al.5 was in fact at Mach 1.76 and 860K if one uses the relationship between static temperature upstream of the injectors and total temperature, given by Guy and Mackley. Such a condition is too hot to be relevant here.

3. The Mach 3.2 result was at a nominal static temperature and pressure of 860K and 0.3bar respectively 20. At this condition, auto-ignition is expected but ignition delay times are long, figure 3. In order to obtain ignition Guy and Mackley added an obstruction on the centre strut to increase compression. That is, ignition occurred at a lower Mach number and higher temperature than indicated on figure 4. The modification resulted in combustor-inlet interaction at equivalence ratios greater than 0.3 and measured combustion efficiencies were low.

4. NASA CR-66952. Apparently a model of the Hypersonic Research Engine (HRE) annular combustor with injection from an orifice row. This reference was not available.

5. Eggers et al.22. A model of the strut combustor of the Airframe integrated engine at the Mach 7 flight condition. The model used a Mach 2.7 nozzle to simulate the required intake flow between the centre and outer strut. The interesting low static temperature result plotted on figure 4 corresponds to run at a reduced stagnation temperature of 1670K. The original reference shows that the M2.7 nozzle was unstarted at this condition. With a pressure rise of a factor 5 occurring somewhere upstream of the strut, this result is also invalid.

6. Russin W.23. A 2D model designed to represent a segment of the HRE annular combustor. Intensive combustion was observed with two stage hydrogen injection into vitiated air with static temperature and pressure of 780K and 0.8bar respectively. The first stage fuel injector was a 5 orifice row located mid way in a 207mm long 39×170mm constant area section. The second stage injector was a 6 orifice row 73mm downstream from the start of the divergence. The total divergence angle was 2.3° giving an initial area change rate of 1% per cm. The hydrogen was unheated yet appeared to burn readily in this cold wall combustor. Combustion efficiency was said to be near one.

Of the combustion experiments included in Huber's survey, only the HRE model (case 5 and maybe 3) demonstrated operation at conditions corresponding to an efficient intake process. The result was repeated in tests of the Aerothermodynamic integration model of the HRE at the NASA Lewis Hypersonic Test Facility although this time with hydrogen heated to about 850K[24]. The Hypersonic test Facility is a clean air blowdown tunnel facility so vitiation contamination was not a factor in this success.

In this section we have concentrated on combustors capable of auto-ignition at low temperature. This is of course not an essential property, the more important question is whether combustion can be maintained if the flame is first ignited by some other means.

5.7 TURBULENT FLAMEHOLDING

Flameholding in the traditional sense (diffusive preheating of reactants by combustion products) appears impossible due to low flame speeds (~10m/s) in comparison to combustor velocity (~1km/s) but combustion generated turbulence can result in sufficient flame speeds in some cases.

In a combustion test facility the flow static temperature can be raised by increasing the total enthalpy. When the fuel ignites, it is then often possible to decrease the temperature to some lower level before "flame out" or "blow off". Thus we can distinguish two processes: ignition, where the flame is established; and flame holding by which combustion is maintained once it has been established. In subsonic combustion the flame holding mechanism is very clear - the upstream diffusion of combustion products preheats the reactants and also provides radicals to enhance reactivity. In supersonic combustion flameholding mechanisms are not well defined, and it is this process that is the focus of this section.

Henry[25] reported an experiment in which premixed hydrogen/air were expanded to Mach 1.5. A coaxial air-hydrogen-oxygen centre pilot was used to ignite the mixture and flame angles were recorded using a schlieren movie. The angles were converted to flame speeds which were found to be close to 10m/s and relatively insensitive to the fuel/air temperature. He concluded that pilots would have to be mounted in wake regions or within the boundary layer, in order to achieve the desired lateral propagation rates. The question remains of how such a pilot location could help ignite the bulk of the fuel/air shear layer in a scramjet, which by definition must be supersonic.

Suttrop[26] presented results showing that the hydrogen diffusion flames downstream of strut injectors in a Mach 1.7, 0.26bar flow blew out when the air static temperature was decreased to 900K. This point is marked on figure 3 and it is seen that it is in a region where autoignition is expected (before the cooling effect of the room temperature hydrogen is considered), so it is quite clear that even with hydrogen fuel a diffusive flame will not necessarily be self sustaining in a supersonic flow.

Turbulent flame propagation models are highly empirical and naturally must simplify the chaotic processes involved. Early flame theories by Damkohler and later Shckelkin, reduce to the simple result for high speed flow that turbulent flame speed is equal to the turbulence velocity u'.[27] To obtain sufficient mixing within a reasonable combustor length, many injection schemes employ what are essentially inviscid flow structures like crossflow jets and/or vortices to enhance the spread of the fuel through the chamber. These structures tend to stretch flames at rates much greater than they would encounter in a plane shear layer, the growth rate of which is restricted to about u'/U. Thus with this type of combustor one could not expect turbulent flame speeds to be sufficient for flame-holding.

Combustors that employ strut injectors tend to inject the fuel in multiple plane shear layers, and with such arrangements it has been shown that flame holding is possible. An excellent and detailed study of such a combustor was made by Beversdorff et al.[28] A fin injector (a strut that doesn't span the entire combustor) designed at TsAGI was tested at Mach 2 with freestream static temperatures of approximately 600K and hydrogen fuel at an equivalence ratio near 1. Upon combustion, turbulence intensities in the wake of the injector increased from 5-8% to 8-40% and the wake flow became subsonic. The interaction between combustion and turbulence is very obvious in this case, and is a phenomena recognized in some turbulent flame theories.[27] The wall pressure increased from 1 to 2atm but the air stream away from the flame remained supersonic. CARS (Coherent anti-Raman scattering) instantaneous static temperature measurements showed that in the combustion zone temperature fluctuated from 600 to 2000K. Given this mixing of high temperature products with low temperature reactants, one might also conclude that chemical kinetics do not have a strong influence on such a turbulent flame.

In Beversdorff's fundamental study, the combustor was relatively short and interaction between the flame and surrounding airstream and wall were relatively mild. With a longer combustor the wall boundary layer is likely to have separated resulting in a dramatic pressure rise upstream of the fuel injector. In fact at the low enthalpy conditions of that test (equivalent to Mach 5.5) with an equivalence ratio of 1, a quasi-normal shock is to be expected with subsonic flow not just confined to the combustion zone.

The increase in turbulence due to heat release, and the existence of large free subsonic combustion zones surrounded by supersonic airflow may account for other reported observations of supersonic hydrogen combustion in very low temperature air.29,30 Whether turbulent flame speed is high enough to maintain combustion in realistic cases is still an open question. For lack of another explanation we might assume that this is the mechanism by which local flames maintained by subsonic pilots, successfully spread through combustors. Henry's experiment25 would indicate that turbulent flame speeds are not high enough but they were conducted with premixed fuel air and in the absence of pressure gradients. Turbulent shear layers and adverse pressure gradients might be essential. The strong adverse pressure gradients present in supersonic combustors (typically 10%/cm) might drive the mixing between the low density combustion products and high density reactants sufficiently fast to spread flames at speeds that are impossible in the isobaric case.

5.8 COMBUSTION INDUCED COMPRESSION

Combustion induced compression refers to the pressure rise from combustion feeding forward into the engine isolator. When this compression is sufficient to elevate the intake exit temperature to the autoignition limit for the fuel, stable combustion is achieved. This mode of operation is fundamental to scramjets.

Dual mode ramjets rely on the pressure rise from combustion feeding forward to the combustor entrance. At low flight Mach numbers the shocks upstream of the combustor (generally in an Isolator) are sufficiently strong that the flow is subsonic and with the static temperature close to the total temperature, combustion proceeds readily. At high flight Mach numbers the flow remains supersonic but the static temperature downstream of the shocks is often sufficient for auto-ignition to occur, at least with hydrogen fuel.

The importance of the upstream compression to scramjet operation has been recognized for many years. Billig and Dugger31 devised methods of modelling the process for cycle performance calculations and there have been many subsequent studies correlating the strength of the pre combustion shock with the heat release, and others on the length of isolator needed to prevent propagation of the disturbance up to the intake. Chinzei et al.32 provide a summary of this work with many references, along with some new data.

A recent shock tube study of the phenomenon attempted to determine the mechanism by which the pressure disturbances propagated upstream.33 A constant area combustor with a rectangular cross section and a central strut with parallel hydrogen injection was operated at Mach 2.5 and 3.8. Shadowgraphs and pressure measurements tracked the shock as it propagated upstream at speeds near 100m/s in laboratory co-ordinates. The flow downstream of the strong convex normal shock was calculated to be transonic and the pressure rise was sufficient to separate the turbulent boundary layers on the combustor walls. O'Byrne et al.33 concluded they had insufficient evidence to be certain if separation or heat release was the dominant process. Interestingly, at the Mach 3.8 condition with the entrance air at 1100K and 1atm, a turbulent flame initially was apparent at the exit

of the injector but it blew out before the combustion wave arrived from downstream. This is further evidence of the difficulty in maintaining turbulent flames close to the auto-ignition limit. Note in this shock tube study, the hydrogen and injector strut were at room temperature.

5.9 PARTIAL SUBSONIC COMBUSTION

Flameholding may be achieved by partial subsonic combustion such as the JHU Dual combustor ramjet, the Aerojet strutjet, and some would argue by the use of two stage injection or combustor wall cavities.

One of the most promising flame-holding techniques for hydrocarbon fuel, and certainly the most thoroughly tested, is the use of a subsonic burner to either pilot the main supersonic fuel jets or produce a fuel rich exhaust jet for subsequent combustion in the supersonic air. Waltrup2 has reviewed and analyzed these techniques, providing many references to experimental work in the USA.

One study of subsonic pilots not included in Waltrup's review is that by Wagner et al. with hydrogen.34,35 Pilot injectors were placed upstream of the primary fuel injectors which were positioned 7.7 step heights downstream of a rearward facing step. After ignition by a plasma jet located between the step and primary fuel injectors, the plasma igniter could be turned off and combustion continued in the Mach 2 flow with static temperatures as low as 560K. Flowfield shadowgraphs showed the flow had separated between the step and primary injectors, and the upstream pilot fuel was burning in this subsonic zone. Total combustion efficiency was 0.47 and the maximum equivalence ratio was 0.29, hence only 14% of the oxygen was being consumed. It is difficult to judge the effectiveness of the pilot scheme in promoting combustion downstream in the combustor where the primary fuel has mixed with the supersonic air. As with Beversdorrf's study28, the supersonic performance of the combustor at Mach 2 is somewhat academic as a real engine would almost certainly produce a strong (normal) precombustion shock with Mach 2 flow at the intake exit.

While fuel rich subsonic combustion followed by supersonic combustion is an obvious solution to the flameholding problem, the use of pilots is not. There is no doubt that fuel can be made to burn in subsonic pockets such as wall cavities but the mechanism by which the flame then propagates across the combustor to light and maintain the flame in the primary supersonic fuel/air stream is not clear.

The HRE with its two stage injection scheme23 perhaps also functioned with subsonic combustion of the first stage fuel. The combustor inlet Mach number of 2.7 makes the HRE experiments a rare source of data on flameholding at representative engine conditions for supersonic combustion.

5.10 PLASMA SOURCES

Ionization sources may be used as an alternative to chemical initiators but although established as ignition sources they have yet to be proved in the flameholding role.

The plasma torch igniters used by Wagner et al. in the study discussed above are described in more detail in Wagner et al.,35 and references to earlier work in the USA and Japan are given. More recent work is referenced by Nagashima et al.36. Argon is a common feed stock for the plasma torch with either hydrogen or oxygen added as a source of radicals to enhance reactivity.

While these low Mach number, low temperature studies provide evidence that plasma jets are effective ignition sources, once lit, the flame remained in the combustors tested without the torches operating. No published data were found on their effect on supersonic combustion efficiency with flames that were not self sustaining. Thus from the available data it is difficult to judge whether a plasma source could be an effective flame-holder in a real engine.

5.11 CONCLUSIONS

1. Low combustor entry temperature is desirable/essential due to intake and nozzle limitations;
2. For both hydrogen and hydrocarbon the optimum temperature/pressures are in regions in which ignition delay is very sensitive to temperature, varying from 0.1ms to >>10ms;
3. Chemical initiators such as silane, fluorine and OTTO can be used but there are penalties in specific impulse, system complexity and handling hazards;
4. Ionization sources may be used as an alternative to chemical initiators but although established as ignition sources they have yet to be proved in the flameholding role;
5. Flameholding in the traditional sense (diffusive preheating and seeding reactants with combustion products) appears impossible due to low flame speeds (~10m/s) in comparison to combustor velocity (~1km/s)

but combustion generated turbulence can result in sufficient flame speeds in some cases. Strong evidence for this has been obtained at low Mach number and static temperatures but at these conditions combustion results in free subsonic regions with very high turbulence. The evidence that flame speeds are sufficient under realistic scramjet conditions is circumstantial. For lack of another explanation we might assume that this is the mechanism by which local flames maintained by subsonic pilots, successfully spread through combustors. Adverse pressure gradients seem to be essential for this spread;

6. Flameholding due to the propagation of pressure disturbances upstream to compress and raise the air temperature to produce autoignition is normal. It allows an increase in engine efficiency beyond that expected for an engine with a self starting intake operating at the same pre-flame temperature;

7. Flameholding may be achieved by partial subsonic combustion such as the JHU Dual combustor ramjet, the Aerojet strutjet, and some argue by the use of two stage injection or combustor wall cavities. In these latter cases the flame must still propagate across the supersonic shear layer and it is this process that is still poorly understood (see 6).

5.12 RECOMMENDATIONS

1. Future supersonic combustion experiments should be conducted at representative inlet temperatures and pressures. Strict control of the static temperature is required so that it is neither too hot (guaranteeing autoignition) or too cold (so that the heat released produces a local subsonic flame).

2. Once ignition is established, temperature should be varied by small amounts to explore the influence of chemical kinetics on the flame-holding. If kinetics are important to the operation of the engine, flame front position and combustion efficiency will be a strong function of temperature, not only of the air but also of the fuel. Heating of the fuel prior to ignition should be beneficial.

3. The effect of strong adverse pressure gradients on a mixed density free shear layer should be investigated to gain a better understanding of the very strong influence of combustor divergence on flameholding. A reasonable start would be to examine the effect of an applied (strong) pressure gradient on a helium jet in supersonic co-flowing air.

4. Piloted-combustion studies should focus on the mechanism and rate of flame propagation in the bulk supersonic flow and not on the pilot flow.

5.13 REFERENCES

[1] Waltrup P. J., "Hypersonic airbreathing propulsion: Evolution and Opportunities", AGARD-CP-428, No. 12, 1987;

[2] Waltrup P. J., "Hypersonic airbreathing missile propulsion", AGARD-CP-600 Vol. 3, 1997;

[3] Northam G. and Anderson G., "Supersonic combustion research at Langley", AIAA-86-0159, 1986;

[4] Curran T., "Scramjet engines: The first forty years", SMI Towards Mach 5: Hypersonic flight conference, London, Nov. 1997;

[5] Huber P., Schexnayder C., and McClinton C., "Criteria for self-ignition of supersonic hydrogen-air mixtures", NASA TP-1457, 1979;

[6] Trexler C., "Inlet performance of the Integrated Langley scramjet module (Mach 2.3 to 7.6)", AIAA-75-1212, 1975;

[7] Billig F., 1995, “Supersonic combustion ramjet missile” J. of Propulsion and Power, Vol. 11 No. 6;

[8] Van Wie D. and Ault D., "Internal flowfield characteristics of a scramjet inlet at Mach 10", J. of Propulsion and Power, Vol. 12, No. 1, 1996;

[9] Smart M., "Design of three-dimensional hypersonic inlets with rectangular-to-elliptical shape transition", J. of Propulsion and Power, Vol. 15, No. 3, 1999;

[10] Molder S., and Romeski J., "Modular hypersonic inlets with conical flow", AGARD-CP-30, paper 9, 1968;

[11] Townend L., 1966, “Ramjet propulsion for hypersonic aircraft”, Tech memo Aero 917, RAE, UK;

[12] Cain T., "Autoignition of hydrogen at high pressure", Combustion and Flame, 111, pp124-132, 1997;

[13] Waltrup P. J., "Liquid fueled supersonic combustion ramjets: A research perspective of the past, present and future", AIAA-86-0158, 1986;

[14] Hunt J., Johnston P., Cubbage J., Dillion J., Richie C. and Marcum D., "Hypersonic airbreathing missile concepts under study at Langley", AIAA-82-0316;

[15] Voland R., and Rock K., "NASP concept demonstration engine and subscale parametric engine tests", AIAA-95-6055, 1995;

[16] Sung C., Li J., Yu G. and Law C., "Chemical kinetics and self-ignition in a model supersonic hydrogen-air combustor", AIAA J., Vol. 37, No. 2, 1999;

[17] Yoshida A. and Tsuji H., "Supersonic combustion of hydrogen in a vitiated airstream using transverse injection", AIAA J., Vol 15., No. 4, 1977;

[18] Cookson R., Flanagan P., and Penny G., "A study of free-jet and enclosed supersonic diffusion flames", Twelfth Combustion Symposium, pp1115-1124, 1969;

[19] Takahashi S., Sato N., Tsue M., Kono M., Nakamura M., Kondo H., and Ujiie Y., "Control of flame-holding in supersonic airflow by secondary air injection", J. of Propulsion and Power, Vol. 14. No. 1, p18-23, 1998;

[20] Guy R. and Mackley E., "Initial wind tunnel tests at Mach 4 and 7 of a hydrogen-burning, airframe-integrated scramjet", 79-7045, Fourth ISABE, 1979;

[21] Northam G., Trexler C., and Anderson G., "Characterisation of a swept-strut hydrogen fuel-injector for scramjet applications", 15th JANNAF Combustion meeting, CPIA Publ. 297, pp393-410, 1979;

[22] Eggers J., Reagon P., and Gooderum P., "Combustion of hydrogen in a two-dimensional duct with step fuel injectors", NASA TP-1159, 1975;

[23] Russin Wm. R., "The effect of initial flow nonuniformity on second stage fuel injection and combustion in a supersonic duct", NASA TM X-72667, 1975;

[24] Anderson W. and Kado L., "Hypersonic research engine project - phase II, Aerothermodynamic Integration model test report", NASA CR-132655, 1975;

[25] Henry J., "Recent research on fuel injection and mixing and piloted-ignition for scramjet combustors", Twelfth Combustion Symposium, pp1175-1182, 1969;

[26] Suttrop F., "Comment on the paper by Billig and Dugger", Twelfth Combustion Symposium, pp1135-1138, 1969;

[27] Beer J. and Chigier N., "Combustion aerodynamics", Applied science publishers, London, 1972;

[28] Beversdorff M., Forster W., Clauss W., Waidmann W., and Woyde M., "Velocity and temperature measurements in a scramjet combustion chamber", Thirteenth International Symposium on air breathing engines, pp385-393, 1997;

[29] Yoon Y., Donbar J., Huh H. and Driscoll J., "Measured supersonic flame properties: Heat release patterns, pressure losses, thermal choking limits", J. Propulsion and Power, Vol. 12, No. 4, pp718-723, 1996;

[30] Segal C., McDaniel J., and Whitehurst R. and Krauss R., "Mixing and chemical kinetics interactions in a Mach 2 reacting flow" J. Propulsion and Power, Vol. 11, No. 2, pp308-314, 1995;

[31] Billig F., and Dugger G., "The interaction of shock waves and heat addition in the design of supersonic combustors", 12th Symposium on Combustion, pp1125-1140, 1969;

[32] Chinzei N., Komuro T., Kudou K., Murakami A., Tani K., Masuya G., and Wakamatsu Y., "Effects of injector geometry on scramjet combustor performance", Tenth International Symposium on air breathing engines, pp1219-1227, 1991;

[33] O'Byrne S., Doolan M., Olsen S., and Houwing A., "Analysis of transient thermal choking process in a model scramjet engine", J. of Propulsion and Power, Vol. 16, No. 5, pp808-814, 2000;

[34] Wagner T., O'Brien W., Northam G., and Eggers J., "Design and evaluation of a new injector configuration for supersonic combustion", ISABE 87-7026, pp390-397, 1987;

[35] Wagner T., O'Brien W., Northam G., and Eggers J., "Plasma torch igniter for scramjets", J. Propulsion and Power, Vol.5 No. 5, pp 548-554, 1987;

[36] Nagashima T., Kitamura H., and Obata S., "Supersonic combustion of hydrogen in tandem transverse injection with oxygen radicals", ISABE 97-7055, pp366-373, 1997.

CHAPTER 6: FUEL-AIR MIXING AND COMBUSTION IN SCRAMJETS

J. Philip Drummond and Glenn S. Diskin
NASA Langley Research Center, Hampton, Virginia
j.p.drummond@larc.nasa.gov, g.s.diskin@larc.nasa.gov

Andrew D. Cutler
The George Washington University
Joint Institute for Advancement of Flight Sciences, Hampton, Virginia
a.d.cutler@larc.nasa.gov

6.1 Introduction

At flight speeds, the residence time for atmospheric air ingested into a scramjet inlet and exiting from the engine nozzle is on the order of a millisecond. Therefore, fuel injected into the air must efficiently mix within tens of microseconds and react to release its energy in the combustor. The overall combustion process should be mixing controlled to provide a stable operating environment; in reality, however, combustion in the upstream portion of the combustor, particularly at higher Mach numbers, is kinetically controlled where ignition delay times are on the same order as the fluid scale. Both mixing and combustion time scales must be considered in a detailed study of mixing and reaction in a scramjet to understand the flow processes and to ultimately achieve a successful design.

Although the geometric configuration of a scramjet is relatively simple compared to a turbomachinery design, the flow physics associated with the simultaneous injection of fuel from multiple injector configurations, and the mixing and combustion of that fuel downstream of the injectors is still quite complex. For this reason, many researchers have considered the more tractable problem of a spatially developing, primarily supersonic, chemically reacting mixing layer or jet that relaxes only the complexities introduced by engine geometry. All of the difficulties introduced by the fluid mechanics, combustion chemistry, and interactions between these phenomena can be retained in the reacting mixing layer, making it an ideal problem for the detailed study of supersonic reacting flow in a scramjet. With a good understanding of the physics of the scramjet internal flowfield, the designer can then return to the actual scramjet geometry with this knowledge and apply engineering design tools that more properly account for the complex physics. This approach will guide the discussion in the remainder of this section.

6.2 Reacting Mixing Layers and Jets

As described earlier, compressible shear/mixing layers and jets provide good model problems for studying the physical processes occurring in high-speed mixing and reacting flow in a scramjet. Mixing layers are characterized by large-scale eddies that form due to the high shear that is present between the fuel and air streams. These eddies entrain fuel and air into the mixing region. Stretching occurs in the interfacial region between the fluids leading to increased surface area and locally steep concentration gradients. Molecular diffusion then occurs across the strained interfaces. There has been a significant amount of experimental and numerical research to study mixing layer and jet flows [1]- [9]. For the same velocity and density ratios between fuel and air, increased compressibility, to the levels present in a scramjet, results in reduced mixing layer growth rates and reduced mixing. The level of compressibility in a mixing layer with air stream 1 and fuel stream 2 can be approximately characterized by the velocity ratio, $r = U_2/U_1$, the density ratio,

s = ρ_2/ρ_1, and the convective Mach number, $M_c = (U_2-U_1)/(a_1+a_2)$ where a is the speed of sound. Increased compressibility reorganizes the turbulence field and modifies the development of turbulent structures. The resulting suppressed transverse Reynolds normal stresses appear to result in reduced momentum transport. In addition, the primary Reynolds shear stresses responsible for mixing layer growth rate also are reduced. The primary mixing layer instability becomes three-dimensional with a convective Mach number above 0.5, reducing the growth of the large scale eddies. Finally, the turbulent eddies become skewed, flat, and less organized as compressibility increases. All of these effects combine to reduce the growth rate of the mixing layer and the overall level of mixing that is achieved.

Several phenomena result in the reduction of mixing with increasing flow velocity, including the velocity differential between fuel and air, and compressibility. Potentially, the existence of both high and low growth and mixing rates are possible, and the engine designer with an understanding of the flow physics controlling these phenomena can advantageously use these effects. The shock and expansion wave structure in and about the mixing layer can interact with the turbulence field to affect mixing layer growth [1]. Shock and expansion waves interacting with the layer result from the engine internal structure. Experiments have shown that the shocks that would result from wall and strut compressions appear to enhance the growth of the two-dimensional eddy structure (rollers) of a mixing layer. This effect is most pronounced when the duct height in the experiment and the shear layer width become comparable. Waves may be produced by the mixing layer itself under appropriate conditions. Localized shocks (often termed shocklets) occur within the mixing layer when the accelerating flow over an eddy becomes supersonic even when the surrounding flow is subsonic. When the overall flow is supersonic, the eddy shocklets will extend as shocks into the flow beyond the individual eddies. These shocklets can retard eddy growth due to increased localized pressure around the eddy.

The growth of a mixing layer produces a displacement effect on the surrounding flow field. This displacement in confined flow produces pressure gradients that can affect the later development of the mixing layer, typically retarding growth. When chemical reaction occurs in a mixing layer, resulting in heat release, the growth of the mixing layer is retarded in both subsonic and supersonic flow [1, 2]. The effect of heat release can also vary spatially as a function of the local stoichiometry and chemical reaction. The retarded growth in both instances can be reversed, however, by allowing the bounding wall to diverge relative to the initial wall angles where retarded growth was noted [1]. While the process of mixing layer growth is affected by the combustor geometry and design, fuel injector design carried out with proper consideration for the inlet and combustor geometry can have a strong influence on overall mixing and combustion efficiency. Considerable effort has been expended over the past fifteen years to achieve efficient fuel injector designs. Injector design will be considered in the next section.

6.3 Scramjet Fuel Injectors

There are several key issues that must be considered in the design of an efficient fuel injector. Of particular importance are the total pressure losses created by the injector and the injection processes, that must be minimized since the losses reduce the thrust of the engine. The injector design also must produce rapid mixing and combustion of the fuel and air. Rapid mixing and combustion allow the combustor length and weight to be minimized, and they provide the heat release for conversion to thrust by the engine nozzle. The fuel injector distribution in the engine also should result in as uniform a combustor profile as possible entering the nozzle so as to produce an efficient nozzle expansion process. At moderate flight Mach numbers, up to Mach 10, fuel injection may have a normal component into the flow from the inlet, but at higher Mach numbers, the injection must be nearly axial since the fuel momentum provides a significant portion of the engine thrust. Intrusive injection devices can provide good fuel dispersal into the surrounding air, but they require active cooling of the injector structure. The injector design and the flow disturbances produced by injection also should provide a region for flameholding, resulting in a stable piloting source for downstream ignition of the fuel. The injector cannot result in too severe a local flow disturbance, that could result in locally high wall static pressures and temperatures, leading to increased frictional losses and severe wall cooling requirements.

A number of options are available for injecting fuel and enhancing the mixing of the fuel and air in

high-speed flows typical of those found in a scramjet combustor [10, 11]. Two traditional approaches for injecting fuel include injection from the combustor walls and in-stream injection from struts. The simplest approach for wall injection involves the transverse injection of the fuel from wall orifices. Transverse injectors offer relatively rapid near-field mixing and good fuel penetration. Penetration of the fuel stream into the cross-flow is governed by the jet-to-freestream momentum flux ratio. The fuel jet interacts strongly with the cross-flow, producing a bow shock and a localized highly three-dimensional flow field. Resulting upstream and downstream wall flow separations also provide regions for radical production and flameholding, but they can also result in locally high wall heat transfer. Compressibility effects that were noted earlier for mixing layer flows also are evident in the mixing regime downstream of a transverse jet. Compressibility again retards eddy growth and breakup in the mixing layer and suppresses entrainment of fuel and air, resulting in a reduction in mixing and reaction.

Improved mixing has also been achieved using alternative wall injector designs. Wall injection using geometrical shapes that introduce axial vorticity into the flow field has been successful. Vorticity can be induced into the fuel stream using convoluted surfaces or small tabs at the exit of the fuel injector. Alternatively, vorticity can be introduced into the air upstream of the injector using wedge shaped bodies placed on the combustor walls. Vorticity addition to the air stream provides more significant mixing enhancement of fuel and air [12]. When strong pressure gradients are present in the flowfield, e.g. at a shock, vorticity aligned with the flow can be induced at a fuel-air interface, where a strong density gradient exists, by virtue of the baroclinic torque. Fuel injection ramps have proven to be an effective means for fuel injection in a scramjet engine [2]. Fuel is injected from the base of the ramp. The unswept ramp configuration provides nearly streamwise injection of fuel to produce a thrust component. The effects of angled injection on axial thrust only go as the cosine of the angle, so small injection angles result in little loss in thrust. Flow separation at the base of the ramp provides a region for flame holding and flame stabilization through the buildup of a radical pool. The ramp itself produces streamwise vorticity as the air stream sheds off of its edges, improving the downstream mixing. The swept ramp design provides all of the features of the unswept ramp, but the sweep results in better axial vorticity generation and mixing. A novel variation on the swept wedge injector, termed the aero-ramp injector [13], utilizes three arrays of injector nozzles at various inclination and yaw angles to approximate the physical swept ramp design.

In-stream injection also has been utilized for fuel injection in a scramjet. Traditional approaches involve fuel injection from the sides and the base of an in-stream strut. Transverse injection results in behavior similar to transverse fueling from the wall, although differences can occur due to much thinner boundary layers on the strut. Injection from the base of the strut results in slower mixing as compared to transverse injection. A combination of transverse and streamwise injection, varied over the flight Mach number range, often has been utilized to control reaction and heat release in a scramjet combustor. As noted earlier, however, streamwise injection has the advantage of adding to the thrust component of the engine. To increase the mixing from streamwise injectors, many of the approaches used to improve wall injection, including non-circular orifices, tabs, and ramps, have been successfully utilized. Several new concepts have emerged as well. Pulsed injection using either mechanical devices or fluidic oscillation techniques have shown promise for improved mixing. Pulsed injection of fuel utilizing a shuttering technique to control injection has been shown to improve mixing [12]. Fuel injection schemes integrated with cavities also provide the potential for improved mixing and flameholding. This type of integrated fuel injection/flameholding device, utilizing fuel injection into a cavity and from its base, integrates the fuel injection with a cavity that provides flameholding, flame stabilization, and mixing enhancement if the cavity is properly tuned. Air exchange rates with the cavity may be low, however, limiting the amount of fuel that can be added. Additional scramjet fuel injector designs continue to be introduced and studied to achieve even higher levels of mixing and combustion efficiency.

Scramjet design is built upon both experimental and computational research. To assure that computational tools properly represent the complex flow physics in a scramjet, careful evaluation of the computational tools is necessary. Benchmark experiments are becoming available that provide the necessary data for evaluating the accuracy of the numerical algorithms and the physical models that the computational tools employ. In addition, these experiments provide in some instances the information necessary to improve the modeling employed by the codes. Two experiments available for assessing high-speed combustion codes are described in the next section. Results obtained from the application of a combustion code to these experiments are also shown and discussed.

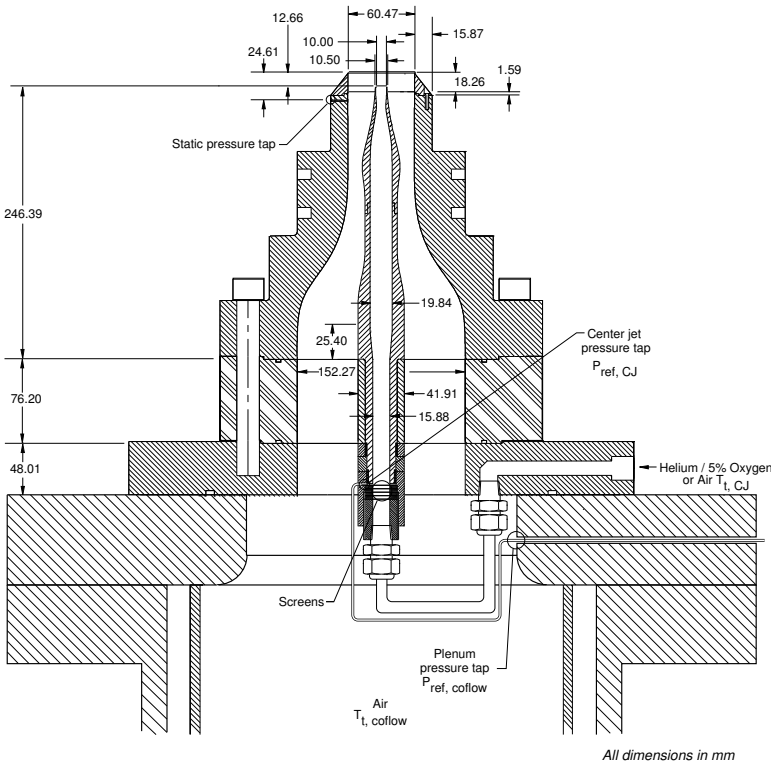

Figure 1: Coaxial jet assembly cross-section

6.4 Mixing and Combustion Experiments

Two basic experiments are being conducted at the NASA Langley Research Center to collect detailed high-speed mixing and combustion data for use in physical model development and code validation. The first experiment concerns coaxial jet mixing of a helium/oxygen center jet with a coflowing air outer jet and was chosen to provide detailed supersonic mixing data. The second experiment was developed to study high-speed mixing and combustion in a simple "scramjet like" engine environment. The experiment utilizes a ducted flow rig containing vitiated supersonic air with a single fuel injector that introduces supersonic gaseous hydrogen from the lower wall. Detailed wall and in flow surveys and noninterference diagnostics are used in both experiments. These experiments will be described in the following sections.

6.4.1 Coaxial Jet Mixing Experiment

A coaxial jet mixing experiment has been developed to study the high-speed compressible mixing of helium and air. Details of the experiment are described in references [14] and [15]. The low-density helium, which serves as a simulant of hydrogen fuel, was chosen to allow detailed studies of mixing without chemical reaction. Oxygen is added to the helium jet as a diagnostic aid for an oxygen flow-tagging technique (RELIEF). Several methods are utilized to characterize the flow field including Schlieren visualization, pitot pressure, total temperature, and gas sampling probe surveying, and RELIEF velocimetry. A schematic of the coaxial jet configuration is shown in Figure 1. The rig consists of a 10 mm inner nozzle from which helium, mixed with 5 percent oxygen by volume, is injected at Mach 1.8 and an outer nozzle 60 mm in diameter from which coflowing air is introduced also at Mach 1.8. The velocity ratio between the two jets is 2.25, the convective Mach number is 0.7, and the jet exit pressures are matched to one atmosphere.

The resulting flow downstream of the nozzles can be seen in Figure 2, which shows a Schlieren image of the flowfield. The development of the mixing layer between the central helium jet and the air jet can be

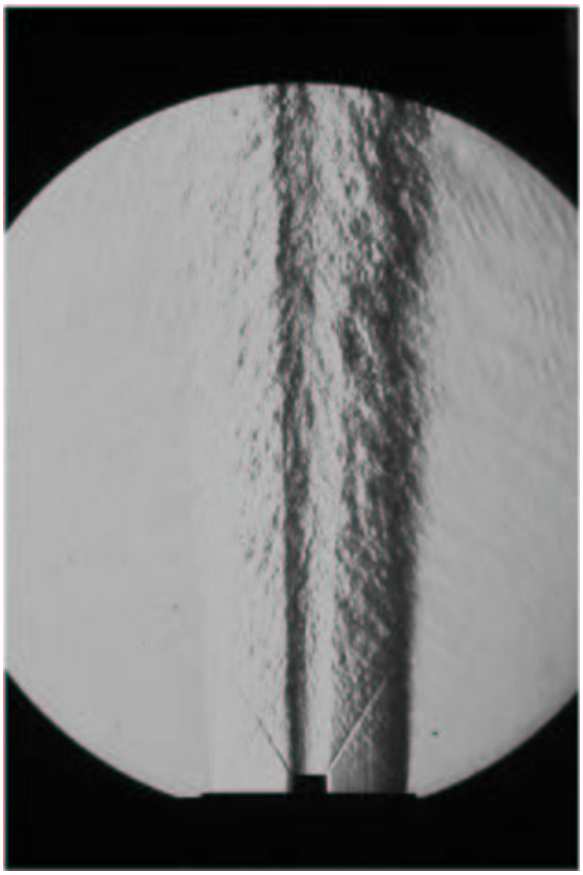

Figure 2: Schlieren image of coaxial jet mixing (conical extension cap removed)

seen along with the shear layer development between the air jet and the surrounding quiescent laboratory air into which the air jet exhausts. Shock-expansion wave structure emanating outward from the centerbody nozzle lip can also be seen. Inward propagating waves from the inner lip, due to the finite thickness of the lip (0.25 mm), can be observed in the air jet once they pass through the helium jet. These waves are not visible in the helium jet due to the low refractive index within the center jet. A third wave can also be observed emanating inward from the outer nozzle lip and traversing both the air jet and the helium jet. Additional results from the experiment will also be considered later in this section when comparisons of the measured data with numerical simulations are made.

6.4.2 SCHOLAR Combustor Experiment

A direct-connect supersonic combustor model, known by its acronym SCHOLAR, has been developed for testing in a combustion heated test facility at the NASA Langley Research Center. This experiment has been designed to provide optical access to a reacting supersonic flowfield typical of the flow present in a scramjet engine. Details of the experiment are described in reference [16]. The model shown in Figure 3a consists of a section 546 mm in length constructed of copper for thermal control followed by a 914 mm long section of carbon steel attached to the aft end of the copper section. The copper section contains a single fuel injector that introduces gaseous hydrogen into the vitiated air stream flowing through the model.

The injector region of the combustor model is shown in Figure 3b. The model consists of a constant area channel initially 38.6 mm high and 87.9 mm wide followed by a 4.8 mm rearward-facing step and a 43.8 mm long constant area section. Combustion heated vitiated air is introduced into the channel at

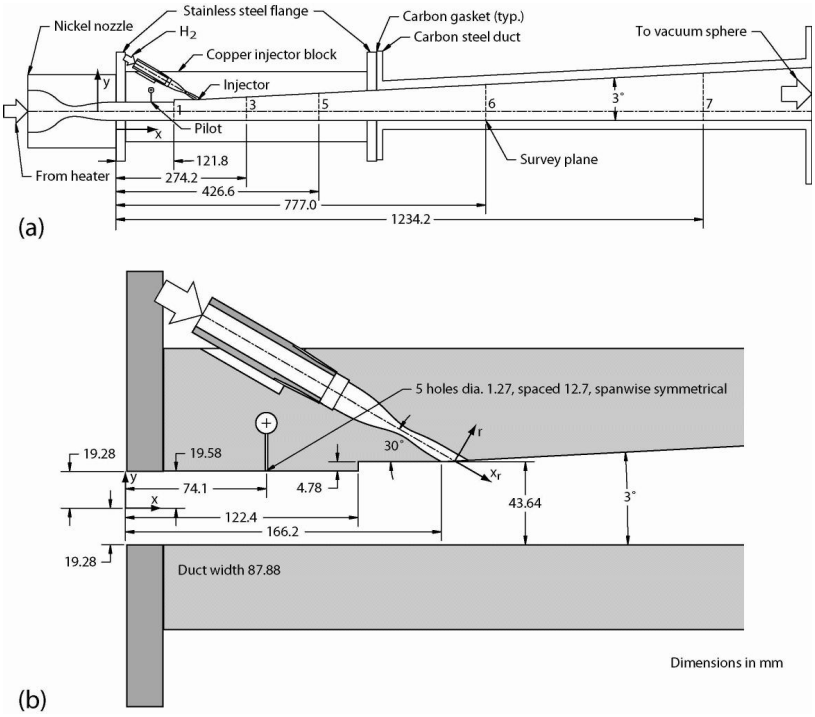

Figure 3: SCHOLAR combustor model: (a) nozzle, copper and steel duct sections; (b) detail near fuel injector and pilots.

Mach 2, 1184 K, and 100405 Pa. The vitiated air contains 20.35 percent water by mass introduced by the facility heater. A small amount of hydrogen fuel at a fuel equivalence ratio of 0.15 is introduced downstream from five pilot injectors along the upper wall at the 74.1 mm station. Each pilot injector is 1.27 mm in diameter. The central pilot injector lies on the duct centerline, and the remaining four injectors are spaced 12.7 mm from one another on either side of the central jet. This fuel is used to pilot the primary Mach 2.5 hydrogen fuel injector further downstream at the 173.2 mm station by igniting and producing a radical pool to enhance ignition of the primary fuel-air mixture. The primary fuel injector is inclined at 30 degrees to the horizontal and has a circular cross-section 7.6 mm in diameter. A 3 degree expansion of the upper wall begins immediately at the primary fuel injector. This 3 degree expansion continues along the upper wall of the carbon steel section that is attached to the copper model.

Five measurement locations for optical access are provided in the copper section of the model. Two additional measurement stations are provided in the carbon steel section. The measurement stations indicated in Figure 3a are slits in both model side walls, through which planar BOXCARS measurement beams enter and exit, allowing single-shot measurements to be made of static temperature (ro-vibrational temperature of N_2 molecules). These measurements are single point measurements, but the location of the measurement is translated during the tests to provide a full plane of data at each station. From these single-shot measurements, averages and RMS values are derived. In additional to optical measurements, wall pressures are measured using an array of orifices.

6.5 Simulation of Mixing and Combustion Experiments

The mixing and combustion experiments described earlier were numerically simulated before data was collected to assist in the experimental design. Additional simulations were also performed during and following the experimental study to compare with the measured data. Initial simulations were made with the SPARK combustion code. Additional studies with other combustion codes are being conducted [15]. Details on the

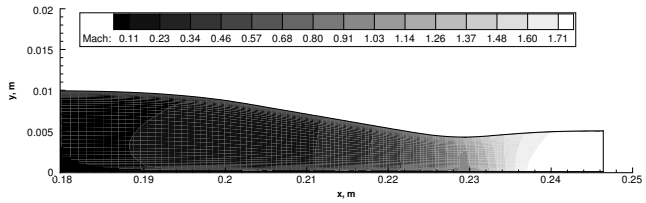

Figure 4: Mach contours in inner nozzle

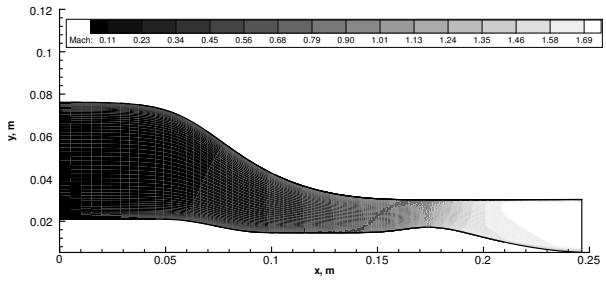

Figure 5: Mach contours in outer nozzle

simulations of both experiments and comparisons with measured data are given in the following sections.

6.6 Simulations of the Coaxial Jet Mixing Experiment

The axisymmetric version of the SPARK code was used to simulate the flowfield in the helium/oxygen center nozzle and the outer air nozzle of the coaxial jet experiment. Details of the code are given in reference [17]. This version of the code solves the axisymmetric full Navier-Stokes equations and species continuity equations describing the production, convection, and mixing of each relevant species. The analysis of the experiment was begun by first solving for the flowfield in the center and outer nozzles using the nozzle contours specified in the last section. The domain of the inner nozzle was discretized with a grid of 201 points in the streamwise direction and 51 points in the radial direction. The domain of the outer nozzle was discretized with a grid of 201 points in the streamwise direction and 101 points in the radial direction. Initial conditions in the subsonic portions of the nozzles were specified at the x = 76.2 mm station. For the inner nozzle at this station, the streamwise velocity was 141.8 m/s, the static temperature was 297.4 K, and the static pressure was 614300 Pa. The helium mass fraction in the inner jet was 0.6995 and the oxygen mass fraction was 0.3005. In the outer nozzle at the 76.2 mm station, the streamwise velocity, static temperature and pressure of the air were 22.94 m/s, 299.74 K, and 578100 Pa, respectively. No slip conditions were specified along the nozzle walls and first order extrapolation was used at the supersonic outflow station of each nozzle. Symmetry conditions were specified along the centerline of the inner nozzle. Turbulence in the outer nozzle was modeled using a Cebeci-Smith model. The flow in the inner nozzle was assumed to be laminar consistent with the behavior observed in the experiment at the outflow of the nozzle. Results from the center and outer nozzle simulations detailing Mach number distributions are given in Figures 4 and 5, respectively. The initial station (x = 76.2 mm) of both nozzles is reset to zero in the calculations. The Mach number ranges from a minimum of 0.1 in the subsonic portion of the nozzles to a maximum of 1.8 at the end of each nozzle. As can be seen from the figures, both nozzles produce very uniform exit flow fields resulting in ideal initial conditions for the mixing study in the region downstream of the nozzle exits.

Results obtained at the end of each nozzle were then used to specify the supersonic inflow conditions for the downstream domain beyond the nozzles where mixing of the jets occurred. The downstream domain was 150 mm long. The upper boundary of the domain was specified at y = 30.24 mm to coincide with the end of the outer nozzle wall. Radially beyond this point, laboratory air is entrained by the outer jet, but measurements have shown relatively low streamwise velocities of only a few meters per second in the entrained flow. Later measurements are planned to confirm these conditions. It is not appropriate to simulate such a low speed flow with a compressible code, so a slip boundary was chosen at y = 30.24 mm so as to consider only the compressible regime. Large scale structure certainly forms at this interface as the two streams viscously interact. Waves from this structure reach the helium-air interface near the nozzle exit. However, the air coflow-ambient air mixing layer does not start to merge with the helium-air mixing layer until the end of the experimental domain. The domain was discretized with a grid of 401 points in the streamwise direction and 201 points in the radial direction. The grid was radially compressed in the region of the helium-air mixing layer. Symmetry boundary conditions were specified along the y = 0 boundary and slip conditions were specified along the upper boundary at y = 30.24 mm. The outflow boundary at x =

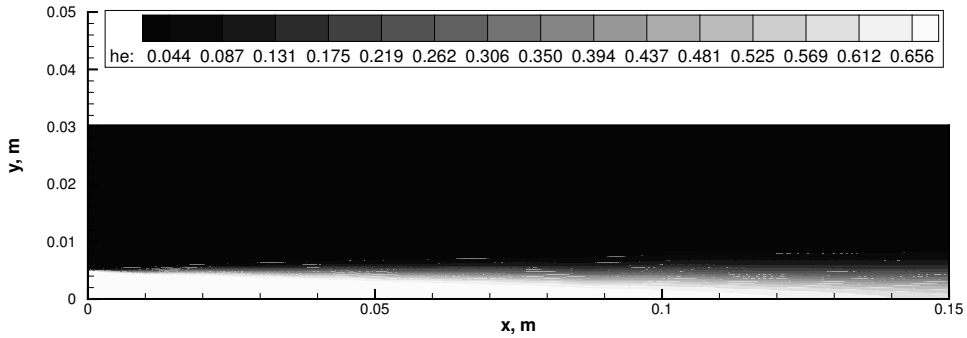

Figure 6: Helium mass fraction contours downstream of nozzles

150 mm remained supersonic, and extrapolation conditions were specified at this location. Turbulence was modeled in the downstream domain with the turbulent jet mixing model of Eggers and Eklund [18, 19].

Results from the downstream calculation are shown in Figures 6 through 8. Helium-air mixing downstream of the nozzles is shown in Figure 6. The helium mass fraction in the figure ranges from a minimum of zero to a maximum of approximately 0.7. There is significant mixing of the helium and air throughout the downstream region although relatively high mass fractions of helium still remain near the centerline.

A comparison of the measured helium mass fraction data with the simulation results at several stations downstream of the nozzles is given in Figure 7. Agreement between the simulation and the data is very good at each station. The code somewhat overpredicts the mixing near the centerline at the x = 0.12 m station, although the prediction improves with increasing radial distance. A comparison of measured pitot pressures with the simulation is shown in Figure 8. Agreement is good in the region of the air coflowing jet, but the simulation somewhat overpredicts the pitot pressure in the helium-air mixing region. The comparison with the experimental data differs at large radial distances greater than 0.025 m as the code does not consider the effects of the laboratory air entrained by the coaxial air jet. The RELIEF streamwise velocity data is compared with the simulation in Figure 9. The prediction agrees well with the data at the first three stations and slightly overpredicts the data at the remaining stations near the centerline. The simulation somewhat underpredicts the the velocity at the final three stations in the mixing region between the helium and air coflowing jets in agreement with the pitot pressure results.

6.6.1 Simulations of the SCHOLAR Combustor Experiment

The three-dimensional version of the SPARK code was used to simulate the flowfield in the SCHOLAR combustor model. Details of the code are given in the references [17, 20]. This version of the code solves the 3-D full Navier-Stokes equations and species continuity equations describing the production, convection, and mixing of chemical species. Calculations have been used in the design and refinement of the experiment. In the calculation the model was rotated from the orientation shown in Figure 3 such that the injector wall was aligned with the lower computational boundary.

Calculations were begun at the x = 0 station of the SCHOLAR model where vitiated air from the facility enters the duct. Vitiated air entered the model at Mach 2.0 yielding a velocity of 1395.7 m/s, a static temperature of 1184 K, and a static pressure of 100405 Pa. The calculated equilibrium mole fractions of the species present in the vitiated air, determined by a quasi-one-dimensional nozzle code, are given in Table 1.

The initial channel cross-section is 38.6 mm high and 87.9 mm wide. The hydrogen fuel injector introduces

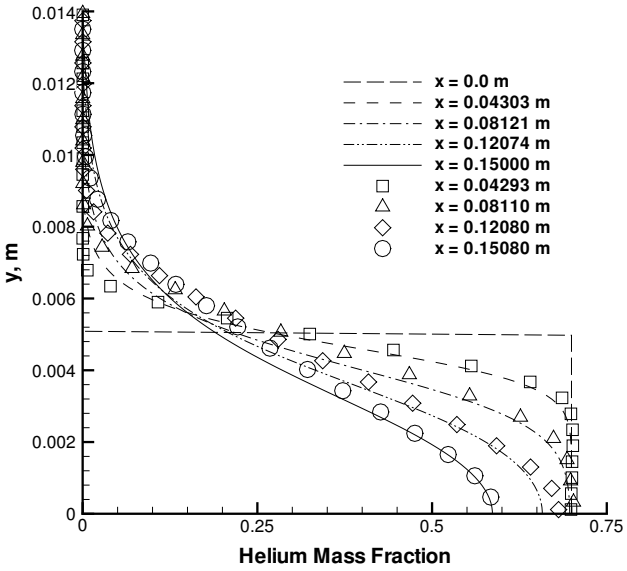

Figure 7: Comparison of helium mass fraction data with simulation results

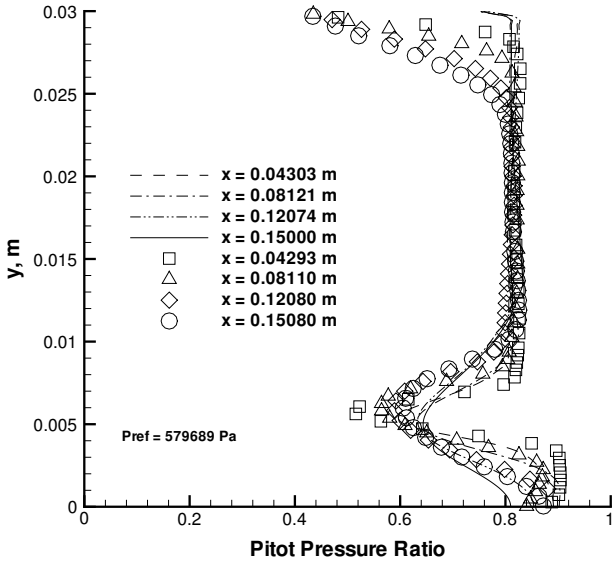

Figure 8: Comparison of pitot pressure data with simulation results

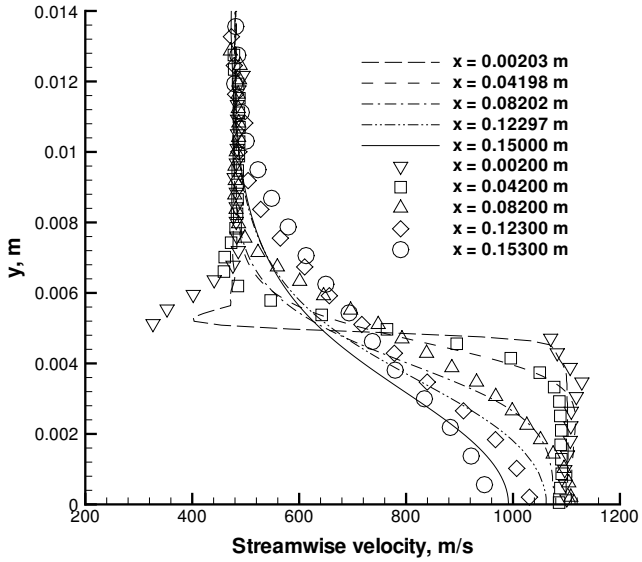

Figure 9: Comparison of RELIEF velocity data with simulation results

Species	Mole Fraction	Species	Mole Fraction
H	6.00000×10^{-08}	O	4.00000×10^{-06}
OH	2.43910×10^{-04}	O_2	1.86499×10^{-01}
HO_2	9.80000×10^{-07}	CO	1.00873×10^{-11}
H_2	2.86000×10^{-06}	CO_2	2.24589×10^{-04}
H_2O	2.92619×10^{-01}	Ar	6.32850×10^{-03}
H_2O_2	2.98644×10^{-09}	HCO	1.26462×10^{-24}
HNO	3.80338×10^{-12}	H_2CO	9.04513×10^{-26}
N	3.70036×10^{-18}	CH_3	4.27856×10^{-40}
N_2	5.12668×10^{-01}	CH_4	9.20779×10^{-39}
NO	1.62088×10^{-03}	C_2H_2	0.0
NO_2	1.19100×10^{-05}	C_2H_4	0.0

Table 1: Vitiate mole fraction at test condition

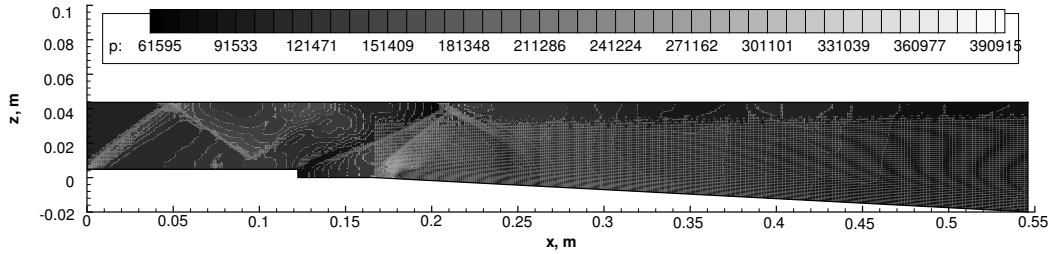

Figure 10: Static pressure contours along streamwise plane

hydrogen through a choked nozzle at Mach 2.5, a static temperature of 134.2 K, and a static pressure of 201300 Pa. The pilot fuel injectors described earlier were activated to improve flameholding under the present test conditions. The pilot injectors are assumed to be choked at the wall surface, resulting in a static temperature and pressure of 251.7 K and 722535 Pa, respectively. No slip conditions were specified along the upper, lower, and near- and far-side channel walls. First order extrapolation was used at the supersonic outflow station located at the 546 mm station for this calculation. This domain was discretized with a grid of 401 points in the streamwise direction, 61 points in the cross-stream direction, and 121 points in the spanwise direction. The grid was compressed near the solid walls and the fuel injector. Turbulence was modeled in the near wall region using the Bauldwin-Lomax model, and in the interior field using the turbulent jet mixing model [18, 19]. Chemistry was modeled using the 9 species, 18 reaction model described in reference [17]. This model provides a detailed description of hydrogen-air chemistry, but does not consider the effects of the small quantities of oxides of nitrogen and hydrocarbon species present in the vitiated air.

The results of flowfield simulations of the SCHOLAR combustor model are shown in Figures 10-16. Figure 10 shows static pressure contours along the streamwise plane centered on the fuel jet. Traversing the combustor from inflow to outflow, a weak bow shock produced by the pilot injectors can be seen. This pressure rise is communicated through the wall boundary layer resulting in a weak shock at the inflow to the combustor. This is followed by the expansion of the flow over the lower wall step. Just downstream, the flow is compressed through a recompression shock followed by a strong bow shock lying ahead of the primary fuel injector. Both the fuel jet and its surrounding air flow then expand beyond the fuel injector. The reflection of the bow shock interacts with the low density hydrogen fuel jet altering the shock angle. Figure 11 shows the static temperature contours along the same streamwise plane. The temperature rise associated with combustion of the pilot fuel near the primary fuel injector, and combustion of the shear layer of the primary injector plume can also be seen. Figure 12 shows the resulting Mach number contours along

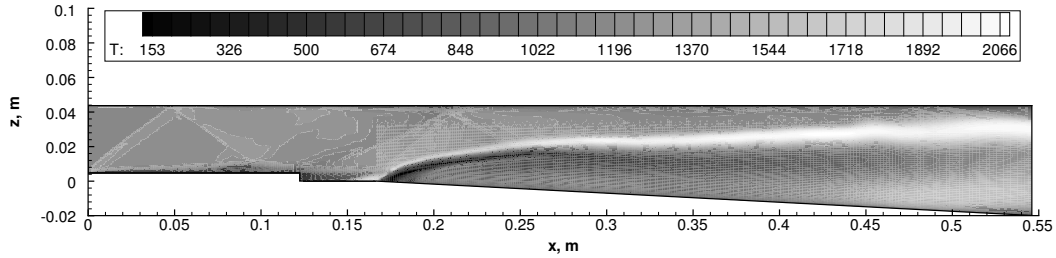

Figure 11: Static temperature contours along streamwise plane

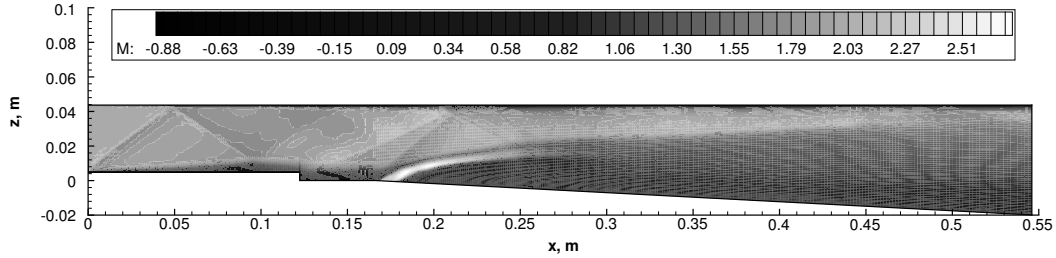

Figure 12: Mach number contours along streamwise plane

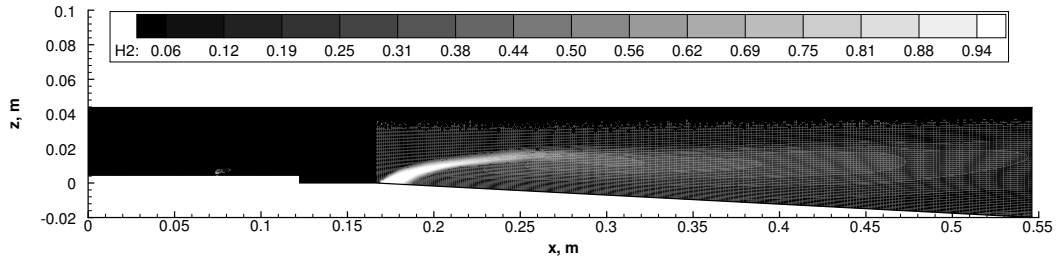

Figure 13: Hydrogen mass fraction contours along streamwise plane

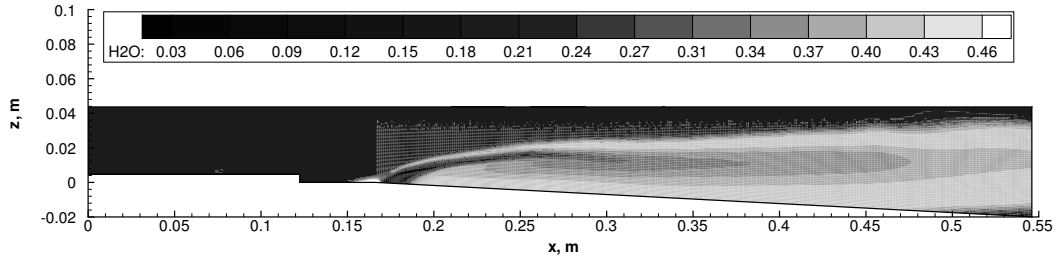

Figure 14: Water mass fraction contours along streamwise plane

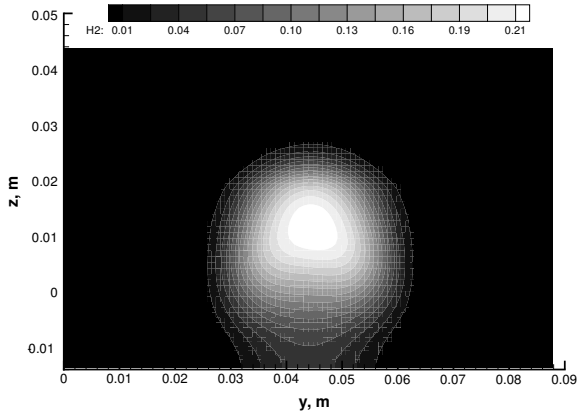

Figure 15: Hydrogen mass fraction at downstream station (0.427 m)

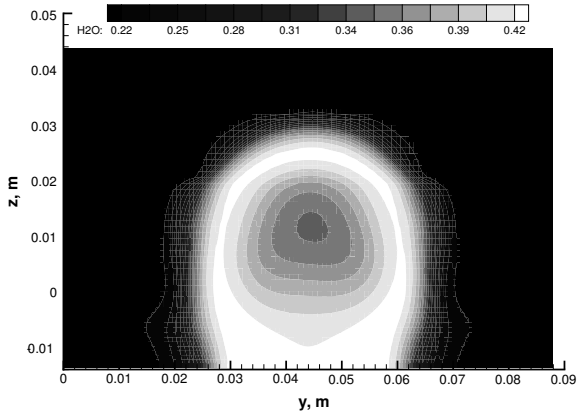

Figure 16: Water mass fraction at downstream station (0.427 m)

the streamwise plane. In addition to the above features, the wall boundary layers can be seen along with regions of recirculation located behind the lower wall step and where the bow shock interacts with the upper wall boundary layer. The plume of the fuel jet can also be seen. Figure 13 also displays the jet in terms of mass fraction contours of hydrogen along the streamwise plane. Figure 14 shows contours of the water mass fraction produced as a result of chemical reaction of the hydrogen fuel and air. The contours range from a minimum mass fraction of zero in the hydrogen jet core to a maximum mass fraction of 0.46 including the water introduced in the air from facility vitiation.

Figures 15 and 16 show contours of hydrogen and water mass fraction, respectively, in a cross-plane at the 0.427 m station bounded by the channel walls. Values of the hydrogen mass fraction range from zero to 0.23 with the highest concentrations existing only in the immediate jet core. Significant amounts of hydrogen have been mixed with facility air and consumed downstream by reaction. Values of the water contours again range from a minimum mass fraction of 0.203 (from vitiation) to a maximum mass fraction of 0.44. Vortices that form as the facility air interacts with the fuel jet lift and spread the jet enhancing fuel-air mixing and reaction. The vortices also convect fluid toward the lower wall and into the remaining fuel jet.

Comparisons of the measured and computed static temperatures at three stations in the copper section of the SCHOLAR model are given in Figures 17 through 19. These stations correspond to stations 1, 3, and 5 in Figure 3a. Measurements were not made for the piloted runs at stations 6 and 7 in the steel section of the SCHOLAR model. Figure 17 shows results at the step in the model wall. The computed results show a rise in temperature ranging from 400K on the walls to 1299K where the pilot fuel is mixing with the facility air and heating, but not undergoing combustion. The measured data ranges from 850K to 1200K in the flow with the fuel and air mixing but not reacting. The asymmetry of the data may simply be attributed to the coarseness of the grid used in surveying the flow relative to the scale of the flow features combined with the slightly asymmetrical location of the grid with respect to the flow. There is no suggestion that the flow itself is not symmetrical. At the 0.274 m station shown in Figure 18, the data now indicate combustion of the pilot fuel whereas the computation shows combustion of the pilot fuel and initial combustion of the primary injector fuel. The computation and the data indicate a maximum temperature of around 2030K and 2300K, respectively. A “cold” core of hydrogen still persists in both the data and the calculation. Figure 19 shows results at the 0.427 m station. Further combustion of the primary injector fuel in the mixing layer between the hydrogen and the facility air is indicated in the calculation. The data indicates increased combustion and temperature rise of the pilot fuel and on the lower surface of the primary injector hydrogen-air mixing layer. No combustion of the fuel is seen in the data along the upper surface of the primary fuel jet at this location.

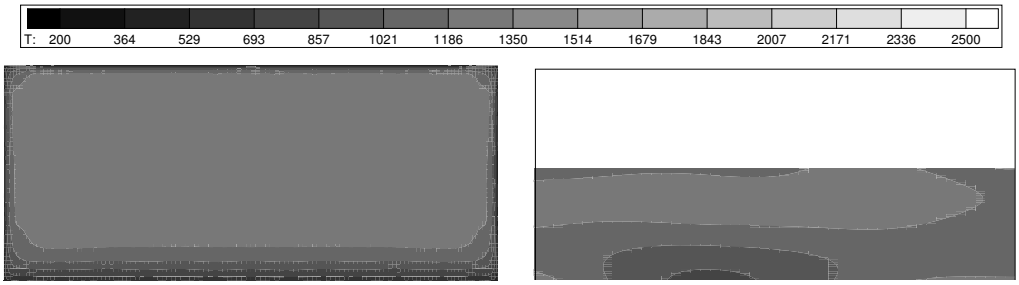

Figure 17: Comparison of computed static temperature (left) with data at 0.122 m station

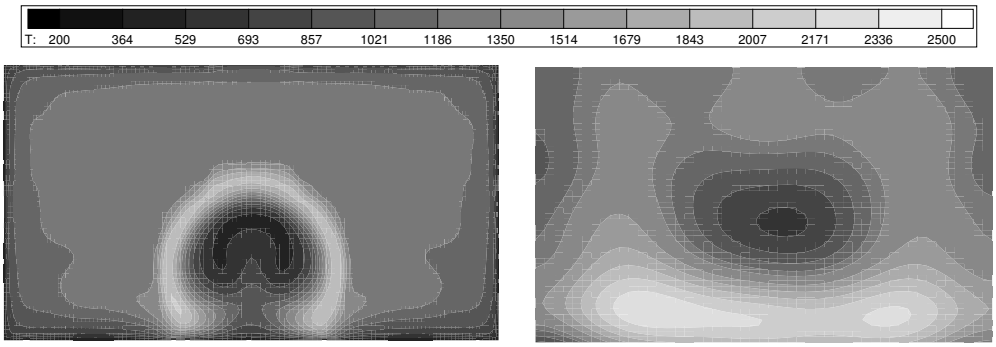

Figure 18: Comparison of computed static temperature (left) with data at 0.274 m station

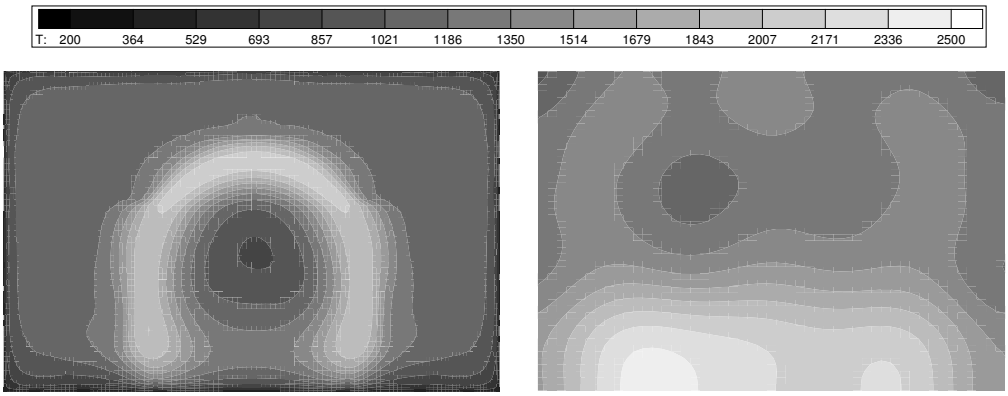

Figure 19: Comparison of computed static temperature (left) with data at 0.427 m station

6.7 Concluding Remarks

Activities in the area of scramjet fuel-air mixing and combustion associated with the Research and Technology Organization Working Group on Technologies for Propelled Hypersonic Flight have been described. Work discussed in this chapter has centered on the design of two basic experiments for studying the mixing and combustion of fuel and air in a scramjet. Simulations were conducted to aid in the design of these experiments. The experimental models were then constructed, and data were collected in the laboratory.

Comparison of the data from the non-reacting coaxial jet mixing experiment with one combustor code were then made and described. The comparisons of the helium mass fraction and pitot pressure data with the simulation were good, although there were some observed differences in the measured and computed pitot pressure in the jet mixing region.

The SCHOLAR combustor experiment flowpath was then analyzed and comparisons were made with CARS temperature data. Computed results indicate that the five pilot injectors ignite just ahead of the primary fuel injector and aid in ignition downstream of the injector. Combustion then occurs at later stations in the hydrogen-air mixing layer around the primary fuel jet. The CARS temperature data also indicates that combustion of the pilot fuel is delayed beyond the step, but occurs further downstream. Near the end of the copper section of the SCHOLAR model, increased temperature due to combustion is noted in both the computation and the data. The highest temperatures in the data (2400K) lie near the lower wall. The highest computed temperatures (2100K) lie around the upper region of the remaining fuel core at this station. Overall, the computation exhibits more significant combustion of the primary fuel jet relative to the degree of combustion indicated by the CARS temperature data.

It is hoped that combustion codes currently employed in scramjet design will be used to simulate both experiments and to compare results with the experimental data. Further discussion of the experiments is given in Chapter 7. Data from the coaxial jet experiment and the SCHOLAR experiment have been made available on the web for the use of other researchers. Shared experiences from the simulations should be very useful in improving the capabilities of each of the codes and the models that these codes employ.

References

[1] Dimotakis, P. E., Turbulent Free Shear Layer Mixing and Combustion. High Speed Flight Propulsion Systems, Chapter 7, Progress in Astronautics and Aeronautics, Vol. 137, 1991.

[2] Drummond, J. P., Carpenter, M. H., and Riggins, D. W., Mixing and Mixing Enhancement in High Speed Reacting Flows. High Speed Flight Propulsion Systems, Chapter 7, Progress in Astronautics and Aeronautics, Vol. 137, 1991.

[3] Givi, P., and Riley, J. J., Some Current Issues in the Analysis of Reacting Shear Layers: Computational Challenges. Major Research Topics in Combustion, Editors: M. Y. Hussaini, A. Kumar and R. G. Voigt, pp. 588-650, Springer-Verlag, New York, NY, 1992.

[4] Drummond, J. P., and Givi, P., Suppression and Enhancement of Mixing in High-Speed Reacting Flow Fields. Combustion in High-Speed Flows, pp. 191- 229, Editors: J. Buckmaster, T. L. Jackson and A. Kumar, Kluwer Academic Publishers, Boston, MA, 1994.

[5] Goebel, S. G., and Dutton, J. C., Velocity Measurements of Compressible, Turbulent Mixing Layers. AIAA Paper 90-0709, January 1990.

[6] Hall, J. L., Dimotakis, P. E., and Rosemann, H., Experiments in Non-reacting Compressible Shear Layers. AIAA Paper 91-0629, January 1991.

[7] Sullins, G. A., Gilreath, H. E., Mattes, L. A., King, P. S., and Schetz, J. A., Instabilities in Confined Supersonic Mixing Layers. Tenth Int. Symposium on Air Breathing Engines, ISABE 91-7096, 1991.

[8] Samimy, M., Zaman, K. B. M .Q., and Reeder, M. F., Effect of Tabs on the Flow and Noise Field of an Axisymmetric Jet. AIAA Journal, Vol. 31, No. 4, pp. 609-619, 1993.

[9] Cox, S. K., Fuller, R. P., Schetz, J. A., and Walters, R. W., Vortical Interactions Generated by an Injector Array to Enhance Mixing in Supersonic Flow. AIAA Paper 94-0708, January 1994.

[10] Seiner, J. M., Dash, S. M., and Kenzakowski, D. C., Historical Survey on Enhanced Mixing in Scramjet Engines. AIAA Paper 99-4869, August 1999.

[11] Bogdanoff, D. W., Advanced Injection and Mixing Techniques for Scramjet Combustors. AIAA Journal of Propulsion and Power, Vol. 10, No. 2, pp. 183-190, 1994.

[12] Cutler, A. D., Harding, G. C., and Diskin, G. S., High Frequency Supersonic Pulsed Injection. AIAA Paper 2001-0517, January 2001.

[13] Schetz, J. A., Cox-Stouffer, S. K., and Fuller, R. P., Integrated CFD and Experimental Studies of Complex Injectors in Supersonic Flows. AIAA Paper 98-2780, June 1998.

[14] Cutler, A. D., Carty, A., Doerner, S., Diskin, G., and Drummond, J. P., Supersonic Coaxial Jet Flow Experiment for CFD Code Validation. AIAA Paper 99-3588, June 1999.

[15] Cutler, A. D., and White, J. A., An Experimental and CFD Study of a Supersonic Coaxial Jet. AIAA Paper 2001-0143, January 2001.

[16] Cutler, A., Danehy, P. M., Springer, R. R., and DeLoach, D. P., CARS Thermometry in a Supersonic Combustor for CFD Code Validation. AIAA Paper 2002-0743, January 2002.

[17] Drummond, J. P., Numerical Simulation of a Supersonic Chemically Reacting Mixing Layer. NASA TM 4055, 1988.

[18] Eggers, J. M., Turbulent Mixing of Coaxial Compressible Hydrogen-Air Jets. NASA TN D-6487, 1971.

[19] Eklund, D. R., et al., Computational/ Experimental Investigation of Staged Injection into a Mach 2 Flow. AIAA Journal, Vol. 32, No. 5, pp. 907-916, 1994.

[20] Carpenter, M. H., Three-Dimensional Computations of Cross-Flow Injection and Combustion in a Supersonic Flow. AIAA Paper 89-1870, June 1989.

CHAPTER 7: FUNDAMENTAL MIXING AND COMBUSTION EXPERIMENTS FOR PROPELLED HYPERSONIC FLIGHT

D. Cutler, G. S. Diskin†, P. M. Danehy‡, J. P. Drummond
Andrew D. Cutler
The George Washington University
Joint Institute for Advancement of Flight Sciences, Hampton, Virginia
a.d.cutler@larc.nasa.gov
J. P. Drummond
NASA Langley Research Center, Hampton, VA 23681
j.p.drummond@larc.nasa.gov

7.1 ABSTRACT

Two experiments have been conducted to acquire data for the validation of computational fluid dynamics (CFD) codes used in the design of supersonic combustors. The first experiment is a study of a supersonic coaxial jet into stagnant air in which the center jet is of a light gas, the coflow jet is of air, and the mixing layer between them is compressible. The jet flow field is characterized using schlieren imaging, surveys with Pitot, total temperature and gas sampling probes, and RELIEF velocimetry. VULCAN, a structured grid CFD code, is used to solve for the nozzle and jet flow. The second experiment is a study of a supersonic combustor consisting of a diverging duct with single downstream-angled wall injector. Nominal entrance Mach number is 2 and enthalpy is nominally that of Mach 7 flight. The primary measurement technique is coherent anti-Stokes Raman spectroscopy (CARS), although surface pressures and temperatures have also been acquired. Modern-design-of-experiment techniques have been used to maximize the quality of the data set.

7.2 NOMENCLATURE

k_s	Thermal conductivity of wall (W/mK)
n_s	Number of samples
n_p	Number of parameters
p_{amb}	Ambient pressure
p_{exit}	Nozzle exit pressure
$p_{ref,CJ}$	Center-jet nozzle reference pressure
$p_{ref,coflow}$	Coflow nozzle reference pressure
Pr_t	Turbulent Prandtl number
q	Heat flux (W/m^2)
Sc_t	Turbulent Schmidt number
t	Time (s)
T	Temperature (K)
T_{amb}	Ambient temperature
$T_{t,CJ}$	Center-jet nozzle total temperature
$T_{t,coflow}$	Coflow nozzle total temperature
u	Velocity
x, y, z	Position coordinates
α_s	Thermal diffusivity of wall (m^2/s)
χ	Mole fraction center-jet gas
σ	Standard deviation

7.3 INTRODUCTION

Computational fluid dynamics (CFD) codes are extensively employed in the design of high-speed air breathing engines. CFD analysis based on the Reynolds averaged Navier-Stokes equations uses models for the turbulent fluxes that employ many ad hoc assumptions and empirically determined coefficients. Typically, these

models cannot be applied with confidence to a class of flow for which they have not been validated. Two studies have been conducted to provide data suitable for code development and testing.

The first experiment (Ref. 1,2,3) is a study of a coaxial jet discharging into stagnant laboratory air, with center jet of a mixture of 5% oxygen and 95% helium by volume and coflow jet of air. The exit flow pressure of both center-jet and coflow nozzles is 1 atmosphere. The presence of oxygen in the center jet is to allow the use of an oxygen flow-tagging technique (Ref.1) to obtain non-intrusive velocity measurements. Both jets are nominally Mach 1.8, but, because of the greater speed of sound, the center jet velocity is more than twice that of the coflow

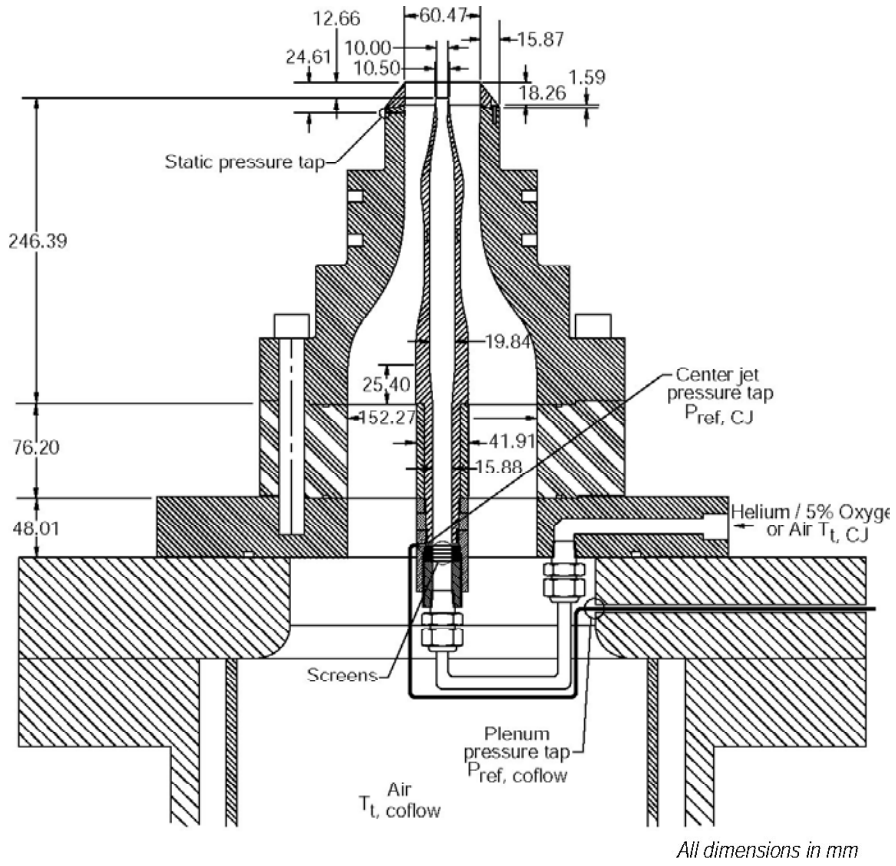

Figure 1 Coaxial jet flow facility

The mixing layer which forms between the center jet and the coflow near the nozzle exit is compressible, with a calculated convective Mach number Ref.2 of ~ 0.7.

This geometry has several advantages: The streamwise development of the flow is generally dominated by turbulent stresses (rather than pressure forces), and thus calculations are sensitive to turbulence modeling. It includes features present in supersonic combustors, including a compressible mixing layer near the nozzle exit and a light-gas/air plume downstream. Since it is a free jet, it provides easy access for both optical instrumentation and probes. Since it is axisymmetric, it requires fewer experimental measurements to fully characterize, and calculations can be performed with more modest computer resources. However, weak shock waves formed at the nozzle exit strengthen and turn normal as they approach the axis, complicating the flow. Care is thus taken in the design of the facility to provide as near as possible to 1-D flow at the exit of both center and coflow nozzles, and to minimize the strength of waves generated at the nozzle exit.Results from this

* Associate Professor, The George Washington University, MS 335.

† Research Scientist, Laser & Electro-optics Branch, MS 468.
‡ Research Scientist, Instrumentation Systems Development Branch, MS 236.
§ Senior Research Scientist, Hypersonic Airbreathing Propulsion Branch, MS 197.
Note: The inclusion of equipment brand names in this paper is for informational purposes only and should not be interpreted as an endorsement of these products by the authors, NASA or the US Government.

experiment are compared to CFD solutions obtained by VULCAN, a previously developed code used in engine analysis (Ref.3).The second experiment is a study of a supersonic combustor consisting of a diverging duct with single downstream-angled wall injector. Thus, the geometry is relatively simple and large regions of subsonic recirculating flow are avoided. Nominal entrance Mach number is 2 and the enthalpy of the test gas (hot air "simulant") is nominally that of Mach 7 flight. It was believed, on the basis of calculations performed (Ref.4) that this would produce mixing-limited flow, that is to say, one for which chemical reaction to equilibrium proceeds at a much greater rate than mixing. It later proved that this was not the case.

The primary experimental technique employed is coherent anti-Stokes Raman spectroscopy, known by its acronym CARS. An introduction to CARS is given by Eckbreth (Ref.5), and an application of CARS to supersonic combustors is given by Smith et al (Ref.5). The species probed is molecular nitrogen and the quantity measured is temperature. Intrusive probes, such as Pitot, total temperature, hot-wire, etc., are not used due to access difficulty and high heat flux in the combustor, and because they may alter the flow. CARS has several advantages over other optical methods. It is a relatively mature and well-understood technique. Signal levels are relatively high and the signal is in the form of a coherent (laser) beam that can be collected through small windows. Incoherent (non-CARS) interferences are rejected by spatial filtering.

Application of a complicated technique like CARS in high-speed engine environments is not routine. Since it is a pointwise (rather than planar) technique, building a "picture" of the internal temperature field of the combustor requires hundreds of facility runs, which is expensive. Thus, modern-design-of-experiments (MDOE) techniques are used to minimize the quantity of data required to meet the goals of this work and to minimize systematic errors associated with random errors. Details of the MDOE aspects are not discussed in this paper, but may be found in Ref. 7.

7.4 SUPERSONIC COAXIAL JET EXPERIMENT

7.4.1 FLOW FACILITY

The coaxial jet assembly is shown in Fig. 1. It is axisymmetric and consists of an outer body and a center body. The passages formed by the space between these bodies, and by the interior passage of the center body, are nozzles designed by the method of characteristics to produce 1-D flow at their exits. The nozzle assembly is joined to the Transverse Jet Facility, located in the laboratories of the Hypersonic
Airbreathing Propulsion Branch at NASA Langley Research Center. The plenum of this facility contains porous plates for acoustic dampening and screens for flow conditioning. Air is provided to the facility from a central air station, and the helium-oxygen mixture is provided to the center body from a bottle trailer containing premixed gas.

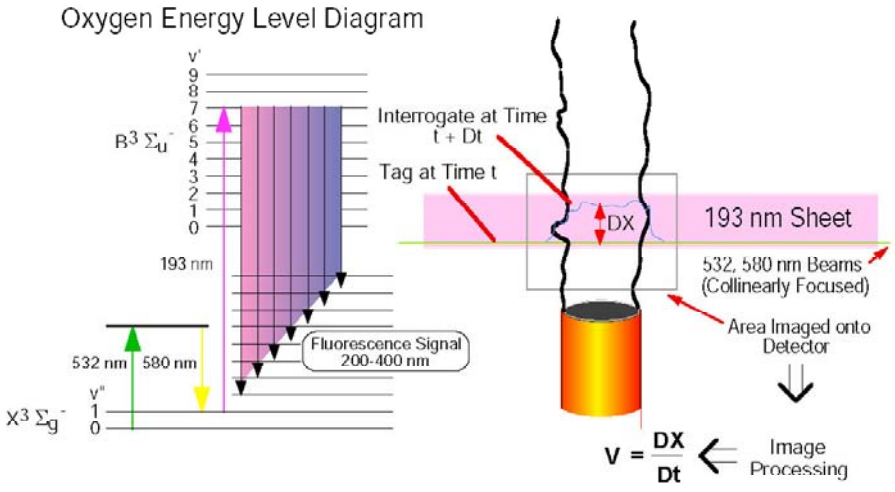

Figure 2 The RELIEF technique

The assembly is instrumented with pressure taps: one in the center body just downstream of the screens, one in the facility plenum, and one in the outer body near the exit of the coflow nozzle (in a region where the flow has reached its exit condition). Thermocouples are located in the gas supply lines. Ambient (barometric) pressure and ambient temperature are read. The values of these various quantities during the probe surveys, and their respective uncertainties (95% probability band) are given in Tab. 1.
Uncertainties are due to facility unsteadiness and variations in set point, and do not include 0.5% in pressures and 2 K in temperatures due to transducer error.

$p_{ref,coflow}$ (kPa)	580 ± 2
$T_{t,coflow}$ (K)	300 ± 6
$p_{ref,CJ}/p_{ref,coflow}$	1.060 ± 0.008
$T_{t,CJ}/T_{t,coflow}$	1.02 ± 0.05
$p_{amb}/p_{ref,coflow}$	0.1758 ± 0.0012
$T_{amb}/T_{t,coflow}$	0.982 ± 0.017
$p_{exit}/p_{ref,coflow}$	0.1748 ± 0.0005

Table 1 Experimental flow parameters

7.4.2 FLOW FIELD MEASUREMENTS

Various types of flow field measurement have been performed. The flow has been visualized with conventional schlieren and shadowgraph. Pitot, gas sampling, and total temperature probes have been employed to survey the flow. Probe survey locations are listed in Tab. 2, and are also shown in Fig. 3(b). References 1 and 2 give details of these measurements.

Survey probe tips are cylindrical and cut square, with outside/inside diameters respectively of the Pitot probe 0.64 mm/0.36 mm, and of both the gas sampling probe and total temperature probe 1.27 mm/0.76 mm. The gas sampling probe and tubing internal diameters are sized to avoid choking the sample gas flow, ensuring shock attachment at the probe tip.

The total temperature probe is a miniature shrouded, vented thermocouple. The probe incorporates a commercial microminiature thermocouple junction at the tip of a 0.20 mm diameter “needle”. Errors in Pitot pressure due to pressure transducer error are 0.5%. Error in total temperature due to thermocouple error is 2 K. In addition, the total temperature probe is found to read about 1% low, due to incomplete stagnation of the flow at the sensor and/or radiation losses.

Number	*x, mm*	*x, mm RELIEF*
1	*0.13*	*2*
2	*3.1*	*5*
3	*10.0*	*12*
4	*17.9*	*17*
5	*27.8*	*27*
6	*42.9*	*42*
7	*61.9*	*62*
8	*81.1*	*82*
9	*100.6*	*102*
10	*121.4*	*123*
11	*150.8*	*153*
12	*181.0*	*190*
13	*220.4*	*220*
14	*261.0*	*258*

Table 2 Experimental survey locations

The mole fraction of the center-jet gas (i.e., the helium-oxygen mixture) in the gas withdrawn from the flow, χ, is found in real time by a hot-film probe based system (Ref.6). The largest contribution to the uncertainty of the system is the manufacturer-quoted ∀1% of full scale in the mass flow controller used to provide a known helium-oxygen/air mixture to calibrate the system. Maximum uncertainty in mole fraction of helium-oxygen is in the range ∀1-1.5%, but uncertainty is less than this near mole fractions 0.0 or 1.0 where there is no uncertainty in the composition of the calibration mixture.

The probes were mounted in a diamond-airfoil strut, and translated in the flow by a two-component stepping-motor driven translation stage. Probe "zero" location was determined using machined fixtures mounted to the nozzle exit (conical extension cap removed). Surveys were conducted across a diameter of the flow.
Analysis of the data to find the best-fit center showed it to be within 0.4 mm (95% of the time) of the measured center. Thus, probe surveys are taken to pass through the axis of the jet ±0.4 mm. Survey data presented have been shifted (by less than ±0.4 mm) so that the best fit center lies at y = 0. Resulting data are found to be almost perfectly symmetrical.

In addition to these "conventional" techniques, the RELIEF[4] (Raman Excitation plus Laser-Induced Electronic Fluorescence) oxygen flow tagging technique, illustrated in Fig. 2, has been used to provide measurements of (instantaneous) axial component velocity. RELIEF is a time-of-flight technique which involves two steps. In the first (Atag≅) step, oxygen in a line segment of the flow is excited to a non-equilibrium vibrational state by stimulated Raman scattering. This is achieved by focusing (50 cm focal length) collinear laser beams at 532nm and 580 nm. These beams are generated by passing a 200 mJ doubled Nd:YAG laser beam (532 nm) through a 6.9 MPa Raman cell containing a 50:50 mixture of helium and oxygen. The Raman cell is seeded with light from a broadband dye laser pumped by doubled residual infrared light from the Nd:YAG laser. The non-equilibrium oxygen returns to equilibrium only slowly as it convects with the flow. In the second "probe" step of the technique, the non-equilibrium region is found by laser-induced fluorescence imaging. This is achieved with a 20 mJ narrow band (approximately 0.5 cm^{-1}) ArF excimer (193 nm) laser beam cylindrically focused to a 10 mm high H 0.5 mm thick sheet in the region where the tagged flow is expected to be. The resulting fluorescence is imaged using a double intensified video-rate CCD camera, with f/4.5 UV lens and extension rings for closeup operation. Data were acquired at 5 Hz.

The resulting data consist of images of displaced line pairs, acquired either at different delay times after the tag, or with one of the lines acquired prior to operation of the jet (i.e., with zero flow velocity). The instantaneous velocity is determined by finding, in subsequent data reduction, the line displacement at various points along it, and dividing by the probe delay time. A calibration is required to establish the relationship between position in the image and position in space. Mean *u*-component velocity and root mean square fluctuation have been obtained by this technique. Uncertainties in this data are approximately ∀3% due to uncertainty in the magnification factor between flowfield and image and uncertainty in the zero point.

7.4.2.1 CALCULATION

The Favre-averaged Navier-Stokes equations are solved using VULCAN, a structured, finite-volume CFD code.
The calculation assumes an axisymmetric flow of a mixture of thermally perfect gases. The calculation was performed on a structured grid generated by a separate, commercial code. There are a total of 188,080 cells, distributed among five blocks. Grid points are clustered near the walls of the nozzles to resolve the boundary layers, at the exit of the center-jet nozzle to resolve the recirculation zone and shocks in the vicinity of the nozzle lip, and to a lesser degree near the axis to resolve shock reflections. The distance from the wall of the centers of the closest cells is less than $y^+ = 1.5$ for all surfaces.

The walls are specified to be adiabatic, and wall velocities are specified to be no slip. Total pressure and temperature conditions are specified at subsonic inflow/outflow planes, while the code switches to extrapolation where the code detects that outflow is supersonic. The flow is assumed to be axisymmetric. At the exterior boundary the composition is air with density of 1.177 kg/m^3 and pressure (p_{amb}) 101.3 kPa. At the coflow nozzle inflow boundary the composition is air with total density 6.735 kg/m^3 and total pressure ($p_{ref,coflow}$) 580.0 kPa. At the center-jet nozzle inflow boundary the composition is 0.7039 by mass He and 0.2961 by mass O_2 with total density 1.3343 kg/m^3 and total pressure 628.3 kPa (computed from $p_{ref,CJ}$ and the area ratio between the reference plane and sonic throat, assuming quasi-1-D flow).

The flow is assumed to be turbulent, and Wilcox=s $\tilde{k}-\tilde{\omega}$ turbulence model is used with the high Reynolds number model (Ref.6). The compressibility correction proposed by Wilcox was not used, but Wilcox's generalization of Pope's modification to the $\tilde{k}-\tilde{\varepsilon}$ model (which attempts to resolve the "round jet/ plane jet

anomaly") was. Turbulent Prandtl number and Schmidt number were set equal to 0.75. More details of the calculation may be found in Ref. 3.

7.4.2.2 RESULTS

Figure 3(a) is a typical schlieren image (with knife edge vertical) showing the jet with coflow nozzle conical extension ring removed. Vertical dark and bright bands are due to transverse gradients of refractive index. Notice the shock-expansion wave structure emanating outward from the (0.25 mm thick) center-body lip. Similar waves propagate in the center jet, but are not visible in the schlieren due to the low refractive index there. The continuation of these initially inward propagating waves, after they have crossed at the axis and passed out of the center jet into the coflow air, is visible. Figure 3(b) is a flooded contour plot of Mach number from the CFD calculation. Although the contour levels are not labeled, the results may be qualitatively compared to the schlieren.

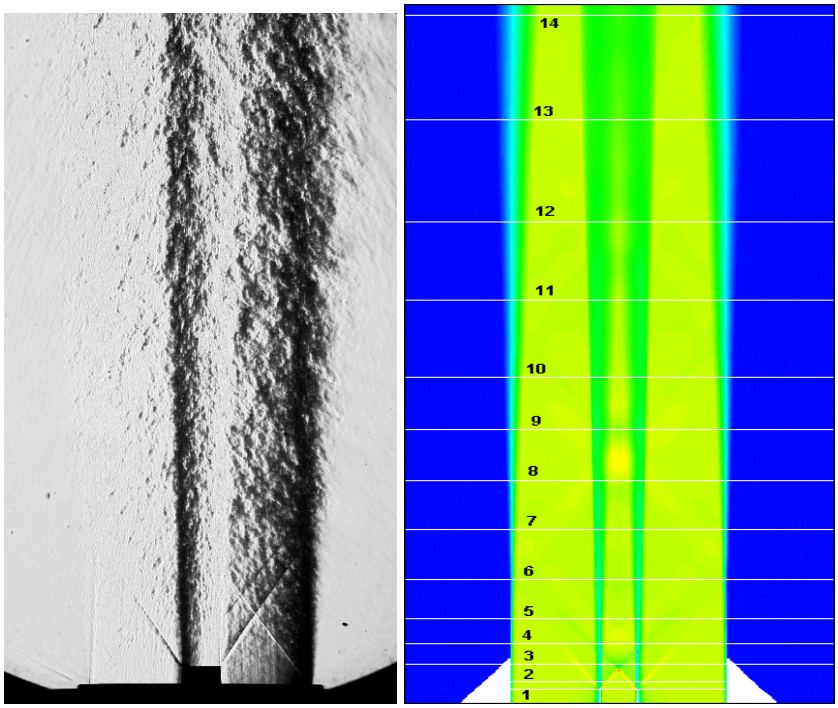

Figure 3: (a) (left) Schlieren image with vertical knife edge (conical extension cap removed) and (b) (right) computed Mach number distribution with data survey lines.

The mole fraction center jet gas data is shown in Fig. 4. The centerjet spreads smoothly, with the peak χ falling below 1.0 downstream of Plane 11. The experimental values are well reproduced by the calculation near the axis, but, moving away from the axis, the calculation is first high and then, near $\chi = 0$, too low. The calculation is discontinuous in slope at $\chi = 0$ (a most unphysical behavior).

The mean velocity data is shown in Fig. 5. At Plane 1 there is a layer with velocity deficit at the boundary between the centerjet and the coflow that is several times the thickness of the nozzle lip. This layer results from the merging of the coflow nozzle inner surface boundary layer and the region of separation at the lip. The spikes in velocity near the edge of the centerjet are due to the shock waves emanating from the nozzle lip. Downstream of the nozzle exit the velocity data is consistent with theχ data, showing a similar spread of the centerjet, but the drop in peak velocity below the nozzle exit value begins significantly upstream, nearer Plane 7. Calculated velocity is high near the axis and low near the edge of the centerjet.

The Pitot pressure is shown in Fig. 6. At Plane 1, as with velocity, there is a layer with reduced Pitot pressure at the boundary between the centerjet and the coflow. Small axisymmetric irregularities in Pitot pressure in the centerjet (-0.005 m $< y <$ 0.005 m) may be attributed to machining flaws in the center-jet nozzle. In general, however, experiment and calculation agree very well, indicating that the calculation of the flow in the

nozzles was good. Downstream of Plane 1 the centerjet spreads, with Pitot pressure near the axis falling downstream of Plane 10 and rising in the wake of the nozzle lip. As with χ, erroneous discontinuities in slope may be observed in the calculation at the outer boundary of the centerjet and the inner boundary the outer (coflow-ambient) shear layer.

The waves seen radiating from the center-jet nozzle lip in the schlieren are found in the calculation, though are not fully resolved. A more detailed inspection shows that the wave from the center-jet nozzle forms a normal shock where it intersects the axis. This results in a small deficit in total pressure at the axis that is visible downstream of the shock in both CFD and experimental Pitot pressure (see Fig. 6). This deficit persists as far downstream as Plane 9 before being obscured by the mixing of the coflow into the center jet.

Figures 4 - 8 show comparisons between the results of the experiment and the results of the CFD calculations.

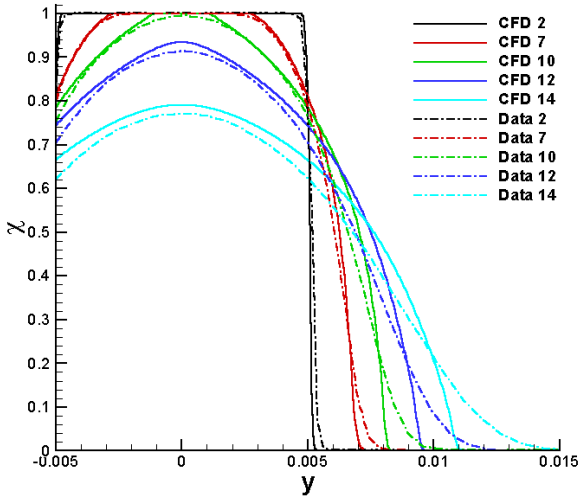

Figure 4: Mole fraction center-jet gas at several data planes.

The range of y in the plots does not correspond to the full range of the data or of the calculation, but is truncated to show more clearly the regions of interest. In these figures, y is given in m and u in m/s.

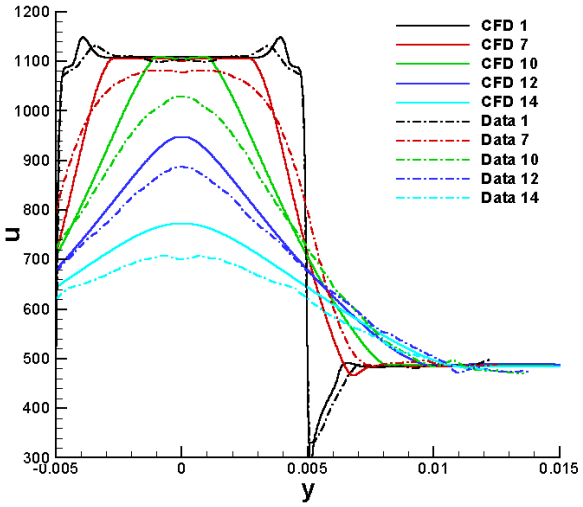

Figure 5: Mean velocity.

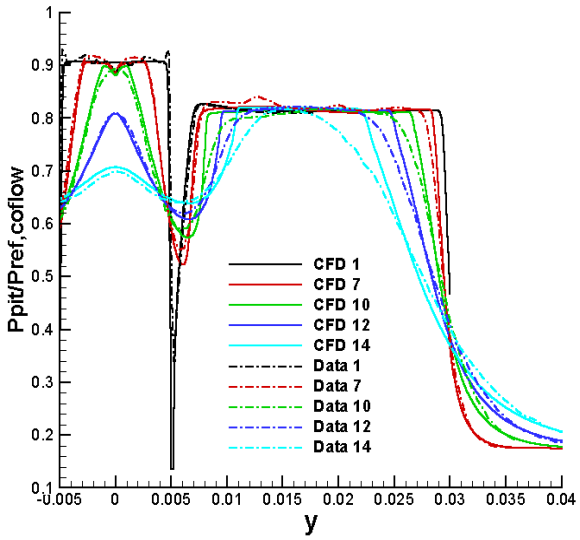

Figure 6: Pitot pressure.

Total temperature was acquired at Plane 9 only (Fig. 7). On the axis and in the coflow experimental data are about 1% below the known supply gas temperatures, due to probe error. Otherwise, the calculation agrees well with the experiment, reproducing both overshoot and undershoot.

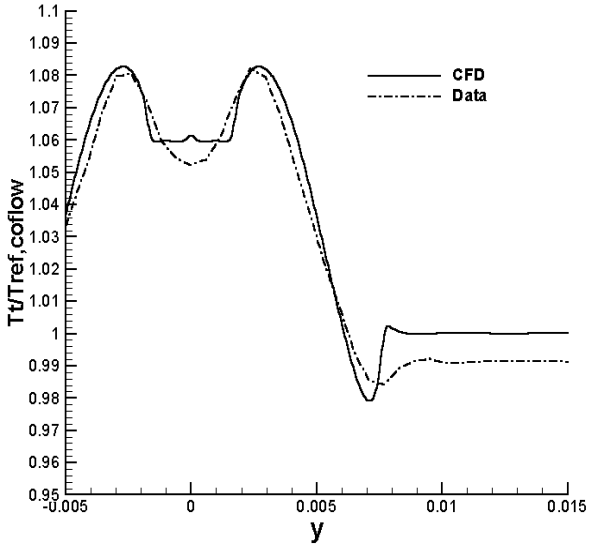

Figure 7: Total temperature at Plane 9.

7.5 SUPERSONIC COMBUSTOR EXPERIMENT

7.5.1 FLOW FACILITY

This experiment was conducted in NASA Langley's Direct-Connect Supersonic Combustion Test Facility (DCSCTF), (Ref.7). "Vitiated air" is produced at high pressure in the "heater", shown in Fig. 8.

Oxygen and air are premixed and hydrogen is burned in the mixture. Flow rates are selected so that the mass fraction of oxygen in the resulting products is the same as that of standard air. The test enthalpy is nominally that of Mach 7 flight. The vitiated air is accelerated through a water-cooled convergent-divergent nozzle and entering the test model. Gas flow rates to the heater are: 0.915±0.008 kg/s air, 0.0284±0.0006 kg/s hydrogen, and 0.300±0.005 kg/s oxygen. The heater stagnation pressure is 0.765±0.008 MPa. These uncertainties are due to the random run-to-run variations and do not include a ±3% uncertainty in the mass flow rate measurements.

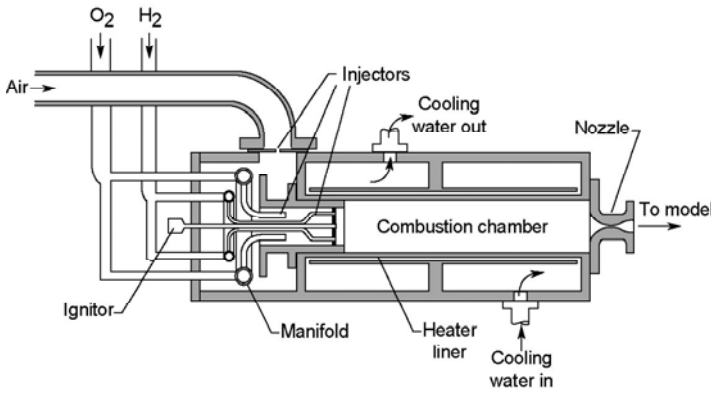

Figure 8: DCSCTF heater and nozzle

Heater and nozzle exit conditions are estimated from the flow rates, heater pressure, and nozzle minimum and exit areas using one-dimensional (1D) analysis (Ref.7). The flow exiting the heater into the nozzle is assumed to be in thermodynamic equilibrium, but has unknown enthalpy due to heat lost to the structure and cooling water. Enthalpy is found from the known mass flow rate, geometrical area of the nozzle (sonic) throat, assuming isentropic flow in the nozzle and 1-D flow at the throat. Nozzle exit conditions are computed similarly from the geometrical exit area. Calculations assuming equilibrium and frozen composition differ in minor species concentration, but not significantly in major species, temperature or pressure. The nominal calculated conditions, and uncertainties due to mass flow rate measurement error and run-to-run variations in heater conditions are: heater stagnation temperature 1827±75 K, exit temperature 1187±60 K, exit pressure 100±1.5 kPa, exit Mach number 1.989±0.005. Errors arising in the calculation due to the assumption of 1D flow (the effects of non-uniform composition, boundary layers, etc.) are not considered.

A study of the flow at the exit of the facility nozzle was conducted previously (Ref. 8). A Pitot probe rake was employed to map the exit Pitot pressure and additionally the flowfield at the exit of the nozzle was visualized. Silane (SiH4) was added to the heater hydrogen and burned to form silica particles in the heater. The particles were illuminated by a pulsed laser-sheet and imaged with a CCD camera. Results were compared to CFD calculations of the nozzle flow. The flow at the nozzle exit was not completely 1D, but the computed Pitot pressure distribution agreed well with measurement. The flow appeared well mixed.

The test model is shown in Fig. 9. There are two main sections: the copper upstream section and the carbon steel downstream section.

Stainless steel flanges and carbon gaskets separate these sections from each other and the nozzle. The internal passage, from left to right, has a constant area segment, a small outward step at the top wall, a second short constant area segment followed by a constant 3° divergence of the top wall. The span is constant at 87.88 mm. Five small pilot fuel injector holes are located ahead of the step, and the main fuel injector is located just downstream of the start of the 3° divergence. The injection angle is 30° to the opposite wall. The injector nozzle is designed by the method of characteristics to produce Mach 2.5, 1D flow at the injector exit. Hydrogen injection is provided at a pressure of 2.12±0.07 MPa, temperature of 302±4 K, and equivalence ratio of

0.99±0.04. On some runs, additional hydrogen injection is provided by the 5 pilot injectors at the same nominal temperature and a total equivalence ratio of 0.148 ±0.008. The pilots are turned on and off at the same time as the main fuel injector.

The duct is uncooled; however, the wall thickness of the copper duct is greater than 32 mm and the carbon steel duct is 19 mm. Thus, fueled run times in excess of 20 s (and unfueled much greater) are possible. With atmospheric temperature air flowing in the model between runs, runs could be repeated every 10 - 15 minutes.

The model is equipped with 7 slots to allow the CARS beams to penetrate the duct, of which slots 1, 3, 5, 6, 7, depicted in Fig. 9(a), are used in this study. The slots are in pairs, one on each side of the duct, 4.8 mm wide, extending the full height of the duct. When not in use the slots are plugged flush to the wall. Windows covering the slots are mounted at the end of short rectangular tubes. The model is instrumented with both pressure taps and wall temperature probes. More details of this instrumentation may be found in Ref. 7.

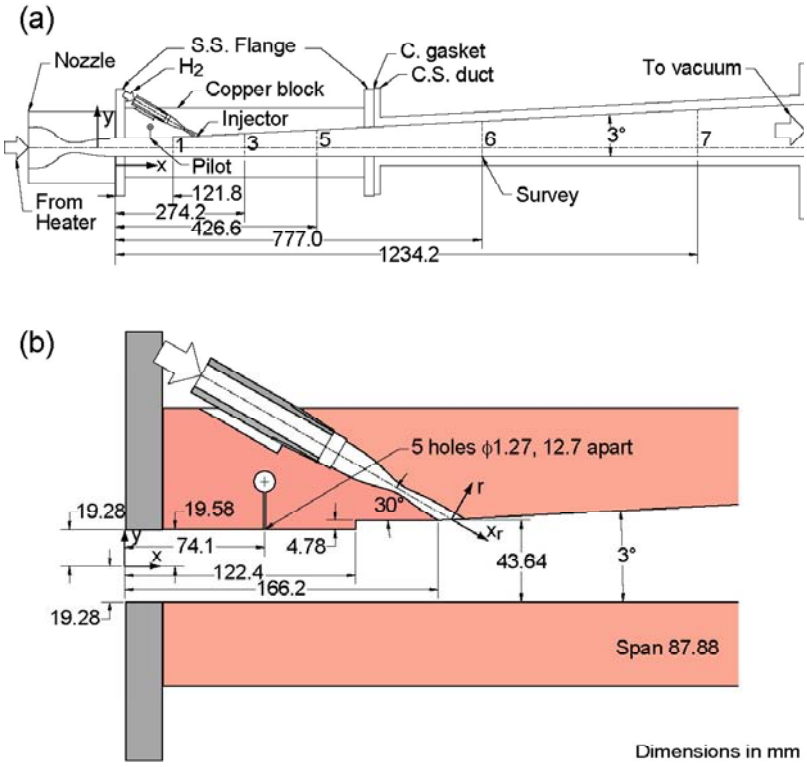

Figure 9: Test model: (a) nozzle, copper and carbon steel (C.S.) duct sections, (b) detail in vicinity of fuel injector and pilots.

7.5.1.1 CARS TECHNIQUE

The CARS system uses an unseeded Spectra-Physics DCR-4 pulsed Nd:YAG laser, frequency doubled to 532 nm. The nominal power at 532 nm is 550 mJ per pulse and repetition rate is 10 Hz. A broadband dye laser utilizing two longitudinally pumped Brewster's angle pumped dye cells is employed in the system. Dye laser wavelength is centered between 605 nm and 606 nm to match the Raman shift of nitrogen by adjusting the dye concentration. The dye laser and two 532 nm beams are combined at a dichroic mirror and relayed via a periscope to a spherical lens. The three beams are crossed at their focal points in a vertical planar BOXCARS configuration[3].

At the focus, the diameters of the 532 nm and dye beams are respectively ~ 0.12 mm and ~ 0.15 mm. The length of the measurement volume is found by translating the CARS measurement volume through a thin planar jet of nitrogen surrounded by a coflowing jet of helium. The length over which CARS signal is recorded

is ~ 4.5 mm and the full width half maximum (FWHM) of the signal distribution is ~ 2.25 mm. The beam energy levels per pulse obtained at the focusing lens are ~85 mJ for each green, and from 12 mJ to 24 mJ for the dye.

The beams (including the CARS signal beam) are relayed via a second spherical (collimating) lens and a second periscope back to the optical bench. The CARS beam is separated, directed through additional filters as needed and a polarizer that allows only horizontally polarized light to pass, then focused to the entrance of a 1 m monochrometer with 1200 groove/mm grating. An EG&G PAR model 1420 intensified, linear, self-scanned silicon photodiode array detector (IPDA) is mounted at the exit plane of the detector. The detector consists of 1024 elements of which the central 598 elements are used. An optical splitter (Ref.8) creates a secondary signal on the detector, identical to the primary but offset by 290 pixels and 6.1% the intensity. When the intensity of the primary signal exceeds the dynamic range of the detector, the secondary signal is used for analysis.

The two top prisms of the periscope are mounted on stepping motor driven vertical translation stages. The two bottom prisms and the vertical translation stages are mounted on similar horizontal stages. By translating the vertical and/or horizontal stages in tandem the measurement volume could be moved in the y and/or z direction. CARS data acquisition is under the control of a personal computer (PC). Two types of acquisition are employed. In the first, data is acquired at a single point in space. In the second, data is acquired while either the vertical or the horizontal stages are in constant velocity motion.

CARS data are acquired in the supersonic combustor during multiple sets of test runs. During a set of runs (which might last as long as 5 hours), access to the model and optical system is prohibited for safety reasons. Test runs consisted of approximately 5 s during which the heater is operating but no fuel is injected in the model, followed by from 11 s to 20 s during which fuel is injected. CARS data is acquired over a period 2 s shorter than the period of fuel injection. Immediately after a run, 10 s of data is acquired with the system operating as before, the dye laser beam blocked by a remotely operated beam block. These “background” scans measure non-CARS interferences such as scattered laser light.

CARS data are analyzed on a separate workstation. Prescans are subtracted from data scans. Background scans (after subtraction of prescans) are averaged and subtracted from data scans. Both primary and secondary (produced by the splitter) CARS signals are contained within the data scan. If the primary is saturated, the secondary is selected for analysis. Data scans are divided, pixel by pixel, by the reference spectrum to remove the effect of the dye laser spectral power distribution, and normalized to unit area (primary or secondary). Data are compared to a library of similarly normalized theoretical spectra to determine the temperature and nitrogen concentration. The pixel location of the start of the theoretical spectra is allowed to allowed to vary for best fit. The combination of temperature, concentration, and pixel location that produces the least mean square deviation between theory and data is selected.

Theoretical CARS spectra are generated using the program CARSFT (Ref.9). The combustion gases are assumed to be a mixture of nitrogen and non-resonant buffer gas, both having non-resonant susceptibility of 8.5×10-18 cm3/erg. The static pressure is assumed to be 1 atmosphere, although, in reality, the pressure varied (see Fig. 10). The Exponential Gap Model for collisional narrowing of the Raman line shape is used. A 532 nm laser line width of 1 cm-1 is assumed. An experimentally determined instrument probe function is used. The peak of the reference CARS spectrum can shift significantly during a set of runs. Techniques developed to derive suitable reference spectra from the CARS data are described in Ref. 7.

The techniques used for acquisition and analysis of CARS data in the supersonic combustor were tested in a “Hencken” adiabatic, flat-flame burner burning hydrogen in air. Equivalence ratio (ratio of hydrogen rate to stoichiometric hydrogen rate for given air flow) was varied and the measured temperature compared to calculations based on measured flow rates and equilibrium chemistry (including minor species). Tests were conducted in which the total laser power was varied from 200 mJ to 550 mJ. Also data were obtained in which, through the use of different neutral density filters, the signal in the primary is saturated, forcing use of the secondary in analysis. No trends are found with either of these variables, indicating that the nitrogen spectrum is not saturated by high laser powers and that the splitter device works well. The average of all the data at an equivalence ratio 1.0 is 2360 K, compared to the theoretical value of 2380 K. The measurements agreed with calculation within ±100 K at an equivalence ratio less than or equal to one. However, for hydrogen rich flames, the measured temperature is consistently 100 K - 150 K high. This problem is being investigated but, for now, it is accepted that measured temperature may be as much as 150 K high in hydrogen rich regions.

7.5.1.2 SURFACE PRESSURE AND TEMPERATURE

Surface pressure and temperature data are presented for two typical runs, one in which the pilot injectors are operating and one in which they are not. These runs are chosen because the gas flow rates to the heater, injector and pilot and the heater pressure are all very close to their respective averages over the total set of runs.

Surface pressure distributions for the pressure taps at the bottom wall centerline, averaged over 1 s intervals, are shown in Fig. 10. The heater is initiated at time t_0 = 1 s and fuel injection commences at time t_1 = 6.0 s (piloted) or 6.4 s (unpiloted). Data are shown 10 s and 22 s into the run. Pressures vary widely in the upstream region due to the complex nature of the shock wave system created by the injectors and step. The pressure for the piloted case is higher than the unpiloted case between the pilot (x = 0.074 m) and about x = 0.7 m, due to combustion of gas from the pilot and main fuel injector. In the unpiloted case, pressure generally falls moving downstream due to divergence of the duct, until 0.5 m where it rises rapidly, peaking at about 0.75 m. Presumably, there is minimal combustion upstream of this region. Downstream of 0.75 m the pressure drops smoothly in both cases but is higher in the unpiloted case, despite the greater total injected fuel rate in the piloted case. Differences between the two cases suggest that significant combustion of the fuel does not take place upstream of 0.5 m in the unpiloted case, but that the combustion then proceeds to completion by 0.75 m. It is not expected that fuel and air are fully mixed at 0.75 m, so that further mixing and combustion is expected to occur downstream.

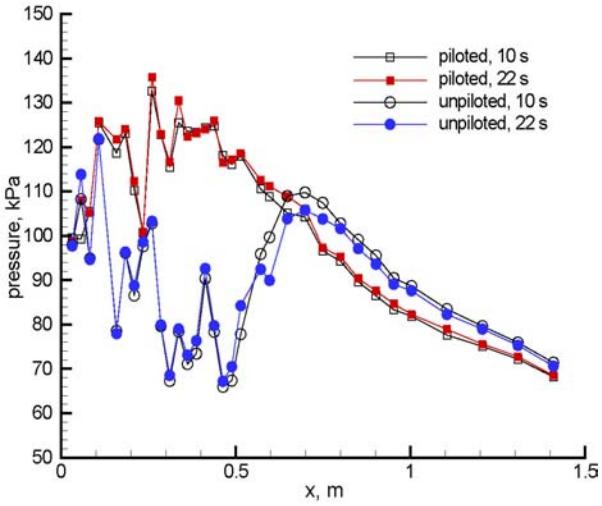

Figure 10: Surface pressure distributions along centerline of bottom wall.

Comparison between measurements at 10 s and at 22 s reveals only small differences. There is no suggestion that the combustion delay experienced by the unpiloted case is affected by the increase in surface temperature that occurs during the course of a run. Surface pressure varies as much as 20 kPa or more between top, bottom, and sidewall taps (not shown) upstream of about 0.65 m, consistent with the effects of shock waves. Downstream of this point, there are no differences between the walls.

Since the duct is uncooled, surface temperatures vary greatly during the course of the run. In the copper section, temperature is typically about ~ 360 K at the start of fuel injection but rises to as high as ~ 610 K. In the carbon steel section, it typically is ~ 440 K at the start and as high as ~ 950 K at the end. These variations in surface temperature are least-squares fit to the solution for wall temperature of a semi-infinite body at initially uniform temperature, subject to steps in surface heat flux at heater start and fuel injection start. Fit parameters include heater flux with heater only, q_0, and heat flux rise due to fuel injection, q_1. The fit is conducted out to t = 11 s. Representative temperature histories and fits are shown in Fig. 11. Fits often diverge from the data beyond about 11 s, indicating that heat flux continues to change slowly during the run. The material property $\sqrt{\alpha_s}/k_s$ is taken to be 36.7 kW K/m^{2}s$^{1/2}$ for the copper duct and 12 kW K/m^{2}s$^{1/2}$ for the steel duct. These values have not been verified experimentally, so this analysis should not be relied upon except in a relative sense (i.e., case to case, location to location within the copper duct, injection to no injection).

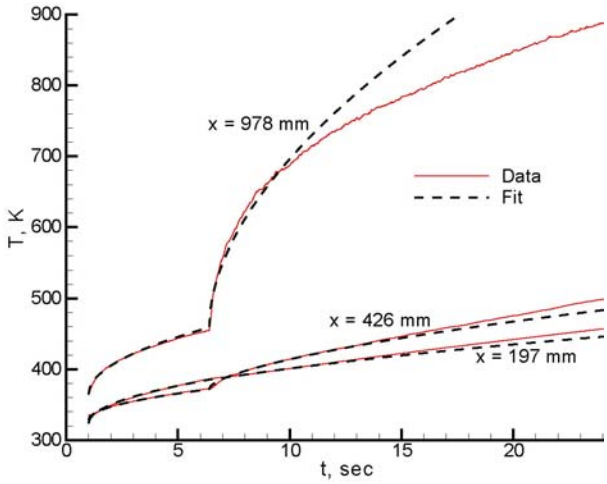

Figure 11: Wall temperature history, unpiloted, top wall: data and fits.

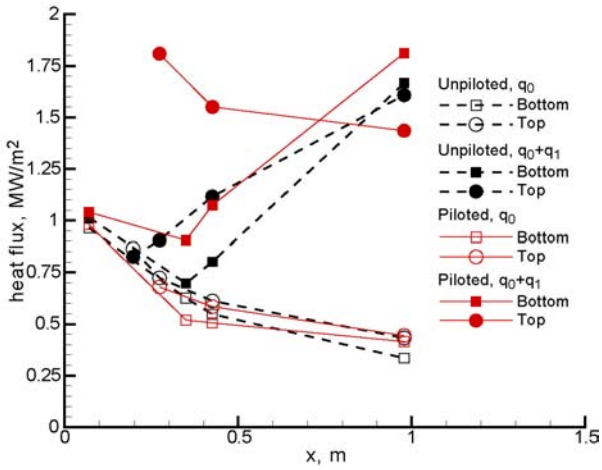

Figure 12: Surface heat flux distributions: top and bottom walls, centerline

Heat fluxes are presented in Fig. 12, on both top and bottom walls, at the centerline. Heat flux varies from 1.0 MW/m^2 to 0.3 MW/m^2 without fuel injection, and from 0.7 MW/m^2 to 1.8 MW/m^2 with injection. Without injection, heat flux varies at a given location 10% to 30% from case to case, reflecting variation in the initial temperature of the wall between runs. With injection, heat flux shows large increases relative to before injection. Large increases occur in the piloted case on the top wall, downstream of the main injector (x = 0.166 m). In the unpiloted case, a smaller heat flux rise occurs ahead of 0.5 m (where the pressure rise starts), indicating either the start of combustion near the wall, or an increase in heat transfer coefficient. (An increase in heat transfer coefficient could occur under the fuel plume due to an injection-induced streamwise vortex pair.)

7.5.2 CARS TEMPERATURES

Data was acquired over 201 facility runs over 10 test days. Except for one day, when laser beams clipped the edge of the duct window slots due to thermal expansion and movements of the duct, the vast majority of the data were found acceptable and analyzed. At each plane, data were acquired at 6 or 7 fixed points near the horizontal centerline. Data were also acquired during 16 s of horizontal motion of the translation stages at 5 mm/s, or from 9 s to 18 s of 5 or 6 mm/s vertical motion, during which time fuel is continuously injected.

All CARS temperature data are fit to a cosine series bivariate function of order 5 at plane 1 or order 6 at the other planes, with the number of fit parameters respectively 21 and 28. Commercial software was used (Ref. 8). 2000 to 4000 data points were acquired per plane and the standard deviation of the data from the fit at the various planes ranges from 196 K to 304 K. Thus, the fitted functions represent an estimate of the mean temperature distribution with mean uncertainty, given by $1.98\sigma\sqrt{n_p / n_s}$ (Ref.10), from 36 K to 59 K depending on the plane. It is important to point out that the uncertainty in the surface fits to the data is lower near the center of the measurement plane and higher near the edge. This uncertainty does not include the previously noted error in fuel rich regions of the flow, or any other non-statistical error.

Figure 13 contains 3-dimensional cutaway views of the duct showing contour plots of the fitted temperature functions. Flow is from top left to bottom right. Recall that the main fuel injector is on the top wall between Planes 1 and 3, and the pilot injectors are in the top wall upstream of Plane 1.

At Plane 1 in the unpiloted case the temperature is fairly uniform, between 1030 K and 1250 K. The mean temperature for all the data points of this plane and case is 1162 K. This mean compares favorably with the value computed assuming 1-D flow from the heater, which is 1187±60 K. In the piloted case, the temperature drops slightly close to the top wall where the (cold) pilot fuel is injected. There is no indication of combustion in this plane.

At Plane 3, in the unpiloted case, the injected fuel plume is a region of low temperature with temperatures as low as ~ 250 K at the center. There is no evidence of combustion of the injected fuel. In the piloted case, there is a band of hot combustion products close to the top wall. The center of main fuel plume may be seen as a cool region with temperature as low as ~ 650 K, which is greater than in the piloted case, suggesting some combustion.

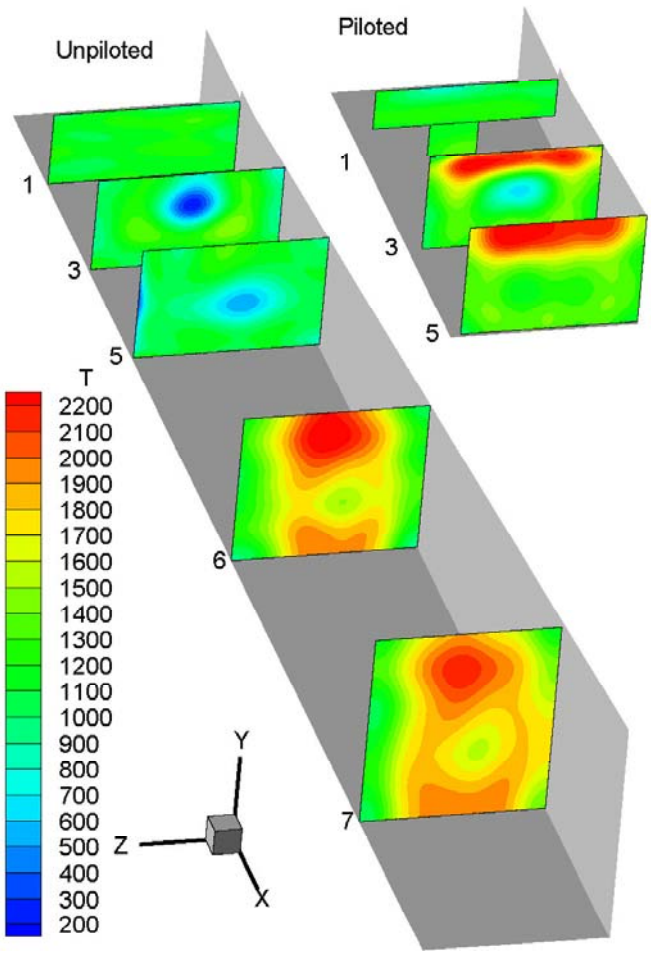

Figure 13: Cutaway views of duct showing contours of mean temperature for unpiloted and piloted cases

For both cases, Plane 5 is similar to Plane 3. In the unpiloted case temperatures have risen near the center of the fuel plume to a minimum of ~ 550 K. In the piloted case the minimum is ~ 1250 K and the height of the region of hot combustion products near the top wall is greater.

At Planes 6 and 7 (unpiloted case only), temperatures have risen abruptly as compared to Plane 5, suggesting nearly complete combustion, i.e., combustion that has consumed all available oxygen or fuel. The hot region close to the top wall (temperatures as high as ~ 2300 K), and to a lesser extent that near the bottom, are probably ones in which the fuel-air ratio is nearly stoichiometric. The cooler region near the center (as low as ~ 1500 K) is probably fuel rich. Injected fuel may not have penetrated to the sidewalls (~ 1200 K to 1300 K). Data at these planes were not acquired in the piloted case due to lack of facility time. However, similarity in the pressure distributions downstream of about x = 0.75 m suggest that the temperature maps would be at least qualitatively similar, except perhaps close to the top wall.

The various data obtained provide a consistent description of the flow field. In the unpiloted case, no significant or only small and intermittent combustion of the injected fuel is observed ahead of x = 0.5 m.

Downstream of x = 0.75 m combustion appears nearly complete. In the piloted case, combustion of the pilot fuel appears to take place between x = 0.122 m (at the step) and 0.274 m. There also appears to be significant combustion of the main injected fuel by this location. These results are not consistent with the CFD calculations performed prior to the commencement of the experimental work[8], which predicted combustion in the vicinity of injection in both unpiloted and piloted cases. Consequently, this experiment provides a test case for CFD that is a more challenging than anticipated.

Accurate calculation will require accurate modeling of the chemical kinetics and turbulence-chemistry interactions as well as accurate modeling of the turbulent mixing.

7.6 SUMMARY

Thus two experiments to acquire data for the validation of computational fluid dynamics (CFD) codes used in the design of supersonic combustors have been described.

The first study was of a supersonic coaxial jet with center jet helium and coflowing jet air. Data include schlieren visualization, gas sampling and Pitot probe surveys, and RELIEF flow tagging velocity measurements. Calculations utilizing a structured finite difference code and Wilcox's $\widetilde{k}-\widetilde{\omega}$ model have been presented. Calculations demonstrated non-physical discontinuities in slope of mole fraction and Pitot pressure due to inadequacies in the turbulence model.

The second study was of a supersonic combustor with single downstream angled hydrogen fuel injector. Data include CARS temperature maps, and wall pressures and temperatures. Modern design of experiments techniques have been used to maximize data value. Contrary to the result of previously performed CFD calculations, it was found that (without pilot injectors) ignition did not occur until significantly downstream of injection. This is attributed to inadequacies in the kinetics model and/or the model for turbulence chemistry interaction.

7.7 ACKNOWLEDGEMENTS

The 1st author would like to acknowledge the support of the NASA Langley Research Center through grant NCC1-370.

7.8 CONCLUSIONS AND RECOMMENDATIONS

Robust design of SCRJ Combustors needs reliable simulations tools. The SPARK code used in the simulations reported here was capable of realistically reproducing non-reactive fuel/air mixing, but still has shortcomings in predicting ignition. This is likely the effect of the hydrogen kinetics and/or of the flame mdel that, by necessity, must approximate the supersonic turbulent combustion.

It is recommended that support be given to study in greater detail turbulelence-kinetics interaction in the Mach range of interest to SCRJ, and that an improved combustion model be developed to be implemented in the SPARK code or other CDF tool.

7.9 REFERENCES

1 Diskin, G. S., "A Experimental and Theoretical Investigation of the Physical Processes Important to the RELIEF Flow Tagging Diagnostic", Ph.D. Dissertation, Princeton University, 1997.

2 Papamoschou, D., Roshko, A., AThe compressible turbulent shear layer: an experimental study," *J. Fluid Mech.*, Vol 197, pp. 453-577, 1988.

3 White, J. A., Morrison, J. H., "A Pseudo-Temporal Multi-Grid Relaxation Scheme for Solving the Parabolized Navier-Stokes Equations", AIAA Paper 99-3360, June 1999.

4 Drummond, J. P., Diskin, G. S., Cutler, A. D., "Fuel-Air Mixing and Combustion in Scramjets," Technologies for Propelled Hypersonic Flight, NATO Research and Technology Organization, Working Group 10, RTO Report AVT 10, January 2001.

5 Smith, M. W., Jarrett, O. Jr., Antcliff, R. R., Northam, G. B., Cutler, A. D., Taylor, D. J., "Coherent anti-Stokes Raman spectroscopy temperature measurements in a hydrogen-fueled supersonic combustor," *Journal of Propulsion and Power*, Vol. 9, No. 2, 1993, pp. 163-168.

6 Wilcox, D. C., *Turbulence Modeling for CFD*, 2nd Edition, DCW Industries, Inc., July 1998.

7 Auslender, A. H., "An Application of Distortion Analysis to Scramjet Combustor Performance Assessment," Final Report, 1996 JANNAF Propulsion and Joint Subcommittee Meeting Scramjet Performance Workshop, Dec. 12, 1996.

8 Eckbreth, A. C., "Optical Splitter for Dynamic Range Enhancement of Optical Multichannel Detectors," *Applied Optics*, July 15, 1983.

9 *Table Curve 3D Version 3.0 User's Manual*, AISN Software Inc., www.spss.com, 1997.
10 Box, G. E. P and Draper, N. R., *Empirical Model Building and Response Surfaces*, New York, John Wiley and Sons, 1987

CHAPTER 8: USE OF SCHOLAR SUPERSONIC COMBUSTION DATA

1D ANALYSIS OF THE SCHOLAR EXPERIMENT

Rodolphe d'Incà, Marc Bouchez
Propulsion Department, MBDA France[1]
8, rue Le Brix / 18020 BOURGES CEDEX / France
marc.bouchez@mbda.fr

8.1 INTRODUCTION

The SCHOLAR experiment has been proposed by NASA Langley Research Center as a test case for the RTO/AVT subgroup2 scramjet. This experiment is a study of a supersonic combustor consisting of a diverging duct with single downstream-angled wall injector. The nominal entrance Mach number is 2 and enthalpy is nominally that of Mach 7 flight (see Chapter 6, 7). The primary measurement technique is intended to be Coherent Anti-Stokes Raman Spectroscopy (CARS), although surface pressures and temperatures have also been acquired.

To analyse these results, 3D reactive computations, using available Navier-Stokes models (for example, the French MSD code) were outside the scope of the present RTO work.

Nevertheless, MBDA proposed to do a first analysis of the SCHOLAR experiment with the 1D method that has been used for the APL scramjet combustor analysis in connection with the question of vitiation. Then, using the pressure measured on the duct, the combustion rate and other associated thermodynamic figures can be estimated in a cross section-averaged way. The obtained 1D static temperature contour has been compared with available CARS measurement maps realized by NASA of the SCHOLAR experiment.

8.2 EXPERIMENTAL COMBUSTOR

8.2.1 COMBUSTOR SCHEMATIC

The combustor is divided into two parts: the main one, made of copper (its schematic is in Fig. 1 below) and a diverging part in carbon.

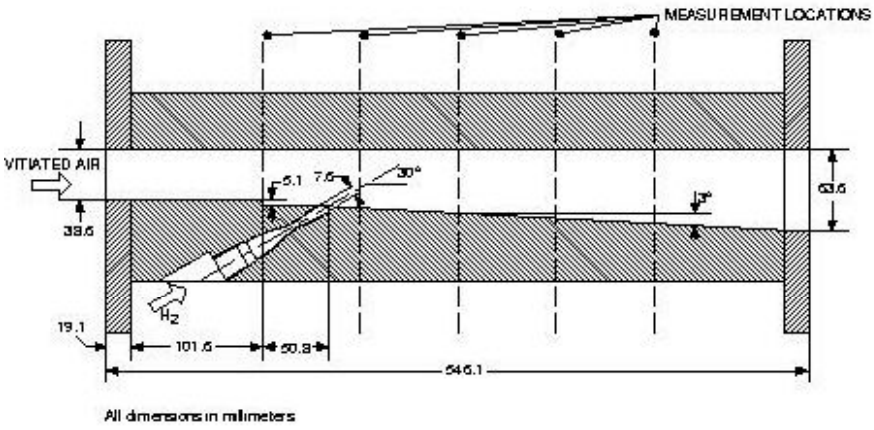

Figure 1 : Combustor schematic. All dimensions in millimeters.

[1] Before 1st of April, 2002 the Company was EADS Aerospatiale Matra Missiles.

[2] See Chapter 6, "Mixing and combustion" of the present report, or paper "Fundamental Mixing And Combustion Experiments For Propelled Hypersonic Flight", by A. D. Cutler, G. S. Diskin, P. M. Danehy, J. P. Drummond, NASA Langley Research Center, to be presented at Joint Propulsion Conference, Indianapolis, July 2002.

8.2.2 INPUT DATA

The input data needed by the simulation are presented in the following tables:

Flow at Air Intake		GH2 Injection	
Mach	**2.0**	**Mach**	**2.5**
Temperature	**1204 K**	**Temperature**	**133 K**
Pressure	**101325 Pa**	**Pressure**	**202650 Pa**

Experiments are carried out at flight conditions corresponding to about Mach 7. Temperatures are sufficiently high to produce self-ignition of the air-hydrogen mixture.

8.2.3 EXPERIMENTAL RESULTS

The only data used here are the pressures along the combustor. Computations have been carried out along the whole combustor, including the copper portion.
These data are in Fig, 2 below:

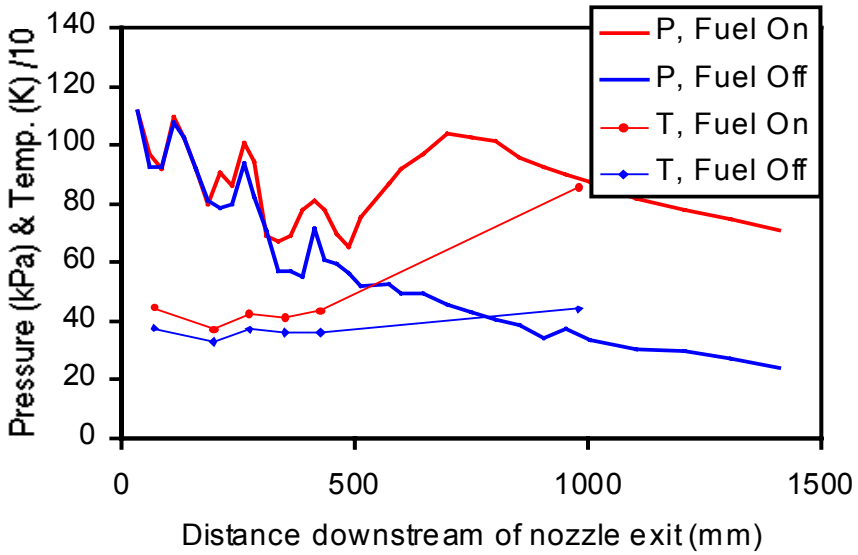

Figure 2 : SCHOLAR wall pressure and wall temperature measurement on the experimental combustor.

8.3 1D ANALYSIS OF THE FLOW

8.3.1 1D ANALYSIS ASSUMPTIONS

The assumptions are the same as for the APL combustor analysis see (Chapter 3). The 1-D PUMA code (a French acronym meaning One-dimensional Program for Analysis of Aerothermochemistry), has been used to provide a preliminary analysis of the results. This code has been extensively used by MBDA for advanced studies of scramjets and to provide a first analysis of experimental results such as CHAMOIS one3, before 3D post-test analysis are available.

We must note the limitations of this 1D study. Some effects that occur in the combustor, like shock wave or recirculation zone behind the rear-facing step, are strongly 2D or 3D: we cannot directly integrate them into the program. That is why we must keep in mind that for some cases (especially for high equivalence ratios),

[3] E. Dufour, M. Bouchez, "Post-Experimental computations of a kerosene-fuelled scramjet", AIAA-2001-1817, Kyoto, Japan, April 2001.

the results are limited by the nature of the flow. The 1D analysis is easy to perform in the frame of the present scope of this RTO report, and allows to perform parametric studies of the physical effect of the composition of the incoming air flow.

The heat release law is tuned until a reasonable agreement is reached between 1-D results and experimental results. For that the balance between the heat release, the effective geometry and the drag has to be identified, in order to decide the contribution of each term to the measured wall pressure increase.

In the present study, the choice is the following:

- To use the "geometrical shape" as the flow boundary (no decrease due to boundary layer or subsonic zone), see Fig. 3

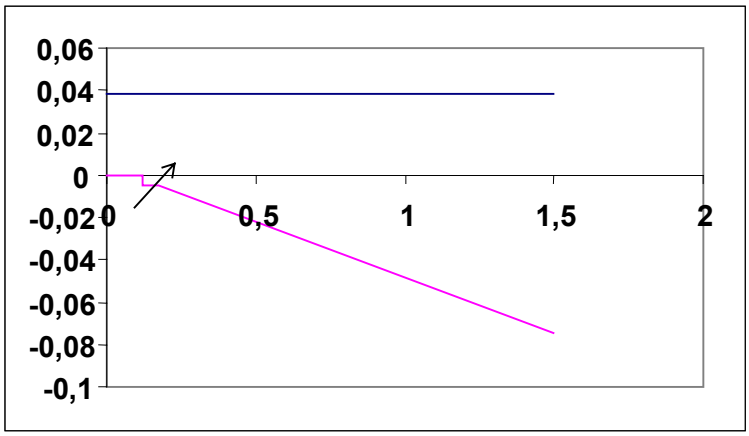

Figure 3 : assumed duct area variation (geometry) of the 1st part of SCHOLAR combustor (m)

- To tune the drag with the non reactive case, and keep the same tuning constant for the reactive cases: the local skin friction coefficient is computed using semi-empirical laws and the 1D parameters of the flow, and sometimes increased by a multiplication factor in order to account for other forms of drag. The multiplication factor is kept the same for any ER from 0 to 1.
- To derive from the pressure on the wall the heat release law, using simple combustion modelling, with a simple reaction.

8.3.2 "FUEL OFF" RESULTS

The computed average pressure along the duct is first compared with wall measurements, without fuel injection (see Fig. 4).

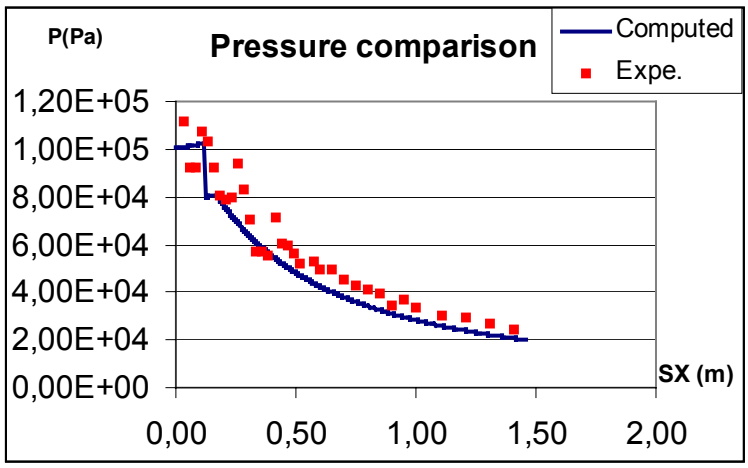

Figure 4: comparison of pressures for "fuel Off" results

From a global point of view, the two graphs seem to be in good agreement. The computed results are a bit lower than the experimental one; this fact probably comes from a too low drag coefficient assumed in the 1D analysis.

In the injector area, there are some differences between measured pressures (which show severals spikes) and the computed ones. The origin of this phenomenon is rooted in the 2D effects of shocks that interact with the boundary layers on the wall and disturb the value given by pressure sensors.

8.3.3 "FUEL ON" RESULTS

The PUMA linked with the PIPEAU inverse code were used to compute the combustion efficiency reproducing to the wall pressure measurements.

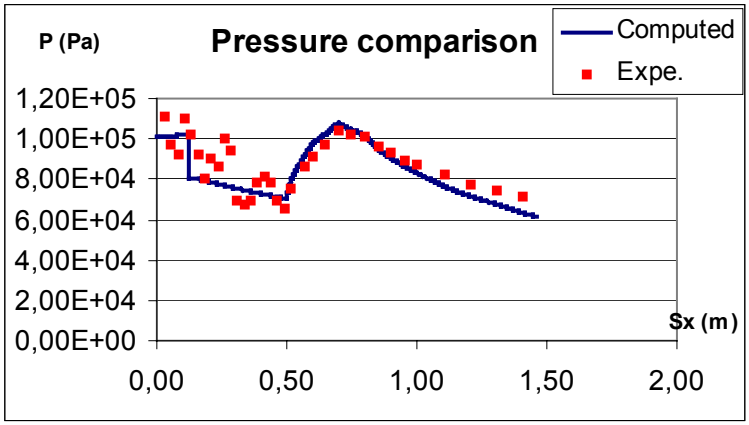

Figure 5: Comparison of pressures for fuel ON

As for the reactive case, there is good agreement between the two curves (see Fig. 5). The pressure speaks are still there and have –despite combustion- the same intensity as in the non-reactive case (quite no effect from dowstream to upstream).

The computed combustion efficiency ETAC(x)can then be seen in Fig. 6:

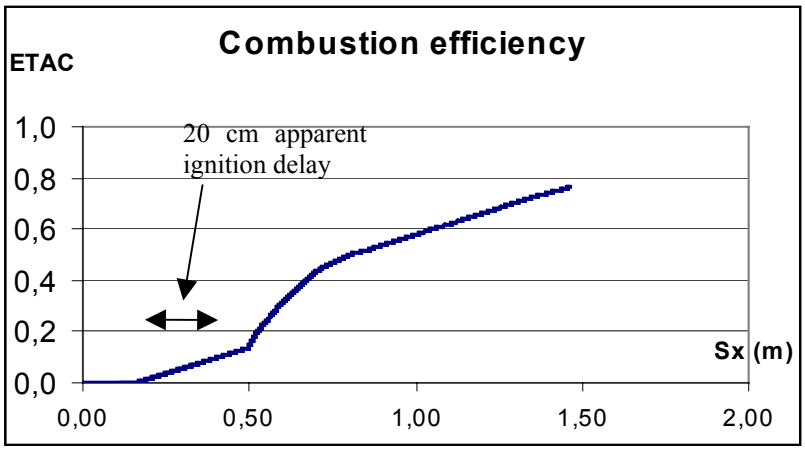

Figure 6: computed combustion efficiency along the SCHOLAR duct

The start of combustion seems to be delayed. This delay can be compared with the formula of A. Ferri[4] giving the self-ignition time for hydrogen /air mixtures :

$$\tau_i(\mu s) = \frac{8.10^{-3}}{P} e^{\frac{9600}{T}}$$ (T(K) and P(Atm) are conditions at injection plane)

This enables computing the length necessary for to start combustion; in our case, this length is equal to 20 cm (at T=1000K).

[4] Review of problems in Application of supersonic combustion – A. Ferri – J. of the Royal Aeron. Society, Vol. 68, p. 645, September 1964

The corresponding Mach , Temperature and water mass fraction vs. x are given in Figs. 7-9 for the two cases 0 and 3:

Case 0: fuel off Case 3: fuel on.

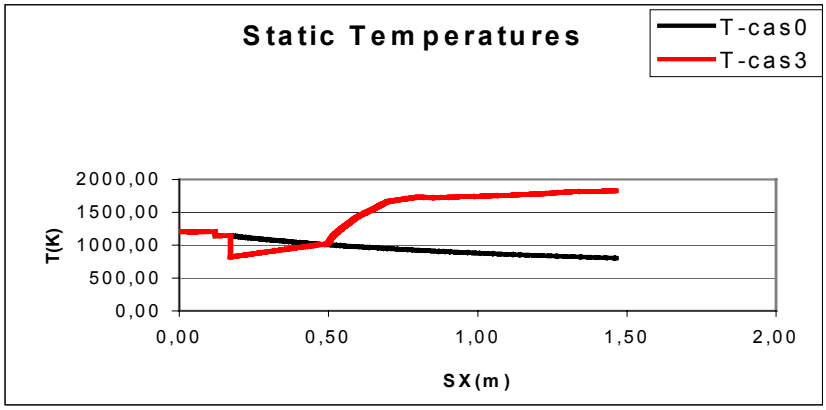

Figure 7: Computed static temperatures with and without injection

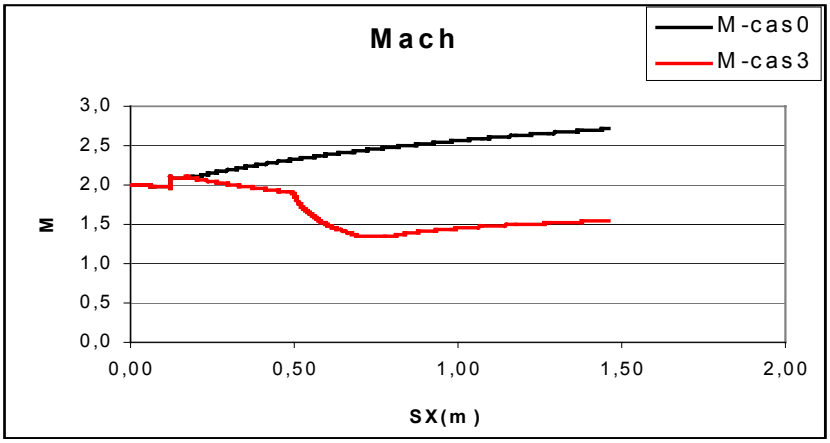

Figure 8: Computed Mach with and without injection

Combustion does take place in the supersonic flow. Once again it can be noticed that heat release is equivalent to a reduction of the duct area (increase of static pressure, decrease of Mach number).

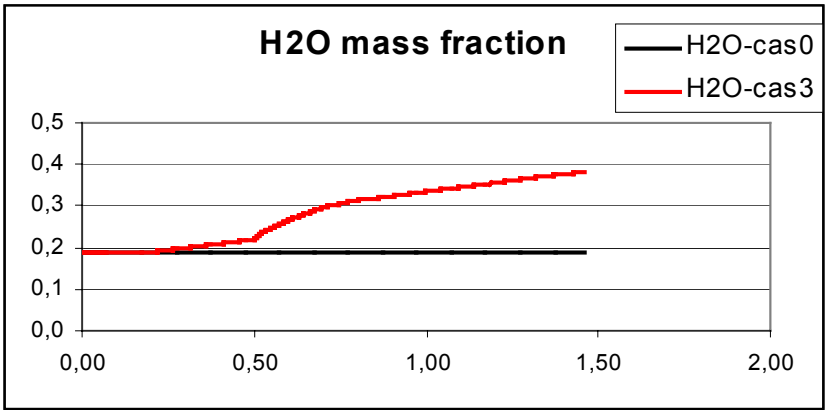

Figure 9: Computed H2O mass fractions with and without injection

The computations took into account the fact that the entrance air is vitiated in this test facility.

8.4 COMPARISON WITH CARS MEASUREMENTS

This 1D analysis was performed in 2001 within the scope of MBDA-France participation to RTO/AVT 10 scramjet subgroup. Afterwards, CARS measurement results were made available.

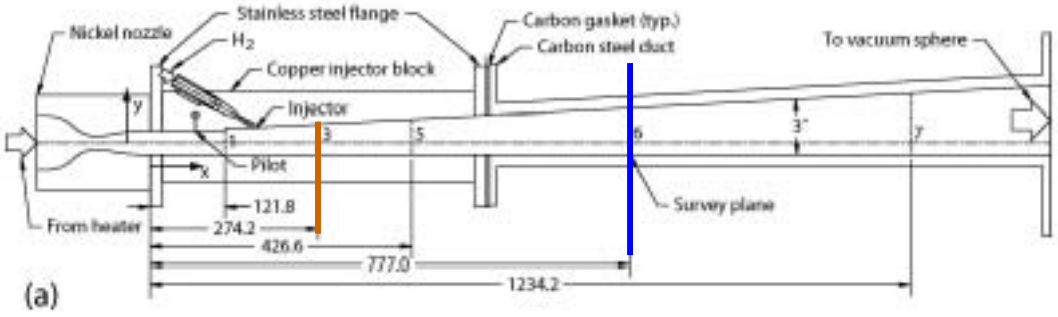

Figure 4 : CARS survey sections in the SCHOLAR experiment

As shown below in Fig. 7, the mean value of static temperature of CARS maps in the survey plane 6 (x≈0,8 m) and of their 1D predictions (1800 K) is quite similar.

In the step / injection zone, the effect of decrease of static temperature (sudden expansion and cold hydrogen injection) can also be seen in the two approaches.

Ignition delay is visible also on CARS maps (difference between “piloted” and “unpiloted”).

8.5 CONCLUSIONS AND RECOMMENDATIONS

This study is one more example of the 1D-analysis of the flow in a scramjet combustor, used worldwide to quickly analyse supersonic combustion tests and to give a first design and cycle analysis in advanced studies.

We obtain quite a good agreement between experimental and computed pressure and with CARS measurements, even though the 1D computation does not take into account the 2D-effects like shocks or local expansion.

Further 3D analyses should be compared with this first simple 1-D analysis.

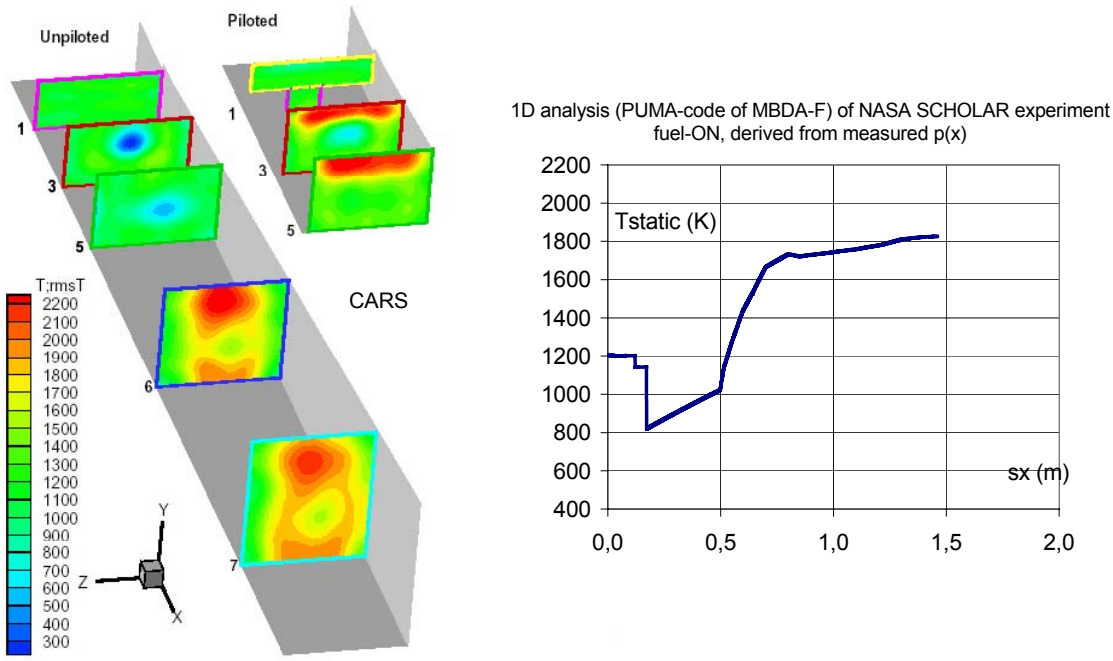

Figure 7: Comparition of 1D analysis with CARS maps

CHAPTER 9: SCRAMJET COMBUSTOR AND FLOWPATH SCALING

I. M. Blankson, S.N.B. Murthy and C. Bruno

I. M. Blankson
Lewis Research Center, NASA GRC
21000 Brookpark Road, Cleveland Ohio 44135
blankson@grc.nasa.gov

S.N.B. Murthy
Chafee Hall, Purdue University
West Lafayette, IN 47907-1003 USA
snbgm@ecn.purdue.edu

C. Bruno
University of Rome "La Sapienza"
Via Eudossiana 18, 00185 ROMA – ITALY
c.bruno@dma.ing.uniroma1.it

9.1 SUMMARY:

The literature on scramjet scaling and flowpath scaling is reviewed and summarized with a focus on specific topics that are directly related to prediction of H_2-fueled scram combustor performance and comparison with test-data. The specific literature on scramjet scaling is unfortunately very limited. In addition, some unsettled issues about the effects of vitiation (e.g. Bruno (Ref. 1)) on combustor flows may compromise the level of certainty of conclusions that may be drawn from these analyses. An analysis of basic equations for a scramjet combustor indicates that, under certain conditions, the product of pressure and cross-sectional area of combustor of similar performance is nearly constant. This is the **Pressure–Length scaling.**

We have also conducted a substantial amount of work on low dimensional performance predictions of scram combustors using predictions obtained by a quasi 1-D SCRAM-3L code. The predictions are based on nonuniformity coefficients applied to flow and state properties in one-dimensional analysis. The geometry includes sudden and gradual area changes and also wall cavities. Detailed 3D predictions carried out with inert, constant thermodynamic properties yield the needed nonuniformity coefficients.

The output consists of variations along the flow in the following properties: P, T, M, V, unreacted hydrogen, and hydrogen that exists as hydrogen in the stream. In addition, the first and second law efficiencies, on exergy-based efficiency, the kinetic energy efficiency, and three efficiencies related to chemical reactions and combustion are calculated; the nominal specific impulse is also predicted. The bulk of these results were presented in Ref. 2.

We have tried to look at representative sets of test data in the US, Australia, Europe, Japan and FSU, but find mostly only pressure distributions along the combustor as reliable data. In fact hardly any data exists on the chemical state of the fluid. The available test data have been utilized in comparisons with predictions in a number of cases. In addition, a large matrix parametric study has been undertaken in which, in addition to geometry and initial conditions, we have varied the injection schemes, the mixing schedules, the ignition, and the friction and heat transfer losses in parametric form to establish their influence. Finally, the experimental data of Pulsonetti and Stalker (Ref. 3) on scaling of scram combustors have been reproduced by prediction. It is clear that low dimensional modeling, coupled with limited exercise of inert 3-d calculations, can yield substantial results. Also, the predictions can be directly compared with measurement; the extent and level of detail in measurements is limited to combustor hardware surface measurements and any predictions of the internal state of the working fluid is well nigh impossible to be checked or verified in any available set of experimental results.

We have also started an extensive study, both theoretical and experimental, on scramjet vehicle flow-path scaling. The experiment involves an "interactions testing" schedule in which the airbreathing hypersonic vehicle is "built – up" sequentially from tip to tail. Three key areas of research are under consideration. (1) Performance measures of scramjet vehicles viewed as coupled inlet-shock isolator-combustor- nozzle systems, which are interdependent and interrelated. (2) Scramjet combustor scaling. (3) The issue of vitiation, and its un-assessed quantitative impact on combustion and thrust development. There is potential for a joint international experiment on vitiation in the near future. The experiment is to be conducted at the NASA Glenn HTF. Finally, a number of

topics are of course of great interest and also crucial for the success of scram combustors as a component of space transportation propulsion systems. These will be mentioned briefly.

9.2 INTRODUCTION

To date, airbreathing propulsion systems have operated successfully up to Mach 3+ and at altitudes as high as 90,000 feet. The turbojet, turbofan, and ramjet (subsonic combustion) have routinely demonstrated high specific impulse performance and use in vehicle applications. In the past decade, the supersonic combustion ramjet (scramjet) has received a considerable amount of attention because of its potential application to transatmospheric vehicles, global-range vehicles, and hypersonic missiles (Ref. 3). Both cruise vehicles and accelerators (space launch) have been considered.

The technical differences between engines operating at speeds above Mach 3 and those for lower speeds stem mainly from the high stagnation enthalpies at high free-stream Mach number. A consequence of this condition is that at Mach 6 and above, conversion of the free-stream kinetic energy to thermal energy can raise the temperature to the level where the air dissociates, changing its thermodynamic properties considerably. Even more important, the temperature can be so high that little gains in temperature rise occur from fuel addition to the air – a result of the dissociation of combustion products. The scramjet was conceived to minimize the problem of dissociation by maintaining combustion at supersonic speed.

The scramjet engine would considerably extend the useful operating range of airbreathing vehicles possibly into the hypervelocity regime. But formidable challenges will have to be overcome. Extending operation of a hypersonic vehicle to hypervelocity speeds puts extreme demands on the propulsion system. This system must survive the severe thermal environment and operate at a high level of efficiency while producing enough net thrust to adequately accelerate the vehicle. At high speed component efficiency becomes critical as a consequence of the increasing kinetic energy in the airflow processed by the engine. For example, at hypervelocity (Mach 16+) the level of energy in the airflow processed by the engine becomes much larger than the energy added by burning hydrogen fuel; therefore, the net thrust (the difference between gross nozzle thrust and the ram drag) becomes only a small fraction of the stream thrust of the airflow entering the engine. Specifically, at Mach 6 the energy associated with heat release of a stoichiometric hydrogen fuel-air mixture is about twice that of the kinetic energy contained in the airflow, whereas at Mach 16 this value is only about one-fourth. At the same time additional factors contribute to increased performance sensitivity: the high inlet area contraction ratio (required to compress the air at high altitudes), high temperatures (to be contained within the engine) and high flow velocities. Consequently, performance sensitivity to component efficiency rapidly increases with increasing vehicle speed throughout the hypersonic flight regime. It is clear that a great deal of work needs to be done to meet these challenges before propulsion at such flight speeds can be realized in practice. Current worldwide efforts and progress on scramjets show a positive trend.

The two main issues considered in this report are related to (i) scramjet combustor scaling (ii) interactions testing including extrapolation to a flight test vehicle. In particular, given the performance of a scramjet engine of a specific type, is there a model or a set of models, which permits the deduction of the performance of the full-scale engine?

The issue may also be stated as follows. In order to obtain a desired level of performance at a particular scale of the engine (under a given set of initial conditions based, for example, on a chosen trajectory), what sets of scaled engine components and initial conditions must be tested to provide adequate scaling parameters with respect to the various performance parameters a of interest.

In addressing these issues, one encounters a lack of knowledge or existence of a set of scaling parameters for scram engine components and the engine as an integrated system. In this report, we will summarize, what is known and then attempt to generate a rational method of generating these scaling parameters. The total scram engine system should consider, in general, the inlet, the isolator, the combustor, and the nozzle. As is typical of internal flows, the phenomena occurring in each component can strongly affect the operation of the other components through their influence on the mass flow. As a system with a single flowpath of the working fluid from inlet entry to nozzle exit, the scramjet engine is subject to a variety of interactions among the components. A systematic analysis of these interactions is the subject of Part 2 of this report.

There the combustor is chosen as the dominant component, and the other components are considered as designed for the combustor. The discussion throughout is centered around the combustor. Thus the combustor is considered in itself, and in combination with the isolator, the isolator and the inlet, the nozzle, and finally, the inlet, isolator, and nozzle; thus a total of five configurations is involved, the last of them consisting of the engine as a whole.

Various processes govern the performance of a scram combustor. These processes in a specific type of combustor can be shown to depend on a set of nondimensional parameters that involve characteristic lengths and

times in addition to impulse (momentum and pressure) and energy (generated and dissipated). Since the scram combustor involves a (high speed) flowfield, there is a continuously, nonlinearly evolving balance among the nondimensional parameters along the combustor, while, ordinarily, only the initial and boundary conditions (for example, along the walls) can be controlled. In some cases, the internal processes along the combustor, such as chemical heat release, can appear to be controllable, but only by means of appropriate initial conditions. The issue, therefore, is the determination of a combination of initial and boundary conditions for the full scale engine based on the performance of one or more small scale engines under different operating conditions.

While a set of characteristic parameters can be identified for the scram combustor processes, the scaling methodology has to be specialized to each specific type of combustor. On one hand, the characteristic parameters must include both detailed and comprehensive (such as exergy-based) performance parameters. On the other, one must establish, for the particular type of combustor, the combination of scales for those parameters that ensure similar or improved performance for the full scale engine. Thus, in the case of a strut engine, for example, the struts serve several purposes, and it is necessary to examine the processes associated with each of those. In particular, some of the processes may be unsteady by nature, as in an isolator, and it is then necessary to account for the wave processes involved.

There are certain topics, which will receive inadequate discussion in this scaling analysis. Fuel injection, for example, is a major consideration in the design of high-speed combustors. The implications of scaling relative to the injection, mixing, ignition, and flame stability, as well as the control scheme regulating the supply of fuel in the different operational modes will not be examined in adequate detail.

The scaling of combustor geometry involves both the cross-sectional dimension as well as the length. Considering the manner in which the length, in addition to affecting the completion of combustion, also affects the overall vehicle volume and mass, it is necessary to establish a method of defining and determining a near-optimum length. These considerations apply both to the final full-scale engine-vehicle system as well as to the flight-test vehicles of interest. The scaling rules deduced by analysis for components need calibration and verification. The usual procedure is to generate one or more scaled-down component models and then test them under various initial conditions. Because of interactions between two or more components along the working fluid flowpath, the method of evolving such models and tests is non-trivial.

This chapter will be divided into 2 parts: I, Combustor scaling, including dimensional analysis, and exergy analysis; the data on scaling by Pulsonetti et al at U. of Queensland (essentially, p x L scaling); predictions obtained by the quasi 1-D SCRAM-3L code, and a final discussion on engine-nozzle integration. SCRAM -3L is an energy balance-type code using a quasi 1-D geometry and 3 streams to simplify mixing and combustion, originally developed at NASA Langley. Mixing and combustion occur across the layers, using real gas properties and nonequilibrium chemistry.

Part II will include engine flowpath scaling; in fact, combustion/engine efficiency depends on length in a non-monotonous way: there is a minimum length for efficient operation, beyond which efficiency starts decreasing again. Engine scaling is the most important task since isolator scaling is well understood, and inlet scaling is also understood. Data on engines are scattered and sorely needed, but CFD data for the Mach 4-8 NASA-Ames vehicle may become available. Final comments will include the recommendations for future experiments and associated calculations, and flight-testing issues.

9.3 PREVIOUS WORK: SCRAM COMBUSTORS AND SCALING

Although general criteria for similitude and scaling have been proposed in hypersonics (see, for instance, Ref. 22), understanding of scaling for SCRJ combustors is still scarce. The status of supersonic combustor technology before about 1985 is summarized in Northam (Ref. 5) with a particular focus on research at Langley. Up to that time, NASA combustor technology was focused on a Mach 4-8 airframe-integrated research aircraft. Scramjet combustor design tools in this era were based largely on experimental studies, and designs were evaluated both in direct connect combustor and in free jet engine experiments. Performance levels for both all-supersonic and dual mode (mixed supersonic and subsonic combustion) were established. Some of the critical problems encountered in this "low" supersonic combustion speed regime were addressed, including fuel mixing, ignition, flame holding, mode transition, and combustor/inlet interactions. The scramjet concepts investigated were shown capable of thermally balanced operation with sufficient thrust and efficiency to accelerate a research aircraft. References 6-7 also contain a wealth of information on scramjets.

At speeds of Mach 8 and below, combustion in ducted flows can generate large local pressure rise, flow deflection and separation. The behavior of this "upstream interaction" has been studied extensively (e.g., Ref. 6), and is characteristic of supersonic combustion in constant area channels below flight speeds of about Mach 8. In such flows involving local separation and a bulk Mach number near unity, local wall static pressure is representative of the pressure across the entire flow at a given axial station. Therefore, a one-dimensional approximation to the flow can provide a reasonable description of the flow behavior.

In Section 4.3 of Chapter 4 a method is outlined that can, in principal be used to scale the effect of air vitiation. In fact, the same method can also be used to scale all physics associated to SCRJ, the only question being the necessity of diving the SCRJ into functional blocks (e.g. inlet, isolator, combustor and nozzle). Each block, obeying the same type of physics, can be dealt with using the guiding principles in Section 4.3.

In essence, each set of physical laws can be cast in non dimensional form showing characteristic numbers (Re, Mach, Damköhler, etc) representative of the ratios between the relevant times (convection/diffusion, convection/sound speed, convection/kinetics, etc). Scaling means making sure these ratios are maintained when varying the scale.

While this all sounds simple, the dependence of these numbers on operational parameters (pressure, temperature, fuel and air concentrations, turbulence intensity and velocity, among others) complicates matters considerably. Although there is hardly any excuse to neglect such a preliminary analysis, it is well known that rigorous scaling maintaining all, or most, of the numbers the same, is impractical.

It is for this reason that less stringent (or: partial) accounting of all the relevant physics has been and is still used to predict the effect of scaling. To some, this approach may sound empirical, while, in fact, often can be justified based on an intuitive, or acquired, sense of which physics is important and which is not in a SCRJ.

McClinton (Ref. 8), in a private communication, outlines the differences between supersonic and hypersonic combustion physics. The latter has been a focused activity at NASA Langley during the last two decades. In hypersonic combustion local Mach number remains high, Mach angles are quite shallow, and significant variations in static pressure are likely to occur across the combustor flow field at a given axial station. Typically, a fully three-dimensional representation of the flow field will be required; and as pointed out by Stalker (Ref. 9), special care must be taken to properly relate the implications of one-dimensional calculations to fully three-dimensional experimental data in a meaningful way. Thus hypersonic combustion flows differ from supersonic combustion flows in that the flow remains hypersonic throughout in a bulk sense, the effects of heat release are smaller, and the pressure field is fully three-dimensional. Common features of hypersonic and supersonic combustion flows include: real gas effects, nonadiabatic wall boundaries, finite-strength shock waves, dissimilar gas injection, turbulent mixing, finite-rate chemical reaction, flow separation, etc. Also, because aerodynamic, fluid mixing, and chemical rate processes are all expected to be important, experimental simulation requires near full-size hardware and duplication of flight conditions. Simulation requirements are discussed in more detail in the Appendix. Hypersonic combustion raises some additional uncertainty and concerns. Firstly, the effects of (extreme) compressibility on turbulence generation and mixing are not well known or understood. Secondly, at about Mach 12 the velocity of the injected (hydrogen) fuel stream equals the velocity of the combustor air stream; and at higher flight speeds the air velocity exceeds the fuel velocity. The behavior of fuel-air mixing under these conditions is also not well known. In fact, compared to flight at Mach 8 and below, there is limited data on which to base confidence in our understanding of or ability to model hypersonic combustion flows. Further discussion will be found in Refs.10-14.

A great deal of research needs to be done before propulsion at such flight speeds can be realized in practice, and most of this research will, of necessity, continue to be done on subscale models. It is therefore important to develop an understanding of the relation between phenomena experienced with subscale models and those which would be experienced with a full scale flight vehicle. This need for a relationship particularly applies to the supersonic combustion process. The manner in which combustion phenomena scale between configurations of different size for subsonic combustion in gas turbine engines and rocket engines was the subject of considerable research some three or four decades ago. Of particular note here is the work of Stewart (Ref. 15). Consult also Benelli (Ref. 16). In theoretical studies of the factors affecting the performance of geometrically similar combustion chambers, Stewart concluded that the two major ones were mixing and reaction kinetics. This led to the further conclusion that, as long as geometric similarity existed between different sized combustion chambers and they were operated at the same inlet temperature, inlet velocity and fuel-air ratio, approximately similar results would be obtained if the product of pressure and characteristic length were maintained constant, (that is P x L = constant, where p is the static pressure and L is a characteristic length). This equation is not without constraints.

Stewart appears to be the first to specifically state the pressure-length scaling law. He qualified it by pointing to importance of fuel atomization and spray characteristics, and others have noted that effects such as radiation may sometimes cause it to be modified. Penner (Ref. 17) performed a scaling study on liquid propellant rocket combustion chambers. For a fixed inlet temperature and fuel oxidiser ratio, he concluded that scaling was possible if the Reynolds' number and ratio of residence time to chemical reaction time (i.e. the first Damköhler number) were the same. For binary reactions, where the reaction rate varies as p, these requirements are satisfied if the above equation is satisfied. And, in a study of ramjet combustors, Stewart and Quigg (Ref. 15) also showed that the above equation yielded good combustor similarity under conditions such that the performance was relatively insensitive to the fuel distribution in the combustor.

Thus it is clear that the above equation could be a basis for scaling a range of aeronautical combustion systems, albeit that caution is required regarding the influence of factors such as the fuel distribution or radiation effects. Incidentally, the above equation has previously been used by Huber et. al. (Ref. 18), as the basis for an approximate correlation of experimental results on ignition in supersonic flows, and this might be seen as offering some promise that it can be applied more extensively to the scaling of supersonic combustor configurations. It seems reasonable to approach the scaling of supersonic combustion by testing the validity of the above equation.

9.4 SCRAM-COMBUSTOR SCALING

Scramjet combustor scaling is of interest in two major contexts:

i. relating design, performance and operation of combustors of different scales, required to operate over defined ranges of combustor entry conditions; and
ii. establishing the influence of combustor scale on overall engine flowpath relative to mission needs.

Under (i), for example, the interest may be in evolving and comparing a series of test articles for a specific flight unit under a number of defined operational conditions. Under (ii), again for example, one may consider a number of variously scaled engines and the combustors utilized in them, given a particular type of mission and class of constraints in usage, including vehicle integration. Thus, under (ii), combustor scaling is still central to a study of the overall engine flowpath. Reference (3) provides an example of a study on scaling of performance of a set of combustors of identical configurational design operated under different conditions of entry pressure and temperature, and Ref. (26) provides a scheme for flowpath scaling of an engine relative to chosen scale design of combustor.

A scramjet combustor may be designed for dual-mode operation, that is for operation under subsonic and supersonic flow conditions. However, attention is concentrated on operation under wholly supersonic flow conditions; some remarks are made at the end of the report on dual-mode operation combustors.

The scaling of scram combustors pertains to the same parameters as involved in their design and operation, namely:

- ranges of operational conditions;
- geometry;
- air and fuel supply;
- cooling and thermal management;
- integration with other components upstream and downstream; and
- dynamic operation and control.

In addition, as stated earlier, scaling may involve consideration of mission requirements and constraints, that have an influence on overall engine flowpath selection.

The influence of these parameters need to be considered in relation to all of the processes involved in the combustor, namely:

- air and fuel mixture preparation and distribution,
- chemical action initiation and progress,
- ignition,
- flame formation and stability,
- progress of combustion,
- completion of combustion and heating of the working fluid, and
- heat transfer at material boundary surfaces.

The general flowfield involves

- multi-dimensional, possibly time-dependent, chemically reactive turbulent flow,
- with embedded shockwaves, that may be interacting with wall boundary layers and one another,
- with regions of flow separation and recirculation, and
- with nonuniformly distributed heat generation and wall heat transfer.

Under a variety of assumptions and approximations, one may describe the flowfield on a one-dimensional basis, as in Refs. (2) and (6). However, the detailed modeling of the processes involved must begin with compressible, Reynolds-averaged, turbulent Navier-Stokes equations in three spatial dimensions, and may need various other more sophisticated approaches in dealing with specific aspects.

Considering the status and feasibility of testing scram combustors and generating data, while long and short duration facilities are available for testing at low and moderate flow speeds (Mach numbers under 5 at entry into the combustor), the ability to generate the combination of operational parameters, on one hand, and the feasibility of making measurements, in addition to those at the combustor walls, in the body of the flow are indeed rather restricted. It is rarely, and only in research-level apparatus, that one is able to obtain anything other than performance on a one-dimensional flowfield basis (Refs. (5) and (6)).

An example that can be cited in this context is the problem of establishing completion of chemical action or progress of combustion. While various types of prediction schemes yield, for example when hydrogen fuel is burnt in air, values for unreacted hydrogen, and partially and fully reacted hydrogen, there are very few measurements from which predictions can be verified with data of any aspect of those parameters. Furthermore, it can be readily anticipated that the distribution of chemical action and combustion is nonuniform over the flow cross-sectional plane, and verification of such distribution requires data scanning the cross-section.

At the same time, it should be stated that, from the point of view of establishing overall performance of a combustor, a one-dimensional approach to measurements and performance prediction seems to yield substantially useful results, at least for purposes of comparing one design, or one set of operational conditions, with another. This has been encouraging, albeit in a limited fashion, in combustors that can be said to be well-behaved; that is, combustors in which the wall pressure distribution is steady and acceptably rational in repeated tests in which one parameter, such as the air flow speed or fuel equivalence ratio, is varied.

The one-dimensional approximation may also be utilized where ignition delay, as evidenced by wall pressure changes, may occur due to complications in chemical kinetics. However, a one-dimensional approach is not useful when it is suspected that there are complex flowfield-related phenomena, for example, separation and formation of recirculation zones, in the region of fuel admission. Even in such cases, the variation of flow and chemical properties in the main combustor can be assessed using a one-dimensional approach in measurements and modeling for purposes of comparing combustors.

In light of the foregoing, scram combustor scaling may be based on a consideration of the following, while noting that the various parameters are indeed closely inter-related:

- fluid flow process;
- ignition and flame stabilization;
- chemical action and combustion;
- thermal balance; and
- test environment.

The latter, namely the test conditions, needs some further explanation.

9.4.1 TEST ENVIRONMENT

The basic operation of a scram combustor rests on air and fuel supply with either auto-ignition of the fuel or ignition with an external source of energy input. In practical testing, whether on ground or in flight, it can be expected that the composition of air will vary due to contamination and vitiation in different cases. For example, humidity of air can vary substantially in flight and ground tests in an uncertain fashion. Also, in long and short duration test facilities, the method of generating high pressure, high enthalpy air with electrical heaters, plasma arcs, and fuel combustion gives rise to

- contamination with charged particles or dissociated and ionized species, or
- vitiation with products of combustion.

The performance data from tests generally display effects due to such causes in

- ignition and flame stability and
- progress of combustion.

The extent of such effects along the combustor and in resulting performance becomes an issue in comparing overall combustor performance of different combustors tested under uncertain conditions.

Two aspects of the issue are

- the method of ensuring test conditions that are identical or definitely scaled, and
- the extent of the effects and their possible influence on the realized performance.

Another aspect of the test environment that is of interest is the use of additives along with air and fuel, for example, for assisting in positive definite ignition of the mixture. Silane is a common additive, and, when utilized, affects the chemical reactions substantially, as intended.

9.4.2 OUTLINE OF THE REPORT

The report deals with the five major aspects, as listed above, and presents the various approaches to scaling developed to-date and the directions for future studies in each area.

Two illustrative examples are also included to illustrate possible approach to

- combustor scaling and
- flowpath scaling relative to a combustor that is scaled.

9.5 APPLICATIONS

The following cases are identified for evolving and illustrating scaling procedures:

- Class A. A combustor of given configuration and size operated under off-design conditions of entry thermodynamic properties;
- Class B. A combustor of given configuration and size operated under off-design conditions of

B.1. fuel equivalence ratio,
B.2. air composition relative to standard air composition, and
B.3. turbulence characteristics of air supply
B.4. fuel additives

- Class C. Groups of combustors of given configuration operated under selected combinations of entry thermodynamic properties.

- Class D. A combustor of given configuration installed in a group of engines, each engine identified with a flight vehicle of given mission.

Under Class A, changes may be considered in pressure, enthalpy, or both of entry air, giving rise to change in density, acoustic speed, flow velocity, and derived values of Mach number, Reynolds number, and mass, momentum, and energy flux. Changes also may occur in specific heats and transport properties.

Under Class B.1, changes are considered only in fuel equivalence ratio, all other entry and operating conditions held fixed.

Under Class B.2, the supply air is considered with contamination with dissociated and ionized species, vitiation with products of combustion that may be utilized for heating the air, and presence of water due to humidity of air or combustion, while the entry thermodynamic state properties may be held fixed.

Under Class B.3, the turbulence scale and intensity are assumed to vary while all entry thermodynamic and flow characteristics are held fixed.

Class C pertains to a group of combustors in which a design parameter is related to an assumed change in an entry thermodynamic state property and which is operated with variations in another entry thermodynamic state property or fuel equivalence ratio. For example, the group of combustors may be of different sizes relative to the pressure of supply air, and each member of the group may be operated with air at different values of entry enthalpy or with a number of values of fuel equivalence ratio. The pressure of supply air may also be looked upon as a means of regulating momentum of entry air per unit cross-sectional area of combustor entry section.

Finally, under Class D, a number of engine configurations is considered, each engine being chosen for a specific flight vehicle application; the engines are based on a chosen combustor configuration; differences in the combustor arise from the manner in which it is integrated into the engine flowpath.

9.5.1 SCRAMJET CONFIGURATION

The four cases A, B, C, and D described above are of interest in different scramjet configurations which may be classified as follows from the point of view of geometry:

i. fixed geometry,
ii. entirely variable geometry in respect of duct wall, injectors, and other features, and
iii. a geometry with special features.

Under III we may include combustors in which a specific relation is invoked between an entry flow parameter and a geometrical feature of the combustor, for example pressure of air supply and a characteristic dimension of the combustor.

9.5.2 SPECIFIC EXAMPLES

From various points of view, one may identify a series of example cases of interest as shown in Table I. The fifteen cases cited are illustrative of various applications in ground and in flight testing.

There is probably no case in which groups of combustors have been tested and data documented, that would provide adequate basis for generating scaling laws relative to the entire set of variables and their effects on performance and operation. Individual studies have been undertaken in most cases under one of the 15 categories.

9.5.2.1 PERFORMANCE PARAMETERS

Scram combustors may be compared with one another on the basis of a number of operational and performance parameters:

- ease of auto-ignition
- flame stabilization
- combustor effectiveness
- kinetic energy efficiency
- stagnation pressure loss
- energy availability generation efficiency
- mixing efficiency of air and fuel
- mixing power loss coefficient
- reactedness efficiency
- reaction completion

Two types of problems are of interest in scaling:

i) those in which the change in operation or performance is to be determined in a relation to the operation or performance of scaled model in a given system that may be referred to as the original; and
ii) those in which the objective is to establish the conditions under which a scaled model may be made to approach a given system (or the reference) in respect of one or more operational or performance parameters.

The second category of problems may involve changes in both design and combustor entry and operating conditions. A necessary caution is that such changes may modify the combustor to an extent that it becomes a new configuration only remotely related to either the original or the scaled model, and, therefore, are outside the scaling exercise.

9.5.2.2 CATEGORIES OF SCALING

Based on the performance parameters, the direct and the indirect problem of scaling can be divided into several steps as follows:

i) gas dynamic scaling,
ii) gas thermal properties scaling,
iii) ignition scaling,
iv) mixing scaling,
v) chemical action and combustion scaling, and
vi) friction and heat transfer.

1. GAS DYNAMIC SCALING

The variables in gas dynamic scaling can be chosen as pressure or enthalpy (or equivalently temperature in many cases) and a typical flow scale of the combustor, such as its diameter of cross-section. The scaling parameters are the flux of mass, momentum, and energy at entry to the combustor, and the corresponding Reynolds number and Mach number.

PRESSURE

Considering that pressure and duct diameter are varied in combination, similarly with respect to Reynolds and Mach number requires that

$$PD = \text{constant} \qquad (1)$$

and

$$V \alpha \sqrt{T} \qquad (2)$$

Considering mass flow, and denoting properties in the Reference with [ ]*, one can write

$$m = \dot{m}^* \sqrt{\frac{T^*}{T}} \cdot \frac{D}{D^*} \qquad (3)$$

Then, in the case P > P* by choice, D < D* and the mass flow in the model must be modified such that m is given by Eq. (9) with the value of gas temperature T chosen. The fuel equivalence ratio is held constant in the Reference and the models.

Now, the choice of pressure may affect the chemical action therefore also the friction and heat transfer processes. These matters are discussed further later as appropriate.

TEMPERATURE

Considering that temperature and duct diameter are varied in combination, similarly with respect to Reynolds and Mach number requires that

$$D/T = \text{constant} \qquad (4)$$

and

$$V/\sqrt{T} = \text{constant} \qquad (5)$$

Considering mass flow, one can write

$$m = m^* \left(\frac{T^*}{T}\right)^{1/2} \cdot \frac{D^*}{D} \cdot \frac{P^*}{P} \qquad (6)$$

Thus, in the case T > T*, D > D*, and the mass flow needs to be set equal to m* that is modified as in Eq. (6), with the values of P chosen. It is observed that the mass flow also depends on the ratio $(T/T^*)^{1/2}$, and, therefore, the pressure P to be employed in the model has to be selected based on the temperature value specified in the model.

It is again necessary to point out that chemical action depends on the temperature of the reactants and, therefore, heat release, friction, and heat transfer are affected during this type of scaling.

2. GAS THERMAL PROPERTIES SCALING

The thermal properties of interest are the specific heats and the gas constant. Only flow variations are considered here, in particular the entry Reynolds and Mach number. Thus

$$D/R = \text{constant} \qquad (7)$$

and

$$V / \sqrt{\gamma RT} = \text{constant} \qquad (8)$$

Considering mass flow, one can write

$$\dot{m} = \dot{m}^* \frac{P\ D}{P^*\ D^*} \sqrt{\frac{\gamma R\ T^*}{\gamma^* R^*\ T}} \qquad (9)$$

It is clear that the choice of pressure and temperature for the gas under consideration for use in the model involves the thermal properties of the gas, and therefore cannot be made entirely arbitrarily. It is useful to note that for a calorically perfect gas $\gamma\ R = c_p\ (r - 1)$.

3. MIXING SCALING

Three parameters involved in mixing are (i) completion of mixing, (ii) power required for mixing, and (iii) mixing enhancement. The parameters can be defined in different schemes of mixing with respect to the means adopted for bringing the mixing fluids into contact and mixing:

- fluid jets at walls
- fluid jets at struts
- vortex generators and other means, and
- shocks.

Turbulence and compressibility effects cause a variety of complications in the identification and application of parameters during scaling.

4. CHEMICAL SCALING

Two main considerations in chemical scaling are

- ignition and
- progress of chemical action.

It is of interest to examine the changes in those with respect to changes in

- air pressure
- air enthalpy
- air composition
- fuel equivalence ratio
- fuel enthalpy and
- fuel composition in terms of possible additives.

Three parameters that enter into chemical scaling are as follows:

- D_1 which is the ratio of flow transit time through a combustor length to the chemical reaction time;
- D_2 which is the ratio of heat added by chemical reaction to the stagnation enthalpy of the flow; and
- GW which is the ratio of enthalpy at the wall temperature to stagnation enthalpy of the flow.

Denoting the characteristic chemical time by t_c, the combustion efficiency by η_c, the heat of combustion by Δhc, and the wall temperature by T_W, one can define

$$D_1 = L/ut_c \qquad (10)$$

$$D_2 = \eta_c\ \Delta h_c / \left(c_p T + u^2/2\right) \qquad (11)$$

$$GW = \frac{c_p / T_w}{\left(c_p T + \frac{u^2}{2} \right)} \tag{12}$$

In cases where it is possible to assume that chemical reactions are predominantly binary, combustion time can be taken to be linear in density and one can set up a relation between D_1 and Re, the Reynolds number; for example,

$$D_1 = \rho L/u \exp(-T) \tag{13}$$

$$= Re \frac{\sqrt{T}}{u^2} \exp(-T) \tag{14}$$

where it is assumed that the coefficient of viscosity is proportional to $\sqrt{T}$. One can write further

$$D_1 = Re \cdot \frac{1}{M} \cdot \frac{\exp(-T)}{u} \tag{15}$$

However, it is virtually impossible in practice to be able to choose u, T, and model size such that the main non-dimensional parameters are prescribed in the reference and the model. In general, in supersonic combustion tests, it is far more common to duplicate primitive variables, especially model length and test gas composition.

AIR PRESSURE

Considering ordinary fuels such as hydrogen and hydrocarbons, ignition reactions can be shown to follow the scaling law

$$PL = \text{constant} \tag{16}$$

Similarly, the completion of chemical reaction can be related to the factor

$$P^n L = \text{constant} \tag{17}$$

where n has a value close to 2.

In the foregoing it is assumed that all other properties are held fixed between the reference and the model.

AIR AND FUEL ENTHALPY

Ignition and progress of chemical reaction are highly sensitive to the enthalpy of the reactants.

At a given value of pressure, ignition time depends on the length of time required for creation of a radical tool that produces a self-sustained reaction. Hence ignition is sensitive to the initial enthalpy level.

Chemical reaction time however is not very sensitive to the temperature of the reactants, since, once ignition has occurred, chemical reactions proceed without need for large activation energies.

AIR COMPOSITION

The composition of air may vary in many respects:

- humidity
- atomic species
- products of combustion, and
- dust and other particulates.

HUMIDITY

The presence of water gives rise to the possibility of third-body reactions both during ignition reactions and subsequently during chemical action with combustion.

ATOMIC OXYGEN

Small quantities of atomic oxygen affect ignition delay. However, once the atomic oxygen is consumed, there is little further effect due its presence.

FRICTION AND HEAT TRANSFER SCALING

The theory of compressible viscous flow is reasonably well developed, taking account of turbulence and pressure gradient, insofar as well-behaved flows are concerned; that is, flows with no strong gradients as in shockwaves, recirculations, or separations (Ref. 19). The calculation scheme, however, does not include possible nonuniform combusting flows. Thus, although in several test data sets, one can establish friction coefficients and associated heat transfer coefficients, no reliable correlations can be set up for their variation with respect to flow and chemical parameters.

CONSTRAINTS IN SCRAMJET OPERATION

Several constraints in the operation of scram combustors are as follows.

- Pressure: Two factors that can be noted are:
    1. the ambient pressure in a combustor must be above a minimum value in the case of each fuel; and
    2. the nature of chemical reactions generally shifts towards the molecular type as the pressure is increased, and therefore the heat of reaction realized is a function of pressure.
- Temperature: Each fuel can be associated with an auto-ignition temperature.

THE AUTO-IGNITION TEMPERATURE MAY BE REALIZED AS A RESULT OF

- mixing between reactants one of which is at a high enthalpy;
- shockwave action when a chock becomes formed in the initial mixing region; or
- a gradual build-up of a pool of radicals produced with a small rate of chemical action over some part of the combustor, followed by the appearance of a flame that becomes stabilized at a suitable location.

WALL EFFECTS

The combustor walls affect the performance of a combustor in several ways:

- Effect of wall confinement on mixing: The growth of a mixing layer and the process of mixing are affected by the boundary walls.
- Combustion of fuel occurring at the wall is affected by the temperature and catalytic action of the wall material surface.
- Friction and heat transfer at the wall are affected by the combustion and heat release that occur adjacent to the wall.

ONE-DIMENSIONAL PERFORMANCE PREDICTIONS

A series of tests have been reported (Ref. 3) in which a scram combustor has been scaled for physical size based on the selection of a value of air pressure for its operation using a law of the form

$$PL^2 = \text{constant} \qquad (18)$$

In particular, two combustors, one referred to as the large combustor (operating at low pressure) and the other as the small combustor (operating at the higher pressure), are selected and tested at various selected values of air enthalpy and chosen value of fuel equivalence ratio. In the following, an attempt has been demonstrated to establish the performance of the combustors on a theoretical basis using one-dimensional flow analysis.

The one-dimensional analysis is described in terms of

i. the basic flowfield
ii. mixing of air and fuel
iii. chemical action, ignition, and combustion, and
iv. friction and heat transfer

i. Basic Flowfield

The basic flowfield consists of

- air that may have been variously processed by the air intake and other ducting present ahead of the combustor entrance, for example, an isolator section; and
- fuel for combustion, that may be a liquid or a gas, with, on occasion, additives.

It is possible that in a particular case, some of the fuel is added to the air before entry into the combustor. In such a case the flow process, including mixing, between air and fuel upstream of the combustor need to be determined with the attendant complexities. More generally, the air and fuel are supplied as two streams at entrance to the combustor. The interaction and mixing between the streams are discussed in the next section. Here, we may note a general description for the two reacting streams and the product generated following chemical action and combustion.

The simplest description for the three streams can be based on one-dimensional flow considerations. At this level, the flowfield description consists of the following:

- one-dimensional flow of each of the three streams with mass, momentum, and energy conservation, individually and in the overall;
- a means of establishing the generation and state of the product stream along the flowfield; and
- processes at the wall boundary of the flow.

It is assumed that the initial conditions of the two reacting streams, as well as the duct geometry along the flow are known. Under the one-dimensional approximation, the only geometrical variable of interest is the duct cross-sectional area normal to the general flow direction.

The mass flow of the two reacting streams along the flow depends on the amount of fluids undergoing chemical action, which, in turn, depends on mixing of the streams among various parameters. If it is assumed that the two reacting streams retain their initial state conditions everywhere along the flow, then the mass flow in the air and the fuel stream can be determined based on the reacted substances becoming part of the product stream, containing products of combustion. Then, at each cross-section along the flow, one has the two reacting streams and the product stream, and it is necessary to make further assumptions in order to proceed: (a) the three streams retain their characteristics in momentum and energy at each cross-section, and (b) a single value of pressure applies to the three streams. The latter is based on the premise that the two reacting streams enter the combustor at the same pressure, and the change in pressure due to chemical action and combustion applies uniformly to all the three streams. The unmixed air and fuel streams continue with their original characteristics so long as they are not mixed. The product stream at each section includes the product carried to that section from the upstream section and the amounts of the two reactants that become mixed (according to the mixing rule) at that section. The reactions at the section depend on the transit time in the section, the mixed fluid temperature and the concentration of various reactants. When the chemical reactions and heat release are accounted for, one obtains values for the modified pressure and the final temperature of the products. Once mixing is complete, the duct section is assumed to consist of a single stream containing partially and wholly reacted products.

ii. Mixing of Fuel and Air

The fuel may be injected in a variety of ways that can be grouped as follows:

- injection at a wall of the combustor, generally at an angle to the airstream with which it is expected to mix; and
- injection with some type of an injector located in the air stream.

It is generally assumed that the useful part of the momentum of injected fluid is the component coincident with the local air flow direction, and that the remaining part of the fuel jet momentum is indeed lost.

The main interest in calculations pertaining to mixing is in the following:

- rate of mixing along the flow,
- the total length required for completion of mixing, and
- the power expended in carrying out the mixing.

Various approaches to determining the foregoing have been evolved:

- correlations of experimental data on specific injection schemes (Ref. (2)), and
- empirical mixing theories.

The so-called standard mixing rule adopted is as follows: The mixing efficiency is prescribed in an exponential formed by writing

$$\eta_m = 1 - \exp(- cc \cdot x) \qquad (19)$$

where x denotes an axial length along the combustor, and

$$cc = \ln(1 - \eta_{max}) / L_{mix} \qquad (20)$$

with η_{max} equal to the maximum mixing efficiency at the end of the mixing length, and L_{mix} equal to the length chosen for mixing. In standard mixing, the maximum mixing efficiency and the mixing length are chosen at typical values, for example 95% and 20 cm. In other cases, mixing is specified with other choices.

iii. Chemical action, ignition, and combustion

Finite rate chemistry is adopted throughout for the calculation of chemical reactions. The fuels that can be handled with the code are

- hydrogen,
- hydrocarbon, and
- hydrogen mixed with silane.

Various chemical reaction schemes for H_2/air can be chosen from literature (Refs.24-25).

Ignition

In general, ignition can be identified as due to

- auto-ignition,
- delayed ignition following a slow accumulation of heat during low rate chemical action, and
- externally-supported ignition.

In the particular group of simulations of scaled combustors, ignition has been assumed to occur at the same location as in the tests under the same conditions.

iv. Friction and Heat Transfer

The prediction scheme requires a friction coefficient to be chosen and used. In a so-called standard friction coefficient assumption, the coefficient is assigned a value, for example 0.003. In other cases, this can be varied.

In all of the predictions, it is assumed that the combustor walls are adiabatic and no heat transfer is allowed.

9.5.2.3 TEST CASES

A detailed description of the test cases can be found in Ref. 3.

All of the cases belong to a single combustor configuration, namely a constant area duct of a given length. Two sets of combustors are considered, one referred to as the large combustor and the other as the small combustor, the large combustor operating with air supply at a reduced, low pressure and the small combustor operating with high pressure air supply. The main design and operating parameters of the combustors are given in Tables 2 and 3. The large combustor is 5 times larger than the small combustor.

As can be seen from Tables 2 and 3, the scaling is based on

PD = constant

in the two combustors. With the Mach numbers being in the same range, similarity is encouraged with respect to Reynolds and Mach numbers.

Predicted Results

The results of prediction calculations are presented in terms of pressure variation along the combustor in various cases, in figures 2-3 as indicated in Tables I.4 and II.

The one-dimensional calculations also provide other efficiency parameters, such as

- kinetic energy efficiency,
- stagnation pressure loss coefficient, and
- completion of chemical reaction.

TABLE I
Example Cases for Scaling

Number	Identification	Variable	Affecting
1.	I.A.1. II.A.1.	supply air pressure	▪ mass flux ▪ flow velocity ▪ Re_1 ▪ M_1 ▪ chemical action ▪ transport processes
2.	I.A.2. II.A.2.	supply air enthalpy	▪
3.	I.B.1. II.B.1.	fuel equivalence ratio	▪ chemical action
4.	I.B.2.1. II.B.2.1.	humidity in air	▪ mass flux ▪ flow velocity ▪ Re_1 ▪ M_1 ▪ chemical activity
5.	I.B.2.2. II.B.2.2.	atomic oxygen in air	▪ chemical activity
6.	I.B.2.3. II.B.2.3.	combustion products in air	▪ chemical activity
7.	I.B.2.4. II.B.2.4.	solids content in air	▪ chemical activity ▪ transport processes
8.	I.B.3. II.B.3.	supply air turbulence	▪ chemical activity ▪ transport processes
9.	I.B.4. II.B.4.	fuel additive	▪ chemical activity ▪ transport process
10.	III.C.1	supply air enthalpy varied at chosen pressures in different groups of combustors	▪ chemical activity ▪ transport processes
11.	III.C.2.	supply air composition varied at chosen pressures in different groups of combustors	▪ chemical activity ▪ transport processes
12.	III.C.3.	fuel additive varied at chosen pressures in different groups of combustors	▪ chemical activity ▪ transport processes

13.	I.D.1. II.D.1.	engine configuration for selected mission	
14.	III.D.1.	engine configuration for selected mission, entry air property varied	
15.	III.D.1.	Engine configuration for selected mission, fuel additive varied	

TABLE 2
Large Combustor Data

Designation	P (kPa)	T (K)	M	ϕ	Figure Number
B	17.0	1100	4.42	1.23	--
C	18.2	1520	4.37	1.41	--
D	14.0	1640	4.38	1.26	--
E	20.9	2080	4.26	1.32	--
F	14.2	1150	4.43	1.23	--
G	7.84	1010	4.47	1.53	--

TABLE 3
Small Combustor Data

Designation	P	T	M	ϕ	Figure Number
B	77.8	1100	4.47	2.39	--
C	91.7	1530	4.29	1.24	--
D	83.1	1760	4.17	1.02	--
E	99.6	2400	3.96	1.35	--
F	66.4	1060	4.48	1.36	--
G	42.9	1080	4.47	1.31	--

9.6 APPROACH IN SCALING TESTS OF PULSONETTI/STALKER

Pulsonetti and Stalker (Ref. 3) conducted shock-tunnel experiments to aid their scaling study. For their study, it was considered desirable to focus on a simple configuration, and thus experiments were conducted with two constant area rectangular combustors of rectangular cross section, which differed in size by a factor of 5. Fuel was injected, parallel to airstream, from the trailing edge of a centrally located strut. The experiments were done in a shock tunnel. Because of the high stagnation enthalpy of shock tunnels, temperatures which allow combustion could be produced at high supersonic Mach number, and this increases the amount of fuel which can be burned without causing thermal choking. Therefore, by suppressing thermal choking and boundary layer separation, shock tunnel experiments can be expected to more clearly reveal the fundamental phenomena of supersonic combustion.

Two sets of tests were conducted to simulate different flight trajectory conditions.

- constant stagnation pressure and different stagnation enthalpies
- constant stagnation enthalpy and different stagnation pressures

A geometric scaling factor of 5 was chosen based on tunnel operating conditions and limits. Turbulent mixing was based on distance for mixing to begin, and distance for mixing to complete. It is argued that pressure-length scaling is valid for ignition reactions. Friction and heat transfer are also argued to follow PxL scaling.
The experimental results of Ref. 3 were used as the primary test case for testing our calculations. In general, the predicted results with SCRAM-3L match the measurements in all cases. Examples of these comparisons are shown in Figs. 1-4 of Ref. 3. It may be noted that the calculations have been performed assuming that ignition occurs where experimental data indicate a rise in temperature. It is also possible to conclude that the type of data obtained in pulse facilities can be generated satisfactorily with the SCRAM-3L procedure.

9.7 CONCLUSIONS

The pressure-length scaling criterion is a good starting point for more detailed studies on combustor scaling. This rule applies to supersonic combustion configurations provided that binary reactions are involved throughout the whole flowfield, or chemical equilibrium prevails (yielding mixing limited combustion). The experiments by Pulsonetti and Stalker (Ref. 3) in constant area ducts support this finding. Further calibration and verification of scaling criteria deduced by analysis for combustors is desirable and recommended.
The results of the SCRAM-3L code are being used to independently deduce scaling rules. The experimental data of Ref. 3 on scaling of scram combustors have been qualitaively reproduced by prediction as shown in Figs.1-4. (See also comments in appendix). It is evident that low dimensional modeling, coupled with limited exercise of inert 3-D calculations, can yield substantial results.
Additionally, the scaling rules deduced by analysis for hypersonic vehicle components need further calibration and verification. The usual procedure is to generate one or more scaled-down component models and then test them under various initial conditions. Because of interactions between two or more components along the working fluid flowpath, the method of evolving such models and tests is non-trivial. As a system with a single flowpath of the working fluid from inlet entry to nozzle exit, the scramjet engine is subject to a variety of interactions among the components. That is the subject of Part 2 of this report.

9.8 RECOMMENDED AREAS FOR EXPLORATION

9.8.1 EFFECTS OF VITIATION: CONTINUATION OF THEORETICAL AND EXPERIMENTAL VALIDATION.

Scramjet combustor scaling is of interest in two major contexts:

- relating design, performance and operation of combustors of different scales, required to operate over defined ranges of combustor entry conditions; and
- establishing the influence of combustor scale on overall engine flowpath relative to mission needs.

Vitiation is still a big unknown and may affect scaling rules. We need to be able to quantitatively assess the influence of flow vitiation on these combustors (uncertainty in size and weight). What I am thinking of is a set of rules that allows one to “correct” vitiated data (in the same way that corrections are made for transonic flows and wall-effects). Both hydrogen and hydrocarbon combustors should be assessed. The experimental program, that France and US are contemplating, is a step in the right direction.

9.8.2 FLIGHT TESTING OF INTEGRATED SCRJ VEHICLE (FLOWPATH), PROPULSION – AIRFRAME INTEGRATION-.

Real advances in hypersonics will be made in quantum leaps and not by the usual incremental evolutionary changes. There are several uncertainties in ground-based procedures for the development of airframe-integrated scramjets.

They include:

- the effects of facility-induced turbulence and facility-induced contaminants (NO, H2, etc.,) on mixing, combustion, thrust
- effects of inadequate simulation of vehicle boundary layer on inlet and engine performance(scale)
- accuracy to which scramjet nozzle analysis and simulation techniques predict nozzle performance chemical kinetics, interactions, etc.

- determining the overall performance of an integrated scramjet propulsion system forebody through nozzle (tip-to-tail)

What is not known is what is really important in these procedures and simulations. Flight experiments should be conducted to provide clarification of the above. Furthermore, integration may only be resolved by flight test.

9.8.3 FACILITIES RESEARCH FOR HYPERSONIC TESTING.

New facility concepts are needed.

- Simulation of the hypersonic flight environment in Ground Facilities:
- Facilities research is needed to evaluate how to attain proper simulated conditions (pressure, temperature, gas medium, flow quality, scales), numerical methods development and application as a guide to ordering the importance of what needs to be simulated. Then, investigate specific suggestions of facilities (existing or planned) to overcome questioned areas, without presenting any facility as more than a partial solution.
- Effects of non-equilibrium free-streams on parameters measured in wind-tunnels
- Scramjet scaling and verification

9.8.4 ELECTROMAGNETIC FIELD INTERACTIONS IN HYPERSONIC FLOWS: PLASMA FLOW AND CONTROL IN HYPERSONIC ENVIRONMENTS, MHD ENERGY BYPASS.

Plasma flows are rapidly becoming a new enabling technology of interest. Besides the use of plasmas in space thrusters, a growing interest is evident in plasma-based aerodynamics, including flow manipulation through MHD forces, power generation, and drag reduction. In particular, unusual characteristics of weakly ionized non-equilibrium plasmas (WINP) for reducing shock-wave drag, mostly due to heating non-uniformities, for a hypersonic vehicle have received significant attention in recent years. In addition, MHD power generation is of interest for scramjet vehicles. In the AJAX concept, the traditional scramjet engine cycle is modified by adding a by-pass of energy from the inlet to the nozzle, i.e. from a MHD generator to a MHD accelerator. The MHD deceleration at the inlet produces flows at lower gas stagnation temperature as compared to ramp compression, and more energy can be added during combustion.

9.8.5 FUELS CONVERSION TECHNOLOGY: CONVERSION OF HYDROCARBON FUELS TO HYDROGEN FOR IN-SITU COMBUSTION (PROCESSES DIFFERENT FROM THE CLASSICAL ENDOTHERMICS).

Non-Catalyst Hydrogen Para-Ortho Conversion, Steam Reforming, Hydrocarbon Fuels reforming for thermal protection of hypersonic structures. This will have a **MAJOR** impact on the design of lifting hypersonic vehicles.

9.9 ACKNOWLEDGEMENTS

The authors are pleased to acknowledge the numerous contributions of their colleagues in NASA, other government labs, and the international aerospace community to the contents of this report. The authors are especially thankful to Prof. Stalker (Australia), Charles (Chuck) McCLinton of NASA Langley, and Dr. Allan Paull (Australia) for providing essential materials, interesting ideas, and making time for critical discussions.

9.10 REFERENCES

[1] Bruno, C., " Modeling and Characterization of Vitiation Effects on Ignition/Combustion in Scramjets". (This NATO (RTO WG10) report, Section 4.3)

[2] Murthy, S. N. B., (2000), "Basic Performance Assessment of Scram Combustors", Progress in Astronautics and Aeronautics, Vol. 189, Chapter 10, p. 597, (Editors: E.T. Curran and S.N.B. Murthy), AIAA,2000

[3] Pulsonetti, M.V., and Stalker, R.J. "A Study of Scramjet Scaling". AIAA Paper No. 96 – 4533. (to be published in AIAA Journal.) (also M.V. Pulsonetti and R.J. Stalker., "Scaling of Supersonic Combustion", (NASA grant NAGW-674)).

[4] I.M. Blankson, "Air-Breathing Hypersonic Cruise: Prospects for Mach 4-7 Waverider Aircraft." Transactions of the ASME, Journal of Engineering for Gas Turbines and Power, pp104 - 115, Jan. 1994.

[5] Northam, G. B.; and Anderson, G. Y. "Supersonic Combustion Ramjet Research at Langley". AIAA Paper 86-0159, January 1986.

[6] Curran, E.T. et al " Fluid Phenomena in Scramjet Combustion Systems", Annual Reviews of Fluid Mechanics, vol 28, pp323 – 360, 1996.

[7] Ferri, A., "Review of SCRAMJET Propulsion Technology". Journal of Aircraft, vol. 5, No.1, Jan.-Feb. 1968.

[8] McClinton, C. R. "Private Communication- Supersonic and hypersonic combustion". 1999 - 2001.

[9] Stalker, R.J., "Thermodynamics and Wave Processes in High Mach Number Propulsive Ducts". AIAA Paper 89-0261, January 1989.

[10] Riggins, D. W.; and McClinton, C. R., "A Computational Investigation of Mixing and Reacting Flows in Supersonic Combustors". AIAA 92-0626, Jan. 1992.

[11] Kamath, P.; and McClinton, C. R., "Computation of Losses in a Scramjet Combustor". AIAA Paper 92-0635, January 1992.

[12] Riggins, D. W.; and McClinton, C. R.: Analysis of losses in Supersonic Mixing and Reacting Flows. AIAA Paper 91-2266, July 1991.

[13] Paull, A., Stalker, R.J., Mee, D.J., "Experiments on supersonic combustion ramjet propulsion in a shock tunnel". J. Fluid Mechanics, Vol. 296, pp. 159-183, 1995.

[14] Stewart, D. G., "Selected Combustion Problems", Advisory Group for Aeronautical Research and Development, pp 384-413, Butterworths Scientific Publications, London. 1956.

[15] Stewart, D. G. And Quigg, G.C., 9th International Symposium on Combustion. Pp. 707 – 921. Academic Press, New York. 1963.

[16] Benelli, G., Bruno, C., and Marcolongo, V., (1992), "Scaling laws for industrial gas turbines", in: Proc. of the Joint French, Italian and Swedish Sections of the Int.l Combustion Institute, Capri, 21-24 Sept.1992, CUEN Publishers, Naples, page III-7.

[17] Penner, S. S. "Chemistry Problems in Jet Propulsion", Chapter XXV. Pergamon Press, 1957.

[18] Huber, P.W., Schexnayder, C.J, and McClinton, C.R. NASA Tech Paper 1457, 1979.

[19] Anderson, J.D., "Hypersonic and High temperature Gas Dynamics". Chapter 17. McGraw-Hill Book Company. New York. 1989.

[20] Shen-Tao Yu, et al., "Basic Equations of Chemically Reactive Flow For Computational Fluid Dynamics", Paper AIAA-98-1051, AIAA 36th Aerospace Sciences Meeting & Exhibit, January 12-15, Reno, NV. USA.

[21] Daso, E. and Blankson, I.M., "Generalized Thermo-Fluid Equations for perfect, Real-Gas, High Temperature and Non-Equilibrium Flows", Paper AIAA-99-0417, AIAA 37th Aerospace Sciences Meeting & Exhibit, January 11-14, Reno, NV. USA.

[22] Viviand, H. "Similitude in Hypersonic Aerodynamics", in: "Hypersonic Flows for Re-entry Problems", Vol. I,edited by J.-A. Desideri, R. Glowinski and J. Periaux, Springer-Verlag, Berlin, 1991, pp.72-97.

[23] Sarma, G.S.R., "Physico-chemical modeling in hypersonic flow simulation", Progress in Aerospace Sciences., Vol. 36, No. 3-4, p. 281. (2000)

[24] Jachimowski, C.J., "An Analytical Study of the Hydrogen-Air Reaction Mechanism with Application to Scramjet Combustion", NASA Technical Paper 2791. (1988),

[25] C. John Marek, "Computation of Kinetics for the Hydrogen/Oxygen System Using the Thermodynamic Method", NASA TM107340, October 1996.

[26] Czysz, P.; and Murthy, S. N. B.: Energy Analysis of High-Speed Flight Systems. High-Speed Flight Propulsion Systems, Progress in Astronautics and Aeronautics Series (Edited by S. N. B. Murthy and E. T. Curran), pp. 143-235, AIAA, 1991.

[27] V. Gusev, N. Blagoveshchensky, S. Zadonsky, "The Integration of a Hypersonic Vehicle airframe with an Airbreathing Engine." AIAA Paper 93-5034. AIAA/DGLR 5th International Aerospace Planes Conference, Munich, Germany.

[28] I.M.Blankson, J.S.Pyle, "NASA's Hypersonic Flight Research Program." AIAA Paper 93 -0308. Thirty-first Aerospace Sciences Meeting , January 11-14, 1993. Reno, NV, USA.

[29] J.W. Haney, "A Waverider Derived Hypersonic X-vehicle." AIAA Paper 95-6162. AIAA 6th International Aerospace Planes and Hypersonic Technologies Conference, Chattanooga, TN.

[30] G.A.Molvik, J.V.Bowles, L.C.Huynh, "Analysis of a Hydrocarbon Scramjet with Augmentsd Preburning." AIAA Paper 92-3425. AIAA/SAE/ASME/ASEE 28th Joint Propulsion Conference. July, 1992. Nashville, TN, USA.

APPENDIX 1. THEORETICAL CONSIDERATIONS

In the combustor, it is assumed that the compressible reactive Navier-Stokes equations contain all the physics needed to derive scaling laws for scramjets (Refs.19-21). In addition, the flow at the combustor entrance is taken to be "clean" and non-vitiated. The subject of vitiation, and its impact on combustor flows is considered by Bruno (Ref.1, this issue.). Vitiated flows contain unwanted chemical and other non-inert contaminants in the air-stream entering the combustor. The question is how to characterize and quantify the effects due to vitiated air, since it will not be the 'air' fed the combustor in actual flight.

Simplified analysis aimed at deriving scaling rules of scramjet combustors may follow two traditional approaches: the formal method (Viviand, Ref. 22, and Ref. 3), and the use of order-of-magnitude arguments. It is illustrative to understand how the pressure-length scaling arises and under what conditions. To fix ideas, a general analysis of a 2D combustor flowfield is considered, where the flow is supersonic throughout. The governing equations are those appropriate to boundary layers or mixing layers, with allowance for a transverse pressure gradient. Streamwise and transverse coordinates are designated by x and y respectively, with corresponding velocities u and v. The Faire-Averaged Navier Stokes equations for the steady flow in a turbulent boundary layer of a viscous, heat conducting, reacting gas mixture with species diffusion, allowing for the momentum equation in the transverse direction may be written as:

$$\frac{\partial(\rho u)}{\partial x}+\frac{\partial(\rho v)}{\partial y}=0$$

(mass continuity)

$$\rho u\frac{\partial u}{\partial x}+\rho v\frac{\partial u}{\partial y}=-\frac{\partial p}{\partial x}+\frac{\partial}{\partial y}\left\{(\mu+\varepsilon)\frac{\partial u}{\partial y}\right\}$$

(momentum in x-direction)

$$\rho u\frac{\partial v}{\partial x}+\rho v\frac{\partial v}{\partial y}=-\frac{\partial p}{\partial y}$$

(momentum in y-direction)

$$\rho u\frac{\partial C_i}{\partial x}+\rho v\frac{\partial C_i}{\partial y}=\frac{\partial}{\partial y}\left\{\rho\left(D+D_T\right)\frac{\partial C_i}{\partial y}\right\}+\frac{d}{dt}\left(\rho C_i\right)$$

(species transport and diffusion)

$$\rho u\frac{\partial h}{\partial x}+\rho v\frac{\partial h}{\partial y}-u\frac{\partial p}{\partial x}=\left(\mu+\varepsilon\right)\left(\frac{\partial u}{\partial y}\right)^2+\frac{\partial}{\partial y}\left\{\left(\frac{k+K}{c_p}\right)\frac{\partial h}{\partial y}\right\}$$
$$+\frac{\partial}{\partial y}\left[\left\{\frac{k}{c_p}\left(L-1\right)+\frac{K}{c_p}\left(L_T-1\right)\right\}\sum_i h_i\frac{\partial C_i}{\partial y}\right]$$

(energy balance)

$$P=\left(\sum_i {C_i}/{m_i}\right)\rho RT$$

(equation of state)

where ρ, p, h are mean values of density, pressure and enthalpy per unit mass, ρI is the density of species "i", mi is the molecular weight, Ci = ρi / ρ is the mean mass fraction , and hi is the mean enthalpy of that species, whence h=ΣCi . hi.

The frozen specific heat at constant pressure is Cp, given by Cp= ΣCi., where Cpi = ∂hi /∂T is the frozen specific heat of species " i ".

The molecular coefficients of viscosity and thermal conductivity are μ and k, D is a binary molecular diffusion coefficient, L = k/ ρ D Cp is the Lewis number, and ℜ is the universal gas constant. ρD is assumed to be the same for all species in the gas mixture, a convenient simplification which will not influence the scaling argument developed below, as the relation between the molecular diffusion coefficients is not expected to vary with scale or pressure. Note that μ , k, and ρ D are functions of temperature.

The turbulent coefficients of viscosity, thermal conductivity, and diffusion are given by

$$\varepsilon=-\frac{\overline{(\rho\hat{v})\hat{u}}}{\partial u/\partial y},\qquad K=\frac{\overline{(\rho\hat{v})\hat{h}_i}}{\partial T/\partial y},\qquad \rho D_T=-\frac{\overline{(\rho\hat{v})\hat{C}_i}}{\partial C_i/\partial y}$$

Where the symbol "^" over a quantity indicates turbulent fluctuations. K and ρDT are each assumed to have one value for all species and, Lt = K/ρ Dt Cp.

The variables are normalized by choosing a reference length l, and using subscript "o" to refer to reference quantities. The resulting equations are:

$$\frac{\partial}{\partial x'}\left(\rho' u'\right)+\frac{\partial}{\partial y'}\left(\rho' v'\right)=0$$

$$\rho' u'\frac{\partial u'}{\partial x'}+\rho' v'\frac{\partial u'}{\partial y'}=-\left(\gamma M_0^2\right)^{-1}\frac{\partial p'}{\partial x'}+\mathrm{Re}^{-1}\frac{\partial}{\partial y'}\left\{\mu'\left(1+\frac{\varepsilon}{\mu}\right)\frac{\partial u'}{\partial y'}\right\}$$

$$\rho' u'\frac{\partial v'}{\partial x'}+\rho' v'\frac{\partial v'}{\partial y'}=-\left(\gamma M_0^2\right)^{-1}\frac{\partial p'}{\partial y'}$$

$$\rho' u' \frac{\partial C_i}{\partial x} + \rho' v' \frac{\partial C_i}{\partial y} = (Sc\,\mathrm{Re})^{-1} \left\{ \rho' D' \left(1 + \frac{D_T}{D} \right) \frac{\partial C_i}{\partial y'} \right\} + \left(\frac{l}{u_0} \right) \frac{d}{dt} (\rho' C_i)$$

$$\rho' u' \frac{\partial h'}{\partial x'} + \rho' v' \frac{\partial h'}{\partial y'} = \left(\frac{\gamma - 1}{\gamma} \right) \frac{\partial p'}{\partial x'} + (\gamma - 1) M_0^2\, \mathrm{Re}^{-1}\, \mu' \left(1 + \frac{\varepsilon}{\mu} \right) \left(\frac{\partial u'}{\partial y'} \right)^2$$
$$+ \mathrm{Pr}^{-1}\, \mathrm{Re}^{-1} \frac{\partial}{\partial y'} \left\{ k' \left(1 + \frac{K}{k} \right) \frac{\partial h'}{\partial y'} \right\}$$
$$+ \mathrm{Pr}^{-1}\, \mathrm{Re}^{-1} \frac{\partial}{\partial y'} \left[k' (L - 1) \left\{ 1 + \frac{K}{k} \left(\frac{L_T - 1}{L - 1} \right) \right\} \sum_i h_i' \frac{\partial C_i}{\partial y} \right]$$

$$P' = \left(\frac{P_0}{\rho_0} \right) \left(\sum_i C_i / m_i \right) \rho' R T$$

$$\mathrm{Re} = \frac{\rho_0 u_0 l}{\mu_0}$$

$$Sc = \frac{\rho_0 D_0}{\mu_0}$$

$$\mathrm{Pr} = \frac{\mu_0 c_p}{k_0}$$

where Re is the Reynolds number, Sc is the Schmidt number, Pr is the Prandtl number, and γ is the ratio of frozen specific heat at the reference condition, which is taken at the combustor entrance so that M_o becomes the combustor entrance Mach number.

Pulsonetti and Stalker concluded from the above equations that two geometrically similar combustors of different size will generate solutions which are similar (i.e. identical in the normalized variables if

i. The combustor entrance Mach number, temperature, and gas composition are the same
ii. γ, Re, Sc, Pr, and Le are the same
iii. The ratios of the turbulent to the molecular transport coefficients are the same.
iv. Either the dependence of boundary layer transition on Reynolds' number is the same in both cases, or the effects of the boundary layers on the duct walls is the same.
v. The reaction term, the last term in the species transport equation is the same.

The reaction term, of course, will vary with the reactants being used (Refs. 18-24). Pulsonetti and Stalker (Ref.3) focused on a model of the hydrogen-air reaction mechanism characterized by an ignition phase (involving two-body reactions), during which sufficient free radicals are produced to allow a second, reaction, phase (involving mainly three-body reactions) to proceed , involving significant heat release reactions. This choice was made to coincide with their associated experiments aimed at clarifying scaling phenomena. Their analyses considers two situations where scaling is possible. First case is where the reactions proceed at such a high rate that chemical equilibrium prevails throughout the flow-field, and mixing limited combustion occurs. The reaction term in the species transport equation vanishes because of the balance between the rate of appearance and disappearance of species. The second case occurs when the rate at which the reactions proceed in the second phase alone is much higher than the rate of local change in the flow-field. Chemical equilibrium

then prevails for this phase only. In terms of the Damköhler (Da) number for a reaction, defined as the ratio of flow residence time to time required for equilibration, a large Da means that the reaction is fast approaching equilibrium. It is then concluded that for radical pool formation reactions typical of the ignition delay period, Da scales as ρL, while heat release kinetics will scale as $\rho^2 L$. Using the ideal gas equation and keeping the combustor entrance Mach number and temperature the same, results in the pressure-length scaling rule for scramjet combustors. Most experimentalists would strongly take exception to large Da assumption: after all, scramjet combustion is precisely a case where kinetics times are of the same order of convection times. However in spite of these assumptions the experimental results of Ref. 3 seem to support the pressure-length scaling criterion for scramjet combustors.

APPENDIX 2. SIMULATION REQUIREMENTS

From an experimenter's viewpoint there are simply too many variables to attempt to duplicate. It can be said that maintaining all similarity parameters the same leads to the inevitable conclusion that the model must be exactly like the real article. The question then becomes, which parameters to keep the same and which to let float. To appreciate the experimenter's nightmare, a list of the various variables encountered in scramjet combustor testing is outlined below (McClinton, private communication) .
The primitive variables available, which describe the flow in a hypersonic combustor are:

P pressure (or r density)

T temperature

u velocity

L model length

ni gas composition

In principle, the composition can be manipulated in any fashion that results in duplication of the flight values of certain well-known dimensionless groups, i.e., simulation parameters. The first-order simulation parameters are:

M Mach number

Re Reynolds number

St Stanton number

D1 Damkohler's first number

D2 Damkohler's second number

GW wall enthalpy ratio

To these may be added certain second-order parameters such as:

Pr Prandtl number

Sc Schmidt number

The physical interpretation of the first three fluid dynamics and heat-transfer parameters is also well known, i.e., the Mach number represents the ratio of kinetic to thermal energy, the Reynolds number the ratio of inertial to viscous forces, and the Stanton number the ratio of heat flux to inviscid energy flux. However, the interpretation of the last three is less well known as they are more specific to hypersonic reacting flows. These three parameters are the ratios of flow transit time through the combustor to chemical reaction time (D1), the ratio of heat added by reaction to the stagnation enthalpy of the inviscid flow (D2) and the ratio of enthalpy at the wall temperature to stagnation enthalpy of the inviscid flow (GW). The second-order parameters represent gas properties, e.g., the ratio of viscosity to thermal conductivity and the ratio of viscosity to diffusivity. However, to the extent that these parameters reflect turbulence characteristics, they are more dependent on the

first-order simulation parameters than on molecular properties of the gas. The first-order parameters can, in turn, be related to the primitive variable as follows:

$$M \sim \frac{u}{\sqrt{T}} \tag{1}$$

$$Re \sim \frac{\rho u L}{\sqrt{T}} \sim \rho L M \tag{2}$$

$$St \sim \frac{q_w}{\rho u H} \tag{3}$$

$$D_1 \sim \frac{L}{u t_c} \tag{4}$$

$$D_2 \sim \frac{\eta_c \Delta h_c}{c_p T + \frac{u^2}{2}} \tag{5}$$

$$GW \sim \frac{c_p T w}{c_p T + \frac{u^2}{2}} \tag{6}$$

where t_c is a characteristic combustion time, q_w is heat flux to the wall, h_c is a combustion efficiency, Dhc is the heat of combustion, cp is a characteristic specific heat and Tw is the temperature of the combustor wall. The overall reaction time for a typical combustion process is generally proportional to both a function of pressure (or density) with an exponential dependency of approximately 1.75 and a function of temperature with an exponential dependency of unity. In certain restricted conditions wherein only binary (two-body) reactions occur, the combustion time is linear in density, leading to a direct relationship between Reynolds number and Damköhler's first number:

$$D_1 \sim \rho L/u \; exp\,(-T)$$

$$\sim Re \frac{\sqrt{T}}{u^2} \; exp\,(-T) \tag{7}$$

Hence, if velocity and temperature were to be duplicated, then simulation of Reynolds number would also satisfy the requirements for simulation of binary reaction time, and vice versa. This is the same conclusion arrived at in Ref. 3 . However, even in the simplest of situations, it is virtually impossible to manipulate the temperature, velocity and model length in a fashion that will simultaneously preserve the values of Mach number, Reynolds number, and Damköhler's numbers. Therefore, it is clear that, in general, in hypersonic combustion experiments it becomes necessary to duplicate the primitive variables, including model length and gas composition, to ensure a faithful representation of the coupled chemical and flow processes. This automatically satisfies all of the simulation parameter requirements, with the possible exception of wall temperature and wall reactivity simulation. It should be noted that the verification of the above conclusions could be affected by the impact of air vitiation in ground test facilities. Bruno (Ref.1, this issue) is modeling air vitiation effects on ignition/combustion and extrapolation from the ground testing data, using vitiated air, to pure-air flight.

APPENDIX 3

PART 2: FLOWPATH SCALING (To be concluded).

Contents:
Propulsion/Airframe Integration (uniqueness of PAI and requirements for flight)
Inlet/Isolator dynamics and scaling
Nozzle Scaling
Engine performance
Flow-path Scaling
Discussion
Conclusions.
Recommendations for future work, future experiments (“interactions testing”),
and associated calculations for interactions testing.

Comments on write up
Think in terms of extrapolation to flight
Grade technologies in terms of TRL

REPORT DOCUMENTATION PAGE

1. Recipient's Reference	2. Originator's References	3. Further Reference	4. Security Classification of Document
	RTO-TR-AVT-007-V2 AC/323(AVT-007)TP/25	ISBNs 92-837-0041-4 978-92-837-0041-8	UNCLASSIFIED/ UNLIMITED

5. Originator

Research and Technology Organisation
North Atlantic Treaty Organisation
BP 25, F-92201 Neuilly-sur-Seine Cedex, France

6. Title

Technologies for Propelled Hypersonic Flight
Volume 2 – Subgroup 2: Scram Propulsion

7. Presented at/Sponsored by

This report documents the results of the Applied Vehicle Technology Panel Working Group 10, Subgroup 2.

8. Author(s)/Editor(s)	9. Date
Multiple	January 2006
10. Author's/Editor's Address	**11. Pages**
Multiple	212

12. Distribution Statement

There are no restrictions on the distribution of this document. Information about the availability of this and other RTO unclassified publications is given on the back cover.

13. Keywords/Descriptors

Aerospace engineering
Aerothermodynamics
Boundary layer
Computerized simulation
Design
Enthalpy
Fluid dynamics
Hypersonic aircraft
Hypersonic characteristics
Hypersonic flight
Hypersonic flow
Hypersonic test vehicles
Hypersonic vehicles
Hypervelocity wind tunnels
Numerical analysis
Plug nozzles
Propulsion
Scramjets
Shock waves
Test facilities

14. Abstract

The RTO AVT Working Group 10 was aimed to address selected critical issues related to propelled hypersonic flight, to review the associated state of the art for analysis and design, as well as to recommend activities for further developments.

The three volumes cover mainly 3 parts corresponding to the output of three subgroups.

Subgroup 1 dealt with reviewing fundamental aspects on plug nozzles such as altitude adaptation aspects, influence of external flow on thrust and addressing design methods. Subgroup 2 addressed the physical modelling aspects associated with scram combustion including fuels, turbulence mixing, ignition and flame holding prediction capabilities. Subgroup 3 screened and repeated a large number of test cases for CFD validation for areas where CFD validation was deemed essential, such as transition, real gas flows, laminar and turbulent shock-boundary layer interaction, as well as base flows with and without plumes. High standards for the selection and evaluation of test cases for CFD validation were applied, resulting in an unprecedented effort to improve technologies for hypersonic flight.

NORTH ATLANTIC TREATY ORGANISATION

RESEARCH AND TECHNOLOGY ORGANISATION

BP 25
F-92201 NEUILLY-SUR-SEINE CEDEX • FRANCE
Télécopie 0(1)55.61.22.99 • E-mail mailbox@rta.nato.int

DIFFUSION DES PUBLICATIONS
RTO NON CLASSIFIEES

Les publications de l'AGARD et de la RTO peuvent parfois être obtenues auprès des centres nationaux de distribution indiqués ci-dessous. Si vous souhaitez recevoir toutes les publications de la RTO, ou simplement celles qui concernent certains Panels, vous pouvez demander d'être inclus soit à titre personnel, soit au nom de votre organisation, sur la liste d'envoi.

Les publications de la RTO et de l'AGARD sont également en vente auprès des agences de vente indiquées ci-dessous.

Les demandes de documents RTO ou AGARD doivent comporter la dénomination « RTO » ou « AGARD » selon le cas, suivi du numéro de série. Des informations analogues, telles que le titre est la date de publication sont souhaitables.

Si vous souhaitez recevoir une notification électronique de la disponibilité des rapports de la RTO au fur et à mesure de leur publication, vous pouvez consulter notre site Web (www.rta.nato.int) et vous abonner à ce service.

CENTRES DE DIFFUSION NATIONAUX

ALLEMAGNE
Streitkräfteamt / Abteilung III
Fachinformationszentrum der
Bundeswehr (FIZBw)
Friedrich-Ebert-Allee 34, D-53113 Bonn

BELGIQUE
Etat-Major de la Défense
Département d'Etat-Major Stratégie
ACOS-STRAT – Coord. RTO
Quartier Reine Elisabeth
Rue d'Evère, B-1140 Bruxelles

CANADA
DSIGRD2
Bibliothécaire des ressources du savoir
R et D pour la défense Canada
Ministère de la Défense nationale
305, rue Rideau, 9e étage
Ottawa, Ontario K1A 0K2

DANEMARK
Danish Defence Research Establishment
Ryvangs Allé 1, P.O. Box 2715
DK-2100 Copenhagen Ø

ESPAGNE
SDG TECEN / DGAM
C/ Arturo Soria 289
Madrid 28033

ETATS-UNIS
NASA Center for AeroSpace
Information (CASI)
Parkway Center, 7121 Standard Drive
Hanover, MD 21076-1320

FRANCE
O.N.E.R.A. (ISP)
29, Avenue de la Division Leclerc
BP 72, 92322 Châtillon Cedex

GRECE (Correspondant)
Defence Industry & Research
General Directorate, Research Directorate
Fakinos Base Camp, S.T.G. 1020
Holargos, Athens

HONGRIE
Department for Scientific Analysis
Institute of Military Technology
Ministry of Defence
H-1525 Budapest P O Box 26

ISLANDE
Director of Aviation
c/o Flugrad
Reykjavik

ITALIE
Centro di Documentazione
Tecnico-Scientifica della Difesa
Via XX Settembre 123
00187 Roma

LUXEMBOURG
Voir Belgique

NORVEGE
Norwegian Defence Research Establishment
Attn: Biblioteket
P.O. Box 25, NO-2007 Kjeller

PAYS-BAS
Royal Netherlands Military
Academy Library
P.O. Box 90.002
4800 PA Breda

POLOGNE
Armament Policy Department
218 Niepodleglosci Av.
00-911 Warsaw

PORTUGAL
Estado Maior da Força Aérea
SDFA – Centro de Documentação
Alfragide
P-2720 Amadora

REPUBLIQUE TCHEQUE
LOM PRAHA s. p.
o. z. VTÚLaPVO
Mladoboleslavská 944
PO Box 18
197 21 Praha 9

ROYAUME-UNI
Dstl Knowledge Services
Information Centre, Building 247
Dstl Porton Down
Salisbury
Wiltshire SP4 0JQ

TURQUIE
Milli Savunma Bakanlığı (MSB)
ARGE ve Teknoloji Dairesi Başkanlığı
06650 Bakanliklar – Ankara

AGENCES DE VENTE

NASA Center for AeroSpace Information (CASI)
Parkway Center, 7121 Standard Drive
Hanover, MD 21076-1320
ETATS-UNIS

The British Library Document Supply Centre
Boston Spa, Wetherby
West Yorkshire LS23 7BQ
ROYAUME-UNI

Canada Institute for Scientific and Technical Information (CISTI)
National Research Council
Acquisitions, Montreal Road, Building M-55
Ottawa K1A 0S2, CANADA

Les demandes de documents RTO ou AGARD doivent comporter la dénomination « RTO » ou « AGARD » selon le cas, suivie du numéro de série (par exemple AGARD-AG-315). Des informations analogues, telles que le titre et la date de publication sont souhaitables. Des références bibliographiques complètes ainsi que des résumés des publications RTO et AGARD figurent dans les journaux suivants :

Scientific and Technical Aerospace Reports (STAR)
STAR peut être consulté en ligne au localisateur de ressources uniformes (URL) suivant:
http://www.sti.nasa.gov/Pubs/star/Star.html
STAR est édité par CASI dans le cadre du programme NASA d'information scientifique et technique (STI)
STI Program Office, MS 157A
NASA Langley Research Center
Hampton, Virginia 23681-0001
ETATS-UNIS

Government Reports Announcements & Index (GRA&I)
publié par le National Technical Information Service
Springfield
Virginia 2216
ETATS-UNIS
(accessible également en mode interactif dans la base de données bibliographiques en ligne du NTIS, et sur CD-ROM)

NORTH ATLANTIC TREATY ORGANISATION

RESEARCH AND TECHNOLOGY ORGANISATION

BP 25
F-92201 NEUILLY-SUR-SEINE CEDEX • FRANCE
Télécopie 0(1)55.61.22.99 • E-mail mailbox@rta.nato.int

DISTRIBUTION OF UNCLASSIFIED RTO PUBLICATIONS

AGARD & RTO publications are sometimes available from the National Distribution Centres listed below. If you wish to receive all RTO reports, or just those relating to one or more specific RTO Panels, they may be willing to include you (or your Organisation) in their distribution.

RTO and AGARD reports may also be purchased from the Sales Agencies listed below.

Requests for RTO or AGARD documents should include the word 'RTO' or 'AGARD', as appropriate, followed by the serial number. Collateral information such as title and publication date is desirable.

If you wish to receive electronic notification of RTO reports as they are published, please visit our website (www.rta.nato.int) from where you can register for this service.

NATIONAL DISTRIBUTION CENTRES

BELGIUM
Etat-Major de la Défense
Département d'Etat-Major Stratégie
ACOS-STRAT – Coord. RTO
Quartier Reine Elisabeth
Rue d'Evère
B-1140 Bruxelles

CANADA
DRDKIM2
Knowledge Resources Librarian
Defence R&D Canada
Department of National Defence
305 Rideau Street
9th Floor
Ottawa, Ontario K1A 0K2

CZECH REPUBLIC
LOM PRAHA s. p.
o. z. VTÚLaPVO
Mladoboleslavská 944
PO Box 18
197 21 Praha 9

DENMARK
Danish Defence Research Establishment
Ryvangs Allé 1
P.O. Box 2715
DK-2100 Copenhagen Ø

FRANCE
O.N.E.R.A. (ISP)
29, Avenue de la Division Leclerc
BP 72
92322 Châtillon Cedex

GERMANY
Streitkräfteamt / Abteilung III
Fachinformationszentrum der Bundeswehr (FIZBw)
Friedrich-Ebert-Allee 34
D-53113 Bonn

GREECE (Point of Contact)
Defence Industry & Research General Directorate, Research Directorate
Fakinos Base Camp, S.T.G. 1020
Holargos, Athens

HUNGARY
Department for Scientific Analysis
Institute of Military Technology
Ministry of Defence
H-1525 Budapest P O Box 26

ICELAND
Director of Aviation
c/o Flugrad, Reykjavik

ITALY
Centro di Documentazione Tecnico-Scientifica della Difesa
Via XX Settembre 123
00187 Roma

LUXEMBOURG
See Belgium

NETHERLANDS
Royal Netherlands Military Academy Library
P.O. Box 90.002
4800 PA Breda

NORWAY
Norwegian Defence Research Establishment
Attn: Biblioteket
P.O. Box 25, NO-2007 Kjeller

POLAND
Armament Policy Department
218 Niepodleglosci Av.
00-911 Warsaw

PORTUGAL
Estado Maior da Força Aérea
SDFA – Centro de Documentação
Alfragide, P-2720 Amadora

SPAIN
SDG TECEN / DGAM
C/ Arturo Soria 289
Madrid 28033

TURKEY
Milli Savunma Bakanlığı (MSB)
ARGE ve Teknoloji Dairesi Başkanlığı
06650 Bakanliklar – Ankara

UNITED KINGDOM
Dstl Knowledge Services
Information Centre, Building 247
Dstl Porton Down
Salisbury, Wiltshire SP4 0JQ

UNITED STATES
NASA Center for AeroSpace Information (CASI)
Parkway Center, 7121 Standard Drive
Hanover, MD 21076-1320

SALES AGENCIES

NASA Center for AeroSpace Information (CASI)
Parkway Center
7121 Standard Drive
Hanover, MD 21076-1320
UNITED STATES

The British Library Document Supply Centre
Boston Spa, Wetherby
West Yorkshire LS23 7BQ
UNITED KINGDOM

Canada Institute for Scientific and Technical Information (CISTI)
National Research Council
Acquisitions
Montreal Road, Building M-55
Ottawa K1A 0S2, CANADA

Requests for RTO or AGARD documents should include the word 'RTO' or 'AGARD', as appropriate, followed by the serial number (for example AGARD-AG-315). Collateral information such as title and publication date is desirable. Full bibliographical references and abstracts of RTO and AGARD publications are given in the following journals:

Scientific and Technical Aerospace Reports (STAR)
STAR is available on-line at the following uniform resource locator:
http://www.sti.nasa.gov/Pubs/star/Star.html
STAR is published by CASI for the NASA Scientific and Technical Information (STI) Program
STI Program Office, MS 157A
NASA Langley Research Center
Hampton, Virginia 23681-0001
UNITED STATES

Government Reports Announcements & Index (GRA&I)
published by the National Technical Information Service
Springfield
Virginia 2216
UNITED STATES
(also available online in the NTIS Bibliographic Database or on CD-ROM)

ISBNs 92-837-0041-4 / 978-92-837-0041-8